

Development of New Breast Cancer Resistance Protein Inhibitors

Dissertation

zur

Erlangung des Doktorgrades (Dr. rer. nat.)

der

Mathematisch-Naturwissenschaftlichen-Fakultät

der

Rheinischen Friedrich-Wilhelms-Universität Bonn

vorgelegt von

Kapil Juvale

aus

Pune, Indien

Bonn 2013

Angefertigt mit Genehmigung der Mathematisch-Naturwissenschaftlichen Fakultät
der Rheinischen Friedrich-Wilhelms-Universität Bonn

„Gedruckt mit Unterstützung des Deutschen Akademischen Austauschdienstes“

1. Gutachter : Prof. Dr. Michael Wiese

2. Gutachter : Prof. Dr. Gerd Bendas

Tag der Promotion : 10.06.2013

Erscheinungsjahr : 2013

Dedicated to my family and friends

*"Without speculation there is no good
and original observation"*

Charles Darwin (1809-1882)

Abstract

Chemotherapy is a major form of treatment for cancers. Unfortunately, the majority of cancers are either resistant to chemotherapy or acquire resistance (MDR) during treatment. The most common mechanism by which human cancers develop multidrug resistance is overexpression of certain ATP-binding cassette (ABC) transporters. Breast Cancer Resistance Protein (BCRP / ABCG2), a member of ATP binding cassette family ABCG has been found to confer multidrug resistance in cancer cells. One of the strategies to overcome resistance due to BCRP overexpression is the investigation of potent and specific BCRP inhibitors. Several inhibitors of BCRP have been developed in last decade in an attempt to overcome the resistance mediated by this transporter, but there are only very few potent and selective BCRP inhibitors such as Ko143. Aim of the current project was to develop new potent and selective BCRP inhibitors. In this work a total of 131 compounds spanning different chemical classes such as chalcone, flavonoid and quinazoline were investigated. Several biological studies were carried out using these compounds to determine their BCRP inhibitory potential, selectivity, toxicity and efficacy to reverse MDR to certain anticancer compounds. The study of all three classes of compounds revealed structural requirements for BCRP inhibition. In this study, chalcones and benzoflavones showed moderate to good BCRP inhibition with selectivity towards BCRP over other transporters. Amongst chalcones and flavones, 7,8-benzoflavones were the most potent BCRP inhibitors. The structural activity relationship of quinazoline compounds revealed the importance of a 2-phenyl substitution in quinazoline scaffold for BCRP inhibition. The quinazoline compounds were the most active compounds among all classes, some of the quinazolines showing even better activity than Ko143. The results obtained from the study of chalcones, flavonoids and quinazolines as BCRP inhibitors are promising for the ongoing research to find potent BCRP inhibitors.

Contents

1	Introduction	1
1.1	Chemotherapy and multidrug resistance (MDR)	1
1.2	ATP-binding cassette transporters	2
1.2.1	P-glycoprotein (P-gp) / ABCB1	4
1.2.1.1	Molecular structure of P-gp	4
1.2.1.2	Substrates and inhibitors of P-gp	6
1.2.2	Multidrug Resistance associated Protein 1 (MRP1) / ABCC1	7
1.2.2.1	Molecular structure of MRP1	7
1.2.2.2	Substrates and inhibitors of MRP1	8
1.2.3	Breast cancer resistance protein (BCRP) / ABCG2	9
1.2.3.1	Molecular structure of BCRP	10
1.2.3.2	Localization of BCRP in human tissues	10
1.2.3.3	Role of BCRP in MDR	11
1.2.3.4	Substrates of BCRP	13
1.2.3.5	Inhibitors of BCRP	13
2	Objectives of the work	17
2.1	Synthesis and evaluation of chalcones and benzochalcones as BCRP inhibitors	18
2.2	Synthesis and evaluation of flavones and benzoflavones as BCRP inhibitors	18
2.3	Synthesis and evaluation of substituted quinazolines as BCRP inhibitors	19
3	Project 1: Chalcones and benzochalcones as BCRP inhibitors	21
3.1	Chalcones as modulators of ABC transporters: an overview	22
3.2	Synthesis of chalcones and benzochalcones	23
3.2.1	Synthesis of chalcones	23
3.2.2	Synthesis of 3',4'- and 5',6'-benzochalcones	25

3.3	Biological investigation of chalcones and benzochalcones	26
3.3.1	Investigation of BCRP inhibition in the Hoechst 33342 accumulation assay	26
3.3.1.1	Structure-activity relationship	30
3.3.2	Screening of chalcones and benzochalcones for P-gp and MRP1 inhibition in the calcein AM accumulation assay	33
3.3.3	MTT cytotoxicity assay	35
3.3.3.1	Investigation of selected chalcones to reverse MDR by MTT assay	35
3.3.3.2	Cytotoxicity of selected chalcones and benzochalcones	37
4	Project 2: Flavones and benzoflavones as BCRP inhibitors	39
4.1	Overview of flavonoids as ABC transporter modulators	40
4.2	Synthesis of benzoflavones	41
4.3	Synthesis of 3-hydroxyflavones and 3-hydroxybenzoflavones	42
4.4	Synthesis of 3-methoxy-flavones and 3-methoxybenzoflavones	44
4.5	Biological evaluation of flavones and benzoflavones	46
4.5.1	Investigation of BCRP inhibition	46
4.5.1.1	Structural features of flavones and benzoflavones for BCRP inhibition	51
4.5.2	Determination of P-gp and MRP1 inhibition in the calcein AM assay	53
4.5.3	Intrinsic cytotoxicity of selected flavones and benzoflavones in the MTT assay	55
4.5.4	Re-sensitization of BCRP overexpressing cells towards SN-38 and Hoechst 33342 cytotoxicity	57
5	Quinazolines as BCRP inhibitors	59
5.1	Quinazolines as modulators of ABC transporters	60
5.2	Synthesis of quinazoline derivatives	61
5.2.1	Synthesis of 2-phenyl-4-anilinoquinazolines	62
5.2.2	Synthesis of 2-(3,4-dimethoxyphenyl)-4-anilinoquinazolines	63
5.2.3	Synthesis of 4-anilinoquinazolines	64
5.2.4	Synthesis of 6,7-dimethoxy-4-anilinoquinazolines	65
5.2.5	Synthesis of 4- <i>N</i> -piperazinylquinazolines	66
5.2.6	Synthesis of 2,4-bis-anilinoquinazolines	67

5.3	Biological evaluation of quinazolines	68
5.3.1	Hoechst 33342 and Pheophorbide A assays for determining BCRP inhibition	68
5.3.2	P-gp and MRP1 inhibition by quinazolines	76
5.3.3	Intrinsic cytotoxicity of selected quinazolines	77
5.3.4	MDR reversal ability of quinazolines	79
6	Summary	81
7	Experimental work	87
7.1	Chemistry	87
7.1.1	General materials and methods	87
7.1.2	General synthesis procedures	89
7.1.2.1	Synthesis of 2-hydroxy-4-methoxyacetophenone . . .	89
7.1.2.2	Synthesis of 4,6-dimethoxy-2-hydroxyacetophenone .	89
7.1.2.3	Synthesis of 2,4-dimethoxyacetophenone	90
7.1.2.4	Synthesis of chalcones	90
7.1.2.5	Synthesis of benzochalcones	108
7.1.2.6	Synthesis of 7,8- and 5,6-benzoflavones	118
7.1.2.7	Synthesis of 3-hydroxy flavones and benzoflavones . .	122
7.1.2.8	3-methoxy flavones and benzoflavones	130
7.1.2.9	Synthesis of pentamethyl ethers of quercetin and morin	137
7.1.2.10	Synthesis of tetramethyl ethers of quercetin and morin	139
7.1.2.11	Synthesis of substituted quinazolin-4(3 <i>H</i>)-ones . . .	141
7.1.2.12	Synthesis of substituted 4-chloroquinazolines	143
7.1.2.13	Synthesis of <i>N</i> -phenylpiperazines	145
7.1.2.14	Synthesis of 4-anilinoquinazolines	149
7.1.2.15	Synthesis of 4- <i>N</i> -piperazinylquinazolines	176
7.1.2.16	synthesis of <i>N</i> ² , <i>N</i> ⁴ -disubstituted quinazolines . .	181
7.2	Biological testing	185
7.2.1	Materials	185
7.2.1.1	Chemicals	185
7.2.1.2	Materials for cell culture and assays	186
7.2.1.3	Instruments	187
7.2.1.4	Buffers used for preparing cells for biological assays .	188
7.2.2	Cell culture	190

7.2.2.1	Cell lines	190
7.2.2.2	Growing and subculturing of cells	191
7.2.2.3	Cryopreservation and defrosting of cells	192
7.2.2.4	Cell counting using CASY1 model TT	192
7.2.3	Assays	193
7.2.3.1	Hoechst 33342 accumulation assay	193
7.2.3.2	Pheophorbide A assay	195
7.2.3.3	Calcein AM accumulation assay	198
7.2.3.4	MTT cytotoxicity assay	200
7.2.3.5	IC ₅₀ and GI ₅₀ calculations using GraphPad Prism . .	202

Bibliography	203
List of Tables	231
List of Figures	233
List of Algorithms	237

Abbreviations

ABC transporter	ATP binding cassette transporter
ATP	adenosin-5'-triphosphate
BCRP	breast cancer resistance protein, ABCG2
Calcein AM	calcein acetoxymethylester
CDCl ₃	deuterated chloroform
d	doublet
dd	double doublet
DMF	dimethylformamid
DMSO	dimethyl sulfoxide
dt	double triplet
FBS	fetal bovine serum
FTC	Fumitremorgin C
GI ₅₀	concentration of compound required for 50 % inhibition of cell growth
HCl	hydrochloric acid
IC ₅₀	concentration of compound required for 50 % inhibitory
KHB	Krebs-HEPES buffer
KOH	potassium hydroxide
m	multiplet
MDR	multidrug resistance
MRP1	multidrug resistance-related protein 1, ABCC1
MTT	3-(4,5-dimethylthiazol-2-yl)-2,5-diphenyltetrazolium bromide
n.a.	no activity
NaOH	sodium hydroxide

NBD	nucleotide binding domain
NMR	nuclear magnetic resonance
PBS	phosphate buffered saline
P-gp	permeability glycoprotein, ABCB1
ppm	parts per million
q	quartet
RT	room temperature
s	singlet
SD	standard deviation
t	triplet
TLC	thin layer chromatography
TMD	transmembrane domain
wt	wild type

1 Introduction

1.1 Chemotherapy and multidrug resistance (MDR)

Cancer is the main cause of millions of deaths worldwide. In addition to surgery, chemotherapy is a major form of treatment for different types of cancers. Unfortunately, the majority of cancers are either resistant to chemotherapy or acquire resistance during treatment [1]. Intrinsic drug resistance relates to the failure of many tumors to respond to initial chemotherapy, while acquired drug resistance occurs when tumors initially respond to chemotherapy but later relapses and appears to be strongly resistant to the original treatment. MDR is a drug resistance by tumor cells, that consists of simultaneous emergence of cellular resistance to toxic action of chemotherapeutic drug originally used and to other chemicals having different chemical structure and mechanism of action. As a result of MDR, chemotherapeutic agents fail to target the tumor cells and cancer becomes untreatable by chemotherapy [2]. A common mechanism by which tumors develop multidrug resistance is overexpression of efflux transport proteins, especially certain ATP-binding cassette (ABC) transporters in the plasma membrane of cancer cells [3]. P-glycoprotein (P-gp) and the multidrug resistance associated protein 1 (MRP1) have been shown to confer resistance to a broad spectrum of chemotherapeutic agents. More recently BCRP (breast cancer resistance protein) has been discovered and proved to cause resistance in tumor cells. [4]

1.2 ATP-binding cassette transporters

Transporters are membrane proteins with multiple membrane-spanning domains, which facilitate the permeation of low molecular weight compounds and ions across the biological membranes. ATP-binding cassette (ABC) transporters have been found to be present in cells of all species, ranging from bacteria to man [5]. ABC transporters belong to a large family of structurally related transmembrane proteins. In eukaryotic organisms, ABC transporters are ubiquitously present, especially in human ABC transporters are widely expressed throughout the body. ABC transporters actively transport chemically diverse substrates across the membrane and are also involved in various cellular processes [6, 7]. The transport of substrates is energy dependent and is driven by ATP hydrolysis.

Till now 49 members of the ABC transporter family have been discovered in humans [8]. These are divided into seven subfamilies from ABC-A to ABC-G depending on the similarity in gene structure, sequence homology and order of the domains [9]. The major ABC transporters involved in multidrug resistance are P-glycoprotein (P-gp / ABCB1 / MDR1), multidrug resistance protein 1 (MRP1 / ABCC1) and breast cancer resistance protein (BCRP / ABCG2) [10].

The functional unit of ABC transporters consists of two nucleotide binding domains (NBDs) and two transmembrane domains (TMDs). The transmembrane domains of ABC transporters consists of six membrane spanning helices. Transported compounds, xenobiotics in most cases, interact with sites present within the TMDs. A minimum of 12 membrane-spanning helices are required for transport of a substrate [11]. But, some transporters like BCRP consists of only one TMD and one NBD, hence are known as half transporters. Such transporters form homo- or hetero-dimer to function as full ABC transporters [12]. A schematic representation of typical ABC transporter is shown in Figure 1.1.

ABC transporters play an important role in tissue defense by removal of toxic xenobiotics [9, 11, 13]. Hence, ABC transporters are found to be expressed in biological barriers like the blood-brain barrier (BBB) [14–16], blood-cerebrospinal-fluid barrier (CSF) [17, 18]. ABC transporters like P-gp and BCRP have also been shown to be present in the placenta protecting the fetus from xenobiotics [19, 20].

ABC transporter have also been shown to play a role in altering absorption, dis-

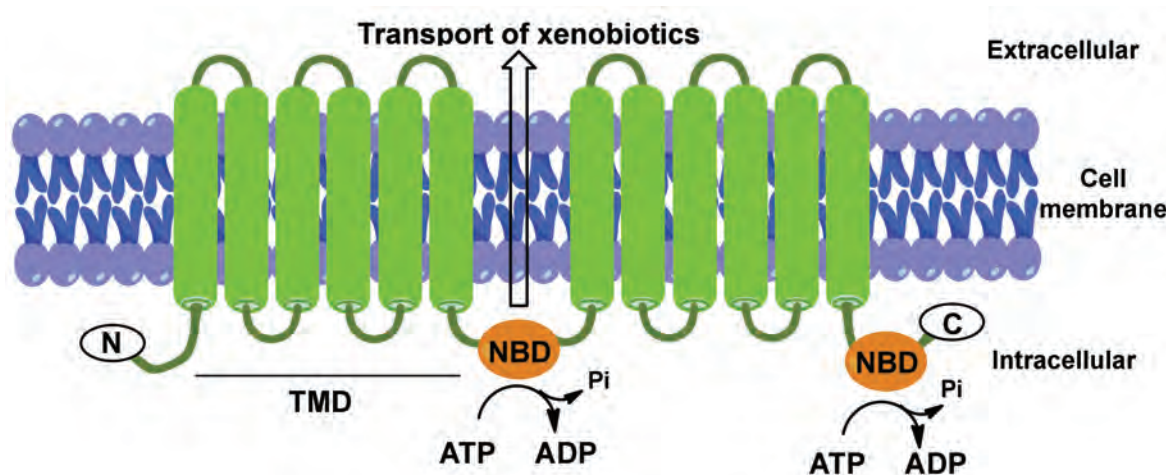


Figure 1.1: Structural features of typical ABC transporters

tribution, metabolism and excretion (ADME) of transported drugs owing to their presence in several organs like intestine and liver [10, 11, 21–23]. This affects the oral bioavailability and tissue distribution, making necessary to identify the influence of transporters on the drug disposition. A list of different ABC transporters and their presence in several tissues is shown in Table 1.1.

Table 1.1: Major ABC transporters and their localization in tissues [11, 24]

ABC transporter	Tissue localization
P-gp / ABCB1	liver, kidney, intestine, placenta, blood-brain barrier, stem cells
MDR2 / ABCB4	liver
MRP1 / ABCC1	lungs, kidney, testes, cardiac muscle, placenta, skeletal muscles
MRP2 / ABCC2	lungs, Liver, kidney, placenta, blood-brain barrier
BCRP / ABCG2	placenta, liver, intestine, breast, stem cells, blood-brain barrier

Apart from detoxification or affecting an ADME, ABC transporters have been identified to cause multidrug resistance. ABC transporters have been found to be highly overexpressed in cancer cells resistant to chemotherapy causing lower accumulation of cytotoxic anticancer drugs. This mechanism of MDR has been found to be most relevant to drugs entering cells by passive diffusion such as the chemotherapeutic agents doxorubicin and paclitaxel [25]. Among all ABC transporters P-gp, the

MRP family proteins (especially MRP1) and BCRP have been found to be mainly responsible for MDR [3, 26, 27]. These transporters are discussed in detail in the next sections.

1.2.1 P-glycoprotein (P-gp) / ABCB1

P-glycoprotein (P-gp) is the first member of the ABC subfamily B (ABCB1) and is also known as MDR1. It was first discovered and characterized in 1976 by Juliano and Ling in multidrug resistant Chinese hamster ovary cells [28, 29]. Human ABCB1 was later identified to be overexpressed in cultured cancer cells having MDR against different anticancer drugs [30]. The active efflux of substrates by P-gp leads to reduced intracellular concentrations, resulting in resistance to a broad range of cytotoxic drugs such as *Vinca* alkaloids, anthracyclines and taxanes.

1.2.1.1 Molecular structure of P-gp

Human ABCB1 consists of 1280 amino acid residues. It has a molecular weight of about 170 kDa, which may vary from 130-180 kDa depending on the type of cells and species in which they are expressed [31]. P-gp is composed of 2 homologous halves of transmembrane domains (TMDs), each consisting of 6 transmembrane helices, an N-terminal and a C-terminal. Each half of the protein consists of an intracellular nucleotide binding domain (NBD) or ATP binding site (see Figure 1.2). The hydrolysis of ATP provides the energy required for the drug transport [32]. The two folded halves of the P-gp molecule have approximately 43 % similarity.

Until now several homology models for P-gp have been suggested. The first models were based on the crystal structures of transporters available from bacteria. Homology models of the P-gp have been used to identify structure of the P-gp as well as detecting binding sites for substrates and inhibitors [33–36]. Later in 2009 the crystal structure of mouse P-gp (Abcb1a) was solved. This crystal structure has 87 % identity to that of human P-gp sequence [37].

Regardless of these models and biochemical data, the molecular mechanism underlying the substrate transport is still not clear. Two different models have been suggested to explain the transport of substrates by P-gp. The ‘Flippase’ model was suggested

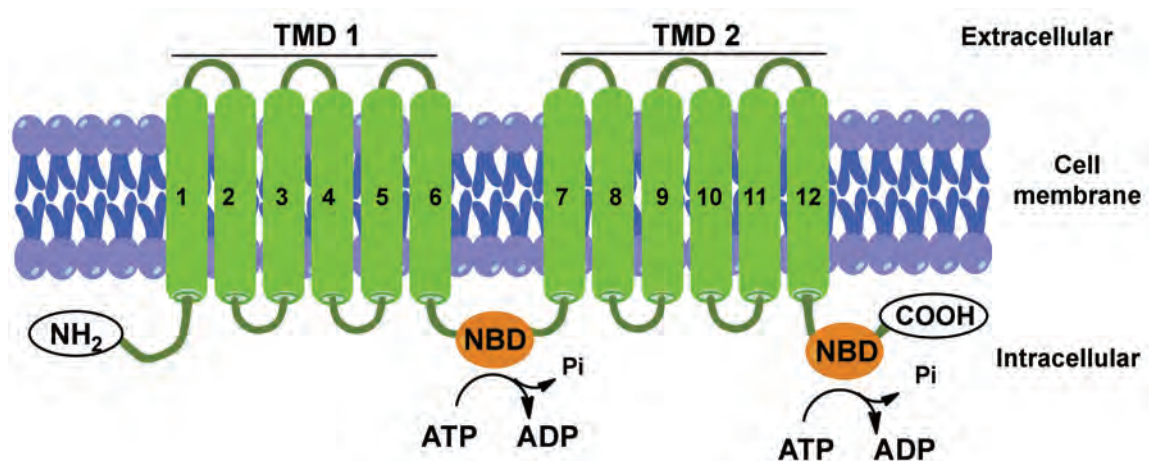


Figure 1.2: Topological model of ABCB1 / P-gp

by Higgins *et al.* in 1992, where it was postulated that substrates congregate with P-gp at the inner side of the plasma membrane. Then, P-gp flips the substrate to the outer side, from where it can diffuse into the extracellular space (see Figure 1.3) [38]. A second ‘hydrophobic vacuum cleaner’ model was suggested by Gottesman *et al.* in 1993, where it was also postulated that the substrate diffuses passively into inner side of the plasma membrane. Here, substrate is detected by the P-gp and ejected directly outside the membrane. It was also suggested that P-gp forms a single transport channel by bringing two halves of P-gp together. The transport of substrates occurs through a single barrel-like structure of transporter (see Figure 1.3) [1].

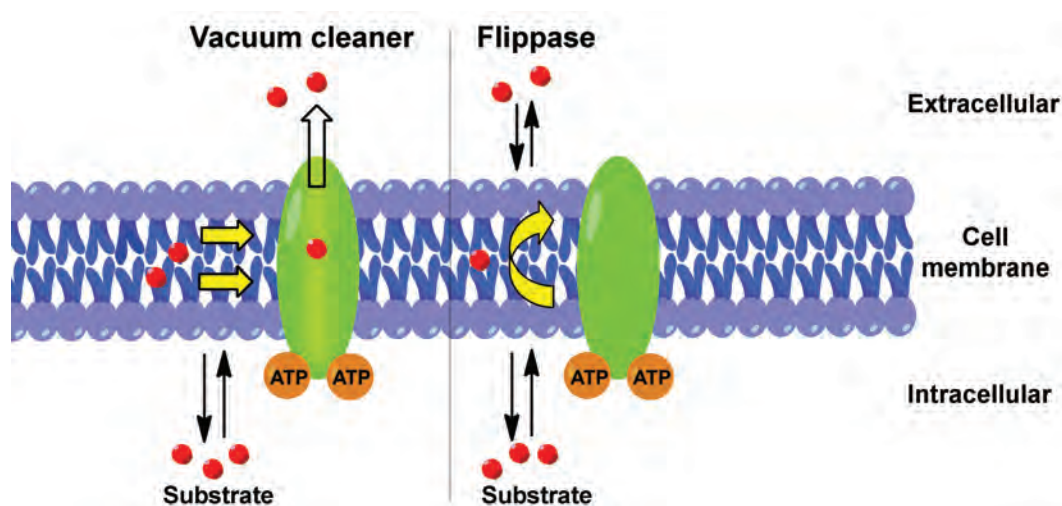


Figure 1.3: Hydrophobic vacuum cleaner and flippase models for substrate transport by P-gp, modified from [39].

1.2.1.2 Substrates and inhibitors of P-gp

Until now many P-gp substrates belonging to different chemical classes have been identified, which include cytotoxic drugs, antibiotics, antiallergics, HIV protease inhibitors, calcium channel blockers, central nervous system drugs, cardiacs, steroids and peptides [39, 40]. Some of these substrates are listed in Table 1.2.

Table 1.2: Substrates and inhibitors of P-gp [39]

Substrates	<p>Anticancer / cytotoxic drugs: <i>Vinca</i> alkaloids: vinblastine, vincristine anthracyclines: daunorubicin, doxorubicin epipodophyllotixins: etoposide, teniposide taxanes: Paclitaxel, docetaxel camptothecins: irinotecan, SN-38</p> <p>Antibiotics: erythromycin, valinomycin</p> <p>HIV protease inhibitors: saquinavir, ritonavir, nelfinavir</p> <p>calcium channel blockers: diltiazem, felodipine, nifedipine, verapamil, tiapamil</p> <p>Fluorescent dyes: calcein-AM, BCECF-AM, rhodamine 123, Hoechst 33342</p> <p>Peptides: gramicidine D, valinomycin</p>
Inhibitors	<p>First generation: verapamil, cyclosporine A, quinidine, quinine, nifedipine, dextniguldipine</p> <p>Second generation: elacridar (GF120918), biricodar (VX-710), PSC-833</p> <p>Third generation: tariquidar (XR-9576), zosuquidar (LY335979), laniquidar (R101933), LY475776</p>

Several efforts have been undertaken in the past to develop potent inhibitors of P-gp. Like substrates, inhibitors of P-gp belong to a broad range of different chemical classes. The calcium channel blocker verapamil was first investigated by Tsuruo *et*

al. and was found to be able to reverse the vincristine and vinblastine resistance in P-gp overexpressing cancer cells [41]. The modulators of P-gp are categorized into three generations. The first generation of inhibitors consists of compounds that were already in clinical use for other therapeutic applications. Drug compounds like verapamil, cyclosporine and quinidine belong to the first generation, but they showed high toxicity at the required inhibitory concentrations [42]. The second generation of compounds consists of less toxic inhibitors of P-gp.

Further development of P-gp inhibitors based on structure-activity relationships led to the third generation of inhibitors which have very low inhibitory concentrations [43]. When compared to second generation inhibitors, these are not cytochrome P450 3A4 substrates and have no effect on the pharmacokinetic profile of co-administered drugs [42–44]. A list of selected P-gp inhibitors is given in Table 1.2.

1.2.2 Multidrug Resistance associated Protein 1 (MRP1) / ABCC1

The multidrug resistance associated protein 1 (MRP1) was first identified by Cole *et al.* in 1992 [45]. MRP1 belongs to the C subfamily of ABC transporters and is the member 1 (ABCC1). It was first discovered in lung cancer cells H69 after continuous incubation of cells with doxorubicin. In normal tissues, similar to P-gp, MRP1 also plays an important role in protection from toxic xenobiotics [17, 46]. It has been found to be present in almost all tissues and organs, being highly expressed in testes, kidneys, lungs, gastrointestinal track and BBB [45, 47]. MRP1 has been found to be overexpressed in a wide variety of solid tumors such as those of lung, breast and prostate and also has been shown to cause MDR against several cytotoxic drugs in different cancers [48].

1.2.2.1 Molecular structure of MRP1

Although MRP1 shows a partly similar resistance profile to that of P-gp, the amino acid sequence identity is only to the extent of 15 % [49]. MRP1 consists of 1531 amino acid residues and has a molecular weight of about 190 kDa. The MRP1 consists of a core structure that is common to many ABC proteins like P-gp, having

two hydrophobic transmembrane domains (TMDs) each followed by a NBD. In addition to the central core, it contains a third TMD0, which has five transmembrane α -helices and an extracellular N-terminus [50]. The TMD1 and TMD2 in the central core play a role in substrate transport while, TMD0 has no transport ability. The structure of MRP1 is depicted in Figure 1.4.

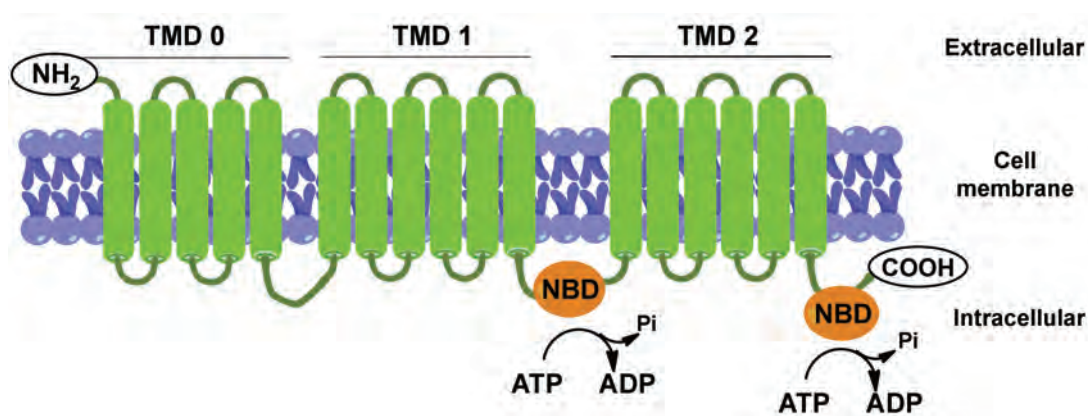


Figure 1.4: Topological model of MRP1

1.2.2.2 Substrates and inhibitors of MRP1

Several substrates of MRP1 have been identified until now. These include a vast variety of hydrophobic compounds, organic anion conjugates and nonconjugated compounds. MRP1 plays major role in transport of glucuronoide, sulfate and glutathion conjugates, protecting the tissues from toxic metabolites. A detailed list of MRP1 substrates is given in Table 1.3.

Until now very few specific MRP1 inhibitors such as MK571 (a leukotriene receptor antagonist) [51] and ONO-1078 (a peptide leukotriene receptor antagonist) [52] have been found. The glutathion transport by MRP1 has been shown to be inhibited by the tricyclic isoxazole compounds LY402913 [53] and LY475776 [54]. Recently Koley *et al.* showed that MK571 was able to inhibit the MRP1 mediated transport of thiodione [55]. The nonspecific organic anion transport inhibitors like probenecid and indomethacin have also been found to inhibit MRP1 [56].

Table 1.3: Substrates of MRP1 [57, 58]

Conjugates	GSH conjugates: leukotriene C4, leukotriene D4, leukotriene E4, hydroxynonenal-SG, melphalan, chlorambucil glucuronide conjugates: glucuronosylbilirubin, estradiol-17- β -D-glucuronide, etoposide glucoronoide sulfate conjugates: dehydroepiandrosterone 3-sulfate, sulfatolithocholyl taurine, estrone 3-sulfate
Anticancer / cytotoxic drugs	<i>Vinca</i> alkaloids: vincristine and vinblastine anthracyclines: doxorubicin and daunorubicin others: etoposide, SN-38, methotrexate
Peptides:	<i>N</i> -acetyl-Leu-Leu-norleucinal (ALLN), GSH, GSSG
Fluorescent dyes	calcein-AM, BCECF

1.2.3 Breast cancer resistance protein (BCRP) / ABCG2

Breast cancer resistance protein (BCRP) belongs to subfamily G, member 2 of ABC transporters. It was first cloned by Doyle *et al.* in 1998 from a doxorubicin resistant MCF-7 breast cancer cell line (MCF-7/AdrVp) and from which it derived its name ‘breast cancer resistance protein’ [59]. These cells were sensitive to *vinca* alkaloids, cisplatin and paclitaxal, which are either P-gp or MRP1 substrates, suggesting the presence of an other ABC transporter. But, unlike the name suggest BCRP is not limited to expression in breast tissue and caner cells. It was later found in mitoxantrone resistant cancer cells and in placenta. Hence it is also known as mitoxantrone resistant protein (MXR) or placental ABC protein (ABCP). Because of its structural and sequence homology to *Drosophila* white, brown and *scarlet* protein genes and the human white homologue (ABCG1), it was named ABCG2 by the Human Genome Nomenclature Committee [60].

1.2.3.1 Molecular structure of BCRP

BCRP is a 655 amino acid protein having a molecular weight of about 72 kDa. In comparison to other ABC transporters, BCRP is a half transporter with reversed NBD-TMD configuration. Although the exact structure of the BCRP is not clear, it has been suggested to have an N-terminal nucleotide binding domain (NBD) and a C-terminal transmembrane domain (TMD) consisting of six transmembrane α -helices [61]. A topology model of the BCRP is shown in Figure 1.5. Owing to its half transporter nature, BCRP is believed to homodimerize or oligomerize to function as an efflux protein [62]. It has been suggested by Xu *et al.* that, BCRP functions as a tetramer bridged by disulphide bonds [63].

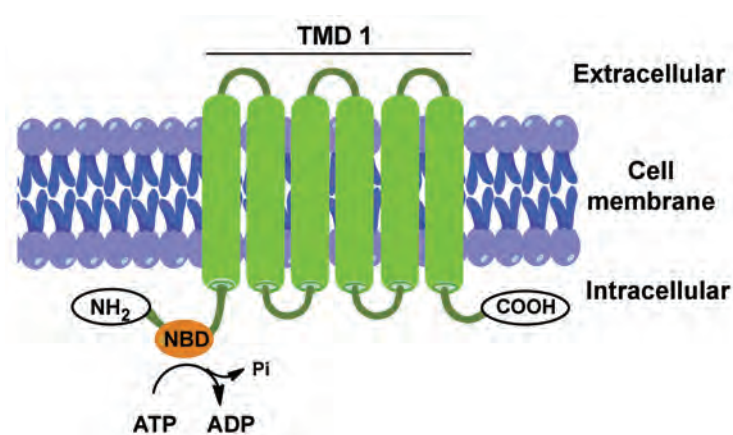


Figure 1.5: Topology model of BCRP

1.2.3.2 Localization of BCRP in human tissues

BCRP has been shown to be present in many normal tissues and it plays an important physiological role. Doyle *et al.* reported the presence of high levels of BCRP in placenta and lower levels in the brain, small intestine, testes, liver, spleen, ovaries and prostate gland [59]. Fetsch *et al.* have shown the presence of BCRP in the adrenal gland, central nervous system, small and large intestine, lungs, stomach and pancreas [64]. The tissue distribution of BCRP shows overlap with P-gp, suggesting its role in tissue protection from xenobiotics.

BCRP has also been found to be expressed in stem cells, especially in the hematopoietic cells [65]. BCRP has been identified to transport the Hoechst 33342 dye from

cells within the ‘side-population’ (SP) region. Despite the exact role of BCRP in stem cells is not known, it has been postulated that BCRP may play role in protection of stem cells [66]. Localization of BCRP and its physiological role is listed in Table 1.4.

Table 1.4: Tissue distribution and physiological role of BCRP [60, 67]

Tissue	Physiological role
Placenta	protection of the fetus from toxins
Liver and biliary tract	hepato-biliary excretion, biliary excretion of drugs, xenobiotics or endogenous compound conjugates
Stem cells	SP-phenotype and protection against hypoxia
Intestine	reduction of drug absorption
Brain	protection against xenobiotics
Breast	secretion of B vitamin required for fat metabolism
Kidney	renal excretion

1.2.3.3 Role of BCRP in MDR

Multidrug resistance caused by overexpression of BCRP was first observed in MCF-7/AdrVp after a long term selection of MCF-7 human breast cancer cell line with doxorubicin [59]. Later an identical transporter (MXR) was identified in a mitoxantrone resistant cell line derived from the S1 human colon carcinoma cells [68]. Several cell lines including MCF-7, S1, gastric carcinoma EPG85-257 and fibrosarcoma EPF86-079, showed resistance to mitoxantrone due to overexpression of BCRP [59, 68, 69]. Several studies showed that the overexpression BCRP leads to resistance to topotecan [70, 71]. Several transfection studies were performed to prove the role of BCRP in the MDR to drugs like mitoxantrone and topotecan. The expression of the BCRP protein and/or mRNA has been detected in numerous types of human cancers, such as solid tumors and hematological malignancies. Immunohistochemical studies of several tumors have shown overexpression of BCRP in more than 40 % of solid tumors [72]. BCRP expression in premature stem cells of different tissues was confirmed, suggesting its role in protection of cancer stem cell subpopulation particularly under hypoxic conditions [8, 73].

Table 1.5: BCRP substrates

Class of drugs / compounds	Drugs / compounds
Anthracenes	mitoxantrone [74, 75] aza-anthrapyrazole [76, 77] bisantrene [78]
Camptothecins	topotecan [78] irinotecan [79, 80] SN-38 [81] 9-amino-camptothecin [82] diflomotecan [83]
Anthracyclines	doxorubicin* [84, 85] daunorubicin* [86]
Antifolate	methotrexate** [87, 88]
Nucleoside analogs	azidothymidine (AZT) [89, 90] lamivudine [89, 90]
Other drug	flavopiridol [91, 92] prazosin [78] imatinib mesylate (STI571) [93] pantoprazole [94] indocarbazole [95] ciprofloxacin [96] erythromycin [97]
Fluorescent dyes	Hoechst 33342 [65] BODIPY-prazosin [75, 78] BCECF-AM [98] 6-carboxy-2',7'-dichlorofluorescein[99]
Conjugates of glucuronoide and sulfate	benzo[a]pyrene-3-glucuronide [100] estrone-3-sulfate [101, 102] dehydroepiandrosterone sulfate [103] 17 β -estradiol sulfate [101]
Porphyrines	pheophorbide A [104, 105] protoporphyrin IX [105] phytoporphyrin [106] pyropheophorbide A methylester [107]

* Transported only by BCRP mutants R482T or R482G

** Transported only by wild-type BCRP (R482).

1.2.3.4 Substrates of BCRP

Mitoxantrone was the first substrate reported for BCRP. It has been shown to confer resistance to different anticancer drugs which include, camptothecins such as topotecan, irinotecan (CPT-11) and SN-38 (an active metabolite of irinotecan). The anthracycline class of compounds has also been shown to be transported in BCRP overexpressing MCF-7/AdrVp3000 and S1-M1-80 cells [85]. But these compounds were not transported in wild type cells expressing BCRP with an amino acid residue arginine at position 482. Anthracyclines were identified to be transported only by the BCRP mutant R482G (glycine at position 482) or R482T (threonine at position 482) found in the S1-M1-80 and MCF-7/AdrVp3000 cell lines respectively [108]. Also, the antifolate drug methotrexate was found to be transported only by wild type BCRP [88, 109].

In addition to its role to confer MDR against chemotherapeutic agents, BCRP has been identified to actively transport structurally different organic molecules, conjugated or unconjugated compounds, such as flavopiridol, estrone-3-sulfate, benzo[a]pyrene-3-glucuronide and prazosin. Several fluorescent dyes like BODIPY-prazosin, Hoechst 33342, pheophorbide A have also been found to be substrates of BCRP. A list of BCRP substrates is given in Table 1.5.

1.2.3.5 Inhibitors of BCRP

BCRP has been shown to play a vital role in the development of MDR in different carcinomas. Hence it was of a great interest to identify modulators of BCRP mediated MDR. Since the discovery of the transporter protein, several efforts have been undertaken to find inhibitors.

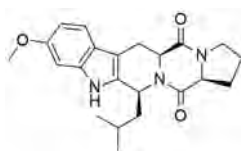
The second generation P-gp inhibitor elacridar (GF120918), an acridone carboxamide derivative was found to be a potent inhibitor of BCRP [110]. The structurally related P-gp inhibitor tariquidar (XR9576) was also shown to inhibit BCRP [107]. Later Rabindran *et al.* discovered that fumitremorgin C (FTC), a tremorgenic mycotoxin produced by the fungus *Aspargillus fumigatus*, was able to effectively reverse the multidrug resistance and increase cellular drug accumulation in BCRP overexpressing cells. FTC efficiently inhibits BCRP *in vitro* at concentrations in the micromolar

range and has little effect on P-gp or MRP1 mediated drug resistance, suggesting its specificity for BCRP [76, 80]. But its *in vivo* study was precluded owing to its neurotoxicity. Novobiocin, a coumermycin antibiotic has been shown to be a specific BCRP inhibitor, however with high IC_{50} values in the range of 20 to 80 μM only [111].

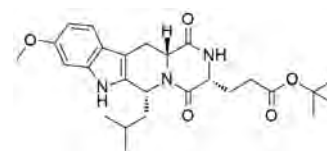
Recently, Allen *et al.* studied various tetracyclic indolyl diketopiperazine analogues of FTC as inhibitors of murine and human BCRP. The most potent analogues Ko132 and Ko134 showed comparable or greater activity than FTC. These compounds showed very low *in vivo* toxicity [112]. The desmethoxy analog of the FTC showed decreased BCRP inhibitory activity, suggesting the importance of the methoxy group at the aromatic indole ring. Hence, the methoxylated analog of Ko134 was synthesized (Ko143, see Figure 1.6), which was found to be the most potent analogue [113].

Figure 1.6: Selected inhibitors of BCRP

Specific inhibitors

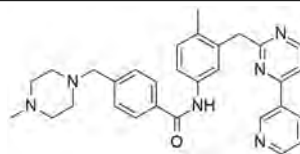


Fumitremorgin C (FTC)

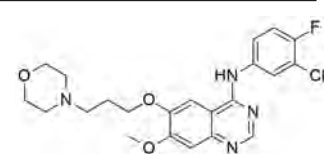


Ko143

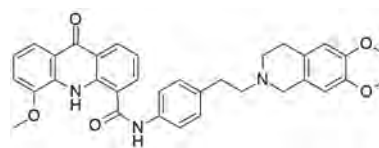
Broad spectrum inhibitors



Imatinib

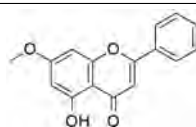


Gefitinib

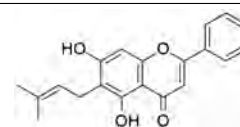


Elacridar (GF120918)

Flavonoids



Techtochrysin



6-Prenylchrysin

Various tyrosin kinase inhibitors (TKIs) like gefitinib, imatinib, EKI-785 and C11033 were analyzed for their interaction with BCRP. Some of these compounds inhibited

BCRP at submicromolar concentrations [114–116]. Very recently Pick *et al.* were able to show the effect of TKIs gefitinib and PD158780 on BCRP expression [117]. Both compounds were found to reduce the total and surface BCRP expression in EGFR-positive MDCK BCRP cells by interacting with the PI3K/Akt signaling pathway.

Several naturally occurring flavonoids have been investigated for their ability to reverse the BCRP mediated MDR. Initially, some flavonoids like chrysin and biochanin A were found to be effective at micromolar concentrations [118]. Later it was shown that tectochrysin and the synthetic analog 6-prenylchrysin were potent inhibitors of BCRP [119]. These compounds are different from GF120918, FTC and Ko143 in a way that they bind to distinct sites on BCRP or induce differential effect on coupling between ATP hydrolysis and drug transport [119].

Whether any of these compounds will be clinically useful in reversing BCRP-mediated multidrug resistance has yet to be determined. Also the molecular mechanism by which these compounds interfere with drug transport by BCRP is still poorly understood. Until now, only a few clinical studies have been performed on BCRP inhibitors. Elacridar (GF120918), a dual P-gp/BCRP inhibitor has been investigated extensively in preclinical and clinical studies [120]. Clinical trials conducted by Furman *et al.* using gefitinib for the inhibition of intestinal P-gp and BCRP showed increased oral bioavailability of irinotecan [121].

In the current study several chalcones, benzochalcones, flavones, benzoflavones and quinazolines have been investigated to find new selective and potent inhibitors of BCRP. Synthesis and biological investigation of these compounds is discussed in the next chapters.

2 Objectives of the work

In the last decade, several BCRP inhibitors have been developed in the pursuit of overcoming the multidrug resistance due to overexpression of BCRP in variety of cancers. These include naturally occurring as well as synthetic compounds having a wide range of chemical structures. BCRP being the latest identified ABC transporter [59], there is very little knowledge about its functional structure and substrate / inhibitor binding sites. Hence there is a need of developing and identifying potent and selective inhibitors of BCRP, which could help in discovering structural requirements as well as possible binding sites. Currently only very few potent and selective inhibitors like ko143 are known, which encourage to synthesize and identify new BCRP inhibitors.

The aim of the dissertation was:

1. To design and synthesize library of compounds of different chemical classes based on the results of previous studies aiming to find new potent and selective BCRP inhibitors.
2. Biological studies of these compounds to determine their inhibitory potencies against BCRP. Based on the results obtained, structural features required for the BCRP inhibition will be elucidated.
3. Checking the selectivity of synthesized compounds towards BCRP inhibition over the other major ABC transporters P-gp and MRP1.
4. To check the effectiveness and toxicity of the lead compounds, to identify their potential for preclinical studies.

In the current work three different classes of compounds were synthesized and investigated for their BCRP inhibition and selectivity and are discussed below.

2.1 Synthesis and evaluation of chalcones and benzochalcones as BCRP inhibitors

Chalcone, precursor of naturally occurring flavonoids, have been extensively studied for their biological activities. Liu *et al.* investigated several chalcones with basic functionality as P-gp inhibitors [122]. These compounds showed very less BCRP inhibition. Later Han *et al.* identified halogenated chalcones as selective BCRP inhibitors [123]. Despite these studies, no structure activity relationship is available. In this work, synthesis of several chalcones with varying substituents on ring A and ring B of the chalcone scaffold, as well as several 3',4'-benzochalcones and 5',6'-benzochalcones was planned. The aim of these modifications was to find out the importance of different substituents and to study the effect of replacing ring A of the chalcone with a naphthyl ring (see Figure 2.1).



Figure 2.1: General structures of investigated chalcones and benzochalcones

2.2 Synthesis and evaluation of flavones and benzoflavones as BCRP inhibitors

Naturally occurring flavonoids have been extensively studied for their ability to modulate ABC transporters like P-gp and BCRP [118, 124–127]. Zhang *et al.* [128] and Pick *et al.* [125] have suggested several structural requirements for BCRP inhibition. It was suggested that presence of a 3-methoxy substituent in flavone leads to an increase in activity. Recently 7,8-benzoflavone was reported to be a potent

inhibitor of BCRP [128, 129]. Based on these studies, several modifications in the flavone moiety were planned to study the effect of different substituents. As only the unsubstituted 7,8-benzoflavone has been investigated till now, different substituted 7,8-benzoflavones were planned to be synthesized to identify more potent derivatives. Also, for comparison purposes several 5,6-benzoflavones will be investigated. These compounds could be synthesized from the chalcones investigated in the chalcone project (see section 2.1). General structures of the synthesized and tested flavone derivatives are given in Figure 2.2.

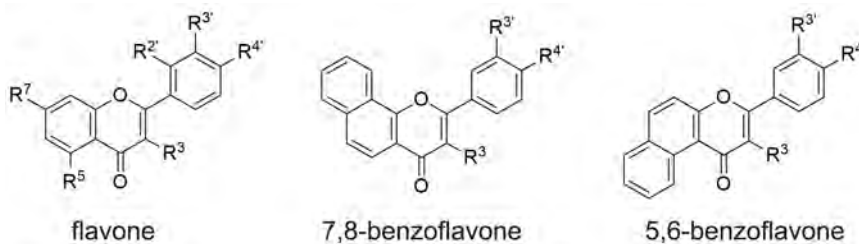


Figure 2.2: General structures of investigated flavones and benzoflavones

2.3 Synthesis and evaluation of substituted quinazolines as BCRP inhibitors

Very recently several Tyrosine kinase inhibitors (TKIs) have been investigated for their BCRP inhibition [117, 130–132]. TKIs having a quinazoline scaffold have been shown to inhibit BCRP in the micromolar range. Some of these compounds were additionally shown to decrease the BCRP expression in cells [117]. In these studies only very few quinazoline compounds have been investigated and hence no structure activity relationship (SAR) is available. Also all compounds investigated earlier lack variation in the substitution at position 2 of the quinazoline nucleus. In the current study it will be attempted to develop a SAR by varying the quinazoline structure at positions 2, 4, 6 and 7 (see Figure 2.3).

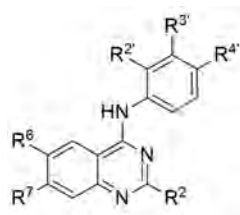


Figure 2.3: General structure of quinazoline type BCRP inhibitors and possible modifications

All synthesized compounds will be checked for BCRP, P-gp and MRP1 inhibition. Also their efficacy and intrinsic toxicity will be checked in the MTT assay.

3 Project 1: Investigation of chalcones and benzochalcones as BCRP inhibitors

Chalcones are naturally occurring compounds with a scaffold of ‘trans-1,3-diaryl-2-propen-1-one’ (see Figure 3.1). Chalcones belong to the flavonoid family and are precursors of flavonoids and isoflavonoids. These compounds are found abundantly in various plant species like *Glycyrrhiza*, *Scutellaria*, *Angelica* and *Piper* and are used as traditional medicines [133]. They are also important intermediates in the synthesis of biologically important heterocycles such as flavones, pyrazolines, oxazolines, benzothiapines, etc.

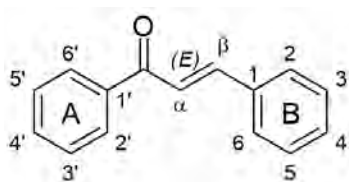


Figure 3.1: Structure of the chalcone scaffold

Until now, the chalcone class of compounds have been extensively investigated for varying biological activities. A wide range of pharmacological activities such as antimicrobial [134], anti-inflammatory [135, 136], antioxidant [137, 138], antitubercular [139], antimalarial [140, 141], antileishmanial [141], anticancer [142–146] and antifungal [147, 148], etc. have been identified.

3.1 Chalcones as modulators of ABC transporters: an overview

Chalcones, being precursors of flavonoids have been investigated as ABC transporter inhibitors. First in 1998 Bois *et al.* investigated several halogenated chalcones for their binding affinity to P-gp [149]. Later, they found a few 4-alkoxy chalcones as potential modulators of P-gp mediated MDR [150]. In 2008, Liu *et al.* reported several chalcones with basic functionalities to be potent inhibitors of P-gp, but these compounds showed no effect on the uptake of mitoxantrone in BCRP overexpressing MCF-7 cells [122].

Han *et al.* investigated a series of non-basic chalcones with halogenated substitutions on ring B of the chalcone. These compounds were found to be good inhibitors of BCRP, showing little or no inhibition of P-gp [151]. Also in 2009 Boumendjel *et al.* showed the ability of JAI-51 (a chalcone derivative with indole ring in place of ring B) to inhibit P-gp and BCRP [152]. Structures of lead compounds found in these studies are depicted in Figure 3.2.

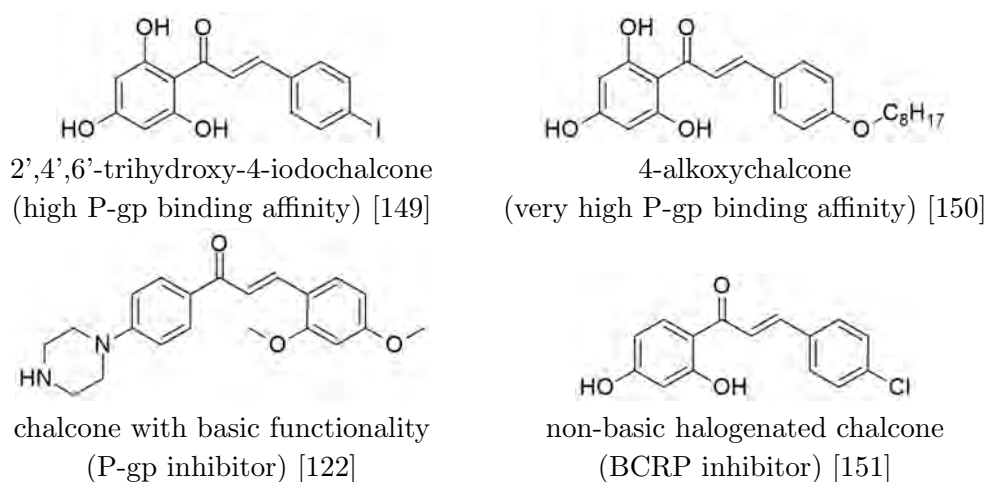


Figure 3.2: Structures of lead chalcones as P-gp and BCRP inhibitors

Despite these studies, structure-activity relationship analyses of chalcones as BCRP inhibitors are not available. In earlier works, only BCRP inhibition of compounds with halogenated ring B was studied. Therefore, it was of great interest to study various chalcone derivatives with varying substituents (especially methoxy) on both

rings A and B. Also, several benzochalcones (naphthyl ring instead of ring A) have been investigated in the current study.

3.2 Synthesis of chalcones and benzochalcones

In the current study, three different types of chalcones were synthesized, namely chalcones, 3',4'-benzochalcones and 5',6'-benzochalcones. All chalcones and benzochalcones were synthesized by Claisen-Schmidt condensation (a modified Aldol condensation reaction) with minor modifications [153, 154]. The classical method for synthesis of chalcones involves reaction of equimolar amounts of acetophenones and aldehydes at room temperature in presence of sodium hydroxide or potassium hydroxide as base catalyst. The general mechanism of the Claisen-Schmidt condensation is given in Figure 3.3. All the investigated chalcones were synthesized by the classical method, while benzochalcones were synthesized using an ultrasound bath with lithium hydroxide as catalyst instead of sodium hydroxide.

3.2.1 Synthesis of chalcones

Chalcones with varying substitutions on ring A and B of the scaffold were synthesized by the classical method for synthesis of chalcones. For the variation of ring A substituents, various multisubstituted acetophenones were used as starting material. For this purpose acetophenone, 2'-hydroxyacetophenone, 2'-4'-dihydroxyacetophenone and 3',4'-dimethoxyacetophenone were obtained from commercial sources. 2',4'-Dihydroxyacetophenone was further converted into 2'-hydroxy-4'-methoxyacetophenone (**1**) by O-methylation reaction using dimethyl sulfate and potassium carbonate (see section 7.1.2.1). 4',6'-dimethoxy-2'-hydroxyacetophenone (**2**) was synthesized by the same procedure from 2',4',6'-trihydroxyacetophenone and excess of dimethyl sulfate (see section 7.1.2.2). The 2',4'-dimethoxyacetophenone (**3**) was synthesized from 2',4'-dihydroxy acetophenone using methyl iodide as methylating agent and potassium carbonate as base (see section 7.1.2.3).

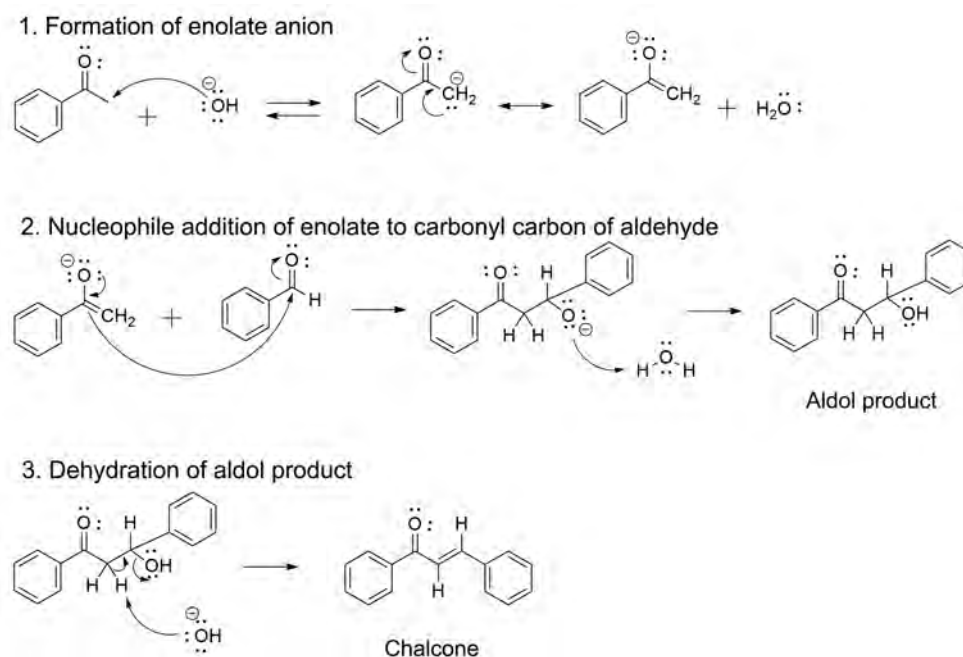
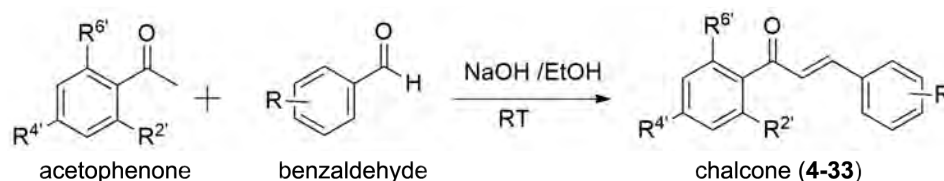


Figure 3.3: Mechanism involved in synthesis of the chalcone by Claisen-Schmidt condensation

Scheme 3.1 General reaction for synthesis of chalcones



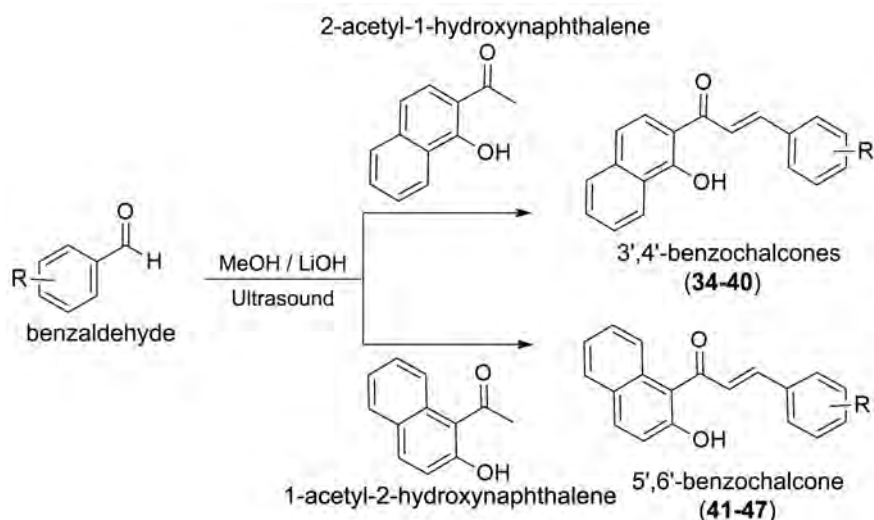
The investigated chalcones (**4-33**) were synthesized using the above mentioned acetophenones. A general procedure for the synthesis is given in section 7.1.2.4 and the general reaction is given in Algorithm 3.1. In short, the selected acetophenone and benzaldehyde were dissolved in ethanol, to the resulting solution 20 % sodium hydroxide was added drop-wise under constant stirring. After addition of sodium hydroxide, the color of the solution changed suddenly to dark yellow / dark orange. The reaction mixture was stirred for 24 to 72 hours until the reaction was complete. The reaction time for chalcones synthesized from unsubstituted acetophenone (**4**, **5**), 2',4'-dimethoxyacetophenone (**22-26**) and 3',4'-dimethoxyacetophenone (**30-33**) was shorter as compared to that for chalcones synthesized from hydroxylated acetophenones. After completion of the reaction, the reaction mixture was poured

onto crushed ice and neutralized with dilute hydrochloric acid, which resulted in precipitation of solid product.

3.2.2 Synthesis of 3',4'- and 5',6'-benzochalcones

In case of benzochalcones, the phenyl ring A of the chalcone scaffold was replaced by a naphthyl ring. In the current study several 3',4'-benzochalcones and 5',6'-benzochalcones were synthesized. During the synthesis of benzochalcones it was observed that, when the reaction was carried out using the classical method (NaOH as base and at RT) the reaction was almost always incomplete even after 72 h of stirring. Hence the reaction was carried out using lithium hydroxide, which is a stronger base and by using ultrasound bath instead of stirring. This led to complete conversion of starting materials into product and a shorter reaction time.

Scheme 3.2 General reaction involved in synthesis of benzochalcones



A general procedure for the synthesis of benzochalcones is given in section 7.1.2.5 and a scheme of the general reaction is depicted in Algorithm 3.2. In short, 2-acetyl-1-hydroxynaphthalene (for synthesis of 3',4'-benzochalcones, **34-40**) or 1-acetyl-2-hydroxynaphthalene (for synthesis of 5',6'-benzochalcones, **41-47**) were dissolved in methanol, lithium hydroxide was added to the solution and the reaction flask was kept in an ultrasound bath for 1-5 hours until completion. Reaction under ultrasound condition reduced the reaction time and also gave almost always pure products. After

completion of the reaction, the reaction mixture was poured onto crushed ice and neutralized using dilute hydrochloric acid, which resulted in formation of a lot of precipitate. The precipitate was filtered and washed with plenty of water to yield the required benzochalcone.

3.3 Biological investigation of chalcones and benzochalcones

In the current study a total of 30 chalcones and 14 benzochalcones bearing varying substituents were synthesized to evaluate their BCRP inhibition potential. For this purpose the Hoechst 33342 accumulation assay, which is a functional assay was applied. In this assay the ability of the synthesized compounds to inhibit the substrate extrusion by BCRP was measured. These compounds were further investigated for their P-gp and MRP1 inhibition in the calcein AM assay. The results obtained from these assays allowed to test the selectivity of the compounds towards BCRP inhibition. A few compounds were found to be potent inhibitors of BCRP, which were further investigated for their ability to reverse resistance to cytotoxic compounds in the MTT assay. These compounds were also tested for their intrinsic cytotoxicity.

3.3.1 Investigation of BCRP inhibition in the Hoechst 33342 accumulation assay

Hoechst 33342 is a benzimidazole derivative and a substrate of BCRP (Figure 3.4). It shows fluorescence when bound to DNA in the cells, especially adenine and thymine rich sequences and also when bound to the cell membrane. It shows very low fluorescence in aqueous solutions in the absence of cells. Hence, the intracellular concentration of Hoechst 3342 can be determined by measuring its fluorescence. Being a substrate of BCRP it is transported outside the cells overexpressing BCRP, leading to decreased fluorescence. Inhibition of the BCRP leads to decreased extrusion of Hoechst 33342 and increased fluorescence. A detailed procedure of the assay is given in section 7.2.3.1.

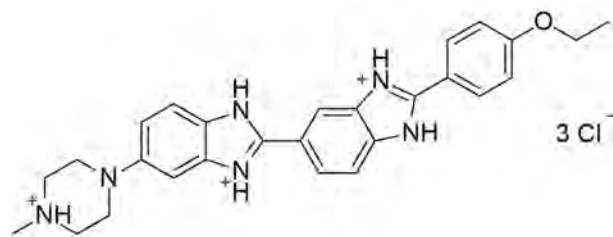


Figure 3.4: Structural formula of Hoechst 33342 (hydrochloride salt)

In general, Hoechst 33342 (final concentration $1 \mu\text{M}$) was added to the cell suspension with or without inhibitor. Fluorescence in KHB in the absence of cells was used for background correction. The fluorescence of Hoechst 33342 was then measured using microplate reader for 120 minutes at a constant interval of 60 seconds. The intracellular concentration of Hoechst 33342 slowly increases and reaches a maximum plateau after certain time. In case of BCRP overexpressing cells without inhibitor, no increase in fluorescence is seen, while in presence of the inhibitor a gradual increase in fluorescence (dependent on the amount of BCRP inhibition) is seen. A representative kinetic diagram for Hoechst 33342 in presence of the standard inhibitor Ko143 in BCRP overexpressing cells is shown in Figure 3.5. Plateau fluorescence values obtained from minutes 100 to 109 were used to generate concentration-response curves with nonlinear regression using a four-parameter logistic equation.

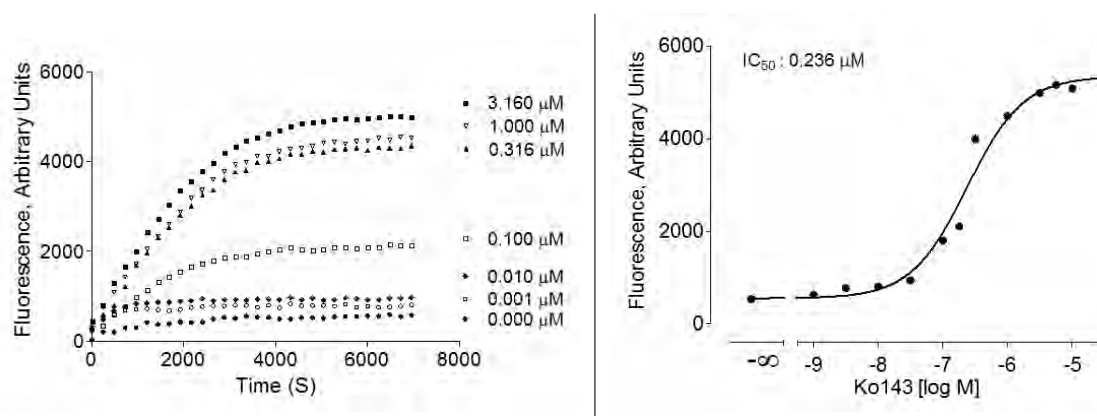


Figure 3.5: Left: Representative fluorescence–time curves of Hoechst 33342 in BCRP overexpressing cells in presence of Ko143. Only a few concentrations and time points are shown for clarity. Right: Concentration–response curve generated from plateau values of fluorescence–time curves.

In these experiments the response obtained in wild type cells not expressing BCRP

was used as control. For comparison purposes in most of the cases XR9577 (WK-X-24) (BCRP and P-gp inhibitor [155, 156]) was used as standard. XR9577 (WK-X-24) was used as a standard for day to day experiments owing to its easy availability and low cost over Ko143. The most potent BCRP inhibitor Ko143 was used as external standard for correlation with inhibitory potencies of synthesized chalcones. All the compounds were investigated for their BCRP inhibition in two different BCRP overexpressing cells viz., MCF-7 MX and MDCK BCRP cells. The activity data obtained for the chalcones and benzochalcones in the Hoechst 3342 accumulation assay is given in Table 3.1 and Table 3.2.

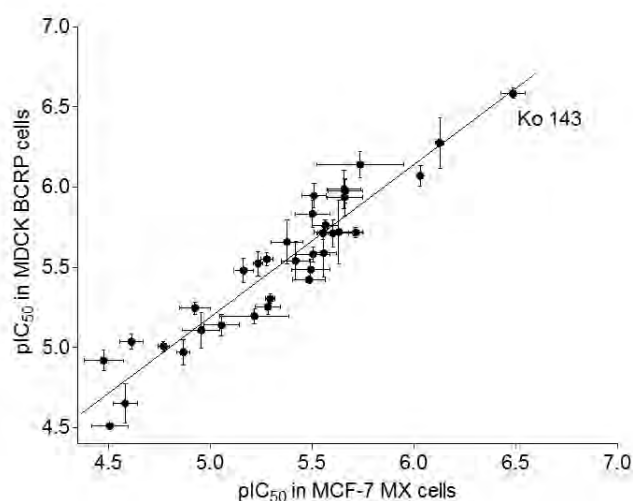
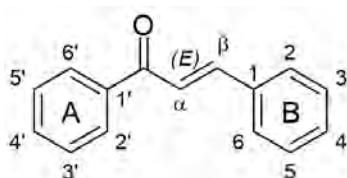


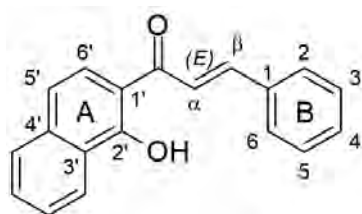
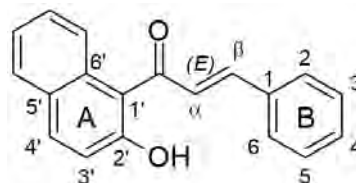
Figure 3.6: Scatterplot of the pIC_{50} values determined in the Hoechst 3342 assay using MCF-7 MX and MDCK BCRP cells. Each point is an average of at least three independent experiments. The squared correlation coefficient $r^2 = 0.89$, $n = 35$.

To determine the correlation between IC_{50} values obtained using MCF-7 MX and MDCK BCRP cells, a scatter plot (see Figure 3.6) was generated for all the investigated compounds. The scatter plot was analyzed by linear regression, which gave a good correlation factor (r^2) of 0.89, suggesting equivalent inhibitory effect in selected MCF-7 MX cells and transfected MDCK BCRP cells.

Table 3.1: Synthesized chalcones and their inhibitory potencies against MCF-7 MX and MDCK BCRP cells in the Hoechst 33342 accumulation assay**Chalcones (4-33)**

Compd	Substituents on ring A	Substituents on ring B	MCF-7 MX IC ₅₀ ± SD (μM)*	MDCK BCRP IC ₅₀ ± SD (μM)*
4	H	3,4-OCH ₃	n.a.	n.a.
5	H	2-Cl	n.a.	n.a.
6	2'-OH	H	n.a.	n.a.
7	2'-OH	4-OCH ₃	n.a.	n.a.
8	2'-OH	3,4-OCH ₃	5.07 ± 0.27	4.97 ± 0.31
9	2',4'-OH	H	n.a.	n.a.
10	2',4'-OH	4-OCH ₃	33.3 ± 7.09	12.0 ± 1.69
11	2',4'-OH	3,4-OCH ₃	0.93 ± 0.03	0.85 ± 0.13
12	2',4'-OH	3-OCH ₃	2.80 ± 0.17	1.94 ± 0.17
13	2',4'-OH	2-Cl	3.21 ± 0.69	3.28 ± 0.50
14	2',4'-OH	4-Cl	6.07 ± 2.37	6.37 ± 0.70
15	2'-OH,4'-OCH ₃	H	31.0 ± 6.39	30.9 ± 1.34
16	2'-OH,4'-OCH ₃	4-OCH ₃	4.20 ± 0.76	2.20 ± 0.75
17	2'-OH,4'-OCH ₃	3,4-OCH ₃	2.17 ± 0.41	1.06 ± 0.17
18	2'-OH,4'-OCH ₃	3-OCH ₃	3.15 ± 0.59	1.47 ± 0.31
19	2'-OH,4'-OCH ₃	2-Cl	6.85 ± 0.76	3.32 ± 0.57
20	2'-OH,4'-OCH ₃	4-Cl	13.5 ± 1.02	10.7 ± 2.82
21	2'-OH,4'-OCH ₃	3,4-Cl	n.a.	n.a.
22	2',4'-OCH ₃	4-OCH ₃	2.34 ± 0.62	1.91 ± 0.78
23	2',4'-OCH ₃	3,4-OCH ₃	2.20 ± 0.40	1.03 ± 0.29
24	2',4'-OCH ₃	2-Cl	3.13 ± 0.57	2.63 ± 0.29
25	2',4'-OCH ₃	4-Cl	3.09 ± 0.44	1.13 ± 0.21
26	2',4'-OCH ₃	3,4-Cl	n.a.	n.a.
27	2'-OH,4',6'-OCH ₃	4-OCH ₃	5.83 ± 0.32	3.00 ± 0.50
28	2'-OH,4',6'-OCH ₃	3,4-OCH ₃	0.75 ± 0.03	0.53 ± 0.22
29	2'-OH,4',6'-OCH ₃	2-Cl	5.27 ± 0.35	2.82 ± 0.26
30	3',4'-OCH ₃	4-OCH ₃	2.19 ± 0.43	1.16 ± 0.34
31	3',4'-OCH ₃	3,4-OCH ₃	3.28 ± 0.64	3.80 ± 0.13
32	3',4'-OCH ₃	2-Cl	3.04 ± 0.21	2.89 ± 0.11
33	3',4'-OCH ₃	4-Cl	2.72 ± 0.42	1.73 ± 0.13

* Data are expressed as mean ± SD (n = 3), n.a. = not active

Table 3.2: Synthesized benzochalcones and their inhibitory potencies against MCF-7 MX and MDCK BCRP cells in the Hoechst 33342 accumulation assay**3',4'-Benzochalcones (34-40)****5',6'-Benzochalcones (41-47)**

Compd	Substituents on the ring B	MCF-7 MX IC ₅₀ ± SD (μ M)*	MDCK BCRP IC ₅₀ ± SD (μ M)*
34	H	24.3 ± 3.11	9.23 ± 1.00
35	4-OCH ₃	16.9 ± 1.02	9.83 ± 0.72
36	3,4-OCH ₃	2.50 ± 0.45	1.95 ± 0.39
37	3-OCH ₃	11.8 ± 1.97	5.68 ± 0.50
38	2-Cl	n.a.	n.a.
39	4-Cl	n.a.	n.a.
40	3,4-Cl	26.1 ± 3.77	22.4 ± 6.88
41	H	2.77 ± 0.41	2.58 ± 0.94
42	4-OCH ₃	3.81 ± 0.62	2.89 ± 0.73
43	3,4-OCH ₃	1.84 ± 0.87	0.72 ± 0.14
44	3-OCH ₃	1.93 ± 0.15	1.93 ± 0.15
45	2-Cl	5.21 ± 0.75	5.58 ± 0.60
46	4-Cl	n.a.	n.a.
47	3,4-Cl	8.78 ± 1.66	7.26 ± 1.10
XR9577	-	0.99 ± 0.15	0.82 ± 0.18
Ko143	-	0.33 ± 0.05	0.25 ± 0.04

* Data are expressed as mean ± SD (n = 3), n.a. = not active

3.3.1.1 Structure-activity relationship

Several substituent requirements on the chalcone scaffold for BCRP inhibition could be suggested.

a) Effect of substituents present on ring A of chalcones:

It was observed that compounds with no substituents on ring A of the chalcone (**4**, **5**) showed no BCRP inhibition. Also presence of a single substituent (hydroxy) at position 2' of the chalcone scaffold (**6-8**) did not improve the inhibition ability of these compounds. Although, compounds bearing multiple substituents at positions 2', 3', 4' and 6' of the ring A showed substantial BCRP inhibition. In case of chalcones with 3,4-dimethoxy substituents on ring B (**11**, **17**, **23**, **28**), it was observed that compounds with hydroxyl group at position 2' (ring A) have slightly increased activity as compared to compounds bearing methoxy substituents. However, no substantial difference was noted for substitution at position 4' of the ring A. Presence of a methoxy group at position 6' had only a very slight effect on the activity. Compounds bearing 3',4'-dimethoxy substituent (**30-33**) showed comparable activity to those having 2',4'-dimethoxy substituents (**22-26**).

b) Effect of substituents present on ring B of chalcones:

In the study by Han *et al.*, effects of chloro substituents present at different positions of ring B of the chalcone scaffold were investigated [123]. It was observed that presence of 2-chloro and 4-chloro substituents led to increased BCRP inhibition. In the current study several compounds with methoxy and chloro substituents on ring B were compared for their BCRP inhibition. It was clearly observed that substitution was needed on ring B of the chalcone, as unsubstituted chalcones (**6**, **9**, **15**) were found to be inactive. Chalcones with 3,4-dimethoxy substitution on ring B showed maximum efficacy of BCRP inhibition, with the chalcones **11**, **17**, **23**, **28** being most potent. A 3-methoxy substituent in case of compounds (**12**, **18**) showed better potencies compared to a 4-methoxy substituent on ring B (**10**, **16**), both having the same substituents at ring A. Chalcones with 2-chloro and 4-chloro substituents were found to be active, while presence of a 3,4-dichloro substituent (**21**, **26**) led to inactivity.

The effect of different substituents on BCRP inhibitory potency of chalcones is summarized in Figure 3.7.

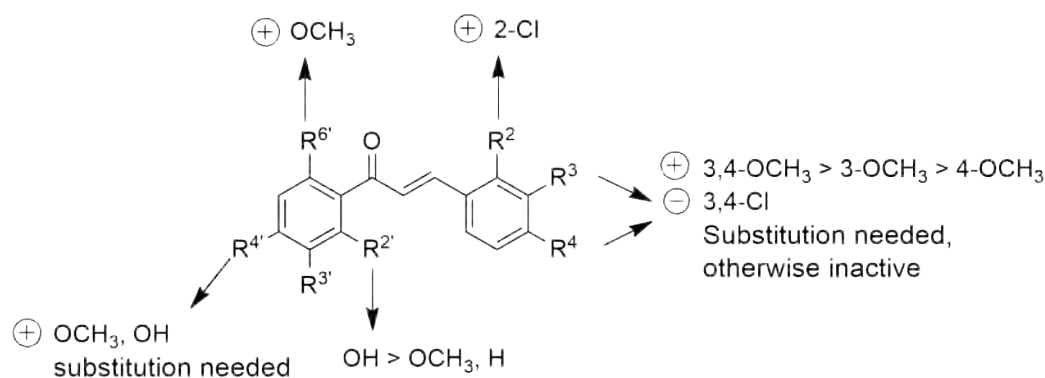


Figure 3.7: Effect of different substituents on the BCRP inhibition by chalcones (**4-33**). \oplus : leads to increase in BCRP inhibition, \ominus : leads to decrease in BCRP inhibition.

c) Effect of substituting ring A with a naphthyl ring:

Several benzochalcones bearing a naphthyl ring instead of ring A of the chalcone scaffold were investigated. For this purpose 3',4'-benzochalcones and 5',6'-benzochalcones were synthesized and tested in the Hoechst 33342 assay for their BCRP inhibition. It was observed that 5',6'-benzochalcones (**41-47**) were more potent as compared to 3',4'-benzochalcones (**34-40**). The effect of variations in substituents on ring B in benzoflavones was similar to the case of chalcones. The 3,4-dimethoxy substituted benzoflavones (**36**, **43**) were more potent compared to those bearing other substituents. Compounds bearing 3,4-dichloro substituents (**40**, **47**) were the least active ones.

When activities of all three types of investigated chalcones are compared, 3',4'-benzochalcones were found to be the least active followed by 5',6'-benzochalcones, while chalcones with retained phenyl ring A structure were the most active. A schematic comparison of activity of chalcones with benzochalcones is depicted in Figure 3.8.



Figure 3.8: Comparison of activities of chalcones and benzochalcones

3.3.2 Screening of chalcones and benzochalcones for P-gp and MRP1 inhibition in the calcein AM accumulation assay

To test the selectivity of the chalcones towards BCRP inhibition, their effect on the other major ABC transporters P-gp and MRP1 was investigated. Calcein acetoxymethyl ester (calcein AM) is a non-fluorescent hydrophobic compound which on hydrolysis by intracellular unspecific esterases converts into fluorescent calcein. Calcein shows fluorescence with an excitation maximum of 496 nm and an emission maximum of 520 nm. Calcein AM has been shown to be a substrate for both P-gp and MRP1, but it is not transported by BCRP [157, 158]. Owing to its high lipid solubility, it can rapidly penetrate the plasma membrane of cells, while calcein being hydrophilic and negatively charged can leave the cells only by active transport. When P-gp or MRP1 is inhibited, this leads to an increase in calcein accumulation, resulting in increased fluorescence. This increase in fluorescence can be used as a parameter of P-gp or MRP1 inhibition. A detailed procedure for the calcein AM accumulation assay is given in section 7.2.3.3.

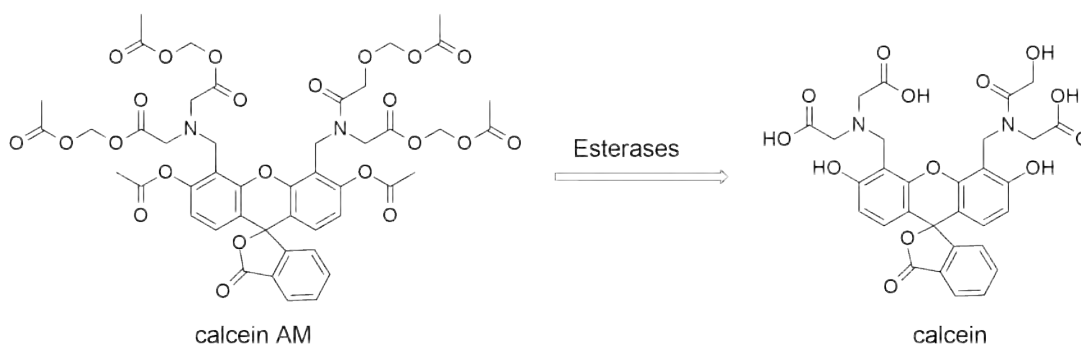
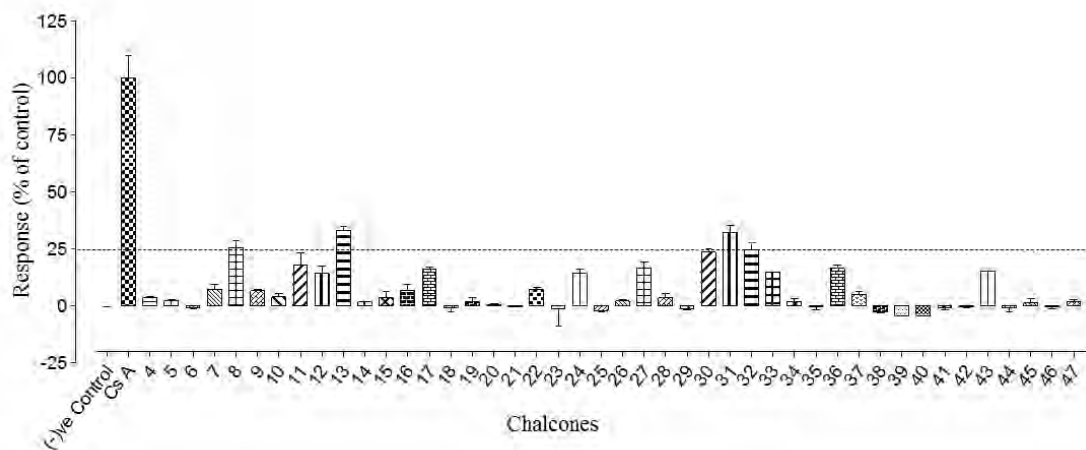


Figure 3.9: Conversion of non-fluorescent calcein AM to fluorescent calcein by intracellular esterases

For the purpose of screening all chalcones were investigated at 10 μM final concentration using calcein AM accumulation assay. For checking P-gp inhibition, P-gp overexpressing A2780 cells were used, while for MRP1 inhibition 2008 MRP1 cells were used. Cyclosporine A, which is a well known inhibitor of both P-gp and MRP1 was used as a standard at 10 μM concentration [159]. For comparing the inhibitory activity of tested compounds, percentage response was calculated considering standard (cyclosporine A) response as 100 %. Response obtained from the cells without any inhibitor was used as a negative control. From the Figure 3.10,

it can be seen that all chalcones showed only very weak inhibitory effect on P-gp, while none of them showed substantial inhibition of MRP1. Only compounds **13** and **31** gave P-gp inhibition response greater than 25 % when compared to cyclosporine A. This indicates that the investigated chalcones are selective BCRP inhibitors.

A) P-gp Inhibition



B) MRP1 inhibition

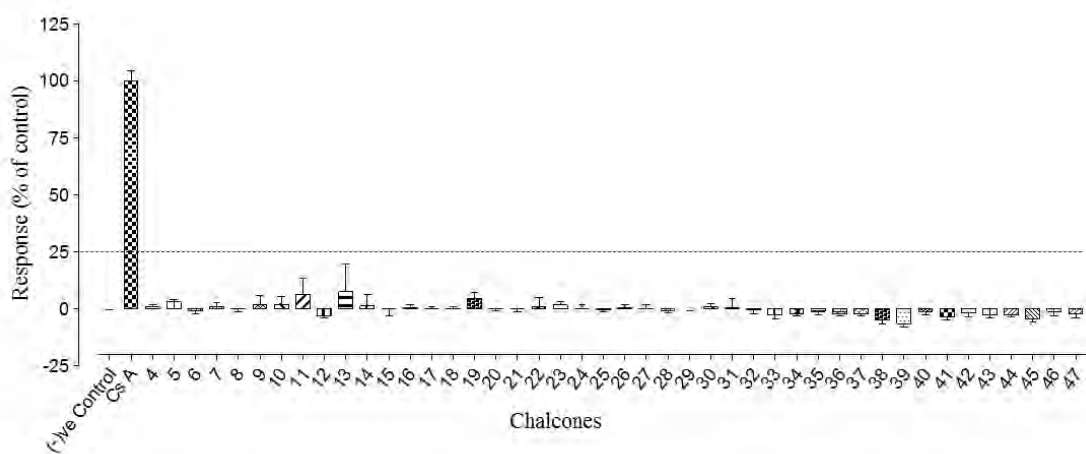


Figure 3.10: Effect of chalcones and benzochalcones (**4-47**) on the accumulation of calcein AM in P-gp (**A**) and MRP1 (**B**) overexpressing cells. All chalcones were investigated at 10 μM concentration (n=3). Cyclosporine A (Cs A), 10 μM , was used as a positive control leading to total inhibition. Data is expressed as response in percentage of standard Cs A, vehicle (KHB) was used as negative control.

3.3.3 MTT cytotoxicity assay

One of the methods to determine the cell viability is a MTT cytotoxicity assay. MTT (Methylthiazolyldiphenyl-tetrazolium bromide or 3-(4,5-dimethylthiazol-2-yl)-2,5-diphenyl tetrazolium bromide) a yellow tetrazole is reduced by mitochondrial succinate dehydrogenase to formazan. Formazan is an insoluble, dark purple colored compound which forms crystals due to its insolubility. The formazan crystals can be dissolved in DMSO and then measured colorometrically. The reduction of MTT is possible only in metabolically active (living) cells and hence only these produce dark purple colored formazan crystals. The reaction involved in the process is shown in Figure 7.7.

The procedure for performing the MTT assay is described in detail in section 7.2.3.4. In short, cells were seeded into 96 well plate and incubated for 6 hours at 5 % CO₂ and 37 °C. Test compound dilutions prepared in PBS were added to cells and incubated again for 72 hours. Then MTT solution was added and plates were further incubated for 1 hour. The formation of formazan crystals was confirmed under microscope. The supernatant was removed and DMSO was added to dissolve the formazan crystals. The color intensity was measured using a microplate reader at 544 nm with background correction at 710 nm.

3.3.3.1 Investigation of selected chalcones to reverse MDR by MTT assay

To investigate the influence of chalcones on the antiproliferative effect of cytotoxic agents in presence of the BCRP transporter, cytotoxicity of mitoxantrone and SN-38 was evaluated in both MDCK BCRP and MCF-7 MX cells. For this purpose, cell viability was determined using MTT assay for the most potent chalcone (**28**) and benzochalcone (**43**). GI₅₀ values of the two anticancer agents were determined in the absence and presence of selected compounds at three different concentrations. Both compounds were able to reverse the resistance of the BCRP expressing cell lines, proving their functional efficacy.

The effect of chalcone **28** on the GI₅₀ of mitoxantrone in MCF-7 / MX cells is shown in Figure 3.11. The compound was investigated at concentrations of 1 μ M, 3 μ M and 5 μ M. It can be clearly seen that, even the lowest concentration of compound

28 ($1\mu M$) was able to reverse the resistance and the higher concentrations led to complete reversal of the resistance.

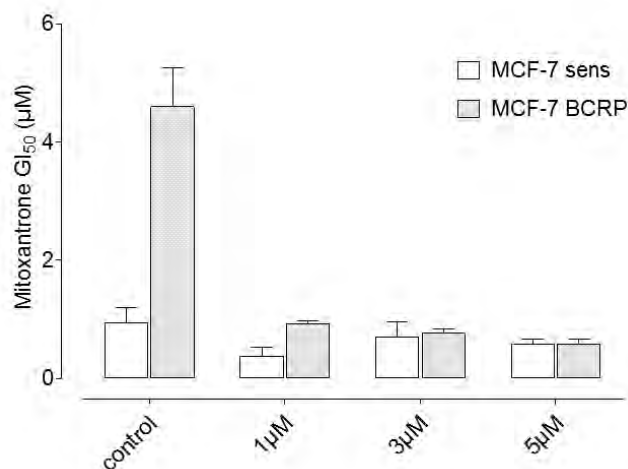


Figure 3.11: Effect of chalcone **28** on the GI₅₀ of mitoxantrone in MCF-7 MX cells. The compound was investigated at 1, 3, and 5 μM concentrations. Untreated cells were used as control. The figure shows average and standard deviation obtained from three independent experiments, $n = 3$.

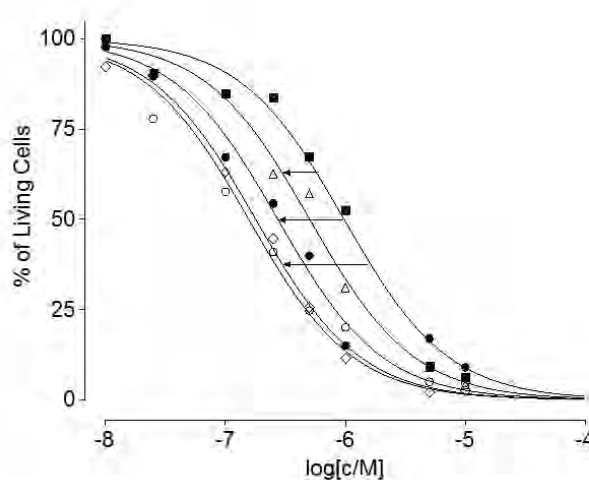


Figure 3.12: Representative dose-response curve of SN-38 in presence of compound **43**. Arrows indicate dose dependent effect of the benzochalcone on sensitisation of MDCK BCRP cells towards SN-38. Open circle: MDCK sensitive cells, closed square: MDCK BCRP cells, triangle: MDCK BCRP cells + 1 μM **43**, closed circle: MDCK BCRP cells + 3 μM **43**, diamond: MDCK BCRP cells + 5 μM **43**.

Compound **43** was investigated for its ability to reverse the SN-38 resistance in

MDCK BCRP cells. For this purpose, three different concentrations ($1\ \mu\text{M}$, $3\ \mu\text{M}$ and $5\ \mu\text{M}$) of benzochalcone **43** were selected. Representative dose–response curves of SN-38 in presence of benzochalcone **43** are shown in Figure 3.12. From the shift in the dose-response curve of MDCK BCRP cells towards lower concentrations, it can be clearly seen that compound **43** was able to sensitize BCRP overexpressing cells towards SN-38 toxicity.

3.3.3.2 Cytotoxicity of selected chalcones and benzochalcones

In the current study several potent and selective inhibitors of BCRP were found, but, to make them potential candidates for future *in vivo* studies it was important that the compounds possessed no or very low intrinsic cytotoxicity. To determine the cytotoxicity of selected potent chalcones and benzochalcone, MTT cytotoxicity assay was applied using MDCK BCRP and MDCK sensitive cells. The concentration-response curves obtained for compounds **11**, **28** and **43** are shown in Figure 3.13. Because of the limited solubility of these compounds in PBS, the highest concentration was prepared by using a methanol in an amount that the final concentration of methanol was not more than 2 %. Blank dilutions containing the same amount of methanol were used to confirm that any cytotoxicity shown at the highest concentration was not due the compound.

Chalcone **11** and benzochalcone **43** showed no cytotoxicity even at a concentration of $100\ \mu\text{M}$. From Figure 3.13 it can be seen that a slight reduction in cell viability at the highest concentrations of these compounds was due to the presence of the small amount of methanol. However, chalcone **28** bearing multiple methoxy groups on both rings of the chalcone moiety, showed cytotoxicity with estimated GI_{50} values of $20.8\ \mu\text{M}$ in MDCK BCRP cells and $23.8\ \mu\text{M}$ in MDCK sensitive cells. Chalcones **11** and **28** differ in structure only at ring A, where the additional methoxy groups on ring A of compound **28** could be responsible for the observed cytotoxicity. Though the GI_{50} value for this compound is approximately 40 times higher than the IC_{50} values for BCRP inhibition, it could limit its usability in *in vivo* studies. Since, compounds **11** and **43** showed no cytotoxicity along with high BCRP inhibitory ability, these compounds are promising for future preclinical studies.

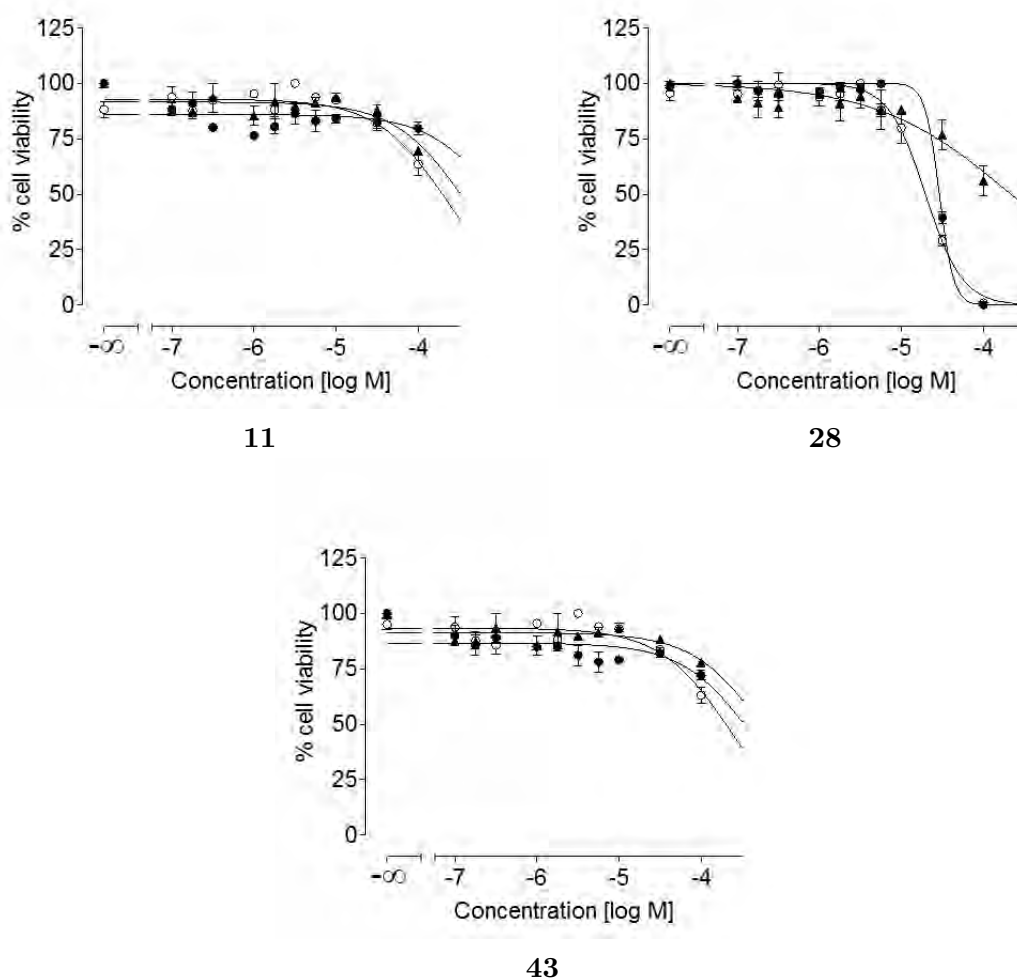


Figure 3.13: Cytotoxicity of chalcones **11**, **28** and benzochalcone **43** in MDCK BCRP and sensitive cells. Open circle: MDCK BCRP cells, closed circle: MDCK sensitive cells and closed triangle: dilution solvent (PBS) containing 2 % methanol at the highest concentration.

In summary, several chalcones, 3',4'-benzochalcones and 5',6'-benzochalcones were investigated for their inhibitory effects and selectivity towards BCRP. In the current work the effect of different substituents on both A and B rings of the chalcone scaffold was investigated. It was clearly observed that among all chalcones, compounds with 3,4-dimethoxy substituents at ring B were most active. The inhibitory effect of the most active compounds was confirmed by MTT cytotoxicity assay. Compounds **11** and **28** were found to be the most potent and selective BCRP inhibitors, being only little less active as compared to the most active BCRP inhibitor Ko143.

4 Project 2: Investigation of flavones and benzoflavones as BCRP inhibitors

Flavonoids are a group of naturally occurring low molecular weight polyphenolic compounds. Flavonoids are found in a wide variety of plants and are present in fruits, roots, stems and flowers. Flavonoids are well known for their beneficial effects on health and are consumed in daily diets in form of tea and wine [160–167]. Different flavonoids have been found to be useful as anti-inflammatory [168], anticancer [169], antidepressant [170, 171], antiallergic [168, 172] and hepatoprotective [173, 174], etc.

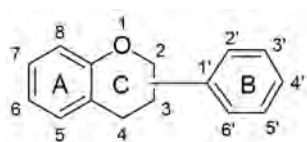


Figure 4.1: Basic structure of flavonoids (benzo[α]pyrane with a phenyl ring at position 2 or 3)

Flavonoids are structurally related compounds with a chromane type of skeleton bearing a phenyl ring at position 2 or 3 of benzo[α]pyrane (see Figure 4.1). These compounds are sub-classified into flavones, isoflavones, flavanones, flavanols, flavonols and anthocyanins depending on the variation in the benzo[α]pyrane structure (see Figure 4.2).

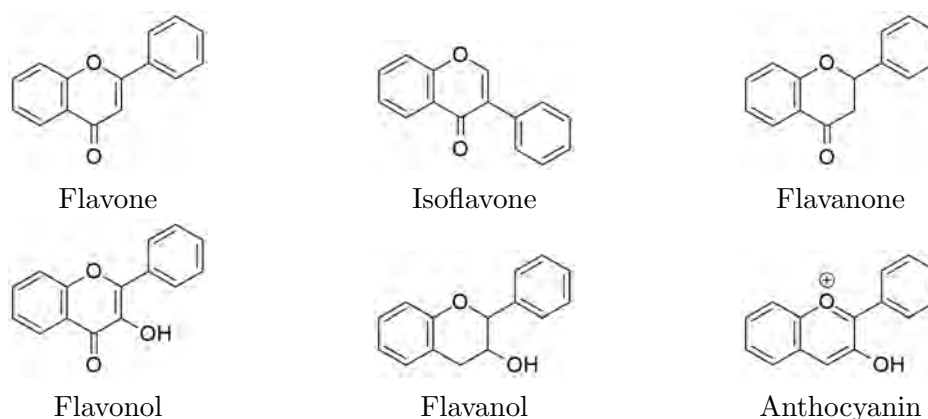


Figure 4.2: Subclasses of flavonoids

4.1 Overview of flavonoids as ABC transporter modulators

In the last decades a variety of flavonoids have been investigated for their modulation of major ABC transporters like P-gp, MRP and BCRP. In 1994 Scambia *et al.* showed the inhibitory effect of the polyhydroxy flavonoid quercetin on the efflux of rhodamine 123 in doxorubicin resistant cells and proposed P-gp as possible target [175]. Subsequently in 1997, Shapiro *et al.* reported a similar inhibitory effect of quercetin on P-gp mediated transport of Hoechst 33342 [176]. Later Ferte *et al.* studied several synthetic flavones and flavanones containing a *N*-benzylpiperazine side chain and found that these compounds were able to modulate the P-gp mediated MDR [177]. Several other groups have reported inhibitory effects of naturally occurring flavonoids like sinensetin, kaempferol, biochanin A, myricetin, morin, baicalein and fisetin among others, on the substrate transport by P-gp [178–180]. Chan *et al.* have reported synthetic apigenin homodimers linked with defined-length poly(ethylene glycol) spacers to be inhibitors of P-gp [181]. Also Wong *et al.* showed MRP1 inhibition by several bivalent apigenin homodimers [182].

Flavonoids as BCRP inhibitors: Flavonoids (especially naturally occurring) have been studied for their BCRP inhibition by several working groups. Imai *et al.* investigated several flavones, isoflavones, flavanones, flavanols and flavonols for their ability to reverse the resistance in BCRP overexpressing K562 (human leukemic) cells. It was shown that all flavones such as acaetin, apigenin, chrysin, etc. were able

to reverse the BCRP mediated resistance, while flavanols and isoflavones were the least active classes [183]. Zhang *et al.* and Ahmed-Belkacem *et al.* have extensively studied several flavonoids and reported SAR (structure-activity relationship) for BCRP inhibition [119, 128]. The latter have also reported 6-prenylchrysin and techtochrysin to be potent inhibitors of BCRP. Recently in our group Anne Pick performed QSAR (quantitative structure-activity relationship) studies on flavonoids extracted from several plant sources [125]. A summary of the results obtained in all three SAR studies performed is depicted in Figure 4.3. In 2005, Zhang *et al.* also reported 7,8-benzoflavone (see Figure 4.3) to be a potent inhibitor of BCRP [128, 129].

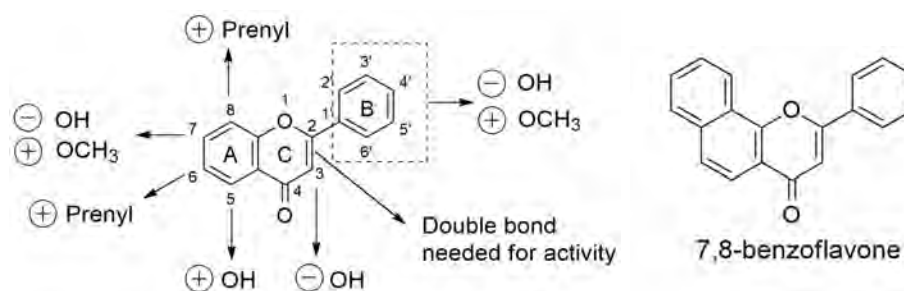


Figure 4.3: Left: Structure-activity relationship of flavonoids for BCRP inhibition based on studies by Zhang *et al.*, Ahmed-Belkacem *et al.* and Pick *et al.* \oplus : leads to increase in BCRP inhibition, \ominus : leads to decrease in BCRP inhibition. Right: Structure of a reported potent BCRP inhibitor 7,8-benzoflavone.

Based on all these studied synthesis of new flavones and benzoflavones was planned with the aim of finding more potent and selective BCRP inhibitors. As only the unsubstituted 7,8-benzoflavone has been reported till now, it was interesting to investigate the effect of substitution on phenyl ring at position 2 of the flavone scaffold. Also several substituted 5,6-benzoflavones were synthesized to check the effect of variation in the position of benzo- substituent in the ring A of the flavone scaffold. Synthesis and biological investigation of these compounds are discussed below.

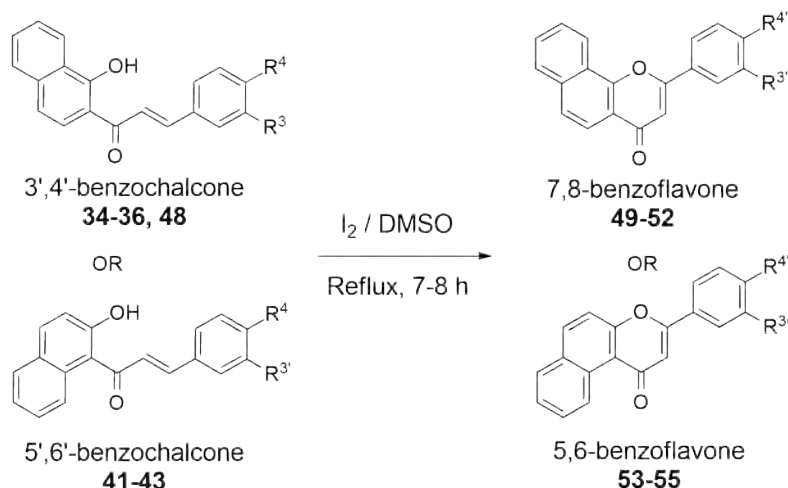
4.2 Synthesis of benzoflavones

In this work, different substituted 7,8-benzoflavones and 5,6-benzoflavones were synthesized to study their ability to inhibit BCRP. The 7,8-benzoflavones were

synthesized from 3',4'-benzochalcones while 5',6'-benzochalcones were used for the synthesis of 5,6-benzoflavones.

Benzochalcones were converted to benzoflavones by cyclisation using iodine as catalyst. The detailed procedure for the synthesis of these compounds is given in section 7.1.2.6. In short, the corresponding 3',4'-benzochalcone or 5',6'-benzochalcone was dissolved in dimethyl sulfoxide (DMSO) and catalytic amount of iodine granules was added. The reaction mixture was refluxed for 7-8 hours until the reaction was complete. Afterwards, the reaction mixture was poured onto crushed ice and extracted with ethyl acetate. The organic phase was evaporated yielding a dark brown solid. The impure benzoflavone was then purified by column chromatography using dichloromethane : methanol (9.5 : 0.5) as eluent. The general reaction involved in the synthesis of benzoflavones is given in Algorithm 4.1.

Scheme 4.1 Synthesis of benzoflavones



4.3 Synthesis of 3-hydroxyflavones and 3-hydroxybenzoflavones

To confirm the negative effect of the presence of a hydroxy substituent at position 3 of the flavone scaffold, several 3-hydroxy flavones and benzoflavones were synthesized. These compounds were further converted to 3-methoxy flavones and benzoflavones (see section 4.4) to compare their activities. The 3-hydroxylated compounds were

synthesized by cyclization of the corresponding chalcones or benzochalcones via Algar-Flynn-Oyamada (AFO) reaction [184]. This reaction involves oxidation of 2'-hydroxy chalcones to 2-aryl-3-hydroxy-4*H*-1-benzopyran-4-ones (flavone-3-ols) in presence of alkaline hydrogen peroxide. Along with formation of 3-hydroxy flavones there is the possibility of formation of aurones as side products. This is dependent on the type of attack by the phenolate on the carbons bearing the oxirane oxygen (see Figure 4.4). It was suggested by Cummins *et al.* that when the reaction was carried out using 6'-methoxychalcones it led to formation of aurones as major products [185]. This was a major obstacle in the synthesis of 3-hydroxy derivatives of flavones and hence only certain chalcones were successfully converted to 3-hydroxy flavones or benzoflavones.

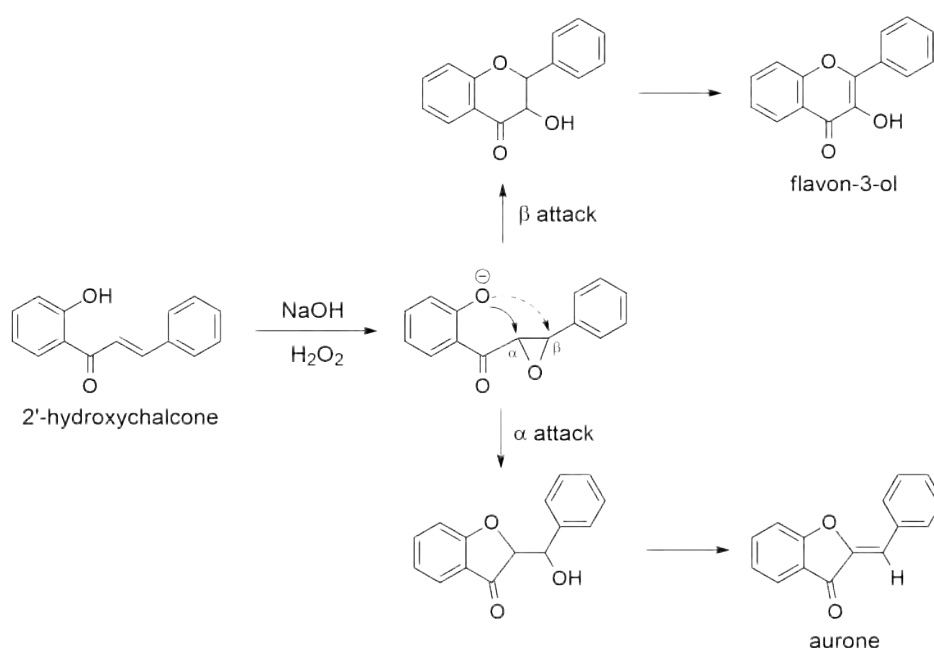
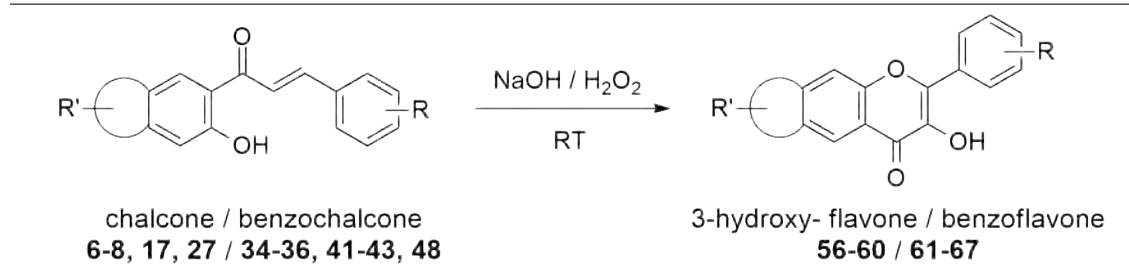


Figure 4.4: Mechanism involved in the synthesis of 3-hydroxyflavones and possible formation of aurones as side products. The mechanism depicted here is adapted from the work of Gormley *et al.* [186] and Cummins *et al.* [185].

A general procedure for the synthesis of 3-hydroxy flavones and benzoflavones is given in section 7.1.2.7. In short, the selected chalcone or benzochalcone was dissolved in ethanol. To the solution, 25 % sodium hydroxide solution was added in small portions, followed by drop wise addition of 25 % hydrogen peroxide. The reaction mixture was stirred at room temperature overnight. After completion of the reaction, the resulting reaction mixture was poured onto crushed ice and neutralized by addition of dilute hydrochloric acid with constant stirring yielding a yellow colored precipitate. All

compounds were recrystallized from ethanol. The general reaction scheme involved in the synthesis of 3-hydroxy flavones and benzoflavones is given in Algorithm 4.2.

Scheme 4.2 Synthesis of 3-hydroxy flavones or benzoflavones from corresponding chalcones or benzochalcones



4.4 Synthesis of 3-methoxy-flavones and 3-methoxybenzoflavones

The work done in our group by Anne Pick suggested that, presence of a 3-methoxy substituent in the flavone scaffold leads to increased BCRP inhibition. Hence, 3-hydroxyflavones and benzoflavones were further converted into 3-methoxy flavones and benzoflavones. Two goals were achieved through these compounds, first to confirm the positive effect of a 3-methoxy substituent seen in naturally occurring flavonoids and second to check the similar effect in benzoflavones.

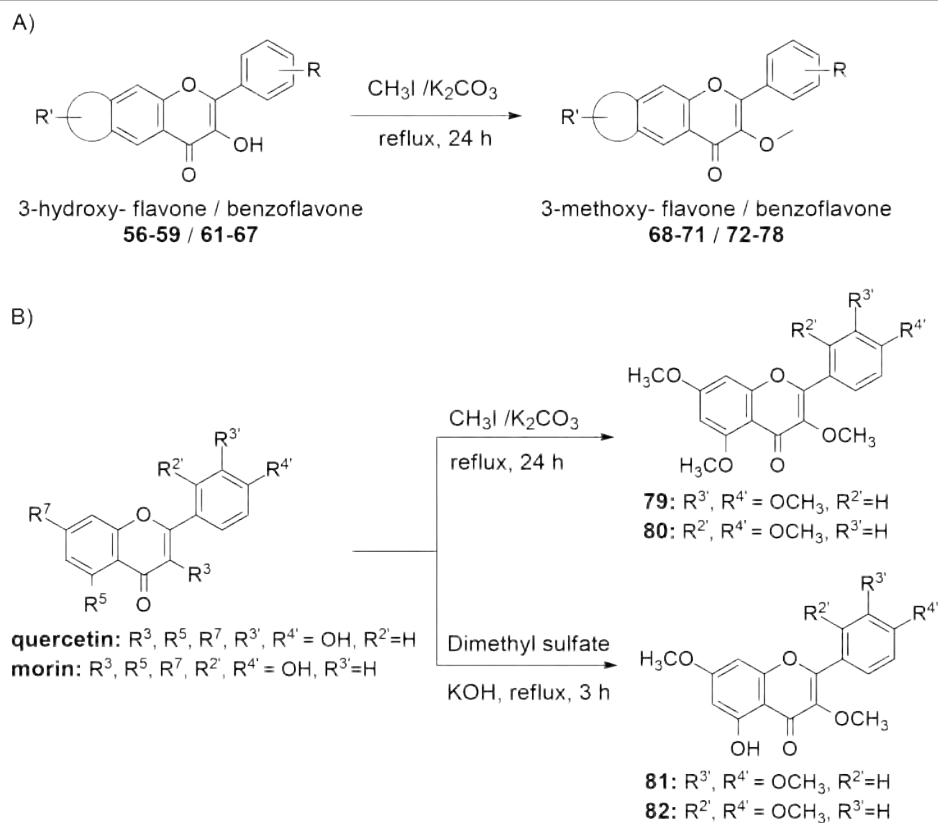
Most of the 3-methoxy compounds were synthesized by O-methylation using methyl iodide, from the corresponding 3-hydroxy flavones (see section 4.3). The naturally occurring pentahydroxy flavonoids quercetin and morin were converted into pentamethyl analogs using methyl iodide while, for tetramethyl analogs dimethyl sulfate was used. The reactions involved in the synthesis of these compounds are given in Algorithm 4.3.

The synthesis procedure for 3-methoxy flavones and benzoflavones is given in section 7.1.2.8. In short, the selected 3-hydroxyflavone or 3-hydroxybenzoflavone was dissolved in acetone and potassium carbonate was added. To the reaction mixture methyl iodide was added drop wise in excess quantity and the mixture was refluxed for 24 h. After completion of the reaction acetone and unreacted methyl iodide was removed under reduced pressure. To the residue, water was added and the

4.4 Synthesis of 3-methoxy-flavones and 3-methoxybenzoflavones

precipitated product was filtered and washed with plenty of water to remove traces of potassium carbonate. The product was recrystallized from ethanol.

Scheme 4.3 Synthesis of 3-methoxy flavones and benzoflavones (**A**). Synthesis of pentamethyl and tetramethyl derivatives of quercetin and morin (**B**).



For synthesis of pentamethylquercetin (3,3',4',5,7-pentamethoxy flavone) or pentamethylmorin (2',3,4',5,7-pentamethoxy flavone) from quercetin (3,3',4',5,7-pentahydroxy flavone) or morin (2',3,4',5,7-pentahydroxy flavone), a similar approach like the above described was used. Here, the amount of methyl iodide was 5 fold excess to that of starting material to assure that all hydroxy groups are methylated.

Initially, a similar approach was also used for the synthesis of tetramethylquercetin (5-hydroxy-3,3',4',7-tetramethoxy flavone) and tetramethylmorine (5-hydroxy-2',3,4',7-tetramethoxy flavone). However, it always resulted in complete methylation of the starting compounds even after controlling the quantity of methyl iodide used. Hence the reaction conditions were modified, where a mixture of acetone / water (2:1) was used as solvent. Dimethyl sulfate was used as methylating agent and potassium

hydroxide was used as base. Small portions of dimethyl sulfate and potassium hydroxide were added to the refluxing reaction mixture in intervals of 10-20 minutes. After completion of the reaction, it was found that a small amount of pentamethyl product was formed along with the desired tetramethyl product. The resulted crude product was eluted on silica (40-63 μm) using hexan:ethylacetate (1:3) as mobile phase to get the pure tetramethyl compounds.

4.5 Biological evaluation of flavones and benzoflavones

The synthesized compounds were investigated for their BCRP inhibition ability by measuring accumulation of Hoechst 33342 and pheophorbide A in MDCK BCRP cells. All compounds were additionally tested for their P-gp and MRP1 inhibition in the calcein AM assay. Cytotoxicity of the representative most active compounds was assessed by MTT-cytotoxicity assay. Also, MDR reversal effectiveness of the most potent compounds was confirmed by checking the chemosensitisation in BCRP overexpressing cells. The assays performed and results obtained are described below.

4.5.1 Investigation of BCRP inhibition

For the estimation of BCRP inhibition of the synthesized flavones and benzoflavones Hoechst 33342 and pheophorbide A assays were utilized. The use of two different substrates for determining the BCRP inhibition allows to check for substrate specificity of the inhibitor. For performing these experiments the more stable MDCK BCRP cells were selected over MC-7 MX cells. It was shown in section 3.3.1 that the results obtained with MDCK BCRP cells are comparable to those obtained using BCRP overexpressing MCF-7 MX cells. The functioning and the principle involved in the Hoechst 33342 assay are already discussed (section 3.3.1 and section 7.2.3.1). The IC_{50} values of the investigated flavones and benzoflavones obtained in the Hoechst 33343 assay using MDCK BCRP cells are given in Table 4.1 and Table 4.2.

In these studies Ko143 was used as standard. Figure 4.5 depicts representative concentration-response curves obtained in the Hoechst 33342 assay for the most active compound **74** compared to the standard Ko143.

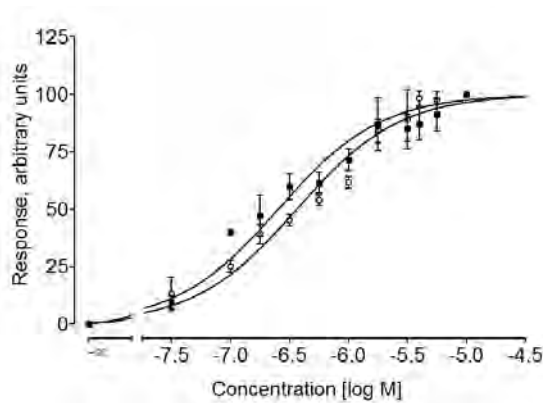


Figure 4.5: Representative concentration-response curves of compound **74** (open circles, $IC_{50} = 0.43 \pm 0.02 \mu M$) and Ko143 (closed squares, $IC_{50} = 0.25 \pm 0.04 \mu M$) obtained in the Hoechst 33342 assay (see Table 4.2). Each data point shown represents the average of 3 independent experiments and error bars indicate the standard deviation.

Pheophorbide A assay: Pheophorbide A is a porphyrine type compound and a substrate of BCRP [104]. An advantage of pheophorbide A is that, it has been shown to be transported only by BCRP and not by P-gp or MRP1 making it a specific substrate of BCRP. It shows fluorescence with excitation maximum of 395 nm and emission maximum at 670 nm. Inhibition of BCRP leads to concentration dependent increase in pheophorbide A accumulation and effectively in its fluorescence. For determination of the intracellular fluorescence of pheophorbide A, flow cytometry technique was applied. A detailed procedure for performing the assay is given in section 7.2.3.2.

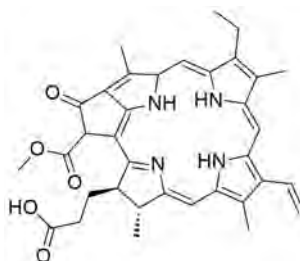


Figure 4.6: Structure of pheophorbide A

In short, different concentrations of selected compounds and cells were seeded in U-shaped microplates and incubated for 30 minutes. After this, pheophorbide A with a final concentration of $0.5 \mu M$ was added and microplates were further incubated for 120 minutes. After incubation the cells were re-suspended. The intracellular

fluorescence of pheophorbide A was measured using FACScalibur flow-cytometer in the FL3 channel.

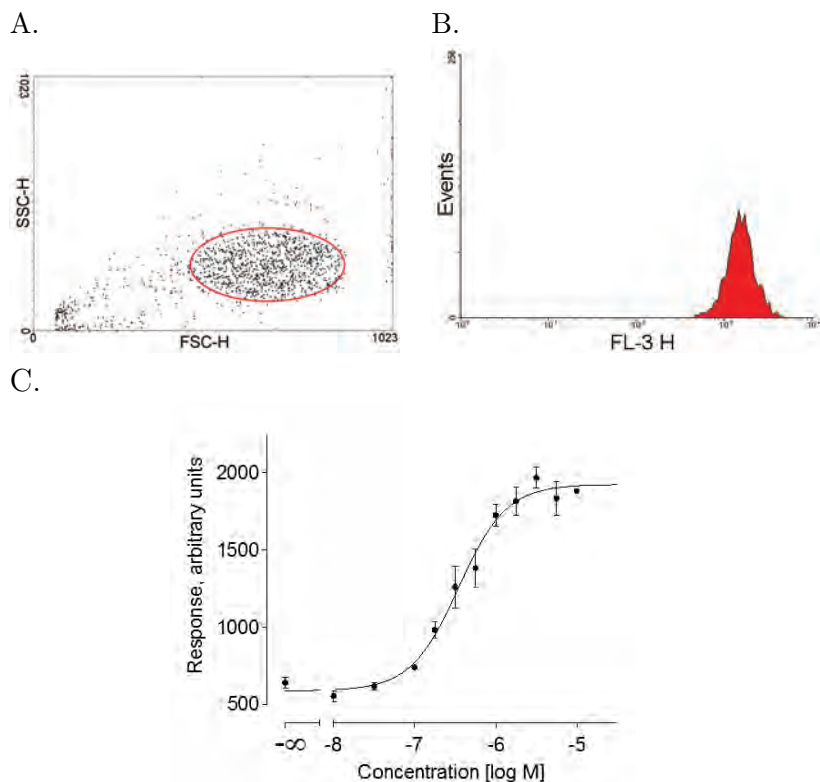
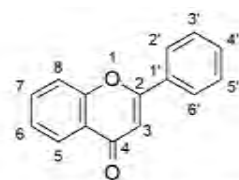


Figure 4.7: (A): A dot plot of cell population (MDCK BCRP) obtained from FSC height against SSC height, the red circle indicates gating of the healthy cell population. (B): Fluorescence intensity of pheophorbide A at FL3 after gating (in presence of 10 μM Ko143 in MDCK BCRP cells). (C): A representative concentration-response curve obtained from the fluorescence data for Ko143 using MDCK BCRP cells in the pheophorbide A assay.

The analysis of the data generated by flow cytometry was performed using BD CellQuest Pro software. A prepared analysis sheet was used, where it was possible to check the plot of FSC count against SSC count, which enables gating of the cell population from debris. Figure 4.7 shows a dot plot of cell population (FSC against SSC) and a histogram obtained by plotting fluorescence (FL-3 height) against the number of gated events. From this fluorescence data a concentration-response curve was generated with the help of a four-parameter logistic equation in GraphPad Prism software. In Figure 4.7 a concentration-response curve for Ko143 ($IC_{50} = 0.33 \mu M$) using MDCK BCRP cells is depicted.

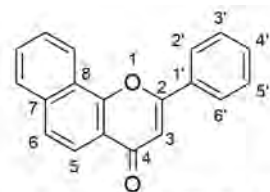
Table 4.1: Synthesized flavones and their inhibitory potencies against MDCK BCRP cells in Hoechst 33342 and pheophorbide A accumulation assays.

Flavone (56-60, 68-71, 79-82)

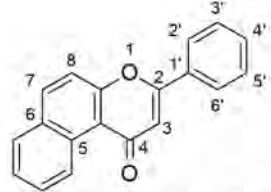
Compd	R ³	R ⁵	R ⁷	R ^{2'}	R ^{3'}	R ^{4'}	Hoechst 33342 assay	Pheophorbide A assay
							IC ₅₀ ± SD (μM)*	IC ₅₀ ± SD (μM)*
3-Hydroxyflavones								
56	OH	H	H	H	H	H	n.a.	n.a.
57	OH	H	H	H	H	OCH ₃	n.a.	n.a.
58	OH	H	H	H	OCH ₃	OCH ₃	n.a.	n.a.
59	OH	H	OCH ₃	H	OCH ₃	OCH ₃	1.01 ± 0.10	1.77 ± 0.14
60	OH	OCH ₃	OCH ₃	H	H	OCH ₃	12.4 ± 0.47	8.95 ± 0.65
3-Methoxyflavones								
68	OCH ₃	H	H	H	H	H	1.21 ± 0.12	1.28 ± 0.17
69	OCH ₃	H	H	H	H	OCH ₃	7.74 ± 0.35	6.50 ± 0.58
70	OCH ₃	H	H	H	OCH ₃	OCH ₃	1.18 ± 0.29	1.34 ± 0.19
71	OCH ₃	H	OCH ₃	H	OCH ₃	OCH ₃	1.18 ± 0.18	2.14 ± 0.31
79	OCH ₃	OCH ₃	OCH ₃	H	OCH ₃	OCH ₃	0.822 ± 0.169	1.88 ± 0.24
80	OCH ₃	OCH ₃	OCH ₃	OCH ₃	H	OCH ₃	5.98 ± 0.45	5.94 ± 0.74
81	OCH ₃	OH	OCH ₃	H	OCH ₃	OCH ₃	0.540 ± 0.079	0.570 ± 0.093
82	OCH ₃	OH	OCH ₃	OCH ₃	H	OCH ₃	3.27 ± 0.15	3.89 ± 0.16

* Data are expressed as mean ± SD (n = 3), n.a. = not active

Table 4.2: Synthesized benzoflavones and their inhibitory potencies against MDCK BCRP cells in Hoechst 33342 and pheophorbide A accumulation assays.



7,8-Benzoflavone (49-52, 61-64, 72-75)



5,6-Benzoflavone (53-55, 65-67, 76-78)

Compd	R ³	R ^{3'}	R ^{4'}	Hoechst 33342	Pheophorbide A
				assay	assay
				IC ₅₀ ± SD	IC ₅₀ ± SD
				(μM)*	(μM)*
Benzoflavones					
49	H	H	H	1.31 ± 0.12	1.40 ± 0.18
50	H	H	OCH ₃	1.28 ± 0.07	1.29 ± 0.09
51	H	OCH ₃	OCH ₃	1.23 ± 0.08	1.13 ± 0.19
52	H	OCH ₃	F	0.522 ± 0.083	0.457 ± 0.124
53	H	H	H	8.32 ± 0.61	6.05 ± 1.62
54	H	H	OCH ₃	2.46 ± 0.15	1.69 ± 0.07
55	H	OCH ₃	OCH ₃	0.590 ± 0.064	0.458 ± 0.053
3-Hydroxybenzoflavones					
61	OH	H	H	2.89 ± 0.73	1.59 ± 0.14
62	OH	H	OCH ₃	6.93 ± 1.58	4.97 ± 0.88
63	OH	OCH ₃	OCH ₃	0.724 ± 0.049	1.52 ± 0.08
64	OH	OCH ₃	F	22.5 ± 4.90	17.9 ± ± 0.29
65	OH	H	H	11.0 ± 2.98	13.6 ± 2.40
66	OH	H	OCH ₃	8.93 ± 2.37	6.12 ± 1.54
67	OH	OCH ₃	OCH ₃	6.12 ± 0.35	4.84 ± 0.99
3-Methoxybenzoflavones					
72	OCH ₃	H	H	2.71 ± 0.41	2.31 ± ± 0.04
73	OCH ₃	H	OCH ₃	1.06 ± 0.26	3.07 ± 0.38
74	OCH ₃	OCH ₃	OCH ₃	0.426 ± 0.019	0.468 ± 0.034
75	OCH ₃	OCH ₃	F	2.44 ± 0.25	4.01 ± 0.77
76	OCH ₃	H	H	11.1 ± 1.37	12.5 ± 0.65
77	OCH ₃	H	OCH ₃	3.07 ± 0.04	8.02 ± 1.39
78	OCH ₃	OCH ₃	OCH ₃	4.27 ± 0.64	5.25 ± 0.67
Ko143		–		0.25 ± 0.04	0.33 ± 0.05

* Data are expressed as mean ± SD (n = 3)

The IC₅₀ values obtained in the pheophorbide A assay for the investigated compounds in MDCK BCRP cells are given in Table 4.1 and Table 4.2. Pheophorbide A assays for flavones **56-60**, **68-71** and **79-82** were performed by Katja Stefan and the results were taken from her master thesis for comparison purposes [187].

4.5.1.1 Structural features of flavones and benzoflavones for BCRP inhibition

In case of flavones, two types of compounds were investigated 1) those having hydroxy substituents at position 3 of the flavone nucleus (**56-60**) and 2) those having methoxy substituents at the same position (**68-71** and **79-82**). Generally, compounds possessing a 3-OH substituent were found to be very less active or even inactive when compared to compounds bearing a 3-OCH₃ substituent, as it can be seen in Table 4.1. The results obtained from the functional assays described in this study are in accordance with the structure-activity relationship proposed earlier by several investigators [125, 128, 188]. It was also observed that presence of methoxy groups on the side ring (at position 2) of flavone led to an increase in activity. Presence of 3',4'-OCH₃ substitution was found to be optimum for BCRP inhibition. The comparison of IC₅₀ values for compounds **79-82** shows the importance of the presence of a 5-OH substituent (in compounds **81** and **82**) for BCRP inhibition. Replacement of 5-OH with 5-OCH₃ leads to a decrease in activity (compare with compounds **79** and **80**). In case of these compounds it was also observed that presence of 2',4'-dimethoxy substituent (**80**, **82**) led to strong decrease in activity when compared to 3',4'-dimethoxy substituted compounds (**79**, **81**). Compound **81**, bearing 3-OCH₃ and 5-OH substituents on the flavone scaffold was found to be the most potent in the flavone series with an IC₅₀ value of 0.54 μ M in Hoechst 33342 assay.

The second series includes 7,8-benzoflavones and 5,6-benzoflavones. Compound **49**, the unsubstituted benzoflavone was shown to be a potent inhibitor of BCRP by Zhang et al. [128] and was included in the current study for comparison purposes. As it can be seen from Table 4.2, also in case of 7,8- and 5,6-benzoflavones the presence of a 3-OH substituent (in compounds **61-67**) led to a decrease in activity. While, particularly in case of 7,8-benzoflavones the presence of a 3-OCH₃ group (compounds **72-74**) led to a strong increase in BCRP inhibition. As in the case of flavones, 3',4'-OCH₃ substituted benzoflavones were more potent BCRP inhibitors

when compared to unsubstituted compounds and those bearing a 4'-OCH₃ substituent only. Compound **52** having a 3'-OCH₃, 4-F substitution was found to be the most active ($IC_{50} = 0.52 \pm 0.08 \mu M$ in the Hoechst 33342 assay) amongst the benzoflavones having no substitution at position 3. However, other derivatives of this compound (**64** and **75**) showed less activity. From Table 4.2, it can be seen that 5,6-benzoflavones are less potent as compared to 7,8-benzoflavones with exception of compound **55** which showed strong BCRP inhibition ($IC_{50} = 0.59 \pm 0.06 \mu M$ in the Hoechst 33342 assay).

The BCRP inhibition analysis done by two different assays gave comparable results with good correlation ($r^2 = 0.89$) between both assays as shown in Figure 4.8. Also the Hill slopes of the dose response curves were similar and not significantly different from one, except for a few experiments. This indicates that the inhibitory activity of these compounds is not substrate specific.

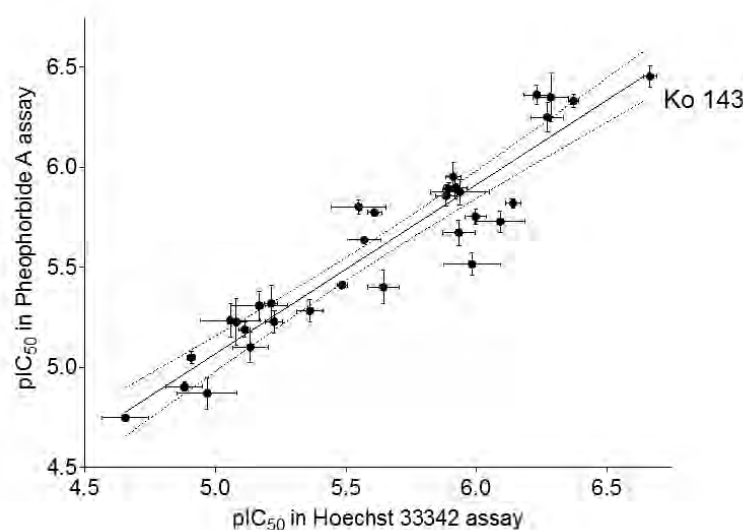


Figure 4.8: Scatterplot of pIC_{50} values for BCRP inhibition obtained in the Hoechst 33342 assay and the pheophorbide A assay. Each point indicates mean of IC_{50} values obtained in three independent experiments and error bars indicate standard deviation. The squared correlation coefficient is $r^2 = 0.89$, $n = 32$.

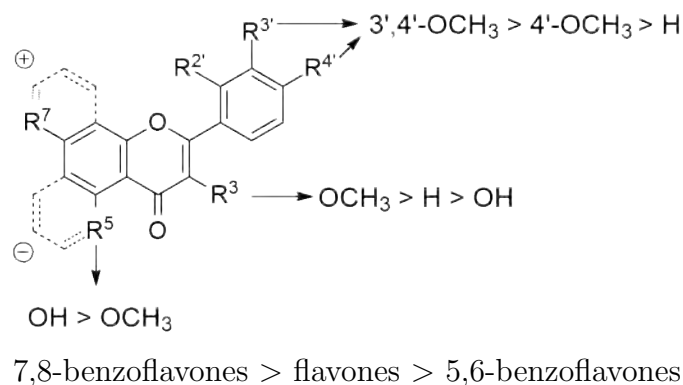


Figure 4.9: Effect of different substituents on BCRP inhibitory activity of flavonoids. Dotted lines indicate 7,8- or 5,6-benzo substitution for benzoflavones. \oplus : leads to increase in BCRP inhibition, \ominus : leads to decrease in BCRP inhibition.

From the activity data of all compounds, it was found that 7,8-benzoflavones are more active as compared to flavones, while 5,6-benzoflavones are the least active class with exception of compound **55**. The effect of different substituents on BCRP activity is summarized in Figure 4.9.

4.5.2 Determination of P-gp and MRP1 inhibition in the calcein AM assay

All compounds were first screened for their P-gp and MRP1 inhibition to investigate selectivity towards BCRP. Screening was performed at 10 μM final inhibitor concentration using calcein AM assay. Functionality and principle involved in the calcein AM assay are described in section 3.3.2 and section 7.2.3.3.

In the screening, cyclosporine A, a P-gp and MRP1 inhibitor, was used as a standard. Most compounds showed no or very weak inhibition of P-gp and MRP1. The effect of the compounds on calcein accumulation in P-gp overexpressing A2780 adr cells is illustrated in Figure 4.10. Figure 4.11 shows the effect of the compounds on accumulation of calcein in MRP1 overexpressing 2008 MRP1 cells. In case of flavones only compound **79** was found to show substantial effect on both P-gp and MRP1. While in case of benzoflavones, only 7,8-benzoflavones showed considerable effect. Compounds showing more than 25 % of response when compared to control (response in non P-gp or MRP1 expressing sensitive cells) were further investigated with a range of different concentrations to calculate their IC_{50} values.

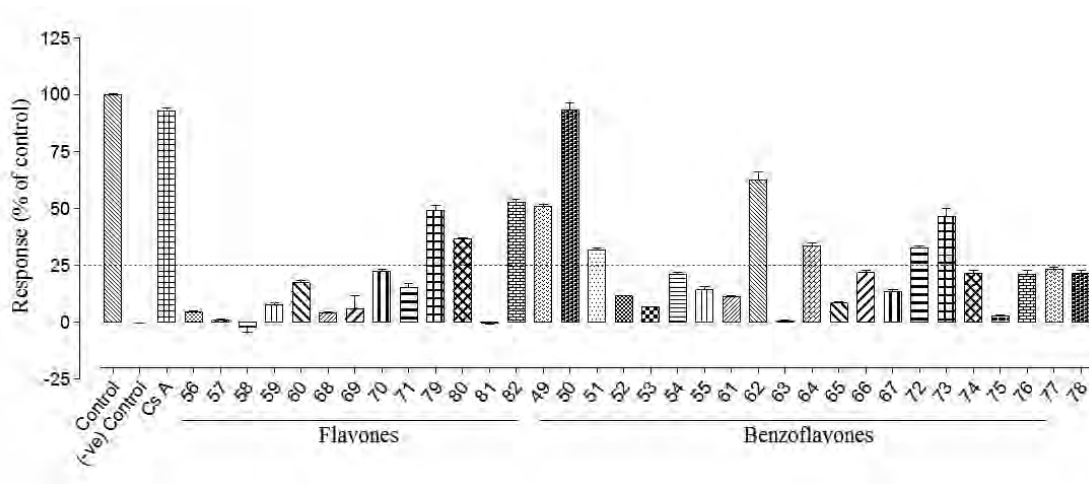


Figure 4.10: Effect of flavones and benzoflavones on accumulation of calcein in P-gp overexpressing A2780 cells. The compounds were investigated at $10 \mu\text{M}$ final concentration. Cyclosporine A (CsA, $10 \mu\text{M}$) was used as a standard. Response in absence of any compound was used as negative control. Data are expressed as response in percentage of control (accumulation of calcein in non P-gp expressing sensitive A2780 cells) and presented as the mean \pm SD of three independent experiments.

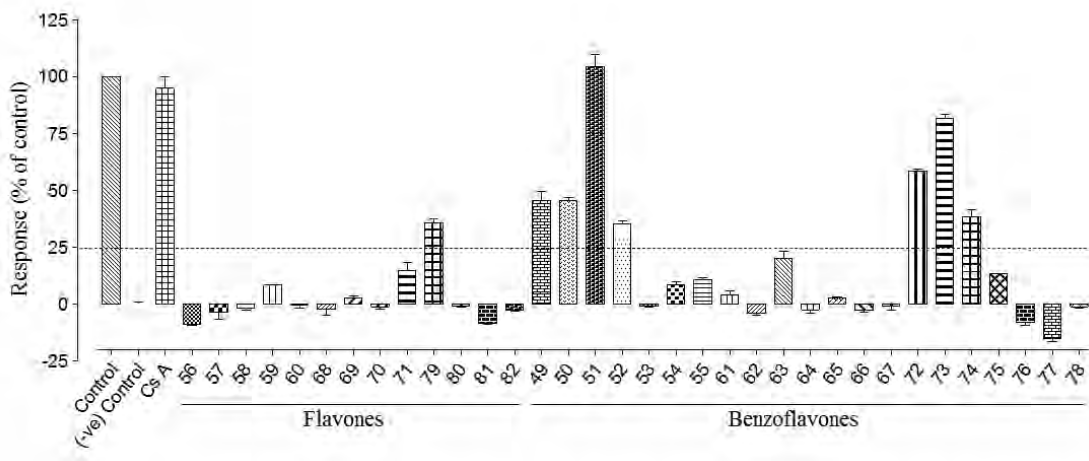


Figure 4.11: Effect of flavones and benzoflavones on accumulation of calcein in MRP1 overexpressing 2008 MRP1 cells. The compounds were investigated at $10 \mu\text{M}$ final concentration. Cyclosporine A (CsA, $10 \mu\text{M}$) was used as a standard. Response in absence of any compound was used as negative control. Data are expressed as response in percentage of control (accumulation of calcein in non MRP1 expressing sensitive 2008 cells) and presented as the mean \pm SD of three independent experiments.

Table 4.3: Inhibitory potencies of selected flavonoids using A2780 adr and 2008 MRP1 cells in calcein AM assay. Data are expressed as mean \pm SD (n=3). Cyclosporine A was used as standard.

Compd	A2780 adr IC₅₀ \pm SD (μM)	2008 MRP1 IC₅₀ \pm SD (μM)
49	24.6 \pm 3.98	11.3 \pm 2.49
50	19.7 \pm 2.82	9.86 \pm 1.05
51	4.00 \pm 0.22	1.76 \pm 0.04
52	n.a.*	15.1 \pm 3.83
63	4.27 \pm 0.59	n.a.
72	n.a	27.5 \pm 4.44
73	n.a	19.0 \pm 2.48
74	21.9 \pm 2.33	21.8 \pm 2.74
79	23.4 \pm 2.78	26.35 \pm 2.65
80	27.1 \pm 3.53	n.a.
Cyclosporine A	0.99 \pm 0.08	2.81 \pm 0.62

* n.a. = not active, showing a response of less than 25 % of control in screening at 10 μ M concentration (see Figure 4.10 and Figure 4.11).

P-gp and MRP1 inhibition data of selected compounds are given in Table 4.3. Compound **51**, a 7,8-benzoflavone bearing 3',4'-OCH₃ substituents was found to be the most potent and active for both P-gp and MRP1 inhibition. It was even more potent than cyclosporine A in MRP1 inhibition. Compound **74**, the most active flavonoid in the current study showed very weak P-gp and MRP1 inhibition with almost 50 times less activity compared to BCRP inhibition.

4.5.3 Intrinsic cytotoxicity of selected flavones and benzoflavones in the MTT assay

In the current study of flavonoids, few flavones and benzoflavones were found to be potent inhibitors of BCRP. To make further investigation of these compounds possible, the intrinsic cytotoxicity was checked in the MTT cytotoxicity assay. For this purpose, from flavones and benzoflavones, the most potent compounds (**59**, **81**, **55** and **74**) from each class were selected. The toxicity studies of these compounds

were performed using MDCK BCRP and sensitive MDCK cells. Owing to low aqueous solubility of these compounds at higher concentrations, the highest concentration (100 μM) was prepared using methanol (not more than 2 % end concentration). To check the effect of this small amount of methanol on cell toxicity, blank experiments were performed using dilution solvents (PBS) containing same amount of methanol.

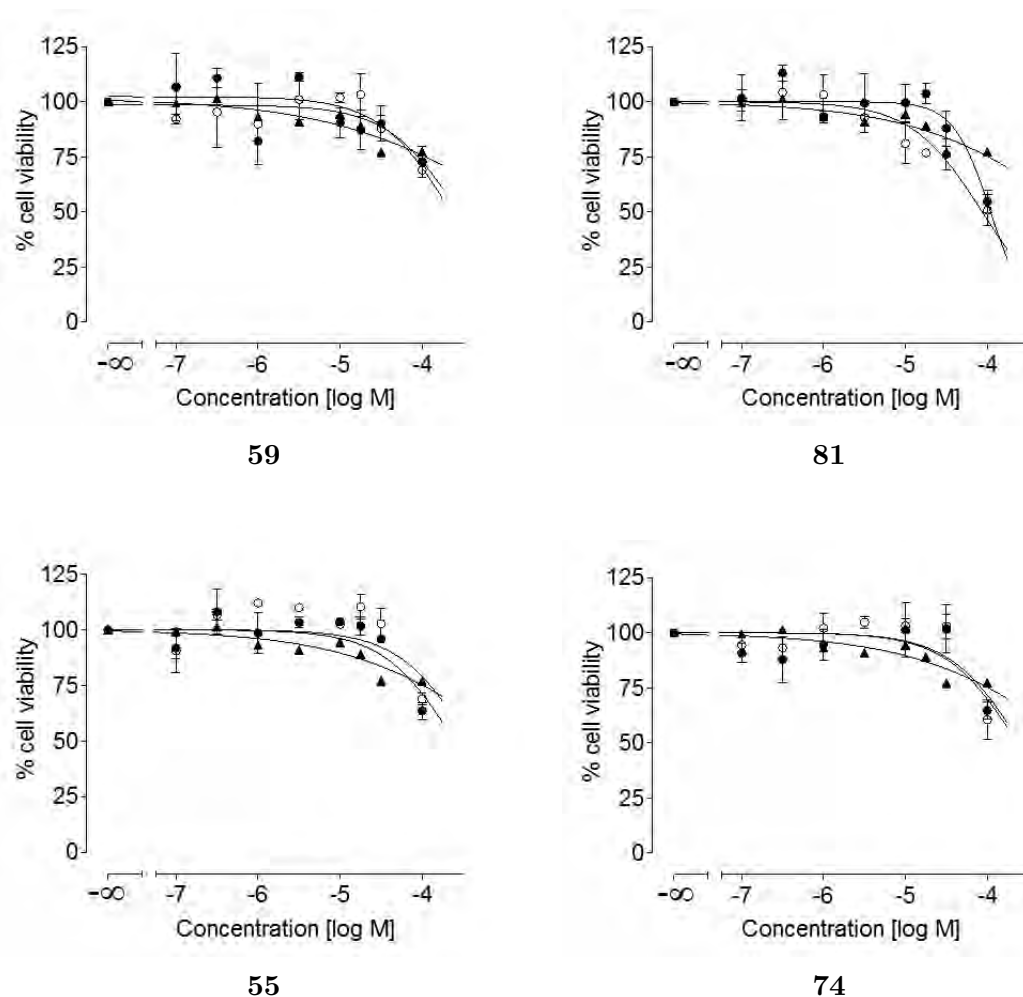


Figure 4.12: Cytotoxicity of selected compounds was determined in the MTT assay using MDCK BCRP and sensitive MDCK cells. Flavones **59** and **81** and benzoflavones **55** and **74** were investigated up to 100 μM concentration, for 72 h. Open circle: MDCK BCRP cells, closed circle: MDCK sensitive cells and closed triangle: dilution solvent (PBS) containing 2 % methanol in highest concentration.

For all compounds, very little toxicity could be observed at 100 μM and none of the compounds showed cytotoxicity at lower concentrations. For most of the compounds GI_{50} could be estimated to be more than 100 μM and only for compound **81** GI_{50}

was estimated to be around 85 μM . These concentrations are much higher than that required for the BCRP inhibition.

4.5.4 Re-sensitization of BCRP overexpressing cells towards SN-38 and Hoechst 33342 cytotoxicity

MTT assay was also used to investigate the effect of flavone (**81**) and benzoflavone (**74**) on the antiproliferative effect of cytotoxic agents in presence of the BCRP transporter. Cytotoxicity of SN-38 (the active metabolite of irinotecan) and Hoechst 33342 was evaluated in MDCK BCRP cells. The cytotoxic effect of both drugs was determined in absence and presence of 5 μM and 10 μM concentrations of the selected compounds. Both compounds were found to be able to reverse the resistance of the BCRP expressing cell lines, proving their functional efficacy. Figure 4.13 shows representative dose–response curves of SN-38 in presence of compound **81** and of Hoechst 33342 in presence of compound **74**.

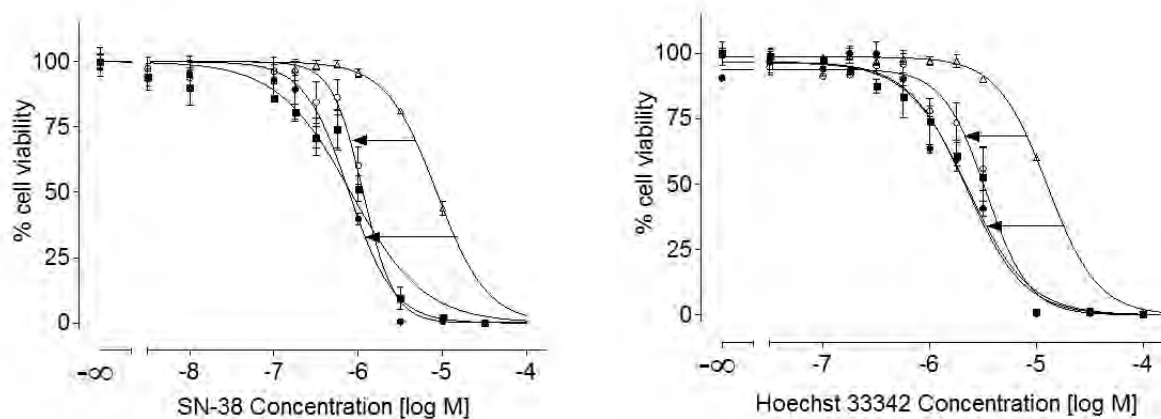


Figure 4.13: Representative shift in dose–response curves of SN-38 and Hoechst 33342 cytotoxicity. Left: effect of compound **81** on SN-38 cytotoxicity in BCRP cells. Right: effect of compound **74** on cytotoxicity of Hoechst 33342. Both compounds were investigated at 5 μM (open circles) and 10 μM (closed circles) concentrations. BCRP cells without inhibitor (open triangles) are more resistant than sensitive cells (closed squares).

The shift in the dose–response curves of MDCK BCRP cells in presence of these compounds towards lower concentrations indicates sensitization to cytotoxicity of SN-

38 and Hoechst 33342. The GI_{50} values of SN-38 in absence of BCRP inhibitor were $8.5 \mu M$ for MDCK BCRP cells and $0.81 \mu M$ for MDCK sensitive cells, indicating resistance to SN-38 in MDCK BCRP cells. In presence of compound **81** ($10 \mu M$), the GI_{50} value for MDCK BCRP cells was reduced to $0.78 \mu M$ indicating complete reversal of resistance. Similar results were observed for Hoechst 33342 cytotoxicity in presence compound **74**, where the GI_{50} of Hoechst 33342 in MDCK BCRP cells was reduced to $2.2 \mu M$ (in presence of inhibitor **74**) from $12.7 \mu M$ (in absence of inhibitor). This outcome, proves their ability to overcome the MDR in BCRP overexpressing cells.

In summary, in the current study several 7,8-benzoflavones, 5,6-benzoflavones were synthesized and investigated for their BCRP inhibition potential along with comparison to multisubstituted flavones. From the activity data obtained in the Hoechst 33342 and pheophorbide A assays it was possible to propose the effect of different substituents as well as the effect of attachment of a benzo-ring at position 7,8 or 5,6 of the flavone moiety. 7,8-benzoflavones were found to be more potent than flavones and 5,6-benzoflavones. The inhibitory effect of these compounds was further confirmed by evaluating the influence of selected compounds on the cytotoxicity of SN-38 and Hoechst 33342 in BCRP overexpressing cells. Most of the synthesized compounds were found to be selective towards BCRP. Cytotoxicity of the most active compounds was determined in the MTT cytotoxicity assay. Compound **74** was found to be a non-toxic potent BCRP inhibitor having 50 times more selectivity towards BCRP. Compound **51**, a substituted 7,8-benzoflavone could be a good broad spectrum MDR modulator as it produced low IC_{50} values for all BCRP, P-gp and MRP1.

5 Project 3: Synthesis and evaluation of quinazolines as BCRP inhibitors

Quinazoline (Figure 5.1) is a heterocyclic compound consisting of two fused six membered aromatic rings, a benzene and a pyrimidine ring and is also known as benzo-1,3-diazine. Quinazoline was first prepared by Gabriel in 1903 [189].

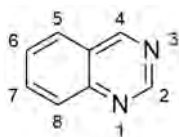


Figure 5.1: General structure of quinazoline

Compounds containing the quinazoline heterocycle have been shown to possess a vast variety of biological activities such as, sedative [190], analgesic [191, 192], anti-diabetic [193], anticonvulsant [194, 195], antiallergic [196, 197], antimalarial [198, 199] and antihypertensive [200, 201], etc. Quinazoline derivatives have been shown to have anticancer activity [202–206]. There are several marketed drugs bearing a quinazoline nucleus, for example prazosin, gefitinib, erlotinib, alfuzosin, trimetrexate, bunazosin, vandetanib, etc. Quinazoline compounds have also been shown to modulate ABC transporters as described below.

Along with being transported by P-gp and BCRP, recently a few TKI quinazolines were identified to be good inhibitors of BCRP. In 2004 Yanase *et al.* showed the inhibitory effect of gefitinib (marketed as Iressa) on BCRP [212], while later in 2006 Leggas *et al.* showed the inhibitory effect of this compound on both P-gp and BCRP [213]. Contradictory results were recently published by Agarwal *et al.* where distribution of gefitinib was found to be limited by P-gp and BCRP through its transport [214]. The BCRP inhibitory effect of gefitinib was recently confirmed in our group by Anne Pick, where it was also shown that gefitinib was able to decrease the overall and surface expression of BCRP in EGFR-positive MDCK BCRP cells by interacting with the PI3K/Akt signaling pathway [117]. Few other quinazoline nucleus bearing compounds such as PD153035 and erlotinib have been shown to inhibit BCRP. Structures of selected quinazoline BCRP substrates and inhibitors are given in Figure 5.2.

In the study done by Anne Pick, a few quinazoline compounds were found to be potent inhibitors of BCRP with IC_{50} values in the sub-micromolar range. But these compounds lack variation in the substituents present on the quinazoline moiety. Hence, with the aim of finding more potent quinazoline compounds and possibly identification of structural requirements for BCRP inhibition, several quinazoline derivatives were synthesized. Synthesis and biological evaluation of these compounds are discussed in the following sections.

5.2 Synthesis of quinazoline derivatives

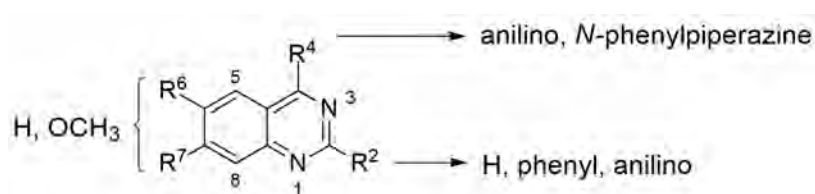


Figure 5.3: Modifications of the quinazoline scaffold

In the current study, several modifications of the quinazoline scaffold were planned with the primary aim of finding more potent BCRP inhibitors showing less toxicity when compared to already available TKI quinazolines. The quinazoline TKIs

investigated until now for BCRP inhibition possess substituents only at positions 4, 6 and 7 of the quinazoline moiety. Hence, in this work compounds with different substitution, starting with 2-phenyl substituted derivatives were investigated for their activity against BCRP. Different combinations of modifications at position 2, 4, 6, 7 of quinazoline were made and are summarized in Figure 5.3.

5.2.1 Synthesis of 2-phenyl-4-anilinoquinazolines

The first variation of the quinazoline scaffold involved synthesis of several quinazoline compounds bearing a phenyl ring at position 2 and a substituted anilino group at position 4 of the quinazoline. In these compounds positions 6 and 7 were kept unsubstituted.

The synthesis of 2-phenyl-4-anilino compounds involved the following steps:

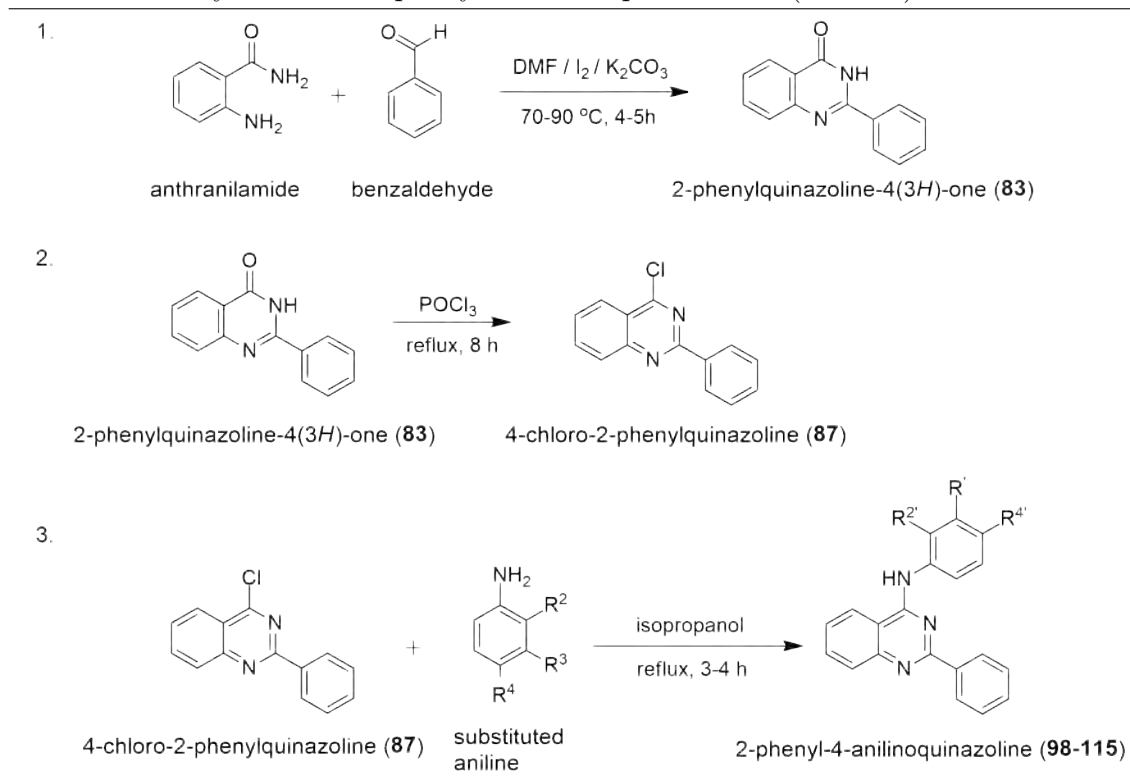
1. Synthesis of 2-phenylquinazoline-4(3*H*)-one (**83**): This compound was synthesized by using method A described in section 7.1.2.11. The quinazolinone compound was synthesized by fusion of anthranilamide with benzaldehyde in presence of iodine and potassium carbonate. Dimethylformamide (DMF) was used as solvent. The reaction mixture was heated for 4-5 hours at 70-90 °C. After completion of the reaction the solution was poured onto crushed ice to get a crude product precipitate. Traces of iodine were removed by washing the product with sodium thiosulfate and later with plenty of water. The product was recrystallized from ethanol to yield pale yellow crystals with 79 % yield. This compound was used further for the synthesis of the 4-chloro derivative.
2. Conversion of 4-quinazolinone to 4-chloro-2-phenylquinazoline (**87**): The quinazolinone (**83**) was converted to 4-chloro-2-phenylquinazoline by chlorination using phosphorus oxychloride (POCl₃) as described in section 7.1.2.12. Compound **83** was refluxed in excess quantity of POCl₃ for 9 hours. After completion of the reaction, excess of POCl₃ was removed under reduced pressure. The residue was added to ice-water and neutralized with ammonium hydroxide. The solution was extracted with dichloromethane and the solvent was removed under reduced pressure to yield pale yellow solid with 87 % yield.
3. Synthesis of 4-anilinoquinazolines (**98-115**) from **87** and substituted anilines: Using the 4-chloro-2-phenylquinazoline (**87**) several 4-anilino derivatives were syn-

5.2 Synthesis of quinazoline derivatives

thesized as described in section 7.1.2.14. In short, 4-chloro-2-phenylquinazoline was dissolved in refluxing isopropanol and the selected aniline was added drop wise. The reaction mixture was refluxed for 3-4 hours. After completion of the reaction in most cases the product precipitated, which was filtered and washed with cold isopropanol to remove traces of the aniline. For compounds bearing methoxy or hydroxy substituents on aniline there was no formation of precipitate. In such cases, the solvent was removed under reduced pressure. Compounds were purified by recrystallization from ethanol.

A synthesis scheme involving these 3 steps is given in Algorithm 5.1 and a list of compounds synthesized is given in Table 5.1.

Scheme 5.1 Synthesis of 2-phenyl-4-anilinoquinazolines (98-115)

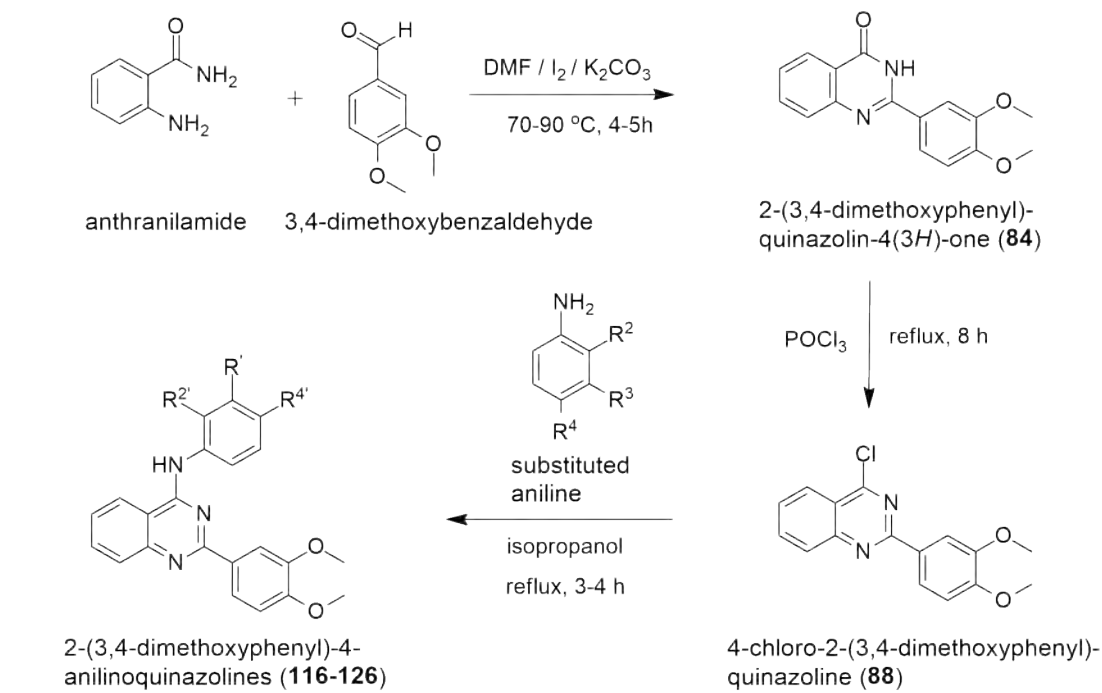


5.2.2 Synthesis of 2-(3,4-dimethoxyphenyl)-4-anilinoquinazolines

The second modification of the quinazolines was the replacement of the 2-phenyl ring by a 2-(3,4-dimethoxyphenyl) substituent. These compounds were synthesized in similar way as described above. The 2-(3,4-dimethoxyphenyl)quinazolin-4(3H)-one

(**84**) was synthesized from anthranilamide and 3,4-dimethoxybenzaldehyde in presence of iodine and potassium carbonate using DMF as solvent. This compound was further converted to 4-Chloro-2-(3,4-dimethoxyphenyl)quinazoline (**88**) by chlorination using POCl₃. Finally compound **88** was reacted with substituted anilines in isopropanol as solvent to get 2-(3,4-dimethoxyphenyl)-4-anilinoquinazolines (**116-126**). A list of synthesized compounds is given in Table 5.2, while a reaction involved in synthesis is shown in Algorithm 5.2

Scheme 5.2 Synthesis of 2-(3,4-dimethoxyphenyl)-4-anilinoquinazolines (**116-126**)

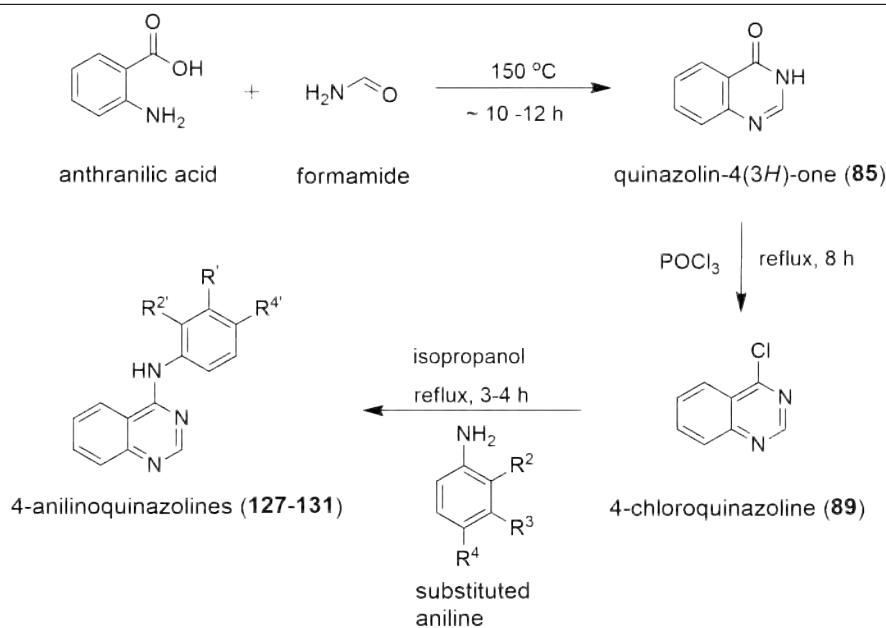


5.2.3 Synthesis of 4-anilinoquinazolines

In the third modification of the quinazoline scaffold a few derivatives bearing no substitution at position 2, 6 and 7 were synthesized to check the importance of the 2-phenyl ring on the BCRP inhibitory activity. The synthesis route was almost the same as described in section 5.2.1 with modification in the synthesis of the quinazolinone. For the synthesis of quinazolin-4(3*H*)-one (**85**), method B described in section 7.1.2.11 was used, where the reactant was used as solvent and no catalyst was used. Compound **85** was synthesized by fusion of anthranilic acid and formamide. The mixture of these two components was heated at 150 °C for approximately 15

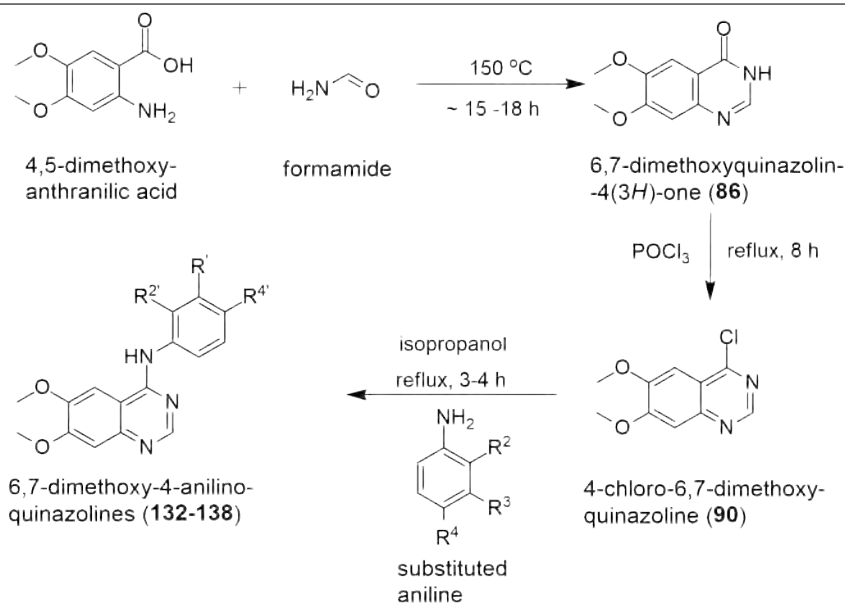
hours. After completion of the reaction, water was added to the reaction mixture and further stirred at room temperature for 30 minutes. The precipitate was filtered and washed with plenty of water. The quinazolinone (**85**) obtained was further converted to 4-chloroquinazoline (**89**) by refluxing with POCl_3 . This compound was further used to synthesize the final 4-anilinoquinazolines (**127-131**) by reacting it with substituted anilines. The reactions involved in synthesis of 4-anilinoquinazolines are given in Algorithm 5.3. All the synthesized compounds are listed in Table 5.3.

Scheme 5.3 Synthesis of 4-anilinoquinazolines (**127-131**)



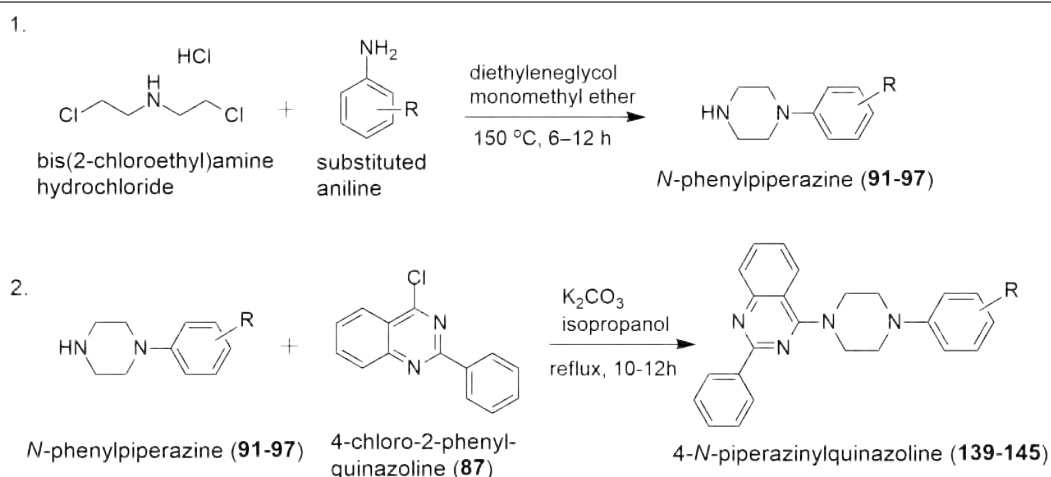
5.2.4 Synthesis of 6,7-dimethoxy-4-anilinoquinazolines

To check if there is any positive effect of substitution at position 6 and 7 of the quinazoline scaffold on BCRP inhibition, several 6,7-dimethoxy-4-anilinoquinazolines (**132-138**) were synthesized. The synthesis was performed as described in section 5.2.3, where 6,7-Dimethoxyquinazolin-4(3H)-one (**86**) was synthesized from 4,5-dimethoxyanthranilic acid (2-amino-4,5-dimethoxybenzoic acid) and formamide without using any catalyst. Compound **86** was converted to 4-Chloro-6,7-dimethoxyquinazoline (**90**) by reacting it with POCl_3 at refluxing temperature. The 4-chloro derivative was reacted with substituted anilines in isopropanol to yield 6,7-dimethoxy-4-anilinoquinazolines (**132-138**). The reactions involved in the synthesis are given in Algorithm 5.4 and a list of compounds is given in Table 5.4.

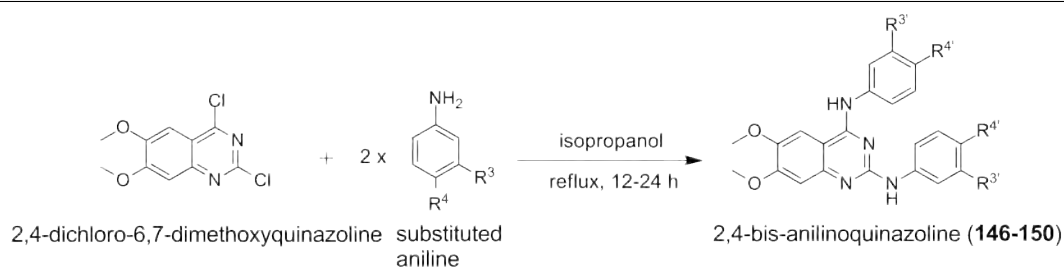
Scheme 5.4 Synthesis of 6,7-dimethoxy-4-anilinoquinazolines (**132-138**)**5.2.5 Synthesis of 4-*N*-piperazinylquinazolines**

Several quinazoline derivatives bearing a *N*-phenyl-piperazine substituent at position 4 were synthesized to compare their activity with the anilinoquinazolines. For the synthesis of 4-*N*-piperazinylquinazolines (**139-145**), 4-chloro-2-phenylquinazoline (**87**) was reacted with several substituted *N*-phenylpiperazines (**91-97**) in presence of potassium carbonate, using isopropanol as solvent. As the compounds did not precipitate after completion of reaction, the solvent was removed under reduced pressure. To the residue water was added, the precipitated product was filtered and washed with water to remove traces of potassium carbonate.

The synthesis of *N*-phenylpiperazines used here is described in section 7.1.2.13. These compounds were synthesized from bis(2-chloroethyl)amine hydrochloride and substituted anilines using diethylene glycol monomethylether as solvent. It gave the hydrochloride salt of the *N*-phenylpiperazine which was converted to the free *N*-phenylpiperazine by treatment with sodium carbonate. Compounds were directly used for synthesis of 4-*N*-piperazinylquinazolines (**139-145**) without further purification. The general reactions involved in synthesis of 4-*N*-piperazinylquinazolines are given in Algorithm 5.5. All synthesized compounds are listed in Table 5.5.

Scheme 5.5 Synthesis of 4-*N*-piperazinylquinazolines (**139-145**)**5.2.6 Synthesis of 2,4-bis-anilinoquinazolines**

The last series of quinazoline compounds contained anilino substituents at position 2 and 4 of the quinazoline scaffold. The anilino substitution at position 2 and 4 was kept the same. A general procedure for synthesis of 2,4-bis-anilinoquinazolines (**146-150**) is given in section 7.1.2.16. These compounds were synthesized from 2,4-dichloro-6,7-dimethoxyquinazoline (procured from Acros Organics, Belgium) by reacting with two moles of substituted anilines in isopropanol as solvent. The reaction mixture was refluxed until the reaction was complete, which resulted in precipitation of the product. Precipitated product was filtered and washed with cold isopropanol and ether. The dried product was recrystallized from ethanol. The general reactions involved in synthesis of compounds **146-150** are given in Algorithm 5.6.

Scheme 5.6 Synthesis of 2,4-bis-anilinoquinazolines (**146-150**)

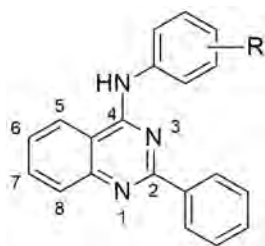
5.3 Biological evaluation of quinazolines

All synthesized compounds were tested for BCRP inhibition in Hoechst 33342 (compounds **98-150**) and pheophorbide A assays (compounds **116-150**). Most potent and promising BCRP inhibitor compounds were further checked for selectivity by testing their ability to inhibit P-gp and MRP1 in the calcein AM assay. Intrinsic cytotoxicity and efficacy of selected compounds were checked in MTT cytotoxicity assay.

5.3.1 Hoechst 33342 and Pheophorbide A assays for determining BCRP inhibition

Functioning and the procedure for performing the Hoechst 33342 accumulation assay are given in section 3.3.1 and section 7.2.3.1, while the pheophorbide A assay is discussed in section 4.5.1 and section 7.2.3.2. Both assays were performed using MDCK BCRP cells and the results obtained are discussed below.

In the first series of quinazolines several 2-phenyl-4-anilinoquinazolines (**98-115**) were synthesized. The IC_{50} values obtained for these compounds in the Hoechst 33342 are given Table 5.1. All compounds in this class of quinazolines were found to be active. From Table 5.1 it is apparent that, from the anilinoquinazolines **98-115**, those bearing a *meta*-substituent on the aniline are more potent than *ortho*- or *para*-substituted analogs (see compounds **100**, **109**, **112**, **113** and **115**). Compounds bearing substituents at *ortho* position of aniline were the least active compounds followed by *para* substituted compounds. Compound **109** was the most potent in the set, with an IC_{50} of $0.13 \mu M$, which is even lower than that of the standard Ko143 ($0.25 \mu M$, see Table 5.6). A comparison of the concentration-response curves for these two compounds is shown in Figure 5.4. It was interesting to see that compound **115** bearing a more polar substituent (OH) was also very active BCRP inhibitor with an IC_{50} value of $0.15 \mu M$.

Table 5.1: Synthesized 2-phenyl-4-anilinoquinazolines and their inhibitory potencies against MDCK BCRP cells in Hoechst 33342 accumulation assays.**2-Phenyl-4-anilinoquinazolines (98-115)**

Compd	R	Hoechst 33342 assay
		IC ₅₀ ± SD (μM)*
98	H	2.57 ± 0.28
99	2-Br	3.75 ± 0.53
100	3-Br	0.57 ± 0.04
101	4-Br	6.83 ± 0.97
102	3-Cl	1.93 ± 0.28
103	3-Cl, 4-F	1.66 ± 0.11
104	2-OCH ₃	2.25 ± 0.07
105	3-OCH ₃	1.32 ± 0.10
106	4-OCH ₃	1.93 ± 0.11
107	3,4- OCH ₃	0.19 ± 0.01
108	2-NO ₂	5.93 ± 0.10
109	3-NO ₂	0.13 ± 0.03
110	4-NO ₂	0.97 ± 0.24
111	3-NO ₂ , 4-F	2.46 ± 0.14
112	3-CN	0.14 ± 0.04
113	3-CF ₃	0.25 ± 0.10
114	4-CF ₃	1.53 ± 0.13
115	3-OH	0.15 ± 0.03

* Data are expressed as mean ± SD (n = 3).

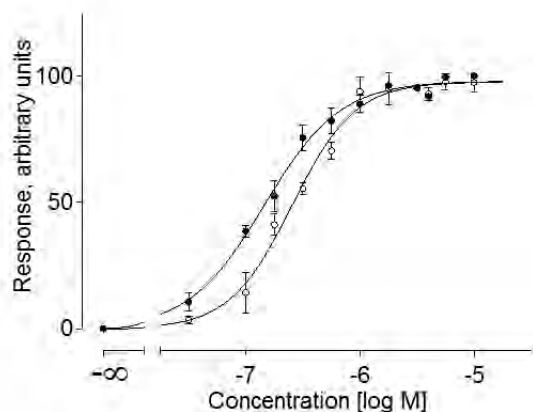
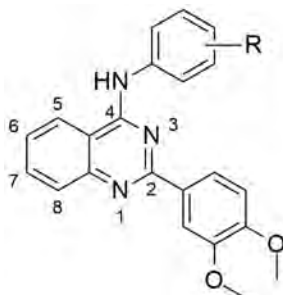


Figure 5.4: Representative concentration-response curves of compound **109** (closed circles, $IC_{50} = 0.13 \pm 0.03 \mu M$) and **Ko143** (open circles, $IC_{50} = 0.25 \pm 0.04 \mu M$) obtained in the Hoechst 33342 assay. Each data point shown represents average of 3 independent experiments with error bars indicating standard deviation.

The second series of quinazolines consists of 2-(3,4-dimethoxyphenyl)-4-anilinoquinazolines (**116-126**), where the influence of methoxy groups at the 2-phenyl ring was investigated. It can be seen from Table 5.2 that in most cases presence of 3,4-dimethoxyphenyl substitution led to a slight increase in the activity, although it was very marginal when compared to 2-phenyl-4-anilinoquinazolines. As in case of compounds **98-115**, similar effect of substituents present on the 4-anilino ring was observed for compounds **116-126**. *Meta* substituted compounds (see **117**, **120**, **122**, **123** and **125**) were highly active when compared to *ortho* (see **119** and **124**) or *para* (see **121** and **126**) substituted compounds. In this series compound **120** was the most potent compound with an IC_{50} value of $0.076 \mu M$ in Hoechst 33342 assay and $0.092 \mu M$ in the pheophorbide A assay. This compound was found to be the most potent amongst all investigated quinazolines in the current work.

Table 5.2: Synthesized 2-(3,4-dimethoxyphenyl)-4-anilinoquinazolines and their inhibitory potencies against MDCK BCRP cells in Hoechst 33342 and pheophorbide A accumulation assays.



2-(3,4-Dimethoxyphenyl)-4-anilinoquinazolines (116-126)

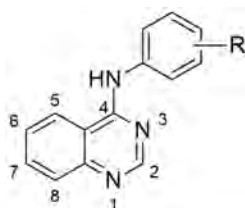
Compd	R	Hoechst 33342	Pheophorbide A
		assay	assay
		IC ₅₀ ± SD (μM)*	IC ₅₀ ± SD (μM)*
116	H	1.99 ± 0.20	4.09 ± 1.60
117	3-Br	0.29 ± 0.03	0.40 ± 0.09
118	3,4-OCH ₃	0.42 ± 0.05	0.61 ± 0.04
119	2-NO ₂	0.64 ± 0.08	1.55 ± 0.29
120	3-NO ₂	0.076 ± 0.019	0.092 ± 0.024
121	4-NO ₂	0.30 ± 0.04	0.32 ± 0.09
122	3-CF ₃	0.30 ± 0.04	0.24 ± 0.05
123	3-CN	0.19 ± 0.01	0.30 ± 0.06
124	2-OH	0.26 ± 0.07	0.29 ± 0.03
125	3-OH	0.14 ± 0.03	0.11 ± 0.01
126	4-OH	0.47 ± 0.05	0.68 ± 0.12

* Data are expressed as mean ± SD (n = 3).

The next modification undertaken was to synthesize compounds without any substituents at position 2 of the quinazoline moiety. As it can be seen from Figure 5.2, all published TKI quinazolines lack substituents at position 2. Hence two different types of 4-anilino quinazolines were synthesized, first without any substitution at positions 2, 6 and 7 of the quinazoline (compounds **127-131**) and second bearing no substitution at position 2, but methoxy substitution at position 6 and 7 (**132-138**). The IC₅₀ values obtained in Hoechst 33342 and pheophorbide A assays are given in Table 5.3 (for compounds **127-131**) and Table 5.4 (for compounds **132-138**).

It was clearly observed that removal of the phenyl substituent at position 2 of the quinazoline led to a drastic decrease in the activity. In these two series of quinazolines, mostly compounds bearing meta substituted anilines were chosen based on earlier results. There was no substantial difference in the activities of the compounds with or without 6,7-dimethoxy substituent. This suggests that, the presence of methoxy substituents at position 6 and 7 of the quinazoline scaffold was not important for the BCRP inhibition. For comparison purposes the TKI quinazoline PD153035 (compound **132**) was included in the current study and gave the same results as reported by Pick *et al.* [117].

Table 5.3: Synthesized 4-anilinoquinazolines and their inhibitory potencies against MDCK BCRP cells in Hoechst 33342 and Pheophorbide A accumulation assays.

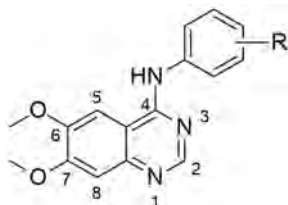


4-Anilinoquinazolines (127-131)

Compd	R	Hoechst 33342 assay	Pheophorbide A assay
		IC ₅₀ ± SD (μM)*	IC ₅₀ ± SD (μM)*
127	3-Br	1.08 ± 0.25	1.48 ± 0.19
128	3-CN	1.18 ± 0.24	2.03 ± 0.55
129	3-NO ₂	1.13 ± 0.37	0.89 ± 0.14
130	3-CF ₃	0.94 ± 0.19	1.55 ± 0.33
131	3,4-OCH ₃	4.79 ± 0.87	3.38 ± 0.76

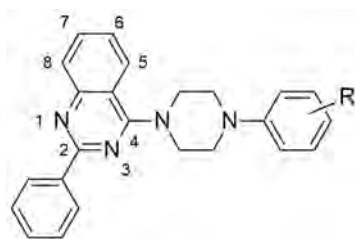
* Data are expressed as mean ± SD (n = 3).

The fifth modification consisted of a piperazine ring instead of an amine linker at position 4 of the quinazoline. The IC₅₀ values for 4-*N*-piperazinylquinazolines (**139-145**) are given in Table 5.5. It was observed that, all compounds with *N*-phenyl-piperazinyl substitution at position 4 showed highly reduced inhibitory activity when compared to compounds **98-115** having the same 2-phenylquinazoline scaffold. This reduction in activity might result from the change in the length and type of the linker at position 4 of quinazoline scaffold, leading to differences in the spacial arrangement of the substituted phenyl ring.

Table 5.4: Synthesized 6,7-dimethoxy-4-anilinoquinazolines and their inhibitory potencies against MDCK BCRP cells in Hoechst 33342 and pheophorbide A accumulation assays.**6,7-Dimethoxy-4-anilinoquinazolines (132-138)**

Compd	R	Hoechst 33342 assay	Pheophorbide A assay
		IC ₅₀ ± SD (μM)*	IC ₅₀ ± SD (μM)*
132	3-Br	1.73 ± 0.15	2.32 ± 0.70
133	3-CF ₃	2.40 ± 0.79	1.98 ± 0.42
134	3-CN	1.06 ± 0.12	0.93 ± 0.06
135	2-NO ₂	3.80 ± 0.53	3.97 ± 0.61
136	3-NO ₂	0.81 ± 0.06	0.91 ± 0.36
137	4-NO ₂	2.92 ± 0.39	2.46 ± 0.50
138	3,4-OCH ₃	7.38 ± 2.19	3.79 ± 0.27

* Data are expressed as mean ± SD (n = 3).

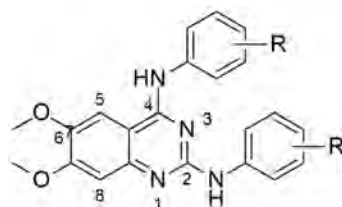
Table 5.5: Synthesized 4-*N*-piperazinylquinazolines and their inhibitory potencies against MDCK BCRP cells in Hoechst 33342 and pheophorbide A accumulation assays.**4-*N*-Piperazinylquinazolines (139-145)**

Compd	R	Hoechst 33342 assay	Pheophorbide A assay
		IC ₅₀ ± SD (μM)*	IC ₅₀ ± SD (μM)*
139	H	8.92 ± 1.82	9.05 ± 1.32
140	3-Br	5.12 ± 0.57	4.98 ± 0.32
141	3-Cl	5.91 ± 1.73	4.87 ± 0.56
142	3-Cl,4-F	8.22 ± 1.36	10.12 ± 1.58
143	3-OCH ₃	8.90 ± 2.35	9.23 ± 1.97
144	3-NO ₂	7.95 ± 0.35	6.99 ± 1.02
145	4-NO ₂	9.35 ± 2.79	8.05 ± 1.78

* Data are expressed as mean ± SD (n = 3).

The last modification carried out included compounds bearing 2,4-bis-anilino substituents at the quinazoline scaffold. Compounds **146-150** bear the same substituent at position 2 and 4 of the quinazoline. The IC_{50} values obtained for these compounds in Hoechst 33342 and pheophorbide A assays are given in Table 5.6. The major problem occurring while testing these compound was their poor aqueous solubility. For testing these compounds, a slightly higher amount of methanol (not more than 5 % in highest concentration) was used. These compounds were also found to be good inhibitors of BCRP with submicromolar IC_{50} values. As it can be seen from Table 5.6, the compound with 3-nitro substituent on the aniline (**149**) yielded lower IC_{50} values over other substituents. Despite of good inhibitory activity of these compounds, low solubility limits their further use.

Table 5.6: Synthesized N^2,N^4 -disubstituted quinazolines and their inhibitory potencies against MDCK BCRP cells in Hoechst 33342 and pheophorbide A accumulation assays.



N^2,N^4 -Disubstituted quinazoline (146-150)

Compd	R	Hoechst 33342 assay	Pheophorbide A assay
		$IC_{50} \pm SD (\mu M)^*$	$IC_{50} \pm SD (\mu M)^*$
146	3-Br	0.67 ± 0.10	0.86 ± 0.14
147	3-CF ₃	0.80 ± 0.02	0.61 ± 0.15
148	3-CN	0.48 ± 0.04	0.47 ± 0.03
149	3-NO ₂	0.33 ± 0.08	0.32 ± 0.06
150	3,4-OCH ₃	1.74 ± 0.26	1.52 ± 0.30
Ko143	-	0.25 ± 0.02	0.33 ± 0.05

* Data are expressed as mean \pm SD (n = 3).

After comparing all the modifications it can be concluded that the presence of 2-phenyl substitution led to strong increase in BCRP inhibition. In all types of quinazolines synthesized, compounds bearing *meta* substitution on the 4-anilino ring of anilinoquinazoline were the most active. When the activity data of compounds

127-131 and **132-138** were compared, it was observed that, substitution at position 6 and 7 of the quinazoline scaffold did not lead to an increase in the activity. This suggests that substitution at position 6 and 7 of the quinazoline is not needed for BCRP inhibition, although substitution at position 2 is desirable. A summary of structural features of the quinazoline scaffold for BCRP inhibition is given in Figure 5.5

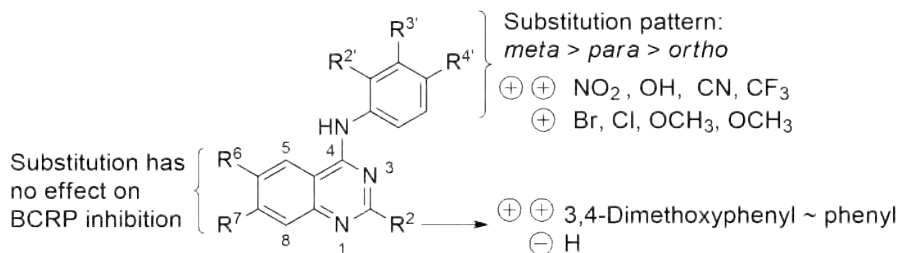


Figure 5.5: Structural features of quinazolines as BCRP inhibitors. ⊕ : showed good activity, ⊕⊕ : showed very high activity, ⊖ : led to decrease in activity.

Compounds **116-150** were investigated in both Hoechst 33342 and Pheophorbide A assays. The comparison of the pIC₅₀ values obtained using these two different substrates gave a good correlation with squared correlation coefficient (r^2) of 0.94. The scatterplot obtained by plotting pIC₅₀ values in the Hoechst33342 assay against the pheophorbide A assay is shown in Figure 5.6.

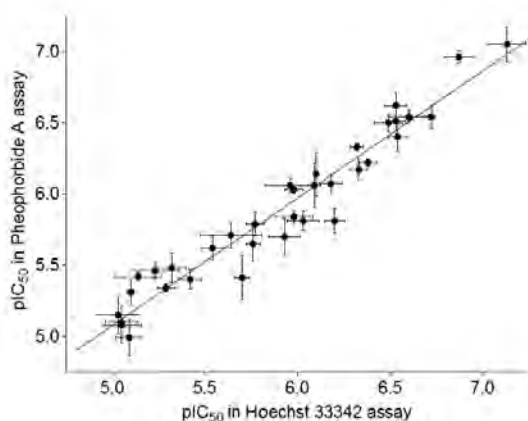
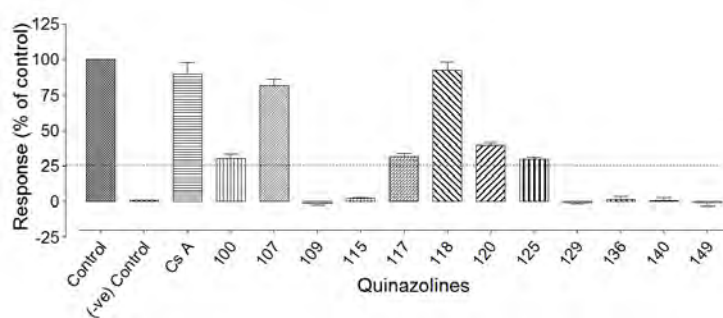


Figure 5.6: Scatterplot of pIC₅₀ values for BCRP inhibition obtained in the Hoechst 33342 assay and the pheophorbide A assay. Each point indicates mean of IC₅₀ values obtained in three independent experiments and error bars indicate standard deviation. The squared correlation coefficient is $r^2 = 0.94$, $n = 36$.

5.3.2 P-gp and MRP1 inhibition by quinazolines

In the current study, all investigated compounds were found to be active against BCRP. In order to check the selectivity of quinazolines towards BCRP inhibition, selected most potent compounds from each class were investigated for P-gp and MRP1 inhibition in the calcein AM assay. The principle of the calcein AM assay is described in section 3.3.2 and section 7.2.3.3. Screening of selected compounds (see Figure 5.7 for compound numbers) was done at a concentration of $10 \mu\text{M}$, in the calcein AM assay using A2780 adr (for P-gp) and 2008 MRP1 (for MRP1) cell lines. Cyclosporine A ($10 \mu\text{M}$) was used as a standard for both P-gp and MRP1 inhibition. The data of the investigated compounds are expressed as % response obtained in sensitive cells (positive control), while the response obtained in absence of any compound was used as negative control.

A)



B)

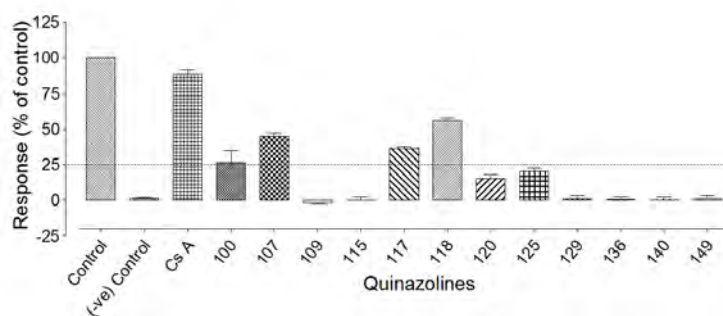


Figure 5.7: Influence of quinazolines at $10 \mu\text{M}$ concentration on accumulation of calcein AM in P-gp (A) and MRP1 (B) overexpressing cells. Cyclosporine A (CsA, $10 \mu\text{M}$) was used as a standard. Response in absence of any compound was used as negative control. Data are expressed as response in percentage of control (accumulation of calcein AM in non P-gp or MRP1 expressing sensitive cells) and presented as the mean \pm SD of three independent experiments.

As seen from Figure 5.7 most of the compounds showed very low inhibitory activity against P-gp and MRP1. Only compounds bearing a 3,4-dimethoxy substitution on the anilino ring of anilinoquinazolines showed more than 50 % inhibition when compared to control. Amongst the most potent BCRP inhibitors, compounds **109** and **115** showed no effect on both P-gp and MRP1, while compounds **120** and **125** showed little effect on P-gp and even less on MRP1. The effect of compounds **120** and **125** on P-gp could be due to the presence of 3,4-dimethoxy substitution on the 2-phenyl ring of these quinazolines. Compounds showing response of more than 25 % of the control were further investigated to determine their IC₅₀ values and these are given in Table 5.7.

Table 5.7: Inhibitory potencies of selected quinazolines using A2780 and 2008 MRP1 cells in the calcein AM assay. Data are expressed as mean \pm SD (n=3). Cyclosporine A was used as standard.

Compd	A2780 adr IC ₅₀ \pm SD (μ M)	2008 MRP1 IC ₅₀ \pm SD (μ M)
100	12.38 \pm 1.72	n.a.*
107	5.85 \pm 0.79	11.18 \pm 0.58
117	11.76 \pm 1.03	14.09 \pm 1.65
118	3.49 \pm 0.23	7.82 \pm 0.62
120	9.56 \pm 0.81	n.a.
125	18.21 \pm 2.10	n.a.
Cyclosporine A	0.92 \pm 0.12	2.70 \pm 0.58

* n.a. = not active, showing a response of less than 25 % of control in screening at 10 μ M concentration (see Figure 5.7).

5.3.3 Intrinsic cytotoxicity of selected quinazolines

Quinazoline compounds have been shown to be inhibitors of tyrosine kinases [215–219]. Tyrosine kinases play an important role in a variety of normal cellular regulatory processes and tyrosine kinase inhibitors are typically used as anticancer agents. Quinazolines like gefitinib and erlotinib are the inhibitors of epidermal growth factor receptor (EGFR) tyrosine kinase, and are marketed for the treatment of cancers with mutated and overactive EGFR (especially for nonsmall cell lung cancer) [220].

Interestingly, from the literature survey it was found that, quinazolines reported as

potent TKIs were lacking a 2-phenyl substitution and most of them possess substitution at position 6 and 7 [218, 221–224]. These findings were more interesting, as the most potent BCRP inhibitors found in the current study (**109**, **112**, **115**, **120** and **125**) lack substitution at position 6 and 7 and bear a phenyl ring at position 2 of the quinazoline scaffold. Despite these findings, it was important to check the possible intrinsic cytotoxicity of the synthesized compounds, as the aim of current study was to find potent and nontoxic inhibitors of BCRP. The cytotoxicity of compounds **109**, **115**, **120** and **125** was checked in MTT cytotoxicity assay. MTT assay was performed as described in section 3.3.3 and section 7.2.3.4. The toxicity studies of these compounds were performed using MDCK BCRP and sensitive MDCK cells. The concentration-response curves obtained are given in Figure 5.8.

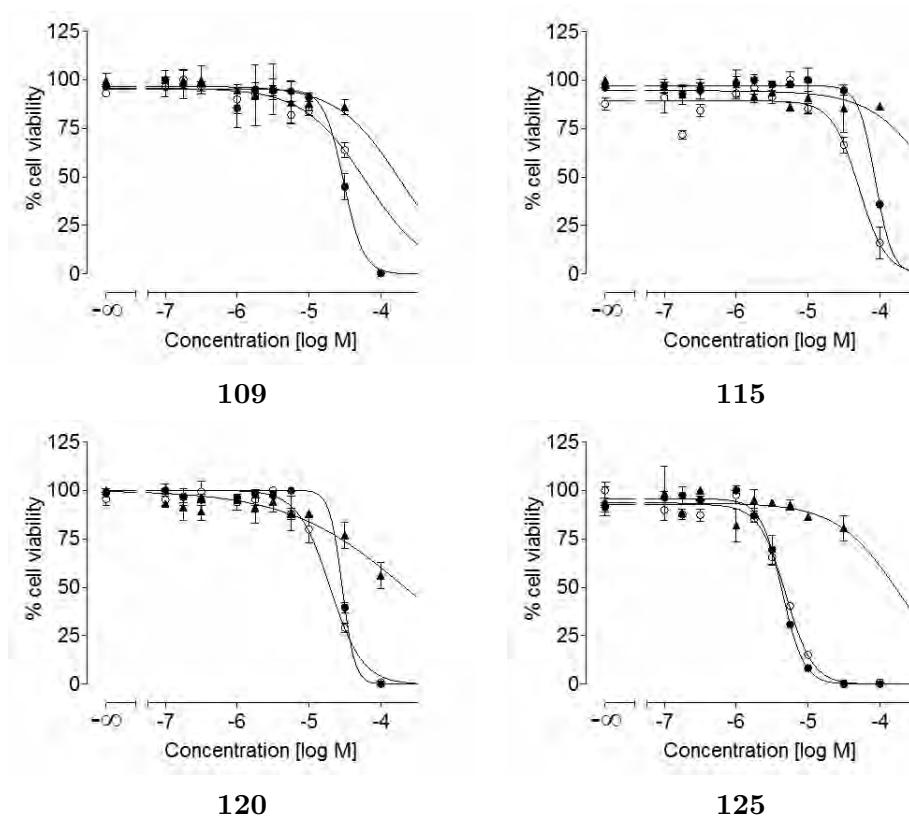


Figure 5.8: Cytotoxicity of selected compounds was determined in the MTT assay using MDCK BCRP and sensitive MDCK cells. Quinazolines **109**, **115**, **120** and **125** were investigated up to $100 \mu\text{M}$ concentration, for 72 h. Open circle: MDCK BCRP cells, closed circle: MDCK sensitive cells and closed triangle: dilution solvent (PBS) containing 2 % methanol in highest concentration.

From Figure 5.8 it can be seen that all four quinazolines tested showed a varying

amount of cytotoxicity. Especially compound **125** bearing 3-hydroxy-anilino substitution at position 4 of the 2-(3,4-dimethoxyphenyl)-4-anilinoquinazolines, showed high intrinsic cytotoxicity which could ultimately limiting from further *in vivo* investigations. In order to check usability of these compounds, therapeutic ratios were calculated from the IC₅₀ values obtained in Hoechst assay and GI₅₀ values from MTT assay using the following formula,

$$\text{Therapeutic ratio} = \frac{\text{GI}_{50}}{\text{IC}_{50}}$$

Table 5.8: Inhibitory activity and cytotoxicity of the most potent quinazolines

Compd	IC ₅₀ in Hoechst 33342 assay (μM)	GI ₅₀ in MTT assay (μM)*	Therapeutic ratio
109	0.13	67.8	521.5
115	0.15	51.11	340.7
120	0.076	20.8	273.7
125	0.14	4.61	32.9

* GI₅₀ values obtained using MDCK BCRP cells in MTT cytotoxicity assay

From the Table 5.8, it is clear that 2-phenyl-4-anilinoquinazolines **109** and **115** are promising BCRP inhibitors owing to their high therapeutic ratio. Compound **125** has the lowest therapeutic ratio, which limits its further use. Increase in the cytotoxicity of compounds **120** and **125** could be the result of extra 3,4-dimethoxy substituents on 2-phenyl ring of anilinoquinazolines.

5.3.4 MDR reversal ability of quinazolines

In all the tests described above, it was revealed that compounds **109** and **115** (belonging to the first series 2-phenyl-4-anilinoquinazolines) were selective inhibitors of BCRP with high therapeutic ratios. To determine the efficacy of these compounds to reverse MDR in BCRP overexpressing cells, MTT assays were performed. Here the ability of these two quinazolines (at 1 μM and 5 μM final concentrations) to reverse resistance to Hoechst 33342 and SN-38 was investigated.

Figure 5.9 shows the shift in the dose–response curves of SN-38 and Hoechst 33342 in MDCK BCRP cells in presence of compounds **109** and **115**. This shift in dose–response curves towards lower concentrations indicates sensitization of MDCK BCRP cells to cytotoxicity of SN-38 and Hoechst 33342. Both compounds were able to significantly reverse the resistance even at concentration as low as 1 μM and a complete reversal of resistance was observed at 5 μM concentration.

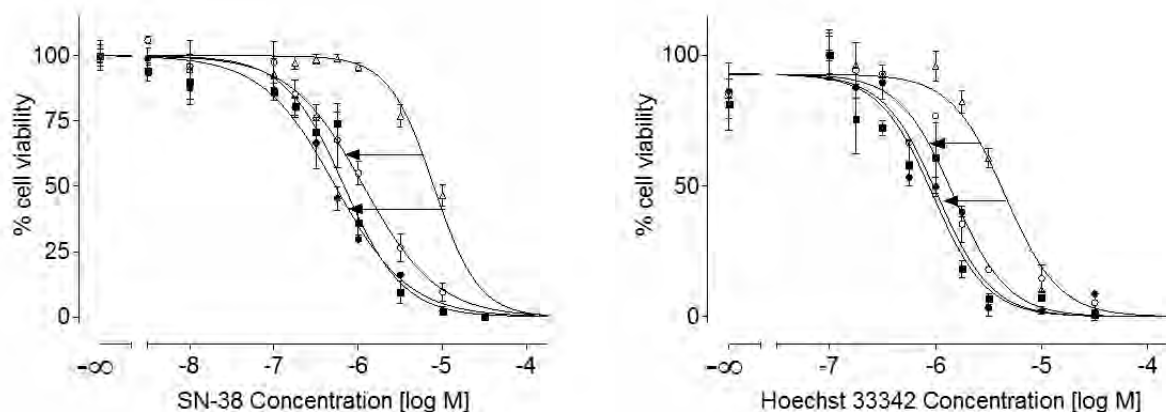


Figure 5.9: Representative dose–response curves of SN-38 and Hoechst 33342 cytotoxicity. Left: effect of compound **109** on SN-38 cytotoxicity in BCRP cells. Right: effect of compound **115** on cytotoxicity of Hoechst 33342. Both compounds were investigated at 1 μM (open circles) and 5 μM (closed circles) concentrations. BCRP cells without inhibitor (open triangles) showed less sensitivity towards SN-38 or Hoechst 33342, than sensitive cells (closed squares).

In summary, a total of 53 quinazoline derivatives spanning six different modifications were synthesized and investigated for BCRP, P-gp and MRP1 inhibition. Compounds bearing a 2-phenyl substituent in 4-anilinoquinazolines (**98-126**) were the most active amongst all variations. It was revealed that a *meta* substituted anilino group present at position 4 of the quinazoline nucleus resulted in increased activity. Nitro, cyano and hydroxy substituted compounds were found to be the most potent BCRP inhibitors. The 2-phenyl-4-anilinoquinazolines **109** and **115** were the most promising selective BCRP inhibitors with high therapeutic ratio. The inhibitory effect of these compounds was confirmed by testing their influence on the cytotoxicity of SN-38 and Hoechst 33342 in BCRP overexpressing cells.

Chapter

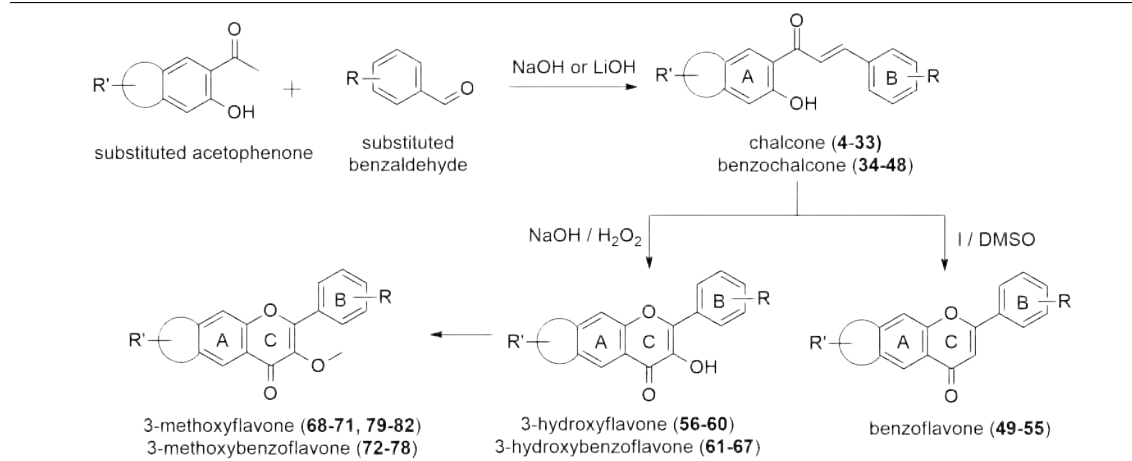
6 Summary

The main aim of the current study was to synthesize a library of structurally different classes of compounds to find new potent, selective and nontoxic BCRP inhibitors. In this work a total of 131 compounds spanning three different structural classes viz. chalcones, flavonoids and quinazolines were synthesized. Several biological studies were carried out using these compounds to determine their BCRP inhibitory potential, selectivity, toxicity and efficacy to reverse MDR to certain cytotoxic compounds.

In the first project a series of substituted chalcones, 3',4'-benzochalcones and 5',6'-benzochalcones were synthesized by the Claisen-Schmidt condensation reaction (see chapter 3). As depicted in Algorithm 6.1 the synthesis of various chalcones and benzochalcones was carried out from the corresponding substituted acetophenone and substituted benzaldehyde. Most of these compounds were synthesized in one step with varying degree of difficulty of formation of product. A classical method of synthesis of chalcones which involves stirring the reaction mixture at room temperature and use of NaOH as base, was modified for the synthesis of benzochalcones. The classical method was successfully replaced with ultrasonication and with the use of the strong base LiOH, which resulted in shorter reaction times. These substances were evaluated for their ability to inhibit BCRP in the Hoechst 33342 accumulation assay using MCF-7 MX and MDCK BCRP cells. Most of the compounds bearing multi-substitutions on ring A of the chalcone were found to be BCRP inhibitors. Chalcones were found to be more potent than 5',6'-benzochalcones followed by 3',4'-benzochalcones. The current study revealed the positive effect of methoxy groups on the inhibitory activity of these compounds. All active compounds were found to be selective towards BCRP

inhibition. Also, it was seen that most active compounds have very low cytotoxicity and these compounds are able to reverse the resistance to mitoxantrone and SN-38 in BCRP overexpressing MDCK cells. In this study the lead chalcones **11** ($IC_{50} = 0.85 \mu M$) and **28** ($IC_{50} = 0.53 \mu M$) bearing methoxy substitution on ring B were found to be both selective and potent inhibitors of BCRP.

Scheme 6.1 Synthesis of chalcones, benzochalcones, flavones and benzoflavones



The second project in this work involved synthesis and investigation of substituted flavones, 7,8-benzoflavones and 5,6-benzoflavones (see chapter 4). To study the effect of substitution at position 3 of flavonoid scaffold, 3-hydroxyflavones, 3-methoxyflavones, benzoflavones, 3-hydroxybenzoflavones and 3-methoxybenzoflavones were synthesized. The synthesis of these compounds was accomplished from the corresponding chalcones (Algorithm 6.1). Selected chalcones and benzochalcones were converted to 3-hydroxyflavones and 3-hydroxybenzoflavones which were subsequently converted to 3-methoxyflavones and 3-methoxybenzoflavones. The naturally occurring flavonoids quercetin and morin were converted to pentamethoxy and tetramethoxy derivatives to study the effect of hydroxy and methoxy substitution at position 5 of the flavonoid scaffold. Benzochalcones were also converted to benzoflavones with unsubstituted position 3. Out of all compounds 7,8-benzoflavones were found to be the most active BCRP inhibitors in the Hoechst 33342 and pheophorbide A assays. In contrast, 5,6-benzoflavones were the least active, which could be a result of blocking the position 5 of the flavonoid scaffold. The substitution at position 5 in flavones was shown to affect the activity, where hydroxy substitution was found to be better than methoxy substitution (see Figure 6.1). The positive effect of methoxy substitution and decremental effect of hydroxy substitution at position 3 of the flavonoid scaffold

was seen in both flavone and benzoflavone classes of investigated flavonoids. Some of the investigated compounds were found to inhibit P-gp and MRP1, although to a lesser extent. Compound **51**, a substituted 7,8-benzoflavone produced low IC_{50} values for all three transporters BCRP, P-gp and MRP1, suggesting its usability as a good broad spectrum MDR modulator. Compound **74** ($IC_{50} = 0.47 \mu M$), a 7,8-benzoflavone bearing methoxy substitution at positions 3, 3' and 4' was found to be the most potent and nontoxic flavonoid with 50 fold selectivity for BCRP. This compound was shown to be able to reverse the resistance to Hoechst 33342 in BCRP overexpressing cells.

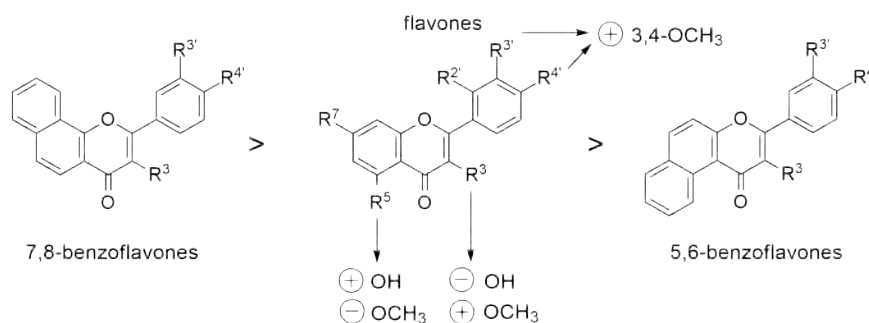
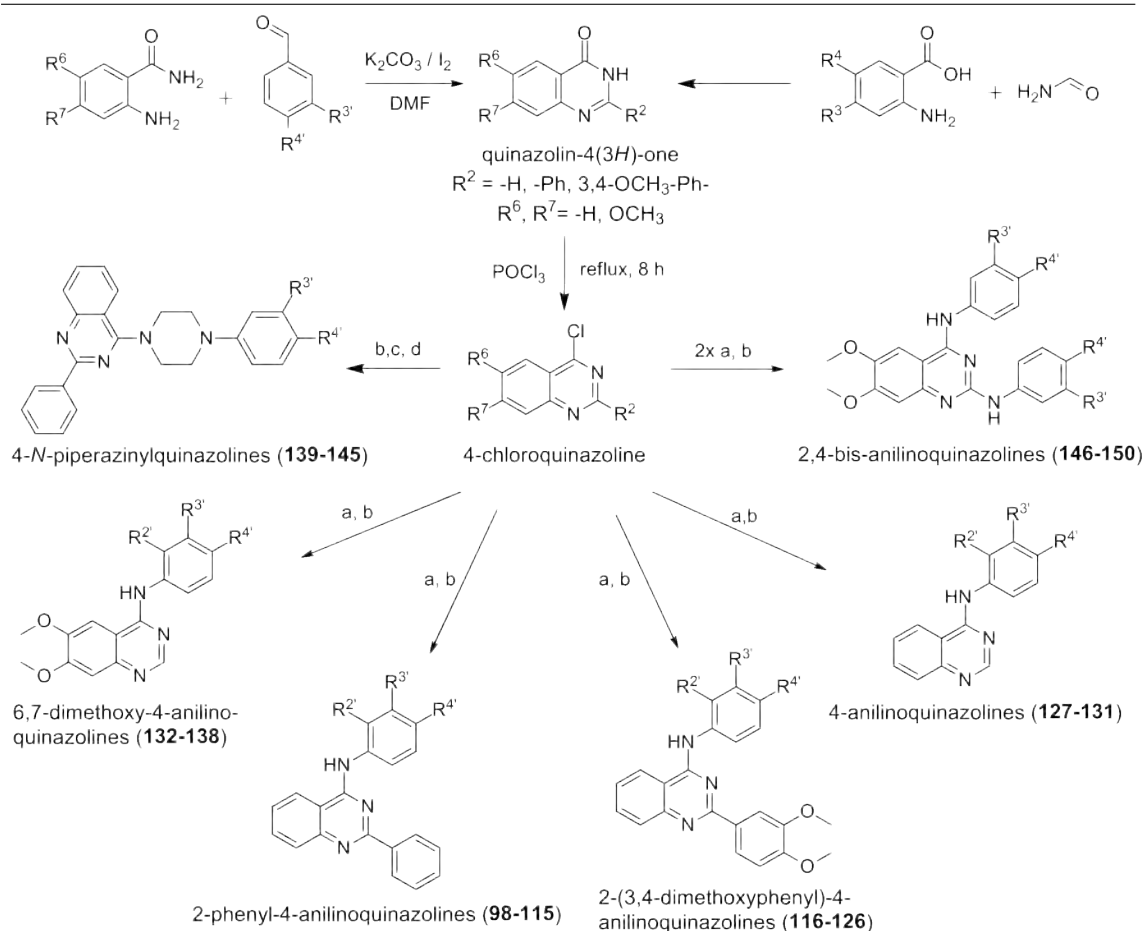


Figure 6.1: Overview of activity of flavonoids as BCRP inhibitors

The last series of compounds investigated in search for potent BCRP inhibitors consisted of quinazoline compounds (see chapter 5). Several substituted quinazolines spanning 6 different modifications at position 2, 4, 6 and 7 of the quinazoline scaffold were synthesized. Most of the synthesized compounds bear anilino substitution at position 4 of the quinazoline nucleus. All the compounds were synthesized using different synthesis routes as depicted in Algorithm 6.2. The first step was the synthesis of substituted 4-quinazolinones which were further converted to 4-chloroquinazolines using $POCl_3$. Four different types of 4-chloroquinazolines were synthesized which were later reacted with a variety of anilines or *N*-phenylpiperazines to obtain six different classes of final quinazoline compounds.

From all types of compounds studied in this work, quinazolines were found to be the most potent inhibitors of BCRP. From the biological studies it could be suggested that 6,7-methoxy groups in quinazoline are not essential for the activity, however presence of a phenyl ring at position 2 is important. It was also found that *meta* substituted anilinoquinazolines were the most potent BCRP inhibitors. From a study of published and marketed tyrosine kinase inhibitors, it was found that they lack the 2-phenyl ring

Scheme 6.2 Summary of synthetic routes used to prepare quinazolines **98-150**. All the reactions were carried out under heating or refluxing conditions, where a: substituted aniline, b: isopropanol, c: substituted *N*-phenylpiperazine and d: potassium carbonate.



and that substitution at position 6 and 7 was essential for tyrosine kinase inhibition, which is in contrast to the structural requirements for BCRP inhibition. Although tyrosine kinase inhibition studies on synthesized compounds was not performed, it could be expected that these compounds will have lower inhibitory potential for tyrosine kinase. In this study compounds **109** ($\text{IC}_{50} = 0.13 \mu\text{M}$), and **115** ($\text{IC}_{50} = 0.15 \mu\text{M}$), both belonging to the 2-phenyl-4-anilinoquinazoline series, were found to be selective and highly potent inhibitors of BCRP with very high therapeutic ratios. These compounds had much lower IC_{50} values than Ko143 (the most potent inhibitor known until now, $\text{IC}_{50} = 0.25 \mu\text{M}$).

The results obtained from the study of chalcones, flavonoids and quinazolines as BCRP inhibitors are promising for the ongoing research to find potent BCRP

inhibitors. Especially, quinazoline lead compounds can be further investigated for their cytotoxicity in different cell lines and for the effect on tyrosine kinase, which could make *in vivo* studies possible.

7 Experimental work

7.1 Chemistry

7.1.1 General materials and methods

Chemicals: All chemicals were procured from Acros Organics (Geel, Belgium), Alfa Aesar (Karlsruhe, Germany), Sigma-Aldrich (Steinheim, Germany) or Merck (Darmstadt, Germany).

Chromatography:

Thin layer chromatography: During the synthesis, reaction progress was monitored using analytical thin layer chromatography (TLC) on silica gel plates (Silica Gel 60 F₂₅₄ from Merck). TLC plates were coated with silica gel containing fluorescent indicator, which on presence of compounds that absorb UV at 254 nm showed dark, quenched spots on a bright background. For detection, a UV cabinet with short-wave UV light source (254 nm) was used.

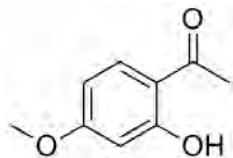
Column chromatography: For the purification of certain compounds column chromatography was performed. For this purpose chromatography columns of different size were selected depending on the yield of the compound. Silica gel 60 (40-63 μm) obtained from Merck, was used as stationary phase. For the preparation of the column, a slurry of silica gel was prepared in the selected mobile phase and was filled in a glass column with due care not to form any bubbles. After packing

the stationary phase, a thin layer of sea sand was applied, which was helpful to keep the stationary phase constant after loading a sample. Compound samples were first dissolved in a small amount of mobile phase before loading on to the column. Slight pressure was applied to column to increase the flow of mobile phase with aid of a hand pump. Collected fractions were checked by TLC and pure fractions were evaporated under reduced pressure to yield the solid compounds.

NMR-Spectroscopy and elemental analysis: Structures and purity of all compounds were confirmed by NMR and elemental analysis. NMR spectra were recorded in DMSO-d₆ or CDCl₃. ¹H NMR spectra were obtained on a Bruker Advance 500 (500 MHz); ¹³C NMR, Bruker Advance 500 (126 MHz); chemical shifts are expressed in δ values (ppm) using the solvent peak as an internal standard (DMSO-d₆ 2.49/39.7 ppm or CDCl₃ 7.26/77.0 ppm); multiplicity of resonance peaks is indicated as singlet (s), doublet (d), triplet (t), quartet (q) and multiplet (m). The ¹³C signals were assigned with the aid of distortion less enhancement by polarization transfer (DEPT) and attached proton test (APT), the *J* values are in Hertz. Elemental analyses were performed on a Vario EL of Elementar (Hanau, Germany). The values for carbon, nitrogen and hydrogen are given in percentage. Found values were all within ± 0.4 % of the theoretical values except when indicated.

7.1.2 General synthesis procedures

7.1.2.1 Synthesis of 2-hydroxy-4-methoxyacetophenone (1)



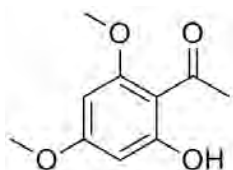
A mixture of 2,4-dihydroxyacetophenone (6 g, 39.5 mmol), dimethyl sulfate (4.1 ml, 43.4 mmol) and potassium carbonate (8.2 g, 59.2 mmol) in 100 ml acetone was stirred at room temperature for 6 h. After completion of the reaction as indicated by TLC, the solid was filtered off and the solvent was evaporated. The residue was chromatographed over silica gel column using petroleum ether/ethylacetate (9:1) as mobile phase to yield 2-hydroxy,4-methoxyacetophenone (5.2 g, 80 %) as white solid.

Molecular weight: 166.17 g/mol

^1H NMR (DMSO- d_6) δ : 12.62 (s, 1H), 7.82 (d, J = 8.9 Hz, 1H), 6.51 (dd, J = 8.9, 2.5 Hz, 1H), 6.33 (d, J = 2.5 Hz, 1H), 3.80 (s, 3H), 2.55 (s, 3H).

^{13}C NMR (DMSO- d_6) δ : 203.09, 165.79, 164.28, 133.33, 113.97, 107.24, 100.87, 55.78, 26.77.

7.1.2.2 Synthesis of 4,6-dimethoxy-2-hydroxyacetophenone (2)



To a refluxing mixture of 2,4,6-trihydroxyacetophenone-monohydrate (5 g, 26.8 mmol) and potassium carbonate (7.5 g, 54.3 mmol) in 50 ml acetone, dimethyl sulfate was added at 3 h intervals (3 x 1.75 ml, 20 mmol). The reaction was refluxed for 15 h

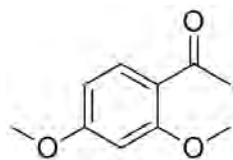
until it was complete. The solid was filtered off and the solvent was evaporated to yield 4,6-dimethoxy-2-hydroxyacetophenone (4.2 g, 80 %) as yellow solid.

Molecular weight: 196.20 g/mol

^1H NMR (DMSO- d_6) δ : 13.74 (s, 1H), 6.10 (d, $J = 2.4$ Hz, 1H), 6.06 (d, $J = 2.4$ Hz, 1H), 3.80 (s, 3H), 3.73 (s, 3H), 2.53 (s, 3H).

^{13}C NMR (DMSO- d_6) δ : 202.91, 166.28, 162.93, 162.02, 157.58, 93.81, 91.15, 56.17, 55.96, 28.81.

7.1.2.3 Synthesis of 2,4-dimethoxyacetophenone (3)



To a mixture of 2,4-dihydroxyacetophenone (6 g, 39.5 mmol) and potassium carbonate (8.2 g, 59.2 mmol) in 100 ml acetone, methyl iodide (6.2 ml, 100 mmol) was added. The resulting reaction mixture was refluxed for 24 h. After completion of the reaction as indicated by TLC, the solid was filtered off and the solvent was evaporated under reduced pressure. The resulting solid was recrystallized from ethanol to yield 2,4-dimethoxyacetophenone (5.95 g, 84 %) as yellow solid.

Molecular weight: 180.20 g/mol

^1H NMR (DMSO- d_6) δ : 7.80 (d, $J = 7.6$ Hz, 1H), 6.82 – 6.73 (m, 2H), 3.59 (d, $J = 7.2$ Hz, 6H), 2.35 (s, 3H).

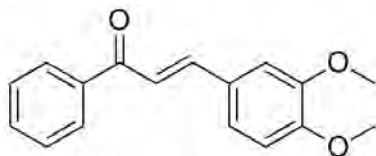
^{13}C NMR (DMSO- d_6) δ : 202.91, 166.28, 162.93, 162.02, 157.58, 93.81, 91.15, 56.17, 55.96, 28.81.

7.1.2.4 General procedure for synthesis of chalcones

To a previously cooled mixture of 5 mmol of the selected acetophenone and 5 mmol of a selected benzaldehyde in 25 ml ethanol, 20 % NaOH (5 ml) was added drop-wise

under vigorous stirring. The mixture was stirred at room temperature for 24–72 h. After completion of the reaction as indicated by TLC, the mixture was poured onto crushed ice and acidified with dilute HCl. Precipitated product was filtered by suction and washed to neutral. The solid was recrystallized from dilute ethanol to yield the chalcone

(E)-3-(3,4-Dimethoxyphenyl)-1-phenylprop-2-en-1-one (4)



Synthesized from acetophenone and 3,4-dimethoxybenzaldehyde, yield 61 %.

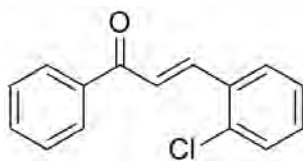
Molecular weight: 268.31 g/mol

^1H NMR (CDCl_3) δ : 7.90 (d, $J = 15.1$ Hz, 1H), 7.80 (dd, $J = 7.4, 1.4$ Hz, 2H), 7.54 (dd, $J = 13.6, 11.3$ Hz, 2H), 7.46 (t, $J = 7.4$ Hz, 2H), 7.21–7.16 (m, 2H), 6.99 (d, $J = 7.4$ Hz, 1H), 3.82 (d, $J = 21.9$ Hz, 6H).

^{13}C NMR (CDCl_3) δ : 191.02, 150.98, 150.02, 144.78, 139.01, 133.69, 130.20, 129.13, 128.52, 123.94, 123.01, 112.69, 111.32, 55.94, 56.15.

Anal. Calcd for $\text{C}_{17}\text{H}_{16}\text{O}_3 \cdot 0.2 \text{H}_2\text{O}$: C, 65.03; H, 9.30. Found: C, 65.21; H, 9.16.

(E)-3-(2-Chlorophenyl)-1-phenylprop-2-en-1-one (5)



Synthesized from acetophenone and 2-chlorobenzaldehyde, yield 64 %.

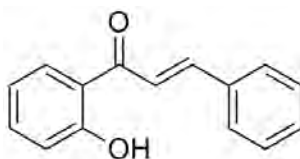
Molecular weight: 242.70 g/mol

^1H NMR (CDCl_3) δ : d 7.97 (d, $J = 14.9$ Hz, 1H), 7.69 (dd, $J = 7.3, 1.5$ Hz, 2H), 7.52–7.49 (m, 1H), 7.48–7.39 (m, 4H), 7.37 (d, $J = 14.8$ Hz, 1H), 7.34–7.25 (m, 2H).

^{13}C NMR (CDCl_3) δ 191.56, 140.83, 138.01, 132.95, 132.04, 131.48, 130.91, 129.14, 128.18, 127.85, 128.15, 127.08, 125.72.

Anal. Calcd for $\text{C}_{15}\text{H}_{11}\text{ClO}$: C, 74.23; H, 4.57. Found: C, 74.08; H, 4.62.

(*E*)-1-(2-Hydroxyphenyl)-3-phenylprop-2-en-1-one (6)



Synthesized from 2-hydroxyacetophenone and benzaldehyde, yield 69 %.

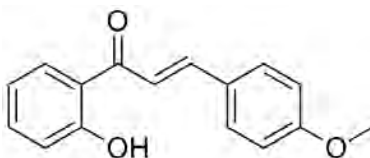
Molecular weight: 224.25 g/mol

^1H NMR (DMSO-d_6) δ : 12.45 (s, 1H), 8.24 (dd, 1H), 8.02 (d, $J = 15.6$ Hz, 1H), 7.92–7.88 (m, 2H), 7.84 (d, $J = 15.6$ Hz, 1H), 7.56 (ddd, $J = 8.4, 7.2, 1.7$ Hz, 1H), 7.48–7.45 (m, 3H), 7.03–6.98 (m, 2H).

^{13}C NMR (DMSO-d_6) δ : 193.75, 161.94, 144.87, 136.42, 134.58, 131.07, 131.00, 129.26, 129.08, 121.99, 120.93, 119.29, 117.85.

Anal. Calcd for $\text{C}_{15}\text{H}_{12}\text{O}_2$: C, 80.34; H, 5.39. Found: C, 80.51; H, 5.28.

(*E*)-1-(2-Hydroxyphenyl)-3-(4-methoxyphenyl)prop-2-en-1-one (7)



Synthesized from 2-hydroxyacetophenone and 4-methoxybenzaldehyde, yield 78 %.

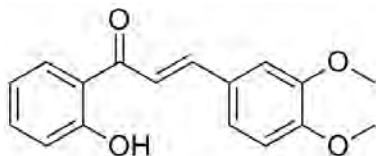
Molecular weight: 254.28 g/mol

^1H NMR (CDCl_3) δ : 12.92 (s, 1H), 7.92–7.88 (m, 2H), 7.61 (d, J = 8.7 Hz, 2H), 7.52 (d, J = 15.4 Hz, 1H), 7.47 (ddd, J = 8.6, 7.2, 1.6 Hz, 1H), 7.01 (dd, J = 8.4, 1.1 Hz, 1H), 6.94 (d, J = 8.8 Hz, 2H), 6.93–6.90 (m, 1H), 3.85 (s, 3H).

^{13}C NMR (CDCl_3) δ : 193.64, 163.52, 162.00, 145.32, 136.11, 130.52, 129.50, 127.33, 120.10, 118.72, 118.56, 117.58, 114.50, 55.43.

Anal. Calcd for $\text{C}_{16}\text{H}_{14}\text{O}_3$: C, 75.57; H, 5.55. Found: C, 75.24; H, 5.72.

(*E*)-3-(3,4-Dimethoxyphenyl)-1-(2-hydroxyphenyl)prop-2-en-1-one (8)



Synthesized from 2-hydroxyacetophenone and 3,4-dimethoxybenzaldehyde, yield 75 %.

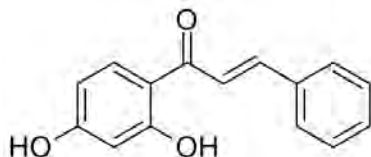
Molecular weight: 284.31 g/mol

^1H NMR (CDCl_3) δ : 12.89 (s, 1H), 7.91 (dd, J = 8.1, 1.6 Hz, 1H), 7.87 (d, J = 15.4 Hz, 1H), 7.50–7.46 (m, 1H), 7.27–7.23 (m, 1H), 7.15 (d, J = 2.0 Hz, 1H), 7.02 (d, J = 1.1 Hz, 1H), 7.00 (d, J = 1.1 Hz, 1H), 6.95–6.88 (m, 2H), 3.94 (d, J = 12.6 Hz, 6H).

^{13}C NMR (CDCl_3) δ : 193.54, 163.51, 151.79, 149.29, 145.62, 136.13, 129.49, 127.57, 123.56, 120.06, 118.69, 118.58, 117.77, 111.14, 110.26, 56.00, 55.98.

Anal. Calcd for $\text{C}_{17}\text{H}_{16}\text{O}_4$: C, 71.82; H, 5.67. Found: C, 71.79; H, 5.48.

(*E*)-1-(2,4-Dihydroxyphenyl)-3-phenylprop-2-en-1-one (9)



Synthesized from 2,4-dihydroxyacetophenone and benzaldehyde, yield 64 %.

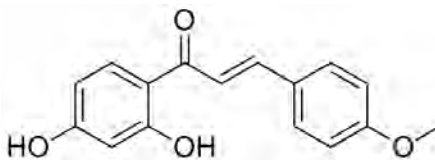
Molecular weight: 240.25 g/mol

^1H NMR (DMSO- d_6) δ : 13.35 (s, 1H), 8.19 (d, J = 9.0 Hz, 1H), 7.96 (d, J = 15.4 Hz, 1H), 7.85 (dd, J = 6.7, 3.2 Hz, 2H), 7.70 (d, J = 15.5 Hz, 1H), 7.46 (dd, J = 5.0, 1.9 Hz, 3H), 6.42 (dd, J = 8.9, 2.4 Hz, 1H), 6.30 (d, J = 2.4 Hz, 1H).

^{13}C NMR (DMSO- d_6) δ : 191.61, 165.93, 165.41, 143.75, 134.75, 133.28, 130.78, 129.36, 129.11, 129.03, 128.65, 121.46, 113.18, 108.41, 102.73.

Anal. Calcd for $\text{C}_{15}\text{H}_{12}\text{O}_3$: C, 74.99; H, 5.03. Found: C, 75.06; H, 5.16.

(*E*)-1-(2,4-Dihydroxyphenyl)-3-(4-methoxyphenyl)prop-2-en-1-one (10)



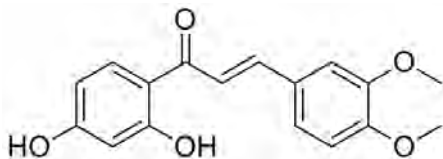
Synthesized from 2,4-dihydroxyacetophenone and 4-methoxybenzaldehyde, yield 79 %.

Molecular weight: 270.28 g/mol

^1H NMR (DMSO- d_6) δ : 13.51 (s, 1H), 10.64 (s, 1H), 8.17 (d, J = 9.0 Hz, 1H), 7.85 (d, J = 8.8 Hz, 2H), 7.79 (d, J = 14.4 Hz, 1H), 7.12 (d, J = 8.7 Hz, 1H), 7.02 (d, J = 8.8 Hz, 2H), 6.41 (dd, J = 8.9, 2.4 Hz, 1H), 6.28 (d, J = 2.4 Hz, 1H), 3.82 (s, 3H).

^{13}C NMR (DMSO- d_6) δ : 191.66, 165.93, 165.17, 161.62, 143.86, 133.09, 131.97, 131.09, 127.43, 118.74, 114.66, 114.58, 113.17, 108.27, 102.73, 55.56.

Anal. Calcd for $\text{C}_{16}\text{H}_{14}\text{O}_4$: C, 71.10; H, 5.22. Found: C, 71.50; H, 4.96.

(E)-1-(2,4-Dihydroxyphenyl)-3-(3,4-dimethoxyphenyl)prop-2-en-1-one (11)

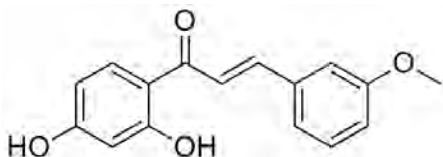
Synthesized from 2,4-dihydroxyacetophenone and 3,4-dimethoxybenzaldehyde, yield 72 %.

Molecular weight: 300.31 g/mol

^1H NMR (DMSO- d_6) δ : 13.55 (s, 1H), 8.20 (d, $J = 9.0$ Hz, 1H), 7.79 (dd, $J = 40.4$, 15.4 Hz, 2H), 7.54 (d, $J = 2.0$ Hz, 1H), 7.38 (dd, $J = 8.4$, 1.9 Hz, 1H), 7.02 (d, $J = 8.4$ Hz, 1H), 6.42 (dd, $J = 8.9$, 2.4 Hz, 1H), 6.28 (d, $J = 2.4$ Hz, 1H), 3.84 (d, $J = 22.4$ Hz, 6H).

^{13}C NMR (DMSO- d_6) δ : 191.68, 165.97, 165.18, 151.59, 149.22, 144.41, 133.12, 127.59, 124.40, 118.73, 113.15, 111.74, 111.02, 108.22, 102.74, 55.93, 55.77.

Anal. Calcd for $\text{C}_{17}\text{H}_{16}\text{O}_5$: C, 67.99; H, 5.37. Found: C, 67.73; H, 5.51.

(E)-1-(2,4-Dihydroxyphenyl)-3-(3-methoxyphenyl)prop-2-en-1-one (12)

Synthesized from 2,4-dihydroxyacetophenone and 3-methoxybenzaldehyde, yield 67 %.

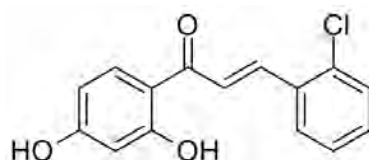
Molecular weight: 270.28 g/mol

^1H NMR (DMSO- d_6) δ : 13.11 (s, 1H), 8.08 (d, $J = 8.2$ Hz, 1H), 7.84 (d, $J = 15.3$ Hz, 1H), 7.61 (d, $J = 15.3$ Hz, 1H), 7.54–6.58 (m, 6H), 3.89 (s, 3H).

^{13}C NMR (DMSO- d_6) δ : 191.66, 165.93, 165.17, 161.62, 143.86, 133.09, 131.97, 131.09, 127.43, 118.74, 114.66, 114.58, 113.17, 108.27, 102.73, 55.56.

Anal. Calcd for $\text{C}_{16}\text{H}_{14}\text{O}_4$: C, 71.10; H, 5.22. Found: C, 70.89; H, 5.37.

(E)-3-(2-Chlorophenyl)-1-(2,4-dihydroxyphenyl)prop-2-en-1-one (13)



Synthesized from 2,4-dihydroxyacetophenone and 2-chlorobenzaldehyde, yield 81%.

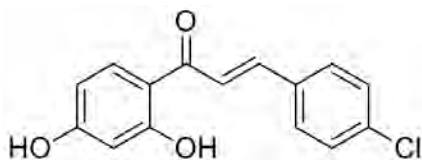
Molecular weight: 274.70 g/mol

^1H NMR (DMSO- d_6) δ : 13.17 (s, 1H), 10.79 (s, 1H), 8.21 (dd, $J = 7.3, 2.2$ Hz, 1H), 8.18 (d, $J = 9.0$ Hz, 1H), 8.09 (d, $J = 15.5$ Hz, 1H), 8.01 (d, $J = 15.5$ Hz, 1H), 7.56 (dd, $J = 7.7, 1.6$ Hz, 1H), 7.46 (ddd, $J = 6.2, 4.4, 1.2$ Hz, 2H), 6.43 (dd, $J = 8.9, 2.4$ Hz, 1H), 6.31 (d, $J = 2.4$ Hz, 1H).

^{13}C NMR (DMSO- d_6) δ : 191.15, 165.99, 165.70, 138.16, 134.53, 133.49, 132.41, 132.18, 130.21, 128.88, 127.84, 124.40, 113.24, 108.61, 102.80.

Anal. Calcd for $\text{C}_{15}\text{H}_{11}\text{ClO}_3$: C, 65.58; H, 4.04. Found: C, 65.39; H, 4.19.

(E)-3-(4-Chlorophenyl)-1-(2,4-dihydroxyphenyl)prop-2-en-1-one (14)



Synthesized from 2,4-dihydroxyacetophenone and 4-chlorobenzaldehyde, yield 84 %.

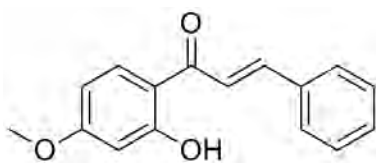
Molecular weight: 274.70 g/mol

^1H NMR (DMSO- d_6) δ : 12.58 (s, 1H), 10.58 (s, 1H), 7.95–7.90 (m, 2H), 7.73 (dd, J = 8.9, 5.2 Hz, 1H), 7.55 (d, J = 8.7 Hz, 1H), 7.52 (d, J = 8.5 Hz, 1H), 7.39–7.29 (m, 2H), 6.36 (dd, J = 8.8, 2.4 Hz, 1H), 6.23 (d, J = 2.3 Hz, 1H).

^{13}C NMR (DMSO- d_6) δ : 202.78, 165.00, 164.33, 142.26, 137.90, 133.80, 131.25, 129.81, 128.85, 122.28, 113.01, 108.23, 102.43.

Anal. Calcd for $\text{C}_{15}\text{H}_{11}\text{ClO}_3$: C, 65.58; H, 4.0. Found: C, 65.52; H, 4.21.

(*E*)-1-(2-Hydroxy-4-methoxyphenyl)-3-phenylprop-2-en-1-one (15)



Synthesized from 2-hydroxy-4-methoxyacetophenone and benzaldehyde, yield 62 %.

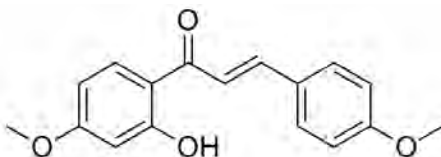
Molecular weight: 254.28 g/mol

^1H NMR (DMSO- d_6) δ : 13.49 (s, 1H), 7.95 (d, J = 15.1 Hz, 1H), 7.63 (d, J = 1.7 Hz, 1H), 7.61 (d, J = 9.3 Hz, 1H), 7.56–7.53 (m, 2H), 7.43–7.35 (m, 3H), 6.65 (dd, J = 7.6, 1.4 Hz, 1H), 6.61 (d, J = 1.6 Hz, 1H), 3.87 (s, 3H).

^{13}C NMR (DMSO- d_6) δ : 192.78, 165.22, 164.48, 144.23, 135.03, 130.98, 129.17, 128.88, 129.87, 128.07, 128.07, 122.22, 114.91, 106.23, 101.47, 56.04.

Anal. Calcd for $\text{C}_{16}\text{H}_{14}\text{O}_3$: C, 75.57; H, 5.55. Found: C, 75.62; H, 5.39.

(*E*)-1-(2-Hydroxy-4-methoxyphenyl)-3-(4-methoxyphenyl)prop-2-en-1-one (16)



Synthesized from 2-hydroxy-4-methoxyacetophenone and 4-methoxybenzaldehyde, yield 71 %.

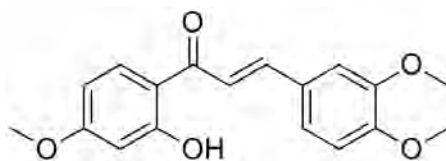
Molecular weight: 284.31 g/mol

^1H NMR (DMSO- d_6) δ : 13.56 (s, 1H), 8.26 (d, J = 9.1 Hz, 1H), 7.87 (d, J = 8.8 Hz, 2H), 7.85 (s, 1H), 7.81 (s, 1H), 7.02 (d, J = 8.8 Hz, 2H), 6.55 (dd, J = 9.0, 2.5 Hz, 1H), 6.50 (d, J = 2.5 Hz, 1H), 3.83 (d, J = 8.1 Hz, 6H).

^{13}C NMR (DMSO- d_6) δ : 192.04, 165.99, 165.85, 161.72, 144.38, 132.67, 131.22, 127.36, 118.65, 114.59, 114.01, 107.43, 101.08, 55.87, 55.55.

Anal. Calcd for $\text{C}_{17}\text{H}_{16}\text{O}_4 \cdot 0.2 \text{H}_2\text{O}$: C, 71.20; H, 5.91. Found: C, 71.14; H, 5.69.

(*E*)-3-(3,4-Dimethoxyphenyl)-1-(2-hydroxy-4-methoxyphenyl)prop-2-en-1-one (17)



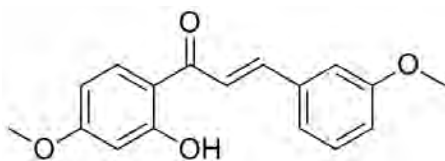
Synthesized from 2-hydroxy-4-methoxyacetophenone and 3,4-dimethoxybenzaldehyde, yield 89 %.

Molecular weight: 314.33 g/mol

^1H NMR (DMSO- d_6) δ : 13.61 (s, 1H), 8.28 (d, J = 9.1 Hz, 1H), 7.87 (d, J = 15.3 Hz, 1H), 7.79 (d, J = 15.3 Hz, 1H), 7.56 (d, J = 2.0 Hz, 1H), 7.41 (dd, J = 8.4, 1.9 Hz, 1H), 7.03 (d, J = 8.4 Hz, 1H), 6.56 (dd, J = 9.0, 2.5 Hz, 1H), 6.51 (d, J = 2.5 Hz, 1H), 3.87–3.81 (m, 9H).

^{13}C NMR (DMSO- d_6) δ : 192.07, 166.00, 165.94, 151.72, 149.23, 144.93, 132.69, 127.54, 124.55, 118.66, 113.98, 111.75, 111.14, 107.46, 101.04, 55.95, 55.88, 55.78.

Anal. Calcd for $\text{C}_{18}\text{H}_{18}\text{O}_5 \cdot 0.25 \text{H}_2\text{O}$: C, 67.81; H, 5.81. Found: C, 67.71; H, 5.77.

(E)-1-(2-Hydroxy-4-methoxyphenyl)-3-(3-methoxyphenyl)prop-2-en-1-one (18)

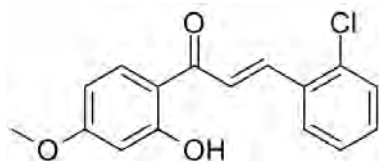
Synthesized from 2-hydroxy-4-methoxyacetophenone and 3-methoxybenzaldehyde, yield 68 %.

Molecular weight: 284.31 g/mol

^1H NMR (DMSO- d_6) δ : 13.40 (s, 1H), 8.29 (d, J = 9.1 Hz, 1H), 8.00 (d, J = 15.5 Hz, 1H), 7.79 (d, J = 15.5 Hz, 1H), 7.51–7.48 (m, 1H), 7.45 (d, J = 7.6 Hz, 1H), 7.37 (t, J = 7.9 Hz, 1H), 7.03 (ddd, J = 8.2, 2.6, 0.9 Hz, 1H), 6.56 (dd, J = 9.0, 2.5 Hz, 1H), 6.51 (d, J = 2.5 Hz, 1H), 3.84 (d, J = 8.2 Hz, 6H).

^{13}C NMR (DMSO- d_6) δ : 192.04, 166.19, 165.88, 159.80, 144.24, 136.06, 132.90, 130.05, 122.06, 121.64, 117.01, 114.01, 113.67, 107.55, 101.06, 55.89, 55.45.

Anal. Calcd for $\text{C}_{17}\text{H}_{16}\text{O}_4$: C, 71.82; H, 5.67. Found: C, 71.66; H, 5.486.

(E)-3-(2-Chlorophenyl)-1-(2-hydroxy-4-methoxyphenyl)prop-2-en-1-one (19)

Synthesized from 2-hydroxy-4-methoxyacetophenone and 2-chlorobenzaldehyde, yield 74 %.

Molecular weight: 288.73 g/mol

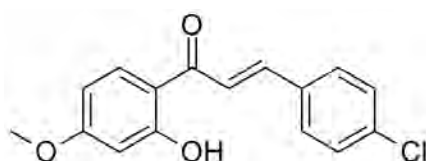
^1H NMR (DMSO- d_6) δ : 13.19 (s, 1H), 8.26 (d, J = 9.1 Hz, 1H), 8.22 (dd, J = 7.4, 2.1 Hz, 1H), 8.11 (d, J = 15.5 Hz, 1H), 8.04 (d, J = 15.4 Hz, 1H), 7.57 (dd, J = 7.7, 1.6

Hz, 1H), 7.47 (ddd, $J = 14.5, 7.1, 1.8$ Hz, 2H), 6.57 (dd, $J = 9.0, 2.5$ Hz, 1H), 6.52 (d, $J = 2.5$ Hz, 1H), 3.85 (s, 3H).

^{13}C NMR (DMSO- d_6) δ : 191.55, 166.38, 165.83, 138.54, 134.58, 133.01, 132.30, 132.26, 130.18, 128.92, 127.82, 124.31, 114.08, 107.72, 101.13, 55.96.

Anal. Calcd for $\text{C}_{16}\text{H}_{13}\text{ClO}_3 / 0.2 \text{ H}_2\text{O}$: C, 65.74; H, 4.62. Found: C, 65.71; H, 4.39.

(*E*)-3-(4-Chlorophenyl)-1-(2-hydroxy-4-methoxyphenyl)prop-2-en-1-one (20)



Synthesized from 2-hydroxy-4-methoxyacetophenone and 4-chlorobenzaldehyde, yield 79 %.

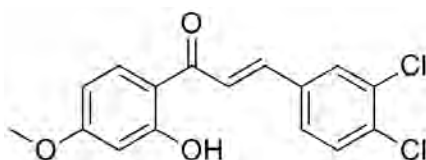
Molecular weight: 288.73 g/mol

^1H NMR (DMSO- d_6) δ : 13.34 (s, 1H), 8.27 (d, $J = 9.1$ Hz, 1H), 8.02 (d, $J = 15.5$ Hz, 1H), 7.94 (d, $J = 8.4$ Hz, 2H), 7.79 (d, $J = 15.5$ Hz, 1H), 7.52 (d, $J = 8.5$ Hz, 2H), 6.56 (dd, $J = 9.0, 2.5$ Hz, 1H), 6.51 (d, $J = 2.5$ Hz, 1H), 3.84 (s, 3H).

^{13}C NMR (DMSO- d_6) δ : 191.87, 166.24, 165.85, 142.72, 135.40, 133.66, 132.90, 130.88, 129.07, 122.19, 114.01, 107.59, 101.08, 55.91.

Anal. Calcd for $\text{C}_{16}\text{H}_{13}\text{ClO}_3$: C, 66.56; H, 4.54. Found: C, 66.31; H, 4.54.

(*E*)-3-(3,4-Dichlorophenyl)-1-(2-hydroxy-4-methoxyphenyl)prop-2-en-1-one (21)



Synthesized from 2-hydroxy-4-methoxyacetophenone and 3,4-dichlorobenzaldehyde, yield 67 %.

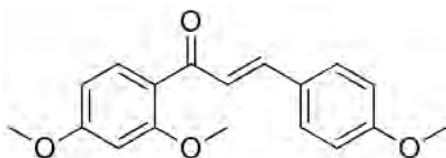
Molecular weight: 323.17 g/mol

^1H NMR (DMSO- d_6) δ : 13.29 (s, 1H), 8.31–8.28 (m, 2H), 8.09 (d, J = 15.5 Hz, 1H), 7.87 (dd, J = 8.4, 2.0 Hz, 1H), 7.76 (d, J = 15.5 Hz, 1H), 7.71 (d, J = 8.3 Hz, 1H), 6.57 (dd, J = 9.0, 2.5 Hz, 1H), 6.51 (d, J = 2.5 Hz, 1H), 3.85 (s, 3H).

^{13}C NMR (DMSO- d_6) δ : 191.75, 166.39, 165.96, 141.37, 135.58, 133.05, 133.02, 131.99, 131.13, 130.40, 129.48, 123.59, 114.03, 107.66, 101.08, 55.96.

Anal. Calcd for $\text{C}_{16}\text{H}_{12}\text{Cl}_2\text{O}_3$: C, 59.46; H, 3.74. Found: C, 59.41; H, 3.79.

(*E*)-1-(2,4-Dimethoxyphenyl)-3-(4-methoxyphenyl)prop-2-en-1-one (22)



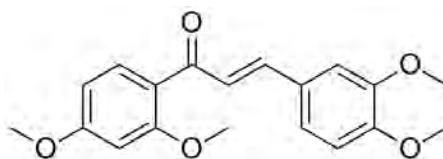
Synthesized from 2,4-dimethoxyacetophenone and 4-methoxybenzaldehyde, yield 85 %.

Molecular weight: 298.33 g/mol

^1H NMR (DMSO- d_6) δ : 7.68–7.64 (m, 2H), 7.58 (d, J = 8.6 Hz, 1H), 7.50 (d, J = 15.8 Hz, 1H), 7.39 (dd, J = 15.8, 0.7 Hz, 1H), 7.01–6.96 (m, 2H), 6.67 (d, J = 2.2 Hz, 1H), 6.65–6.61 (m, 1H), 3.88 (s, 3H), 3.84 (s, 3H), 3.79 (d, J = 3.7 Hz, 3H).

^{13}C NMR (DMSO- d_6) δ : 189.51, 163.84, 161.15, 160.16, 141.45, 131.97, 130.23, 127.58, 124.92, 121.82, 114.59, 106.03, 98.80, 56.05, 55.69, 55.44.

Anal. Calcd for $\text{C}_{18}\text{H}_{18}\text{O}_4$: C, 72.47; H, 6.08. Found: C, 72.58; H, 5.95.

(E)-1-(2,4-Dimethoxyphenyl)-3-(3,4-dimethoxyphenyl)prop-2-en-1-one (23)

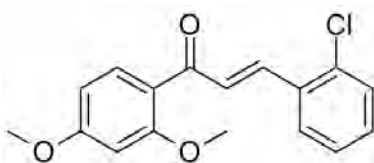
Synthesized from 2,4-dimethoxyacetophenone and 3,4-dimethoxybenzaldehyde, yield 76 %.

Molecular weight: 328.36 g/mol

^1H NMR (DMSO- d_6) δ : 7.56 (d, J = 8.5 Hz, 1H), 7.47 (d, J = 15.8 Hz, 1H), 7.39 (d, J = 15.7 Hz, 1H), 7.30 (d, J = 1.9 Hz, 1H), 7.26 (dd, J = 8.3, 2.0 Hz, 1H), 6.99 (d, J = 8.3 Hz, 1H), 6.68 (d, J = 2.2 Hz, 1H), 6.63 (dd, J = 8.6, 2.2 Hz, 1H), 3.88 (s, 3H), 3.84 (s, 3H), 3.80 (d, J = 7.4 Hz, 6H).

^{13}C NMR (DMSO- d_6) δ : 189.79, 163.74, 160.08, 151.03, 149.12, 142.03, 131.85, 127.81, 125.21, 122.70, 121.93, 111.91, 110.95, 105.99, 98.85, 56.03, 55.73, 55.70, 55.70.

Anal. Calcd for $\text{C}_{19}\text{H}_{20}\text{O}_5$: C, 69.50; H, 6.14. Found: C, 69.29; H, 6.01.

(E)-3-(2-Chlorophenyl)-1-(2,4-dimethoxyphenyl)prop-2-en-1-one (24)

Synthesized from 2,4-dimethoxyacetophenone and 2-chlorobenzaldehyde, yield 69 %.

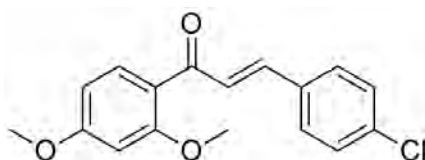
Molecular weight: 302.75 g/mol

^1H NMR (DMSO- d_6) δ : 7.92 (dd, J = 7.2, 2.3 Hz, 1H), 7.82 (d, J = 15.8 Hz, 1H), 7.64 (d, J = 8.6 Hz, 1H), 7.59 (d, J = 15.8 Hz, 1H), 7.56–7.53 (m, 1H), 7.43 (ddd, J = 6.7, 5.7, 1.8 Hz, 2H), 6.69 (d, J = 2.3 Hz, 1H), 6.65 (dd, J = 8.6, 2.3 Hz, 1H), 3.90 (s, 3H), 3.85 (s, 3H).

^{13}C NMR (DMSO- d_6) δ : 189.06, 164.39, 160.57, 135.96, 134.07, 132.74, 132.30, 131.61, 130.13, 129.92, 128.23, 127.93, 121.14, 106.31, 98.75, 56.13, 55.76.

Anal. Calcd for $\text{C}_{17}\text{H}_{15}\text{ClO}_3$: C, 67.44; H, 4.99. Found: C, 67.73; H, 5.183.

(E)-3-(4-Chlorophenyl)-1-(2,4-dimethoxyphenyl)prop-2-en-1-one (25)



Synthesized from 2,4-dimethoxyacetophenone and 4-chlorobenzaldehyde, yield 72 %.

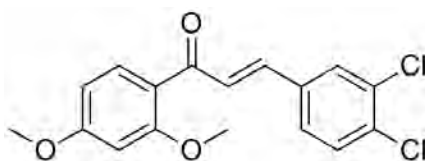
Molecular weight: 302.75 g/mol

^1H NMR (DMSO- d_6) δ : 7.95 (dd, $J=7.1, 2.3$ Hz, 1H), 7.79 (d, $J=15.6$ Hz, 1H), 7.69 (d, $J=8.4$ Hz, 1H), (d, $J=7.4$ Hz, 2H), 7.43 (dd, $J=11.2, 7.7$ Hz, 3H), 6.69 (d, $J=2.3$ Hz, 1H), 6.65 (dd, $J=8.6, 2.3$ Hz, 1H), 3.91 (s, 3H), 3.89 (s, 3H).

^{13}C NMR (DMSO- d_6) δ : 189.08, 164.42, 161.22, 135.76, 133.99, 132.84, 132.26, 131.57, 130.78, 130.03, 128.74, 128.02, 121.12, 106.45, 98.64, 56.23, 55.68.

Anal. Calcd for $\text{C}_{17}\text{H}_{15}\text{ClO}_3$: C, 67.44; H, 4.99. Found: C, 67.25; H, 5.02.

(E)-3-(3,4-Dichlorophenyl)-1-(2,4-dimethoxyphenyl)prop-2-en-1-one (26)



Synthesized from 2,4-dimethoxyacetophenone and 3,4-dichlorobenzaldehyde, yield 67 %.

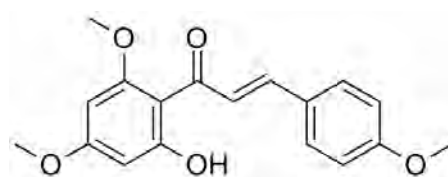
Molecular weight: 337.20 g/mol

^1H NMR (DMSO- d_6) δ : 8.01 (d, J = 2.0 Hz, 1H), 7.73 (dd, J = 8.4, 2.0 Hz, 1H), 7.67 (d, J = 8.4 Hz, 1H), 7.63–7.57 (m, 2H), 7.49 (d, J = 15.9 Hz, 1H), 6.68 (d, J = 2.3 Hz, 1H), 6.64 (dd, J = 8.6, 2.3 Hz, 1H), 3.89 (s, 3H), 3.85 (s, 3H).

^{13}C NMR (DMSO- d_6) δ : 189.23, 164.32, 160.56, 138.40, 136.02, 132.40, 132.24, 131.90, 131.17, 130.32, 129.27, 128.14, 121.33, 106.22, 98.80, 56.17, 55.78.

Anal. Calcd for $\text{C}_{17}\text{H}_{14}\text{Cl}_2\text{O}_3$: C, 60.55; H, 4.18. Found: C, 60.72; H, 4.23.

(*E*)-1-(2-Hydroxy-4,6-dimethoxyphenyl)-3-(4-methoxyphenyl)prop-2-en-1-one (27)



Synthesized from 2-hydroxy-4,6-dimethoxyacetophenone and 4-methoxybenzaldehyde, yield 55 %.

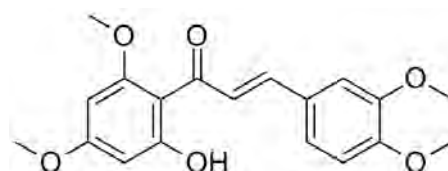
Molecular weight: 314.33 g/mol

^1H NMR (DMSO- d_6) δ : 13.75 (s, 1H), 7.60 (d, J = 8.7 Hz, 2H), 7.14 (d, J = 16.1 Hz, 1H), 6.94 (d, J = 8.8 Hz, 2H), 6.80 (d, J = 16.1 Hz, 1H), 6.31–6.27 (m, 2H), 3.78 (s, 3H), 3.70 (s, 6H).

^{13}C NMR (DMSO- d_6) δ : 193.33, 161.93, 161.32, 158.12, 143.76, 130.40, 127.55, 127.06, 127.02, 125.04, 114.58, 111.45, 93.81, 91.26, 90.97, 55.93, 55.57, 55.46.

Anal. Calcd for $\text{C}_{18}\text{H}_{18}\text{O}_5 \cdot 0.5 \text{H}_2\text{O}$: C, 67.64; H, 6.27. Found: C, 67.47; H, 6.00.

(*E*)-3-(3,4-Dimethoxyphenyl)-1-(2-hydroxy-4,6-dimethoxyphenyl)prop-2-en-1-one (28)



Synthesized from 2-hydroxy-4,6-dimethoxyacetophenone and 3,4-dimethoxybenzaldehyde, yield 71 %.

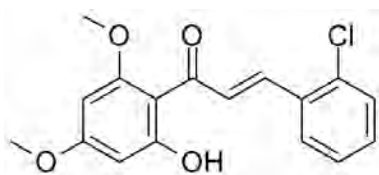
Molecular weight: 344.36 g/mol

^1H NMR (DMSO- d_6) δ : 13.40 (s, 1H), 7.62 (d, $J = 7.4$ Hz, 2H), 7.29 (s, 2H), 7.01 (d, $J = 8.7$ Hz, 1H), 6.14 (d, $J = 2.3$ Hz, 1H), 6.11 (d, $J = 2.3$ Hz, 1H), 3.88 (s, 3H), 3.82 (s, 3H), 3.81 (d, $J = 2.1$ Hz, 6H).

^{13}C NMR (DMSO- d_6) δ : 192.41, 165.39, 165.36, 161.88, 151.28, 149.15, 143.13, 127.77, 125.38, 122.92, 111.97, 111.02, 106.63, 94.06, 91.18, 56.27, 56.17, 55.76, 55.67.

Anal. Calcd for $\text{C}_{19}\text{H}_{20}\text{O}_6 \cdot 0.33 \text{H}_2\text{O}$: C, 65.13; H, 5.95. Found: C, 65.00; H, 6.12.

(*E*)-3-(2-Chlorophenyl)-1-(2-hydroxy-4,6-dimethoxyphenyl)prop-2-en-1-one (29)



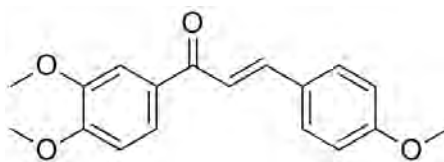
Synthesized from 2-hydroxy-4,6-dimethoxyacetophenone and 2-chlorobenzaldehyde, yield 68 %.

Molecular weight: 318.75 g/mol

^1H NMR (DMSO- d_6) δ : 13.22 (s, 1H), 7.92–7.88 (m, 2H), 7.77 (d, $J = 15.7$ Hz, 1H), 7.57–7.54 (m, 1H), 7.46–7.42 (m, 2H), 6.15 (d, $J = 2.3$ Hz, 1H), 6.13 (d, $J = 2.3$ Hz, 1H), 3.88 (s, 3H), 3.82 (s, 3H).

^{13}C NMR (DMSO- d_6) δ : 192.04, 165.94, 165.61, 162.08, 136.79, 134.10, 132.65, 131.79, 130.47, 130.20, 128.36, 128.01, 106.51, 94.06, 91.26, 56.38, 55.83.

Anal. Calcd for $\text{C}_{17}\text{H}_{15}\text{ClO}_4$: C, 64.06; H, 4.74. Found: C, 63.69; H, 4.80.

(E)-1-(3,4-Dimethoxyphenyl)-3-(4-methoxyphenyl)prop-2-en-1-one (30)

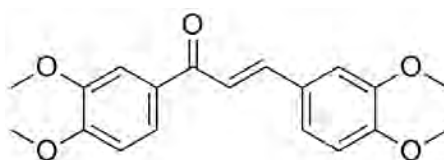
Synthesized from 3,4-dimethoxyacetophenone and 4-methoxybenzaldehyde, yield 81 %.

Molecular weight: 298.33 g/mol

^1H NMR (DMSO- d_6) δ : 7.87 (dd, J = 8.4, 1.9 Hz, 1H), 7.83 (d, J = 8.8 Hz, 2H), 7.79 (d, J = 15.5 Hz, 1H), 7.67 (d, J = 15.5 Hz, 1H), 7.59 (d, J = 1.9 Hz, 1H), 7.09 (d, J = 8.4 Hz, 1H), 7.01 (d, J = 8.7 Hz, 2H), 3.86 (d, J = 5.6 Hz, 6H), 3.81 (s, 3H).

^{13}C NMR (DMSO- d_6) δ : 187.41, 161.34, 153.22, 148.93, 143.15, 130.91, 130.78, 127.62, 123.27, 119.64, 114.51, 111.06, 110.97, 55.91, 55.76, 55.50.

Anal. Calcd for $\text{C}_{18}\text{H}_{18}\text{O}_4$: C, 72.47; H, 6.08. Found: C, 72.12; H, 6.20.

(E)-1,3-Bis(3,4-dimethoxyphenyl)prop-2-en-1-one (31)

Synthesized from 3,4-dimethoxyacetophenone and 3,4-dimethoxybenzaldehyde, yield 81 %.

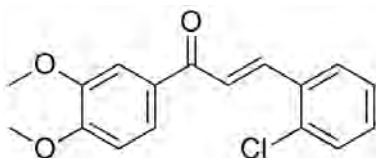
Molecular weight: 328.36 g/mol

^1H NMR (DMSO- d_6) δ : 7.80 (d, J = 15.5 Hz, 1H), 7.66–7.63 (m, 1H), 7.51 (d, J = 2.0 Hz, 1H), 7.41 (d, J = 2.0 Hz, 1H), 7.09 (d, J = 8.5 Hz, 1H), 7.04 (d, J = 2.3 Hz, 1H), 7.02 (d, J = 3.5 Hz, 1H), 6.76 (d, J = 1.0 Hz, 1H), 3.86–3.80 (m, 12H).

^{13}C NMR (DMSO- d_6) δ : 197.32, 153.17, 153.09, 149.10, 148.61, 143.59, 130.88, 129.90, 123.59, 123.33, 122.74, 119.73, 111.72, 110.93, 110.43, 55.86, 55.81, 55.57, 55.54.

Anal. Calcd for $\text{C}_{19}\text{H}_{20}\text{O}_5$: C, 69.50; H, 6.14. Found: C, 69.34; H, 6.23.

(E)-3-(2-Chlorophenyl)-1-(3,4-dimethoxyphenyl)prop-2-en-1-one (32)



Synthesized from 3,4-dimethoxyacetophenone and 2-chlorobenzaldehyde, yield 73 %.

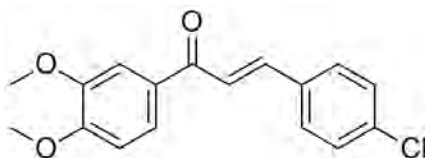
Molecular weight: 302.75 g/mol

^1H NMR (DMSO- d_6) δ : 7.99 (d, $J = 4.4$ Hz, 1H), 7.65 (dd, $J = 8.5, 2.0$ Hz, 1H), 7.52 (dd, $J = 7.8, 1.7$ Hz, 1H), 7.42 (d, $J = 2.0$ Hz, 1H), 7.36 (dd, $J = 7.9, 1.3$ Hz, 1H), 7.25–7.22 (m, 1H), 7.18–7.14 (m, 1H), 7.04 (d, $J = 8.5$ Hz, 2H), 3.83 (s, 3H), 3.79 (s, 3H).

^{13}C NMR (DMSO- d_6) δ : 196.75, 153.22, 148.65, 141.75, 137.78, 133.08, 129.66, 129.41, 128.37, 127.75, 127.29, 124.94, 122.77, 110.98, 110.47, 55.85, 55.61.

Anal. Calcd for $\text{C}_{17}\text{H}_{15}\text{ClO}_3 \cdot 0.25 \text{H}_2\text{O}$: C, 66.45; H, 5.08. Found: C, 66.67; H, 5.293.

(E)-3-(4-Chlorophenyl)-1-(3,4-dimethoxyphenyl)prop-2-en-1-one (33)



Synthesized from 3,4-dimethoxyacetophenone and 4-chlorobenzaldehyde, yield 77 %.

Molecular weight: 302.75 g/mol

^1H NMR (DMSO- d_6) δ : 7.95 (d, J = 15.6 Hz, 1H), 7.92 (s, 1H), 7.90 (dd, J = 8.5, 2.0 Hz, 2H), 7.68 (d, J = 15.6 Hz, 1H), 7.60 (d, J = 2.0 Hz, 1H), 7.51 (d, J = 8.6 Hz, 2H), 7.10 (d, J = 8.5 Hz, 1H), 3.86 (d, J = 7.8 Hz, 6H).

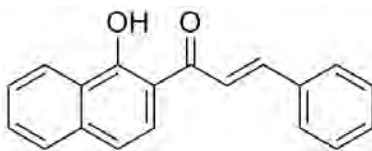
^{13}C NMR (DMSO- d_6) δ : 187.38, 153.50, 148.99, 141.70, 134.99, 133.96, 130.63, 130.63, 130.55, 129.03, 129.03, 123.62, 122.90, 111.08, 110.99, 55.95, 55.78.

Anal. Calcd for $\text{C}_{17}\text{H}_{15}\text{ClO}_3$: C, 67.44; H, 4.99. Found: C, 67.19; H, 5.01.

7.1.2.5 General procedure for synthesis of benzochalcones

To a mixture of 5 mmol of a selected acetophenone and 5 mmol of a selected benzaldehyde in a 50 ml round bottom flask, 20 ml methanol and 35 mmol of LiOH was added. The reaction mixture was kept in an ultrasonic bath for 1 to 5 hours, until reaction completion was indicated by TLC. After completion of the reaction the mixture was poured onto crushed ice and acidified with dilute HCl. Precipitated product was filtered by suction and washed to neutral. The solid was recrystallized from dilute ethanol to yield the corresponding benzochalcone

(*E*)-1-(1-Hydroxynaphthalen-2-yl)-3-phenylprop-2-en-1-one (34)



Synthesized from 2-acetyl-1-hydroxynaphthalene and benzaldehyde, yield 88 %.

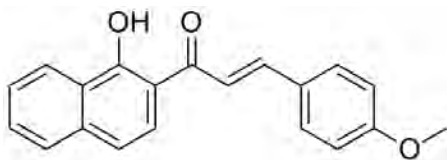
Molecular weight: 274.31 g/mol

^1H NMR (DMSO- d_6) δ : 15.00 (s, 1H), 8.37 (dd, J = 8.3, 0.7 Hz, 1H), 8.30 (d, J = 9.0 Hz, 1H), 8.18 (d, J = 15.5 Hz, 1H), 7.97 (dd, J = 6.2, 3.4 Hz, 2H), 7.93 (d, J = 8.3 Hz, 1H), 7.73 (ddd, J = 8.1, 6.9, 1.2 Hz, 1H), 7.60 (ddd, J = 8.2, 6.9, 1.1 Hz, 1H), 7.51–7.48 (m, 3H), 7.46 (d, J = 8.9 Hz, 1H).

^{13}C NMR (DMSO- d_6) δ : 193.72, 163.37, 145.42, 137.22, 134.59, 131.19, 130.60, 129.45, 129.08, 127.74, 126.30, 125.17, 124.58, 123.78, 121.18, 118.38, 113.47.

Anal. Calcd for C₁₉H₁₄O₂: C, 83.19; H, 5.14. Found: C, 82.87; H, 5.26.

(E)-1-(1-Hydroxynaphthalen-2-yl)-3-(4-methoxyphenyl)prop-2-en-1-one (35)



Synthesized from 2-acetyl-1-hydroxynaphthalene and 4-methoxybenzaldehyde, yield 84 %.

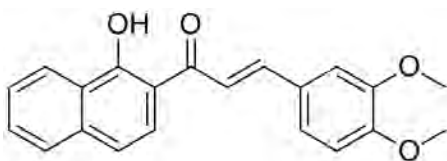
Molecular weight: 304.34 g/mol

¹H NMR (DMSO-d₆) δ: 15.18 (s, 1H), 8.36 (d, *J* = 8.2 Hz, 1H), 8.29 (d, *J* = 9.0 Hz, 1H), 8.04 (d, *J* = 15.4 Hz, 1H), 7.94 (d, *J* = 9.2 Hz, 3H), 7.92 (d, *J* = 3.9 Hz, 1H), 7.72 (ddd, *J* = 8.1, 6.9, 1.3 Hz, 1H), 7.59 (ddd, *J* = 8.2, 5.0, 1.1 Hz, 1H), 7.45 (d, *J* = 8.9 Hz, 1H), 7.05 (d, *J* = 8.8 Hz, 2H), 3.84 (s, 3H).

¹³C NMR (DMSO-d₆) δ: 193.59, 163.26, 161.97, 145.58, 137.11, 131.53, 130.45, 127.71, 127.29, 126.22, 125.13, 123.73, 118.42, 118.25, 114.63, 113.47, 55.57.

Anal. Calcd for C₂₀H₁₆O₃*0.25 H₂O: C, 77.95; H, 5.58. Found: C, 77.83; H, 5.37.

(E)-3-(3,4-Dimethoxyphenyl)-1-(1-hydroxynaphthalen-2-yl)prop-2-en-1-one (36)



Synthesized from 2-acetyl-1-hydroxynaphthalene and 3,4-dimethoxybenzaldehyde, yield 79 %.

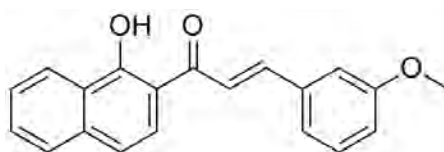
Molecular weight: 334.37 g/mol

^1H NMR (DMSO- d_6) δ : 14.08 (s, 1H), 8.36 (d, J = 8.2 Hz, 1H), 8.25 (d, J = 9.0 Hz, 1H), 8.14 (d, J = 15.4 Hz, 1H), 7.94 (d, J = 9.2 Hz, 3H), 7.92 (d, J = 3.9 Hz, 1H), 7.72 (m, 2H), 7.59 (d, J = 8.2, 1H), 7.47 (d, J = 8.9 Hz, 1H), 3.83 (d, 6H).

^{13}C NMR (DMSO- d_6) δ : 193.60, 158.12, 150.2, 149.90, 144.56, 135.26, 130.93, 129.67, 127.68, 127.35, 126.52, 124.99, 123.25, 122.24, 121.93, 121.12, 120.83, 113.57, 110.67, 55.92, 55.57.

Anal. Calcd for $\text{C}_{21}\text{H}_{18}\text{O}_4$: C, 75.43; H, 5.43. Found: C, 75.37; H, 5.51.

(E)-1-(1-Hydroxynaphthalen-2-yl)-3-(3-methoxyphenyl)prop-2-en-1-one (37)



Synthesized from 2-acetyl-1-hydroxynaphthalene and 3-methoxybenzaldehyde, yield 67 %.

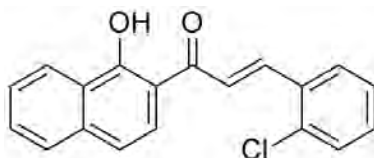
Molecular weight: 304.34 g/mol

^1H NMR (DMSO- d_6) δ : 14.05 (s, 1H), 8.33 (d, J = 8.7 Hz, 2H), 8.18 (d, J = 15.4 Hz, 1H), 7.93 (dd, J = 15.4, 7.3 Hz, 3H), 7.86 (d, J = 8.8 Hz, 1H), 7.72 (dddd, J = 14.0, 8.2, 6.9, 1.3 Hz, 2H), 7.63–7.60 (m, 1H), 7.44–7.41 (m, 1H), 3.85 (s, 3H).

^{13}C NMR (DMSO- d_6) δ : 219.48, 193.80, 163.41, 159.87, 147.20, 145.50, 137.26, 136.00, 130.36, 127.78, 126.34, 125.95, 124.60, 124.36, 123.81, 123.71, 121.45, 117.39, 113.88, 55.54.

Anal. Calcd for $\text{C}_{20}\text{H}_{16}\text{O}_3 \cdot 0.33 \text{H}_2\text{O}$: C, 77.64; H, 5.68. Found: C, 77.59; H, 5.44.

(E)-3-(2-Chlorophenyl)-1-(1-hydroxynaphthalen-2-yl)prop-2-en-1-one (38)



Synthesized from 2-acetyl-1-hydroxynaphthalene and 2-chlorobenzaldehyde, yield 72 %.

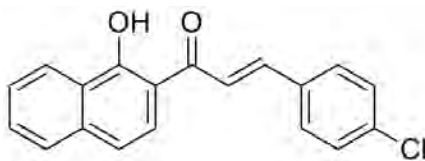
Molecular weight: 308.76 g/mol

^1H NMR (DMSO- d_6) δ : 14.81 (s, 1H), 8.39–8.35 (m, 1H), 8.32 (dd, J = 7.5, 2.1 Hz, 1H), 8.29 (d, J = 9.0 Hz, 1H), 8.23 (d, J = 3.0 Hz, 2H), 7.93 (d, J = 8.1 Hz, 1H), 7.73 (ddd, J = 8.2, 6.9, 1.3 Hz, 1H), 7.63–7.57 (m, 2H), 7.51–7.44 (m, 3H).

^{13}C NMR (DMSO- d_6) δ : 193.37, 163.51, 139.61, 137.33, 134.79, 132.53, 132.17, 130.78, 130.23, 129.12, 127.85, 127.78, 126.39, 125.17, 124.55, 123.97, 123.87, 118.52, 113.49.

Anal. Calcd for $\text{C}_{19}\text{H}_{13}\text{ClO}_2$: C, 73.91; H, 4.24. Found: C, 74.05; H, 4.19.

(*E*)-3-(4-Chlorophenyl)-1-(1-hydroxynaphthalen-2-yl)prop-2-en-1-one (39)



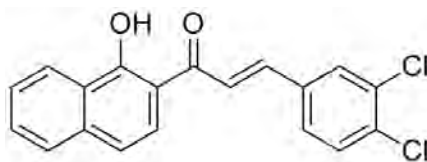
Synthesized from 2-acetyl-1-hydroxynaphthalene and 4-chlorobenzaldehyde, yield 76 %.

Molecular weight: 308.76 g/mol

^1H NMR (DMSO- d_6) δ : 14.95 (s, 1H), 8.37 (d, J = 8.4 Hz, 1H), 8.31 (d, J = 9.0 Hz, 1H), 8.20 (d, J = 15.5 Hz, 1H), 8.02 (d, J = 8.6 Hz, 2H), 7.95 (d, J = 5.2 Hz, 1H), 7.93 (d, J = 1.6 Hz, 1H), 7.74–7.70 (m, 1H), 7.64–7.61 (m, 1H), 7.56 (d, J = 8.5 Hz, 2H), 7.46 (d, J = 8.8 Hz, 1H).

^{13}C NMR (DMSO- d_6) δ : 193.63, 163.40, 143.92, 137.25, 135.72, 133.57, 131.14, 130.67, 129.14, 127.76, 126.34, 125.17, 124.55, 123.80, 121.96, 118.43, 113.48.

Anal. Calcd for $\text{C}_{19}\text{H}_{13}\text{ClO}_2$: C, 73.91; H, 4.24. Found: C, 73.85; H, 4.33.

(E)-3-(3,4-Dichlorophenyl)-1-(1-hydroxynaphthalen-2-yl)prop-2-en-1-one (40)

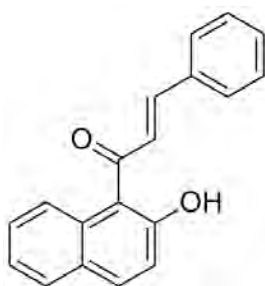
Synthesized from 2-acetyl-1-hydroxynaphthalene and 3,4-dichlorobenzaldehyde, yield 64 %, mp 161 °C.

Molecular weight: 343.20 g/mol

^1H NMR (DMSO- d_6) δ : 14.89 (s, 1H), 8.37 (d, J = 1.9 Hz, 1H), 8.33 (d, J = 9.1 Hz, 1H), 8.27 (d, J = 15.5 Hz, 1H), 7.94 (dd, J = 8.4, 2.3 Hz, 2H), 7.74 (d, J = 8.3 Hz, 2H), 7.71 (ddd, J = 8.2, 5.0, 1.3 Hz, 1H), 7.60 (m, J = 11.3, 8.2, 6.9, 1.2 Hz, 2H), 7.47 (d, J = 8.8 Hz, 1H).

^{13}C NMR (DMSO- d_6) δ : 193.57, 163.53, 142.58, 137.36, 135.49, 133.35, 132.09, 131.21, 130.81, 130.63, 129.78, 127.82, 126.43, 125.27, 124.56, 123.87, 123.38, 118.49, 113.54.

Anal. Calcd for $\text{C}_{19}\text{H}_{12}\text{Cl}_2\text{O}_2$: C, 66.49; H, 3.52. Found: C, 66.23; H, 3.61.

(E)-1-(2-Hydroxynaphthalen-1-yl)-3-phenylprop-2-en-1-one (41)

Synthesized from 1-acetyl-2-hydroxynaphthalene and benzaldehyde, yield 59 %.

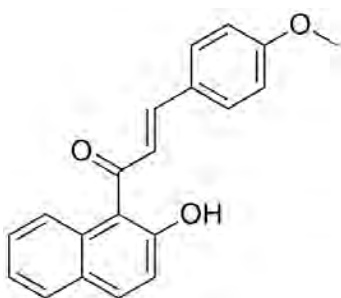
Molecular weight: 274.31 g/mol

^1H NMR (DMSO- d_6) δ : 8.23 (d, J = 8.5 Hz, 1H), 7.71 (d, J = 15.7 Hz, 1H), 7.58 (d, J = 7.3 Hz, 2H), 7.45–7.39 (m, 3H), 7.37 (t, J = 7.4 Hz, 2H), 7.33–7.28 (m, 1H), 7.16 (ddd, J = 8.4, 6.9, 1.5 Hz, 1H), 6.94–6.85 (m, 1H), 6.61 (d, J = 9.2 Hz, 1H).

^{13}C NMR (DMSO- d_6) δ : 190.38, 175.79, 136.69, 135.95, 134.84, 133.55, 132.31, 129.58, 128.85, 128.66, 127.87, 127.69, 126.22, 124.34, 123.14, 118.88, 116.93.

Anal. Calcd for $\text{C}_{19}\text{H}_{14}\text{O}_2$: C, 83.19; H, 5.14. Found: C, 83.04; H, 5.28.

(*E*)-1-(2-Hydroxynaphthalen-1-yl)-3-(4-methoxyphenyl)prop-2-en-1-one (42)



Synthesized from 1-acetyl-2-hydroxynaphthalene and 4-methoxybenzaldehyde, yield 62 %.

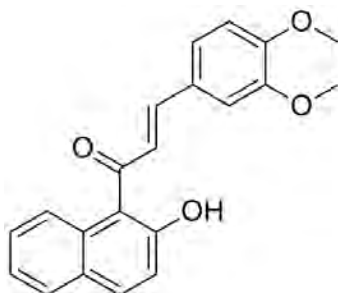
Molecular weight: 304.34 g/mol

^1H NMR (DMSO- d_6) δ : 10.15 (s, 1H), 7.88 (d, J = 8.8 Hz, 1H), 7.84 (d, J = 8.0 Hz, 1H), 7.62 (d, J = 8.8 Hz, 2H), 7.56 (dd, J = 8.4, 0.9 Hz, 1H), 7.41 (ddd, J = 8.4, 6.8, 1.4 Hz, 1H), 7.31 (dt, J = 8.0, 3.9 Hz, 1H), 7.28–7.22 (m, 2H), 7.10 (d, J = 16.1 Hz, 1H), 6.94 (d, J = 8.8 Hz, 2H), 3.78 (s, 3H).

^{13}C NMR (DMSO- d_6) δ : 196.35, 161.46, 152.86, 144.30, 131.66, 131.11, 130.57, 128.40, 128.30, 127.79, 127.19, 127.04, 126.70, 123.47, 123.19, 120.40, 118.53, 114.61, 114.08, 55.48.

Anal. Calcd for $\text{C}_{20}\text{H}_{16}\text{O}_3$: C, 78.93; H, 5.30. Found: C, 78.76; H, 5.30.

(E)-3-(3,4-Dimethoxyphenyl)-1-(2-hydroxynaphthalen-1-yl)prop-2-en-1-one (43)



Synthesized from 1-acetyl-2-hydroxynaphthalene and 3,4-dimethoxybenzaldehyde, yield 68 %.

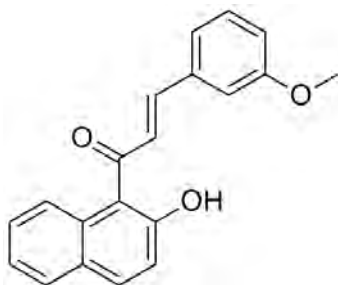
Molecular weight: 334.37 g/mol⁴⁸

¹H NMR (DMSO-d₆) δ : 10.12 (s, 1H), 7.88 (d, J = 8.8 Hz, 1H), 7.84 (d, J = 8.0 Hz, 1H), 7.54 (dd, J = 8.4, 0.9 Hz, 1H), 7.41 (ddd, J = 8.4, 6.8, 1.4 Hz, 1H), 7.33–7.30 (m, 1H), 7.29 (d, J = 2.2 Hz, 1H), 7.25 (dd, J = 12.5, 9.5 Hz, 2H), 7.21–7.17 (m, 1H), 7.15 (d, J = 16.0 Hz, 1H), 6.94 (d, J = 8.4 Hz, 1H), 3.77 (d, J = 2.8 Hz, 6H).

¹³C NMR (DMSO-d₆) δ : 196.59, 152.73, 151.32, 149.16, 144.94, 131.69, 130.95, 128.29, 127.77, 127.28, 127.15, 126.94, 123.45, 123.26, 123.16, 120.50, 118.55, 111.76, 110.92, 55.75, 55.72.

Anal. Calcd for C₂₁H₁₈O₄: C, 75.43; H, 5.43. Found: C, 75.50; H, 5.35.

(E)-1-(2-Hydroxynaphthalen-1-yl)-3-(3-methoxyphenyl)prop-2-en-1-one (44)



Synthesized from 1-acetyl-2-hydroxynaphthalene and 3-methoxybenzaldehyde, yield 63 %.

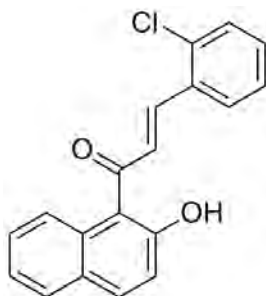
Molecular weight: 304.34g/mol

^1H NMR (DMSO- d_6) δ : 8.29 (d, J = 8.5 Hz, 1H), 7.72 (d, J = 15.7 Hz, 1H), 7.41 (d, J = 9.3 Hz, 2H), 7.36 (d, J = 15.7 Hz, 1H), 7.27 (d, J = 7.9 Hz, 1H), 7.16 (dd, J = 6.9, 1.4 Hz, 2H), 7.13–7.11 (m, 1H), 6.92–6.85 (m, 2H), 6.60 (d, J = 9.2 Hz, 1H), 3.77 (s, 3H).

^{13}C NMR (DMSO- d_6) δ : 190.67, 159.70, 140.32, 138.24, 137.75, 136.00, 134.67, 133.48, 132.71, 129.84, 128.83, 127.84, 126.24, 124.34, 123.06, 120.13, 116.89, 114.46, 112.75, 55.23.

Anal. Calcd for $\text{C}_{20}\text{H}_{16}\text{O}_3$: C, 78.93; H, 5.30. Found: C, 78.67; H, 5.46.

(*E*)-3-(2-Chlorophenyl)-1-(2-hydroxynaphthalen-1-yl)prop-2-en-1-one (45)



Synthesized from 1-acetyl-2-hydroxynaphthalene and 2-chlorobenzaldehyde, yield 56 %.

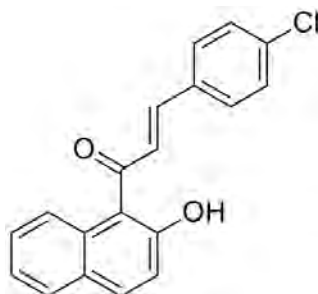
Molecular weight: 308.76 g/mol

^1H NMR (DMSO- d_6) δ : 8.53 (d, J = 8.6 Hz, 1H), 7.82 (d, J = 15.6 Hz, 1H), 7.76 (dd, J = 7.3, 2.2 Hz, 1H), 7.65 (d, J = 15.6 Hz, 1H), 7.48 (dd, J = 7.0, 2.3 Hz, 1H), 7.40 (d, J = 9.1 Hz, 2H), 7.34–7.30 (m, 2H), 7.15 (ddd, J = 8.5, 6.8, 1.5 Hz, 1H), 6.87 (ddd, J = 7.9, 6.9, 1.2 Hz, 1H), 6.57 (d, J = 9.2 Hz, 1H).

^{13}C NMR (DMSO- d_6) δ : 190.19, 176.91, 136.23, 135.64, 134.82, 133.80, 133.20, 129.85, 129.77, 129.73, 128.76, 127.80, 127.67, 127.60, 126.46, 124.33, 122.92, 118.89, 116.50.

Anal. Calcd for C₁₉H₁₃ClO₂: C, 73.91; H, 4.24. Found: C, 73.84; H, 4.31.

(E)-3-(4-Chlorophenyl)-1-(2-hydroxynaphthalen-1-yl)prop-2-en-1-one (46)



Synthesized from 1-acetyl-2-hydroxynaphthalene and 4-chlorobenzaldehyde, yield 68 %.

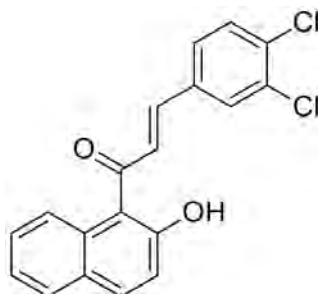
Molecular weight: 308.76 g/mol

¹H NMR (DMSO-d₆) δ: 10.00 (s, 1H), 8.16 (d, *J* = 8.9 Hz, 1H), 7.92 (d, *J* = 8.6 Hz, 1H), 7.67 (dd, *J* = 6.5, 5.1 Hz, 3H), 7.62 (d, *J* = 8.4 Hz, 2H), 7.51 (d, *J* = 8.5 Hz, 2H), 7.28 (d, *J* = 9.0 Hz, 1H), 7.12 (d, *J* = 9.0 Hz, 1H), 5.83 (dd, *J* = 13.2, 3.1 Hz, 1H).

¹³C NMR (DMSO-d₆) δ: 192.74, 163.20, 137.79, 134.31, 133.31, 130.95, 129.68, 129.04, 129.00, 128.83, 128.74, 128.65, 128.13, 125.12, 124.92, 119.11, 112.01.

Anal. Calcd for C₁₉H₁₃ClO₂: C, 73.91; H, 4.24. Found: C, 73.68; H, 4.26.

(E)-3-(3,4-Dichlorophenyl)-1-(2-hydroxynaphthalen-1-yl)prop-2-en-1-one (47)



Synthesized from 1-acetyl-2-hydroxynaphthalene and 4-chlorobenzaldehyde, yield 71 %.

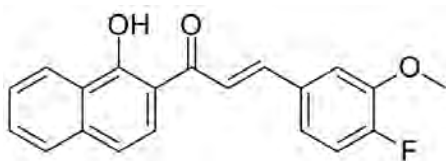
Molecular weight: 343.20 g/mol

^1H NMR (DMSO- d_6) δ : 8.42 (d, J = 8.5 Hz, 1H), 7.82 (dd, J = 12.2, 8.7 Hz, 2H), 7.59 (dd, J = 11.2, 5.1 Hz, 2H), 7.41 (dd, J = 5.3, 4.1 Hz, 2H), 7.31 (d, J = 15.7 Hz, 1H), 7.15 (ddd, J = 8.5, 6.9, 1.5 Hz, 1H), 6.92–6.86 (m, 1H), 6.60 (d, J = 9.2 Hz, 1H).

^{13}C NMR (DMSO- d_6) δ : 190.07, 176.41, 138.00, 136.07, 134.86, 133.78, 131.60, 131.40, 130.92, 130.44, 129.58, 129.13, 127.83, 127.54, 126.43, 124.40, 122.99, 119.00, 116.65.

Anal. Calcd for $\text{C}_{19}\text{H}_{12}\text{Cl}_2\text{O}_2$: C, 66.49; H, 3.52. Found: C, 66.60; H, 3.42.

(*E*)-3-(4-Fluoro-3-methoxyphenyl)-1-(1-hydroxynaphthalen-2-yl)prop-2-en-1-one (48)



Synthesized from 2-acetyl-1-hydroxynaphthalene and 4-fluoro-3-methoxybenzaldehyde, yield 69 %.

Molecular weight: 322.33 g/mol

^1H NMR (DMSO- d_6) δ : 15.08 (s, 1H), 8.36 (d, J = 8.4 Hz, 1H), 8.30 (d, J = 8.9 Hz, 1H), 8.10 (d, J = 15.4 Hz, 1H), 8.03 (dd, J = 12.8, 1.7 Hz, 1H), 7.96 – 7.84 (m, 2H), 7.71 (t, J = 7.0 Hz, 2H), 7.59 (t, J = 7.2 Hz, 1H), 7.43 (d, J = 8.6 Hz, 1H), 7.30 – 7.21 (m, 1H), 3.92 (s, 3H).

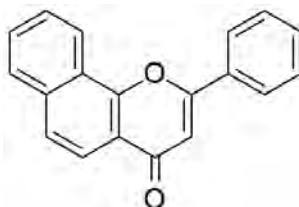
^{13}C NMR (DMSO- d_6) δ : 193.34, 152.77, 150.82, 149.80, 149.72, 137.24, 130.50, 128.00, 127.95, 127.71, 126.19, 125.30, 123.84, 115.59, 115.45, 113.97, 113.57, 56.39.

Anal. Calcd for $\text{C}_{20}\text{H}_{15}\text{FO}_3$: C, 74.52; H, 4.69. Found: C, 74.25; H, 4.74.

7.1.2.6 General procedure for synthesis of 7,8- and 5,6-benzoflavones

An appropriate benzochalcone (2 mmol) and I₂ (0.14 g) were dissolved in DMSO (10 ml). The resulting solution was refluxed for 7-8 h. After completion of the reaction as indicated by TLC, the solution was cooled to room temperature and poured onto crushed ice. 1 N HCl solution (50 ml) was added and stirred for 15 min. This solution was extracted with ethyl acetate. The organic phase was washed 3 times with brine and evaporated under reduced pressure to get crude product. It was further purified by column chromatography using silica gel as solid phase and dichloromethane: methanol (9.5:0.5) as eluent to yield pure benzoflavones.

2-Phenyl-4*H*-benzo[*h*]chromen-4-one (49)



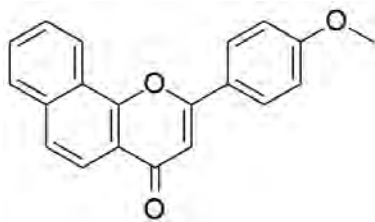
Synthesized from (*E*)-1-(1-hydroxynaphthalen-2-yl)-3-phenylprop-2-en-1-one, yield 68 %.

Molecular weight: 272.30 g/mol

¹H NMR (DMSO-d₆) δ: 8.63 – 8.57 (m, 1H), 8.21 – 8.15 (m, 2H), 8.07 – 8.02 (m, 1H), 7.95 (d, *J* = 8.7 Hz, 1H), 7.87 (d, *J* = 8.6 Hz, 1H), 7.78 – 7.74 (m, 2H), 7.63 – 7.58 (m, 3H), 7.13 (s, 1H).

¹³C NMR (DMSO-d₆) δ: 176.92, 162.00, 152.86, 135.55, 131.82, 131.34, 129.63, 129.35, 128.34, 127.78, 126.46, 125.47, 123.60, 122.36, 120.08, 119.74, 108.25.

Anal. Calcd for C₁₉H₁₂O₂: C, 83.81; H, 4.44. Found: C, 83.72; H, 4.52.

2-(4-Methoxyphenyl)-4*H*-benzo[*h*]chromen-4-one (50)

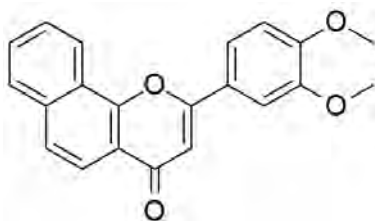
Synthesized from (*E*)-1-(1-hydroxynaphthalen-2-yl)-3-(4-methoxyphenyl)prop-2-en-1-one, yield 72 %.

Molecular weight: 302.32 g/mol

¹H NMR (DMSO-*d*₆) δ: 8.70 – 8.66 (m, 1H), 8.22 – 8.18 (m, 2H), 8.13 – 8.09 (m, 1H), 8.00 (d, *J* = 8.7 Hz, 1H), 7.93 (d, *J* = 8.6 Hz, 1H), 7.84 – 7.80 (m, 2H), 7.18 – 7.15 (m, 2H), 7.09 (s, 1H), 3.88 (s, 3H).

¹³C NMR (DMSO-*d*₆) δ: 176.83, 162.22, 152.78, 135.54, 129.60, 128.38, 128.35, 127.80, 125.37, 123.63, 123.52, 122.37, 120.17, 119.68, 114.83, 106.80, 55.65.

Anal. Calcd for C₂₀H₁₄O₃: C, 79.46; H, 4.67. Found: C, 79.33; H, 4.73.

2-(3,4-Dimethoxyphenyl)-4*H*-benzo[*h*]chromen-4-one (51)

Synthesized from (*E*)-3-(3,4-dimethoxyphenyl)-1-(1-hydroxynaphthalen-2-yl)prop-2-en-1-one, yield 64 %.

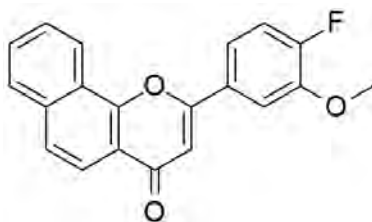
Molecular weight: 332.35 g/mol

¹H NMR (DMSO-*d*₆) δ: 8.66 – 8.62 (m, 1H), 8.12 – 8.08 (m, 1H), 7.99 (d, *J* = 8.6 Hz, 1H), 7.92 (d, *J* = 8.6 Hz, 1H), 7.85 (dd, *J* = 8.5, 2.2 Hz, 1H), 7.83 – 7.79 (m, 2H), 7.66 (d, *J* = 2.2 Hz, 1H), 7.18 (s, 2H), 3.93 (s, 3H), 3.87 (s, 3H).

^{13}C NMR (DMSO- d_6) δ : 176.89, 162.22, 152.79, 152.06, 149.27, 135.55, 129.58, 128.39, 127.84, 125.35, 123.63, 122.31, 120.16, 119.98, 119.67, 112.01, 109.58, 107.16, 56.00, 55.86.

Anal. Calcd for $\text{C}_{21}\text{H}_{16}\text{O}_4$: C, 75.89; H, 4.85. Found: C, 75.56; H, 5.02.

2-(4-Fluoro-3-methoxyphenyl)-4*H*-benzo[*h*]chromen-4-one (52)



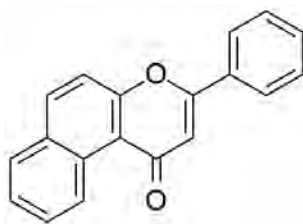
Synthesized from (*E*)-3-(4-fluoro-3-methoxyphenyl)-1-(1-hydroxynaphthalen-2-yl)prop-2-en-1-one, yield 76 % .

Molecular weight: 320.32 g/mol

^1H NMR (DMSO- d_6) δ : 8.70 – 8.64 (m, 1H), 8.12 – 8.04 (m, 3H), 7.98 (d, $J = 8.7$ Hz, 1H), 7.94 – 7.89 (m, 1H), 7.83 – 7.78 (m, 2H), 7.40 – 7.33 (m, 1H), 7.15 (s, 1H), 3.95 (s, 3H).

^{13}C NMR (DMSO- d_6) δ : 176.83, 160.98, 152.80, 152.71, 150.76, 135.57, 129.67, 128.36, 127.84, 125.51, 123.99, 123.74, 123.57, 122.53, 120.10, 119.69, 114.33, 113.98, 107.63, 56.47.

Anal. Calcd for $\text{C}_{20}\text{H}_{13}\text{FO}_3$: C, 74.99; H, 4.09. Found: C, 74.68; H, 4.25.

3-Phenyl-1*H*-benzo[*f*]chromen-1-one (53)

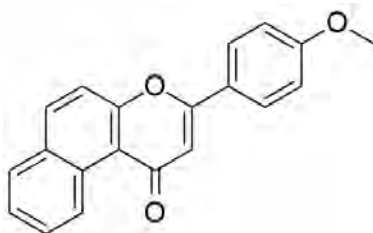
Synthesized from (*E*)-1-(2-hydroxynaphthalen-1-yl)-3-phenylprop-2-en-1-one, yield 59 %.

Molecular weight: 272.30 g/mol

¹H NMR (DMSO-*d*₆) δ : 9.98 – 9.90 (m, 1H), 8.35 (d, *J* = 9.0 Hz, 1H), 8.16 – 8.12 (m, 2H), 8.11 – 8.07 (m, 1H), 7.87 (d, *J* = 9.0 Hz, 1H), 7.77 (ddd, *J* = 8.5, 6.9, 1.5 Hz, 1H), 7.67 (ddd, *J* = 8.1, 6.9, 1.2 Hz, 1H), 7.63 – 7.58 (m, 3H), 7.18 (s, 1H).

¹³C NMR (DMSO-*d*₆) δ : 179.32, 160.38, 157.15, 135.90, 131.78, 130.88, 130.51, 129.81, 129.29, 129.17, 128.71, 126.72, 126.31, 126.21, 118.28, 116.37, 109.90.

Anal. Calcd for C₁₉H₁₂O₂: C, 83.81; H, 4.44. Found: C, 83.72; H, 4.52.

3-(4-Methoxyphenyl)-1*H*-benzo[*f*]chromen-1-one (54)

Synthesized from (*E*)-1-(2-hydroxynaphthalen-1-yl)-3-(4-methoxyphenyl)prop-2-en-1-one, yield 65 %.

Molecular weight: 302.32 g/mol

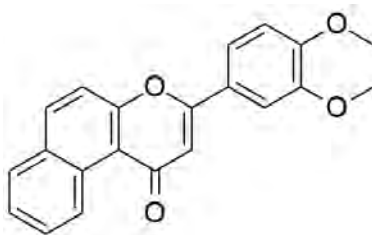
¹H NMR (DMSO-*d*₆) δ : 9.99 – 9.95 (m, 1H), 8.35 (d, *J* = 9.0 Hz, 1H), 8.12 (d, *J* = 9.0 Hz, 2H), 8.11 – 8.08 (m, 1H), 7.88 (d, *J* = 9.0 Hz, 1H), 7.77 (ddd, *J* = 8.5, 6.9,

1.5 Hz, 1H), 7.67 (ddd, $J = 8.1, 6.9, 1.2$ Hz, 1H), 7.14 (d, $J = 9.0$ Hz, 2H), 7.09 (s, 1H), 3.87 (s, 3H).

^{13}C NMR (DMSO- d_6) δ : 179.24, 162.17, 160.52, 157.01, 135.67, 130.49, 129.87, 129.07, 128.67, 128.15, 126.62, 126.23, 123.01, 118.27, 116.24, 114.76, 108.45, 55.67.

Anal. Calcd for $\text{C}_{20}\text{H}_{14}\text{O}_3$: C, 79.46; H, 4.67. Found: C, 79.51; H, 4.59

3-(3,4-Dimethoxyphenyl)-1*H*-benzo[*f*]chromen-1-one (55)



Synthesized from (*E*)-3-(3,4-dimethoxyphenyl)-1-(2-hydroxynaphthalen-1-yl)prop-2-en-1-one, yield 77 %.

Molecular weight: 332.35 g/mol

^1H NMR (DMSO- d_6) δ : 9.98 – 9.94 (m, 1H), 8.33 (d, $J = 9.0$ Hz, 1H), 8.07 (dd, $J = 8.3, 1.0$ Hz, 1H), 7.88 (d, $J = 9.0$ Hz, 1H), 7.78 – 7.72 (m, 2H), 7.69 – 7.62 (m, 2H), 7.16 (s, 1H), 7.13 (d, $J = 8.6$ Hz, 1H), 3.91 (s, 3H), 3.85 (s, 3H).

^{13}C NMR (DMSO- d_6) δ : 179.30, 160.51, 157.01, 151.97, 149.26, 135.60, 130.48, 129.89, 129.04, 128.66, 126.60, 126.26, 123.10, 119.78, 118.33, 116.23, 111.94, 109.46, 108.72, 56.03, 55.86.

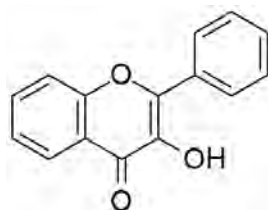
Anal. Calcd for $\text{C}_{21}\text{H}_{16}\text{O}_4$: C, 75.89; H, 4.85. Found: C, 76.03; H, 4.67.

7.1.2.7 General procedure for synthesis of 3-hydroxy flavones and benzoflavones

An appropriate chalcone or benzochalcone (5 mmol) was dissolved in EtOH (25 ml). NaOH 25% (10 ml) and H_2O_2 25% (10 ml) were added in small portions to the

solution. This solution was stirred overnight at room temperature. After completion of reaction as indicated by TLC, the reaction mixture was poured onto crushed ice and was acidified with dilute HCl. Yellow-brown precipitate was filtered under suction, washed with water. The crude product was recrystallized from ethanol to give 3-hydroxy flavones or benzoflavones.

3-Hydroxy-2-phenyl-4*H*-chromen-4-one (56)



Synthesized from (*E*)-1-(2-hydroxyphenyl)-3-phenylprop-2-en-1-one, yield 59 %.

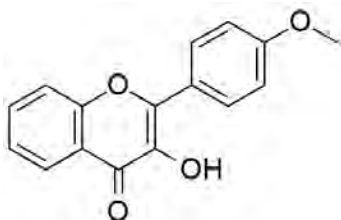
Molecular weight: 238.24 g/mol

^1H NMR (DMSO- d_6) δ : 11.86 (s, 0H), 8.30 – 8.21 (m, 2H), 7.69 (ddd, $J = 1.6, 7.1, 8.6, 1\text{H}$), 7.58 (d, $J = 8.5, 1\text{H}$), 7.53 (dd, $J = 4.7, 10.3, 2\text{H}$), 7.49 – 7.43 (m, 1H), 7.40 (t, $J = 7.5, 1\text{H}$), 7.07 (dd, $J = 2.8, 5.9, 1\text{H}$).

^{13}C NMR (DMSO- d_6) δ : 173.49, 155.44, 144.98, 138.46, 133.64, 131.07, 130.20, 128.60, 128.31, 127.77, 126.30, 125.47, 124.53, 120.66, 118.28.

Anal. Calcd for $\text{C}_{15}\text{H}_{10}\text{O}_3 \cdot \text{H}_2\text{O}$: C, 70.31; H, 4.72. Found: C, 70.22; H, 4.83.

3-Hydroxy-2-(4-methoxyphenyl)-4*H*-chromen-4-one (57)



Synthesized from (*E*)-1-(2-hydroxyphenyl)-3-(4-methoxyphenyl)prop-2-en-1-one, yield 61 %.

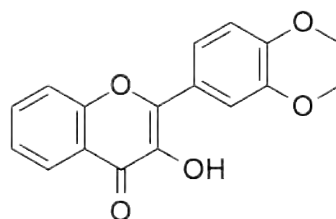
Molecular weight: 268.26 g/mol

^1H NMR (DMSO- d_6) δ : 9.39 (s, 1H), 8.20 (d, $J = 9.2$ Hz, 2H), 7.91 – 7.86 (m, 1H), 7.82 – 7.69 (m, 2H), 7.45 (ddd, $J = 8.0, 6.8, 1.3$ Hz, 1H), 7.12 (d, $J = 9.2$ Hz, 2H), 3.84 (s, 3H).

^{13}C NMR (DMSO- d_6) δ : 172.77, 160.60, 154.59, 145.74, 138.28, 133.61, 131.45, 129.54, 124.87, 123.73, 121.50, 118.44, 114.19, 55.50.

Anal. Calcd for $\text{C}_{16}\text{H}_{12}\text{O}_4$: C, 71.64; H, 4.51. Found: C, 71.53; H, 4.64.

2-(3,4-dimethoxyphenyl)-3-hydroxy-4*H*-chromen-4-one (58)



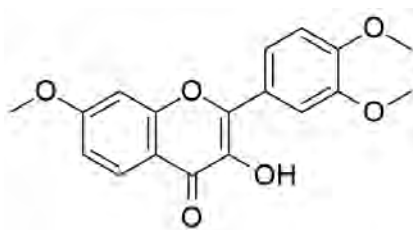
Synthesized from (*E*)-3-(3,4-dimethoxyphenyl)-1-(2-hydroxyphenyl)prop-2-en-1-one, yield 66 %.

Molecular weight: 298.29 g/mol

^1H NMR (DMSO- d_6) δ : 12.58 (s, 1H), 7.90 – 7.86 (m, 2H), 7.69 (d, $J = 8.7$ Hz, 1H), 7.02 – 6.99 (m, 2H), 6.48 (dt, $J = 5.9, 2.4$ Hz, 2H), 3.81 (s, 3H), 3.78 (s, 3H).

^{13}C NMR (DMSO- d_6) δ : 171.97, 167.12, 165.28, 163.56, 162.98, 131.76, 131.47, 123.13, 113.95, 107.17, 105.78, 100.86, 55.69, 55.57.

Anal. Calcd for $\text{C}_{17}\text{H}_{14}\text{O}_5$: C, 68.45; H, 4.73. Found: C, 68.19; H, 4.91.

2-(3,4-Dimethoxyphenyl)-3-hydroxy-7-methoxy-4*H*-chromen-4-one (59)

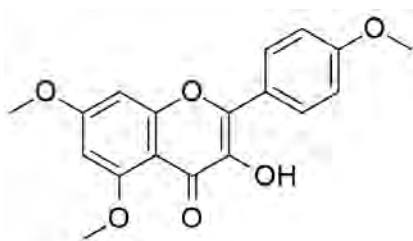
Synthesized from (*E*)-3-(3,4-dimethoxyphenyl)-1-(2-hydroxy-4-methoxyphenyl)prop-2-en-1-one, yield 62 %.

Molecular weight: 328.32 g/mol

¹H NMR (DMSO-*d*₆) δ : 9.27 (s, 1H), 7.98 (d, $J = 8.9$, 1H), 7.85 (dd, $J = 2.1$, 8.6 Hz, 1H), 7.79 (d, $J = 2.1$ Hz, 1H), 7.28 (d, $J = 2.3$ Hz, 1H), 7.13 (d, $J = 8.7$, 1H), 7.03 (dd, $J = 2.4$, 8.9 Hz, 1H), 3.92 (s, 3H), 3.84 (d, $J = 3.1$ Hz, 6H).

¹³C NMR (DMSO-*d*₆) δ : 172.18, 163.66, 156.47, 150.32, 148.59, 144.94, 138.06, 126.20, 123.94, 121.41, 115.29, 114.64, 111.70, 111.10, 100.49, 56.22, 55.90, 55.76.

Anal. Calcd for C₁₈H₁₆O₆*0.5 H₂O: C, 64.09; H, 5.08. Found: C, 63.94; H, 5.17.

3-Hydroxy-5,7-dimethoxy-2-(4-methoxyphenyl)-4*H*-chromen-4-one (60)

Synthesized from (*E*)-1-(2-hydroxy-4,6-dimethoxyphenyl)-3-(4-methoxyphenyl)prop-2-en-1-one, yield 70 %.

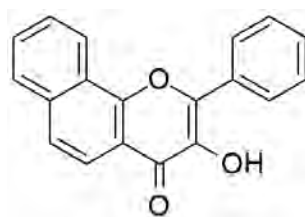
Molecular weight: 328.32 g/mol

¹H NMR (DMSO-*d*₆) δ : 9.12 (d, $J = 1.7$ Hz, 1H), 7.66 (d, $J = 8.9$ Hz, 2H), 6.90 (d, $J = 8.9$ Hz, 2H), 6.35 (s, 2H), 3.75 (s, 6 H), 3.69 (s, 3H).

^{13}C NMR (DMSO- d_6) δ : 191.14, 162.18, 159.23, 158.24, 148.88, 131.44, 127.52, 116.02, 114.13, 108.89, 91.27, 55.99, 55.62, 55.29.

Anal. Calcd for $\text{C}_{18}\text{H}_{16}\text{O}_6$: C, 65.85; H, 4.91. Found: C, 65.67; H, 5.11.

3-Hydroxy-2-phenyl-4*H*-benzo[*h*]chromen-4-one (61)



Synthesized from (*E*)-1-(1-hydroxynaphthalen-2-yl)-3-phenylprop-2-en-1-one, yield 57 %.

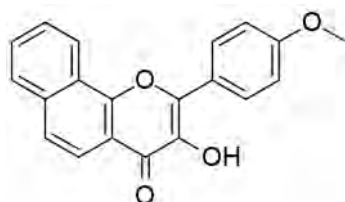
Molecular weight: 288.30 g/mol

^1H NMR (DMSO- d_6) δ : 9.78 (s, 1H), 8.66 (dd, $J = 6.1, 3.4$ Hz, 1H), 8.34 (dd, $J = 8.5, 1.2$ Hz, 2H), 8.10 (dd, $J = 6.0, 3.3$ Hz, 1H), 8.05 (d, $J = 8.7$ Hz, 1H), 7.89 (d, $J = 8.7$ Hz, 1H), 7.84 – 7.79 (m, 2H), 7.74 (d, $J = 8.7$ Hz, 1H), 7.64 – 7.60 (m, 2H).

^{13}C NMR (DMSO- d_6) δ : 172.80, 151.96, 144.74, 140.52, 135.24, 131.61, 129.92, 129.73, 128.87, 128.48, 127.90, 127.68, 125.04, 124.89, 123.76, 123.21, 122.46, 120.28, 117.66.

Anal. Calcd for $\text{C}_{19}\text{H}_{12}\text{O}_3$: C, 79.16; H, 4.20. Found: C, 79.28; H, 4.15.

3-Hydroxy-2-(4-methoxyphenyl)-4*H*-benzo[*h*]chromen-4-one (62)



Synthesized from (*E*)-1-(1-hydroxynaphthalen-2-yl)-3-(4-methoxyphenyl)prop-2-en-1-one, yield 59 %.

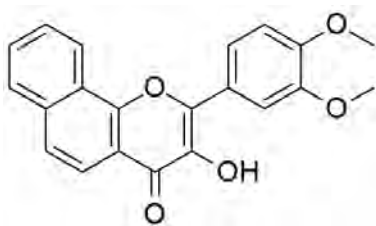
Molecular weight: 318.32 g/mol

^1H NMR (DMSO- d_6) δ : 9.60 (s, 1H), 8.68 – 8.62 (m, 1H), 8.32 (d, $J = 8.9$ Hz, 2H), 8.14 – 8.07 (m, 1H), 8.04 (d, $J = 8.7$ Hz, 1H), 7.89 (d, $J = 8.7$ Hz, 1H), 7.81 (dd, $J = 6.0, 3.3$ Hz, 2H), 7.18 (d, $J = 9.0$ Hz, 2H), 3.87 (s, 3H).

^{13}C NMR (DMSO- d_6) δ : 172.46, 160.52, 151.70, 145.18, 139.53, 135.14, 129.58, 129.39, 128.46, 127.83, 124.75, 123.91, 123.73, 122.37, 120.30, 117.64, 114.38, 55.50.

Anal. Calcd for $\text{C}_{20}\text{H}_{14}\text{O}_4$: C, 75.46; H, 4.43. Found: 75.37; H, 4.54.

2-(3,4-Dimethoxyphenyl)-3-hydroxy-4*H*-benzo[*h*]chromen-4-one (63)



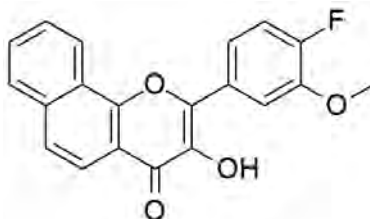
Synthesized from (*E*)-3-(3,4-dimethoxyphenyl)-1-(1-hydroxynaphthalen-2-yl)prop-2-en-1-one, yield 61 %.

Molecular weight: 348.35 g/mol

^1H NMR (DMSO- d_6) δ : 9.61 (s, 1H), 8.61 (s, 1H), 8.10 (d, $J = 9.1$, 1H), 8.04 (d, $J = 8.7$, 1H), 7.95 (d, $J = 8.5$, 1H), 7.91 (d, $J = 2.0$, 1H), 7.89 (d, $J = 8.8$, 1H), 7.83 – 7.79 (m, 2H), 7.20 (d, $J = 8.6$, 1H), 3.88 (d, $J = 12.2$, 6H).

^{13}C NMR (DMSO- d_6) δ : 172.44, 151.70, 150.44, 148.68, 145.14, 139.66, 135.17, 129.60, 128.49, 127.92, 124.00, 123.72, 117.63, 111.96, 111.19, 55.83, 55.80.

Anal. Calcd for $\text{C}_{21}\text{H}_{16}\text{O}_5 \cdot 0.5 \text{H}_2\text{O}$: C, 72.41; H, 4.63. Found: C, 72.35; H, 4.71.

2-(4-Fluoro-3-methoxyphenyl)-3-hydroxy-4*H*-benzo[*h*]chromen-4-one (64)

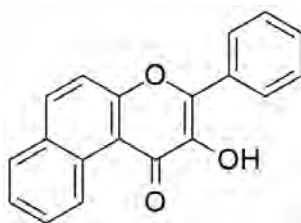
Synthesized from (*E*)-3-(4-fluoro-3-methoxyphenyl)-1-(1-hydroxynaphthalen-2-yl)prop-2-en-1-one, yield 54 %.

Molecular weight: 336.31 g/mol

¹H NMR (DMSO-*d*₆) δ : 9.85 (s, 1H), 8.72 – 8.63 (m, 1H), 8.22 – 8.08 (m, 3H), 8.04 (d, *J* = 8.7 Hz, 1H), 7.90 (d, *J* = 8.7 Hz, 1H), 7.86 – 7.77 (m, 2H), 7.41 (t, *J* = 8.9 Hz, 1H), 3.95 (s, 3H).

¹³C NMR (DMSO-*d*₆) δ : 172.56, 151.77, 150.32, 148.47, 144.01, 143.78, 140.07, 135.22, 129.70, 128.46, 127.90, 124.90, 124.64, 124.29, 123.68, 122.52, 120.26, 117.67, 115.10, 114.13, 56.36.

Anal. Calcd for C₂₀H₁₃FO₄: C, 71.43; H, 3.90. Found: C, 71.54; H, 3.78.

2-Hydroxy-3-phenyl-1*H*-benzo[*f*]chromen-1-one (65)

Synthesized from (*E*)-1-(2-hydroxynaphthalen-1-yl)-3-phenylprop-2-en-1-one, yield 63 %.

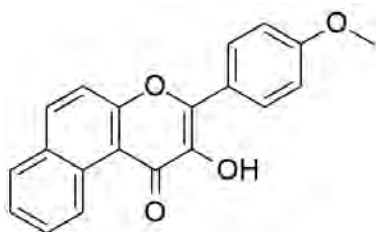
Molecular weight: 288.30 g/mol

^1H NMR (DMSO- d_6) δ : 8.49 (d, $J = 8.5$ Hz, 1H), 7.96 (d, $J = 9.0$ Hz, 1H), 7.86 – 7.82 (m, 2H), 7.78 (d, $J = 9.0$ Hz, 1H), 7.71 (td, $J = 7.5, 1.4$ Hz, 1H), 7.65 (d, $J = 9.0$ Hz, 1H), 7.61 (dt, $J = 13.4, 4.6$ Hz, 1H), 7.55 – 7.48 (m, 2H), 7.35 (ddd, $J = 8.0, 6.8, 1.1$ Hz, 1H), 7.16 (d, $J = 8.9$ Hz, 1H).

^{13}C NMR (DMSO- d_6) δ : 172.28, 165.73, 159.67, 156.12, 142.48, 135.82, 134.73, 134.56, 129.88, 128.77, 127.98, 127.94, 124.59, 123.33, 119.04, 113.08.

Anal. Calcd for $\text{C}_{19}\text{H}_{12}\text{O}_3 \cdot \text{H}_2\text{O}$: C, 74.50; H, 4.61. Found: C, 74.57; H, 4.88.

2-Hydroxy-3-(4-methoxyphenyl)-1*H*-benzo[*f*]chromen-1-one (66)



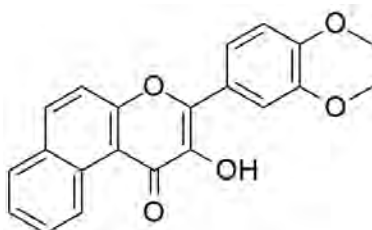
Synthesized from (*E*)-1-(2-hydroxynaphthalen-1-yl)-3-(4-methoxyphenyl)prop-2-en-1-one, yield 57 %.

Molecular weight: 318.32 g/mol

^1H NMR (DMSO- d_6) δ : 9.33 (s, 1H), 8.67 (dd, $J = 7.2, 1.7$ Hz, 1H), 7.79 – 7.71 (m, 2H), 7.54 (d, $J = 7.5$ Hz, 1H), 7.49 (d, $J = 7.5$ Hz, 2H), 7.42 (dtd, $J = 19.9, 7.4, 1.6$ Hz, 2H), 6.97 (d, $J = 7.5$ Hz, 2H), 3.81 (s, 3H).

^{13}C NMR (DMSO- d_6) δ : 172.28, 167.89, 161.06, 159.95, 143.82, 134.65, 131.57, 131.44, 130.02, 128.79, 128.03, 127.00, 126.96, 124.54, 123.41, 118.94, 116.64, 114.47, 55.42.

Anal. Calcd for $\text{C}_{20}\text{H}_{14}\text{O}_4$: C, 75.46; H, 4.43. Found: C, 75.27; H, 4.67.

3-(3,4-Dimethoxyphenyl)-2-hydroxy-1*H*-benzo[*f*]chromen-1-one (67)

Synthesized from (*E*)-3-(3,4-dimethoxyphenyl)-1-(2-hydroxynaphthalen-1-yl)prop-2-en-1-one, yield 66 %.

Molecular weight: 348.10 g/mol

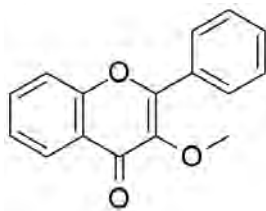
¹H NMR (DMSO-*d*₆) δ : 9.83 (s, 1H), 7.55 (dd, *J* = 8.4, 2.0 Hz, 2H), 7.43 (d, *J* = 2.0 Hz, 2H), 7.29 (d, *J* = 2.0 Hz, 1H), 7.18 (ddd, *J* = 14.2, 7.5, 4.5 Hz, 1H), 7.03 (d, *J* = 8.5 Hz, 2H), 6.42 (d, *J* = 15.9 Hz, 1H), 3.81 (s, 3H), 3.79 (s, 3H).

¹³C NMR (DMSO-*d*₆) δ : 167.98, 167.22, 152.78, 150.95, 149.15, 148.47, 127.22, 123.32, 123.12, 122.74, 116.86, 112.11, 111.74, 111.47, 111.17, 110.55, 55.80, 55.62.

Anal. Calcd for C₂₁H₁₆O₅: C, 72.41; H, 4.63. Found: C, 72.18; H, 4.92.

7.1.2.8 General procedure for synthesis of 3-methoxy flavones and benzoflavones

To a solution of 3-hydroxyflavone or 3-hydroxybenzoflavone (2 mmol) in acetone (25 ml), K₂CO₃ (2 mmol) and methyl iodide (3 mmol) were added. The resulting mixture was refluxed for 24 h. After completion of the reaction acetone and methyl iodide were removed under reduced pressure. To the resulting solid water was added, the precipitated product was filtered and washed with water to remove traces of K₂CO₃. The product was dried at room temperature and recrystallized from ethanol to yield corresponding 3-methoxy flavones and benzoflavones.

3-Methoxy-2-phenyl-4*H*-chromen-4-one (68)

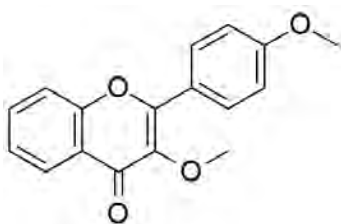
Synthesized from 3-hydroxy-2-phenyl-4*H*-chromen-4-one, yield 74 %.

Molecular weight: 252.26 g/mol

^1H NMR (CDCl_3) δ : 8.26 (dd, $J = 8.0, 1.7$ Hz, 1H), 8.12 – 8.06 (m, 2H), 7.66 (ddd, $J = 8.5, 7.1, 1.7$ Hz, 1H), 7.55 – 7.48 (m, 4H), 7.39 (ddd, $J = 8.0, 7.1, 1.0$ Hz, 1H), 3.89 (s, 3H).

^{13}C NMR (CDCl_3) δ : 175.14, 155.60, 155.28, 141.53, 133.45, 130.72, 128.53, 128.50, 125.83, 124.66, 117.98, 60.13.

Anal. Calcd for $\text{C}_{16}\text{H}_{12}\text{O}_3$: C, 76.18; H, 4.79. Found: C, 75.92; H, 4.96.

3-Methoxy-2-(4-methoxyphenyl)-4*H*-chromen-4-one (69)

Synthesized from 3-hydroxy-2-(4-methoxyphenyl)-4*H*-chromen-4-one, yield 64 %.

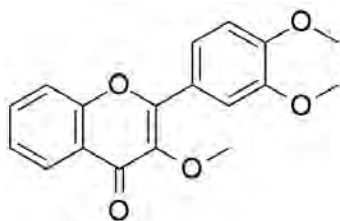
Molecular weight: 282.29 g/mol

^1H NMR (DMSO-d_6) δ : 8.09 (d, $J = 1.3$ Hz, 1H), 8.08 – 8.06 (m, 1H), 8.06 – 8.04 (m, 1H), 7.80 (ddd, $J = 8.6, 7.0, 1.7$ Hz, 1H), 7.75 – 7.71 (m, 1H), 7.47 (ddd, $J = 8.0, 7.0, 1.1$ Hz, 1H), 7.16 – 7.11 (m, 2H), 3.85 (s, 3H), 3.80 (s, 3H).

^{13}C NMR (DMSO- d_6) δ : 173.80, 161.38, 155.10, 154.76, 140.22, 134.01, 130.20, 125.08, 125.01, 123.68, 122.75, 118.47, 114.35, 59.61, 55.58.

Anal. Calcd for $\text{C}_{17}\text{H}_{14}\text{O}_4$: C, 72.33; H, 5.00: C, 72.47; H, 5.38.

2-(3,4-Dimethoxyphenyl)-3-methoxy-4*H*-chromen-4-one (70)



Synthesized from 2-(3,4-dimethoxyphenyl)-3-hydroxy-4*H*-chromen-4-one, yield 73 %.

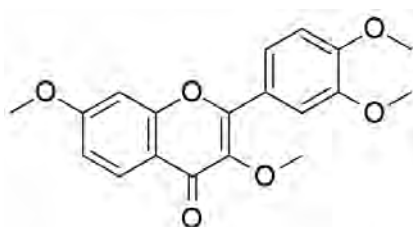
Molecular weight: 312.32 g/mol

^1H NMR (DMSO- d_6) δ : 8.08 (dd, $J = 7.9, 1.6$ Hz, 1H), 7.81 (ddd, $J = 8.5, 6.9, 1.6$ Hz, 1H), 7.78 – 7.75 (m, 1H), 7.72 (dd, $J = 8.5, 2.1$ Hz, 1H), 7.68 (d, $J = 2.1$ Hz, 1H), 7.48 (ddd, $J = 8.0, 6.9, 1.2$ Hz, 1H), 7.16 (d, $J = 8.6$ Hz, 1H), 3.86 (d, $J = 1.8$ Hz, 6H), 3.82 (s, 3H).

^{13}C NMR (DMSO- d_6) δ : 173.81, 155.07, 154.75, 151.26, 148.62, 140.35, 134.00, 125.10, 125.00, 123.65, 122.76, 122.14, 118.57, 111.78, 111.68, 59.64, 55.82.

Anal. Calcd for $\text{C}_{18}\text{H}_{16}\text{O}_5$: C, 69.22; H, 5.16. Found: C, 69.28; H, 5.13.

2-(3,4-Dimethoxyphenyl)-3,7-dimethoxy-4*H*-chromen-4-one (71)



Synthesized from 2-(3,4-dimethoxyphenyl)-3-hydroxy-7-methoxy-4H-chromen-4-one, yield 71 %.

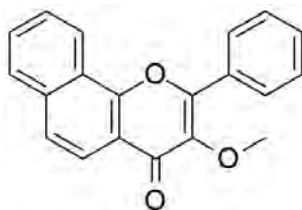
Molecular weight: 342.34 g/mol

^1H NMR (DMSO- d_6) δ : 7.96 (d, $J = 8.9$ Hz, 1H), 7.71 (dd, $J = 8.5, 2.1$ Hz, 1H), 7.66 (d, $J = 2.1$ Hz, 1H), 7.27 (d, $J = 2.3$ Hz, 1H), 7.15 (d, $J = 8.6$ Hz, 1H), 7.05 (dd, $J = 8.9, 2.4$ Hz, 1H), 3.91 (s, 3H), 3.86 (s, 6H), 3.81 (s, 3H).

^{13}C NMR (DMSO- d_6) δ : 173.21, 163.86, 156.57, 154.50, 151.11, 148.60, 140.10, 126.36, 122.83, 121.93, 117.44, 114.71, 111.73, 111.56, 100.73, 59.62, 56.26, 55.84, 55.80.

Anal. Calcd for $\text{C}_{19}\text{H}_{18}\text{O}_6$: C, 66.66; H, 5.30. Found: C, 66.38; H, 5.64.

3-Methoxy-2-phenyl-4*H*-benzo[*h*]chromen-4-one (72)



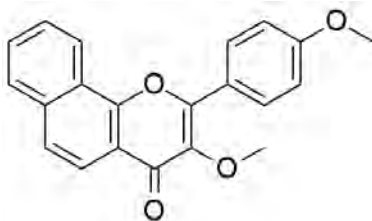
Synthesized from 3-hydroxy-2-phenyl-4H-benzo[*h*]chromen-4-one, yield 62 %.

Molecular weight: 302.32 g/mol

^1H NMR (DMSO- d_6) δ : 8.59 (dd, $J = 6.1, 3.4$ Hz, 1H), 8.21 – 8.18 (m, 2H), 8.14 – 8.10 (m, 1H), 8.04 (d, $J = 8.7$ Hz, 1H), 7.94 (d, $J = 8.7$ Hz, 1H), 7.85 – 7.79 (m, 2H), 7.68 – 7.61 (m, 3H), 3.90 (s, 3H).

^{13}C NMR (DMSO- d_6) δ : 173.83, 154.36, 152.10, 142.14, 135.39, 130.99, 130.70, 129.82, 129.02, 128.44, 128.40, 127.97, 125.34, 123.56, 122.40, 120.22, 120.05, 59.82.

Anal. Calcd for $\text{C}_{20}\text{H}_{14}\text{O}_3$: C, 79.46; H, 4.67. Found: C, 79.29; H, 4.81.

3-Methoxy-2-(4-methoxyphenyl)-4*H*-benzo[*h*]chromen-4-one (73)

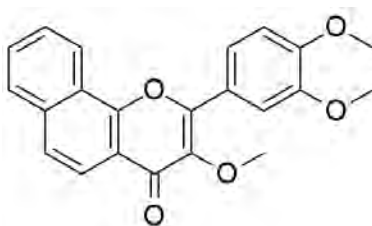
Synthesized from 3-hydroxy-2-(4-methoxyphenyl)-4*H*-benzo[*h*]chromen-4-one, yield 59 %.

Molecular weight: 332.35 g/mol

^1H NMR (DMSO- d_6) δ : 8.59 – 8.54 (m, 1H), 8.20 – 8.16 (m, 2H), 8.11 – 8.07 (m, 1H), 8.01 (d, J = 8.7 Hz, 1H), 7.90 (d, J = 9.0 Hz, 1H), 7.80 (ddd, J = 4.7, 2.2, 0.8 Hz, 2H), 7.19 (d, J = 9.1 Hz, 2H), 3.88 (s, 6H).

^{13}C NMR (DMSO- d_6) δ : 173.58, 161.33, 154.37, 151.85, 141.34, 135.31, 130.13, 129.67, 128.41, 127.87, 125.16, 123.53, 122.87, 122.31, 120.23, 119.96, 114.52, 59.58, 55.56.

Anal. Calcd for $\text{C}_{21}\text{H}_{16}\text{O}_4$: C, 75.89; H, 4.85. Found: C, 75.58; H, 5.04.

2-(3,4-Dimethoxyphenyl)-3-methoxy-4*H*-benzo[*h*]chromen-4-one (74)

Synthesized from 2-(3,4-dimethoxyphenyl)-3-hydroxy-4*H*-benzo[*h*]chromen-4-one, yield 69 %.

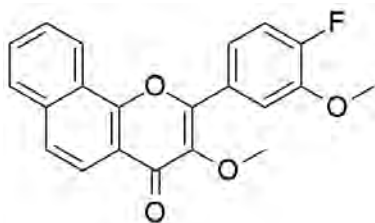
Molecular weight: 362.38 g/mol

^1H NMR (DMSO- d_6) δ : 8.58 (dd, $J = 3.5, 6.2$ Hz, 1H), 8.12 (dd, $J = 3.1, 6.2$ Hz, 1H), 8.03 (d, $J = 8, 7$ Hz, 1H), 7.92 (d, $J = 8.6$ Hz, 1H), 7.84 (d, $J = 2.1$ Hz, 1H), 7.83-7.82 (m, 1H), 7.81 (d, $J = 3.3$ Hz, 1H), 7.77 (d, $J = 2.1$ Hz, 1H), 7.22 (d, $J = 8.6$ Hz, 1H), 3.92 (d, $J = 11.4$ Hz, 6H), 3.76 (s, 3H).

^{13}C NMR (DMSO- d_6) δ : 173.61, 154.45, 151.90, 151.22, 148.72, 135.37, 129.72, 128.47, 128.00, 125.24, 123.57, 122.89, 122.33, 121.99, 120.27, 119.99, 111.98, 111.62, 59.67, 55.85, 55.81.

Anal. Calcd for $\text{C}_{22}\text{H}_{18}\text{O}_5$: C, 72.92; H, 5.01. Found: C, 72.68; H, 5.25.

2-(4-Fluoro-3-methoxyphenyl)-3-methoxy-4*H*-benzo[*h*]chromen-4-one (75)



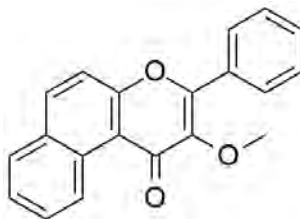
Synthesized from 2-(4-fluoro-3-methoxyphenyl)-3-hydroxy-4*H*-benzo[*h*]chromen-4-one, yield 74 %.

Molecular weight: 350.34 g/mol

^1H NMR (DMSO- d_6) δ : 8.41 (dd, $J = 7.5, 1.6$ Hz, 1H), 7.75 (dt, $J = 8.1, 1.4$ Hz, 2H), 7.61 (d, $J = 7.1$ Hz, 1H), 7.44 (dtd, $J = 25.6, 7.2, 1.5$ Hz, 2H), 6.88 – 6.81 (m, 3H), 3.61 (s, 3H), 3.55 (s, 3H).

^{13}C NMR (DMSO- d_6) δ : 173.68, 158.40, 155.41, 154.67, 151.95, 151.02, 150.80, 136.86, 134.25, 129.19, 129.16, 128.22, 128.27, 127.72, 125.19, 124.54, 124.15, 123.62, 123.57, 123.22, 121.35, 115.26, 115.04, 114.78, 114.72, 61.45, 59.80, 57.76.

Anal. Calcd for $\text{C}_{21}\text{H}_{15}\text{FO}_4$: C, 71.99; H, 4.32. Found: C, 72.18; H, 4.24.

2-Methoxy-3-phenyl-1*H*-benzo[*f*]chromen-1-one (76)

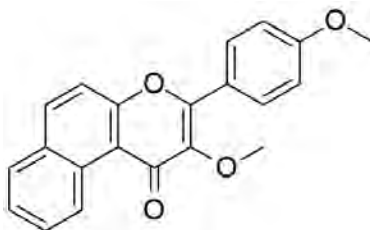
Synthesized from 2-hydroxy-3-phenyl-1*H*-benzo[*f*]chromen-1-one, yield 54 %.

Molecular weight: 302.32 g/mol

¹H NMR (DMSO-*d*₆) δ : 8.78 (dd, *J* = 7.5, 1.6 Hz, 1H), 7.82 – 7.76 (m, 2H), 7.58 – 7.54 (m, 1H), 7.49 (td, *J* = 7.5, 1.5 Hz, 1H), 7.42 (td, *J* = 7.5, 1.5 Hz, 1H), 7.32 (dd, *J* = 7.5, 1.3 Hz, 2H), 7.24 (t, *J* = 7.3 Hz, 2H), 7.21 – 7.15 (m, 1H), 3.49 (s, 3H).

¹³C NMR (DMSO-*d*₆) δ : 172.01, 156.52, 152.44, 136.05, 133.83, 131.19, 130.92, 130.85, 130.59, 128.69, 128.47, 128.01, 127.98, 126.47, 125.09, 119.04, 116.89, 59.51.

Anal. Calcd for C₂₀H₁₄O₃: C, 79.46; H, 4.67. Found: C, 79.14; H, 4.88.

2-Methoxy-3-(4-methoxyphenyl)-1*H*-benzo[*f*]chromen-1-one (77)

Synthesized from 2-hydroxy-3-(4-methoxyphenyl)-1*H*-benzo[*f*]chromen-1-one, yield 63 %.

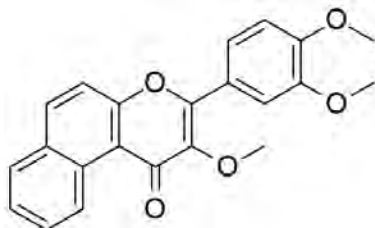
Molecular weight: 332.35 g/mol

¹H NMR (DMSO-*d*₆) δ : 8.75 (dd, *J* = 7.5, 1.7 Hz, 1H), 7.81 – 7.75 (m, 2H), 7.66 – 7.58 (m, 1H), 7.51 (dtd, *J* = 25.1, 7.3, 1.7 Hz, 2H), 7.32 (d, *J* = 7.5 Hz, 2H), 6.89 (d, *J* = 7.5 Hz, 2H), 3.77 (s, 3H), 3.59 (s, 3H).

^{13}C NMR (DMSO- d_6) δ : 173.14, 160.42, 155.62, 152.44, 138.05, 133.73, 130.92, 130.85, 129.87, 128.01, 127.98, 126.47, 125.09, 123.08, 119.04, 114.85, 113.56, 59.97, 58.03.

Anal. Calcd for $\text{C}_{21}\text{H}_{16}\text{O}_4$: C, 75.89; H, 4.85. Found: C, 75.68; H, 5.03.

3-(3,4-Dimethoxyphenyl)-2-methoxy-1*H*-benzo[*f*]chromen-1-one (78)



Synthesized from 3-(3,4-dimethoxyphenyl)-2-hydroxy-1*H*-benzo[*f*]chromen-1-one, yield 68 %.

Molecular weight: 362.38 g/mol

^1H NMR (DMSO- d_6) δ : 8.79 (dd, $J = 7.4, 1.6$ Hz, 1H), 7.85 – 7.78 (m, 2H), 7.68 – 7.62 (m, 1H), 7.45 (dtd, $J = 25.1, 7.4, 1.5$ Hz, 2H), 7.08 – 6.91 (m, 2H), 6.79 (d, $J = 7.8$ Hz, 1H), 3.59 (s, 6H), 3.51 (s, 3H).

^{13}C NMR (DMSO- d_6) δ : 176.04, 155.52, 153.59, 152.27, 149.41, 137.83, 133.83, 130.92, 130.85, 128.01, 127.98, 126.47, 125.09, 123.58, 122.40, 119.04, 114.85, 112.34, 111.89, 61.45, 56.78.

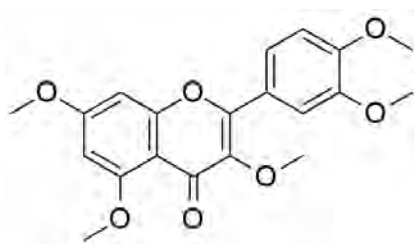
Anal. Calcd for $\text{C}_{22}\text{H}_{18}\text{O}_5$: C, 72.92; H, 5.01. Found: C, 73.05; H, 5.12.

7.1.2.9 General procedure for synthesis of pentamethyl ethers of quercetin and morin

To a solution of quercetin hydrate or morin (10 mmol) in acetone (50 ml), K_2CO_3 (30 mmol) and methyl iodide (70 mmol, excess) were added. The resulting mixture was refluxed for 24 h. After completion of the reaction acetone and methyl iodide

were removed under reduced pressure. To the resulting solid water was added, the precipitated product was filtered and washed with water to remove traces of K_2CO_3 . The product was dried at room temperature and recrystallized from ethanol to yield pentamethylquercetine or pentamethylmorin.

2-(3,4-Dimethoxyphenyl)-3,5,7-trimethoxy-4*H*-chromen-4-one (79)



Synthesized from quercetin, yield 82 %.

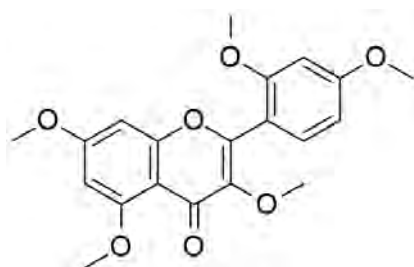
Molecular weight: 372.37 g/mol

1H NMR (DMSO- d_6) δ : 7.69 (s, 1H), 7.67 (d, $J = 2.1$ Hz, 1H), 6.96 (d, $J = 8.3$ Hz, 1H), 6.48 (d, $J = 2.3$ Hz, 1H), 6.33 (d, $J = 2.3$ Hz, 1H), 3.94 (s, 9H), 3.88 (s, 3H), 3.86 (s, 3H).

^{13}C NMR (DMSO- d_6) δ : 174.00, 163.87, 161.02, 158.78, 152.52, 150.79, 148.65, 141.18, 123.41, 121.60, 111.26, 110.76, 109.49, 95.72, 92.42, 59.93, 56.39, 56.05, 55.95, 55.75.

Anal. Calcd for $C_{20}H_{20}O_7$: C, 64.51; H, 5.41. Found: C, 64.34; H, 5.62.

2-(2,4-Dimethoxyphenyl)-3,5,7-trimethoxy-4*H*-chromen-4-one (80)



Synthesized from morin, yield 76 %.

Molecular weight: 372.37 g/mol

^1H NMR (DMSO- d_6) δ : 7.34 (d, $J = 8.4$ Hz, 1H), 6.69 (d, $J = 2.3$ Hz, 1H), 6.64 (dd, $J = 8.5, 2.3$ Hz, 1H), 6.61 (d, $J = 2.3$ Hz, 1H), 6.47 (d, $J = 2.3$ Hz, 1H), 3.83 (d, $J = 2.1$ Hz, 9H), 3.79 (s, 3H), 3.60 (s, 3H).

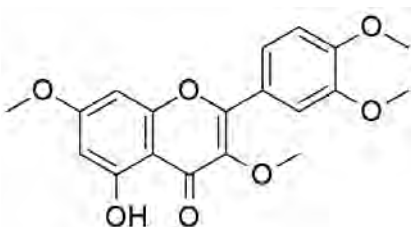
^{13}C NMR (DMSO- d_6) δ : 172.12, 163.71, 162.44, 160.64, 158.85, 158.38, 152.86, 141.48, 131.46, 114.37, 112.26, 109.11, 105.34, 98.78, 96.01, 93.05, 59.57, 56.30, 56.10, 55.91, 55.63.

Anal. Calcd for $\text{C}_{20}\text{H}_{20}\text{O}_7$: C, 64.51; H, 5.41. Found: C, 64.67; H, 5.34.

7.1.2.10 General procedure for synthesis of tetramethyl ethers of quercetin and morin

Quercetin hydrate or morin (10 mmol) was added to a mixture of acetone (150 ml) and water (75 ml). To the resulting solution, 30% aqueous KOH (6 ml) was added and refluxed for 10 minutes. Dimethyl sulfate (2.4 ml) was added and refluxed for 20 min. More amount of KOH (3 ml) was added producing a dark brown solution. To this solution an additional amount of dimethyl sulfate (2.4 ml) was added and refluxed for additional 20 min. After this KOH (3.0 ml) and dimethyl sulfate (3.5 ml) were added again and the solution was refluxed further for 1.5 h and allowed to cool to room temperature. Evaporation of acetone gave a dark yellow to brown residue. This residue was purified by column chromatography using hexan:ethylacetate (1:3) as mobile phase. The first two fractions were combined and evaporated to give pure tetramethylquercetin or tetramethylmorin.

2-(3,4-Dimethoxyphenyl)-5-hydroxy-3,7-dimethoxy-4*H*-chromen-4-one (81)



Synthesized from quercetin, yield 51 %.

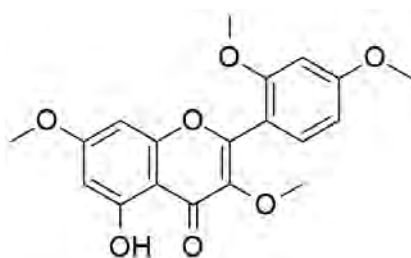
Molecular weight: 358.34 g/mol

^1H NMR (DMSO- d_6) δ : 12.61 (s, 1H), 7.71 (dd, $J = 8.6, 2.1$ Hz, 1H), 7.65 (d, $J = 2.1$ Hz, 1H), 7.15 (d, $J = 8.7$ Hz, 1H), 6.77 (d, $J = 2.1$ Hz, 1H), 6.37 (d, $J = 2.2$ Hz, 1H), 3.87 – 3.84 (m, 9H), 3.82 (s, 3H).

^{13}C NMR (DMSO- d_6) δ : 178.20, 165.34, 160.81, 156.51, 155.59, 151.52, 148.67, 138.51, 122.25, 122.22, 111.79, 111.52, 105.39, 97.95, 92.70, 59.94, 56.27, 55.85.

Anal. Calcd for $\text{C}_{19}\text{H}_{18}\text{O}_7 \cdot 0.5 \text{H}_2\text{O}$: C, 62.12; H, 5.21. Found: C, 62.27; H, 5.32.

2-(2,4-Dimethoxyphenyl)-5-hydroxy-3,7-dimethoxy-4*H*-chromen-4-one (82)



Synthesized from morin, yield 48 %.

Molecular weight: 358.34 g/mol

^1H NMR (DMSO- d_6) δ : 12.62 (s, 1H), 7.39 (d, $J = 8.5$ Hz, 1H), 6.72 (d, $J = 2.3$ Hz, 1H), 6.66 (dd, $J = 8.5, 2.3$ Hz, 1H), 6.61 (d, $J = 2.2$ Hz, 1H), 6.38 (d, $J = 2.2$ Hz, 1H), 3.84 (d, $J = 7.2$ Hz, 6H), 3.81 (s, 3H), 3.69 (s, 3H).

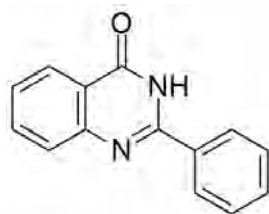
^{13}C NMR (DMSO- d_6) δ : 178.24, 165.31, 162.85, 161.27, 158.56, 157.10, 156.82, 139.54, 131.58, 111.72, 105.77, 105.53, 98.80, 97.98, 92.48, 60.12, 56.24, 55.99, 55.67.

Anal. Calcd for $\text{C}_{19}\text{H}_{18}\text{O}_7 \cdot 0.5 \text{H}_2\text{O}$: C, 62.12; H, 5.21. Found: C, 61.99; H, 5.36.

7.1.2.11 General procedure for synthesis of substituted quinazolin-4(3H)-ones

Method A: To a stirred mixture of anthranilamide (20 mmol) and a selected substituted benzaldehyde (20 mmol) in 20 ml DMF, iodine (3.17 g, 25 mmol) and anhydrous potassium carbonate (2.76 g, 20 mmol) were added. Then the mixture was heated at 70-90 °C for 4-5 hours. The mixture was poured on to crushed ice and the precipitate formed was filtered. The product was washed with 100 ml 20 % solution of sodiumthiosulfate to remove traces of iodine, followed by washing with water. The product was recrystallized from ethanol to yield pale yellow to dark yellow crystals.

Method B: A mixture of 2-aminobenzoic acid (anthranilic acid) or 2-amino-4,5-dimethoxybenzoic acid (20 mmol) and formamide (20 mmol) was heated at 150 °C for 10-18 hours. To the resulting mixture 50 ml water was added, which resulted in precipitation of a lot of solid. The reaction mixture was stirred for another 30-45 minutes and the resulting precipitate was filtered and washed with a lot of water. The product was recrystallized from ethanol to yield white to pale yellow crystals.

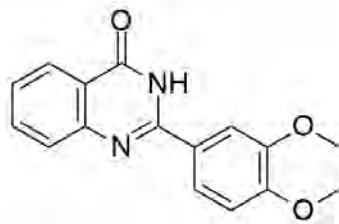
2-Phenylquinazoline-4(3H)-one (83)

Synthesized from anthranilamide and benzaldehyde using method A, yield 79 %.

Molecular weight: 222.24 g/mol

^1H NMR (DMSO- d_6) δ : 11.56 (s, 1H), 8.23 (d, $J = 7.6$ Hz, 1H), 7.98 (dd, $J = 7.9$ Hz, 1H), 7.79 (dd, $J = 8.1, 4.2$ Hz, 2H), 7.68-7.52 (m, 2H), 7.46-7.38 (m, 3H), 7.22 (t, $J = 8.2$ Hz, 1H).

^{13}C NMR (DMSO- d_6) δ : 164.23, 157.08, 143.68, 138.92, 131.47, 129.01, 127.22, 126.91, 125.12, 124.37, 123.06, 119.56.

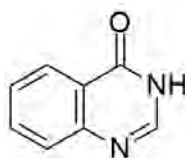
2-(3,4-Dimethoxyphenyl)quinazolin-4(3H)-one (84)

Synthesized from anthranilamide and 3,4-dimethoxybenzaldehyde using method A, yield 86 %

Molecular weight: 282.29 g/mol

^1H NMR (DMSO- d_6) δ : 12.37 (s, 1H), 8.14 – 8.10 (m, 1H), 7.89 – 7.84 (m, 1H), 7.82 – 7.80 (m, 1H), 7.79 – 7.77 (m, 1H), 7.70 (dd, $J = 8.2, 0.5$ Hz, 1H), 7.46 (ddd, $J = 8.1, 7.1, 1.2$ Hz, 1H), 7.09 (dd, $J = 10.0, 5.7$ Hz, 1H), 3.85 (dd, $J = 16.6, 7.6$ Hz, 6H).

^{13}C NMR (DMSO- d_6) δ : 162.76, 152.27, 151.72, 149.04, 148.71, 134.57, 127.32, 126.16, 125.97, 125.14, 121.30, 120.84, 111.55, 110.93, 55.85, 55.84.

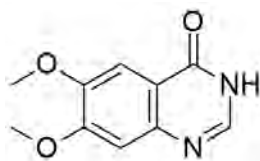
Quinazolin-4(3H)-one (85)

Synthesized from anthranilic acid and formamide as described in method B, yield 85 %.

Molecular weight: 146.15 g/mol

^1H NMR (DMSO- d_6) δ : 12.20 (s, 1H), 8.11 (ddd, $J = 7.9, 1.6, 0.5$ Hz, 1H), 8.07 (s, 1H), 7.80 (ddd, $J = 8.2, 7.1, 1.6$ Hz, 1H), 7.65 (ddd, $J = 8.2, 1.0, 0.4$ Hz, 1H), 7.51 (ddd, $J = 8.1, 7.2, 1.2$ Hz, 1H).

^{13}C NMR (DMSO- d_6) δ : 160.86, 148.84, 145.51, 134.40, 127.28, 126.83, 125.93, 122.75.

6,7-Dimethoxyquinazolin-4(3H)-one (86)

Synthesized from 2-Amino-4,5-dimethoxybenzoic acid and formamide as described in method B, yield 89%.

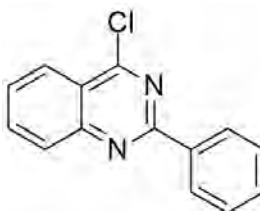
Molecular weight: 206.20 g/mol

^1H NMR (DMSO- d_6) δ : 12.02 (s, 1H), 7.96 (s, 1H), 7.43 (s, 1H), 7.12 (s, 1H), 3.87 (d, $J = 17.4$ Hz, 6H).

^{13}C NMR (DMSO- d_6) δ : 160.16, 154.60, 148.70, 145.01, 143.94, 115.75, 108.17, 105.10, 56.05, 55.83.

7.1.2.12 General procedure for synthesis of substituted 4-chloroquinazolines

To phosphorus oxychloride (30 ml), the selected quinazolin-4(3H)-one (10 mmol) was added at 0°C and stirred for 10 minutes. The resulting mixture was refluxed for 9 hours. After removal of the excess solvent, the residue was dissolved in ice-water (50 mL) and the solution was neutralized with ammonium hydroxide. The solution was extracted 3 times with dichloromethane (50 mL). The organic layer was washed with brine (100 mL), dried over MgSO_4 , and the solvent was removed under reduced pressure. The formed solid was recrystallized from ethanol. For further use compounds were confirmed by NMR analysis.

4-Chloro-2-phenylquinazoline (87)

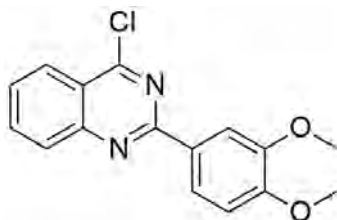
Synthesized from 2-phenylquinazoline-4(3H)-one, yield 87%.

Molecular weight: 240.69 g/mol

^1H NMR (DMSO- d_6) δ : 8.41-8.36 (m, 2H), 8.01 (ddd, $J = 8.0, 1.43, 0.62$ Hz, 1H), 7.78 (ddd, $J = 8.2, 1.71, 0.52$ Hz, 1H), 7.59 (m, 1H), 7.48 (m, 1H), 7.39-7.31 (m, 3H).

^{13}C NMR (DMSO- d_6) δ : 164.2, 159.8, 153.5, 137.3, 135.6, 132.3, 130.2, 129.8, 128.1, 127.3, 123.9, 120.8.

4-Chloro-2-(3,4-dimethoxyphenyl)quinazoline (88)



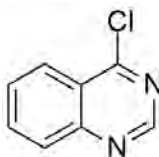
Synthesized from 2-(3,4-dimethoxyphenyl)quinazolin-4(3H)-one, yield 78 %.

Molecular weight: 300.74 g/mol

^1H NMR (DMSO- d_6) δ : 8.19 – 8.15 (m, 1H), 8.12 (d, $J = 8.0$ Hz, 1H), 7.96 – 7.89 (m, 1H), 7.89 – 7.82 (m, 2H), 7.60 (ddd, $J = 8.1, 7.3, 1.1$ Hz, 1H), 7.20 (d, $J = 8.5$ Hz, 1H), 3.90 (d, $J = 19.6$ Hz, 6H).

^{13}C NMR (DMSO- d_6) δ : 161.20, 154.77, 153.24, 148.66, 135.55, 127.59, 126.44, 123.40, 123.21, 120.00, 112.16, 111.63, 56.09, 56.06.

4-Chloroquinazoline (89)



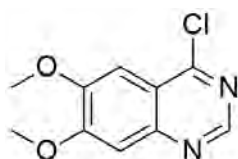
Synthesized from quinazolin-4(3H)-one, yield 82 %.

Molecular weight: 164.59 g/mol

^1H NMR (DMSO- d_6) δ : 8.31 (s, 1H), 8.01 (dd, 1H, $J = 7.6, 1.2$ Hz), 7.79 (t, 1H, $J = 8.0$ Hz), 7.69 (d, 1H, $J = 7.9$ Hz), 7.51 (t, 1H, $J = 7.2$ Hz).

^{13}C NMR (DMSO- d_6) δ : 161.07, 146.01, 144.71, 133.85, 126.92, 125.31, 124.05, 118.21.

4-Chloro-6,7-dimethoxyquinazoline (90)



Synthesized from 6,7-dimethoxyquinazolin-4(3H)-one, yield 71 %.

Molecular weight: 224.64 g/mol

^1H NMR (DMSO- d_6) δ : 8.51 (s, 1H), 7.45 (s, 1H), 7.23 (s, 1H), 3.91 (s, 3H), 3.88 (s, 3H).

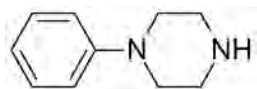
^{13}C NMR (DMSO- d_6) δ : 159.26, 155.08, 149.32, 148.72, 115.11, 107.00, 105.54, 105.18, 56.31, 56.27, 56.04.

7.1.2.13 General procedure for synthesis of *N*-phenylpiperazines

In an atmosphere of dry nitrogen, a mixture of substituted aniline (5 mmol), bis(2-chloroethyl)amine hydrochloride (5 mmol) and diethylene glycol monomethylether (0.75 ml) was heated at 150 °C for 6-12 hours. After cooling to room temperature, the mixture was dissolved in MeOH (4-5 mL) followed by addition of diethyl ether (150 ml). The precipitate was filtered off and washed with diethyl ether to provide the HCl salt. The HCl salt was further converted to the free amine by treatment with Na_2CO_3 solution and extracted with ethylacetat 2 times. The combined organic

layers were dried over MgSO_4 , and concentrated in vacuum to provide the free amine. The product was used without further purification and its structure was confirmed by NMR spectroscopy before use.

1-Phenylpiperazine (91)



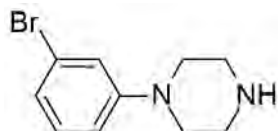
Synthesized from aniline and bis(2-chloroethyl)amine hydrochloride, oily compound, yield 59 %.

Molecular weight: 162.23 g/mol

^1H NMR (DMSO-d_6) δ : 8.34 (s, 1H), 7.12 (t, $J = 7.34$ Hz, 2H), 6.82 – 6.77 (m, 3H), 3.48 (m, 2H), 3.29 (m, 2H), 2.79 – 2.71 (m, 4H),

^{13}C NMR (DMSO-d_6) δ : 151.22, 130.45, 119.97, 116.45, 50.01, 45.70.

1-(3-Bromophenyl)piperazine (92)

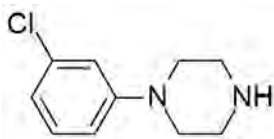


Synthesized from 3-bromoaniline and bis(2-chloroethyl)amine hydrochloride, oily compound, yield: 63 %

Molecular weight: 241.13 g/mol

^1H NMR (DMSO-d_6) δ : 8.02 (s, 1H), 7.09 – 7.05 (m, 1H), 7.02 – 6.98 (m, 1H), 6.93 (ddd, $J = 7.8, 1.8, 0.8$ Hz, 1H), 6.79 (ddd, $J = 8.4, 2.4, 0.7$ Hz, 1H), 3.11 (dd, $J = 6.1, 3.9$ Hz, 4H), 2.99 (dd, $J = 6.1, 3.9$ Hz, 4H).

^{13}C NMR (DMSO-d_6) δ : 152.86, 130.24, 123.16, 122.22, 118.68, 114.39, 49.71, 45.80.

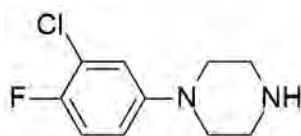
1-(3-Chlorophenyl)piperazine (93)

Synthesized from 3-chloroaniline and bis(2-chloroethyl)amine hydrochloride, oily compound, yield 68 %

Molecular weight: 196.68 g/mol

^1H NMR (CDCl_3) δ : 8.07 (s, 1H), 7.13 (t, $J = 8.1$ Hz, 1H), 6.84 (t, $J = 2.2$ Hz, 1H), 6.77 (dddd, $J = 17.5, 8.4, 2.2, 0.8$ Hz, 2H), 3.14 (dd, $J = 6.2, 3.9$ Hz, 4H), 3.02 (dd, $J = 6.2, 3.9$ Hz, 4H).

^{13}C NMR (CDCl_3) δ : 152.58, 134.89, 129.98, 119.44, 115.86, 115.78, 113.99, 113.79, 77.25, 77.00, 76.74.

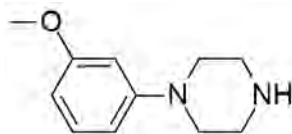
1-(3-Chloro-4-fluorophenyl)piperazine (94)

Synthesized from 3-chloro-4-fluoroaniline and bis(2-chloroethyl)amine hydrochloride, oily compound, yield 54 %

Molecular weight: 214.67 g/mol

^1H NMR (DMSO-d_6) δ : 8.21 (s, 1H), 6.89 (t, $J = 8.1$ Hz, 1H), 6.69 (dd, $J = 5.9, 1.8$ Hz, 1H), 6.58-6.47 (m, 1H), 3.37 (dd, $J = 5.9, 3.4$ Hz, 4H), 3.02 (dd, $J = 6.3, 3.7$ Hz, 4H).

^{13}C NMR (DMSO-d_6) δ : 153.14, 151.23, 148.76, 118.00, 116.41, 115.84, 77.25, 76.99, 76.74.

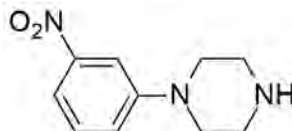
1-(3-Methoxyphenyl)piperazine (95)

Synthesized from 3-methoxyaniline and bis(2-chloroethyl)amine hydrochloride, oily compound, yield 61 %

Molecular weight: 192.26 g/mol

^1H NMR (DMSO- d_6) δ : 8.75 (s, 1H), 6.76 (t, $J = 2.7$ Hz, 1H), 6.68 (dd, $J = 48.7$, 16.5 Hz, 4H), 6.61 – 6.54 (m, 1H), 3.83 – 3.79 (m, 3H), 3.71 – 3.66 (m, 2H), 3.50 – 3.45 (m, 2H), 2.86 – 2.79 (m, 4H).

^{13}C NMR (DMSO- d_6) δ : 160.34, 158.23, 129.69, 129.59, 108.16, 104.25, 101.58, 54.98, 49.04, 45.39.

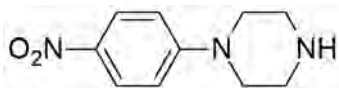
1-(3-Nitrophenyl)piperazine (96)

Synthesized from 3-nitroaniline and bis(2-chloroethyl)amine hydrochloride, oily compound, yield 68 %

Molecular weight: 207.23 g/mol

^1H NMR (DMSO- d_6) δ : 8.15 (s, 1 H), 7.61 (t, $J = 2.3$ Hz, 1H), 7.55 (ddd, $J = 8.0$, 2.2, 0.9 Hz, 1H), 7.45 (t, $J = 8.2$ Hz, 1H), 7.37 (ddd, $J = 8.4$, 2.6, 0.8 Hz, 1H), 3.22 – 3.18 (m, 4H), 2.91 – 2.85 (m, 4H).

^{13}C NMR (DMSO- d_6) δ : 152.09, 149.01, 130.23, 121.36, 112.71, 108.40, 48.19, 45.06.

1-(4-Nitrophenyl)piperazine (97)

Synthesized from 4-nitroaniline and bis(2-chloroethyl)amine hydrochloride, oily compound, yield 59 %

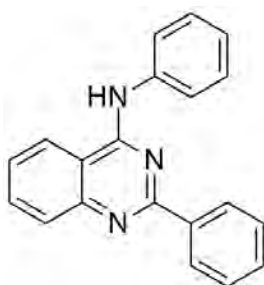
Molecular weight: 207.23 g/mol

^1H NMR (DMSO- d_6) δ : 8.14 (s, 1H), 8.08 – 8.01 (m, 2H), 7.03 – 6.97 (m, 2H), 3.44 – 3.39 (m, 4H), 2.91 – 2.83 (m, 4H).

^{13}C NMR (DMSO- d_6) δ : 155.01, 136.96, 125.83, 112.68, 46.93, 44.85.

7.1.2.14 General procedure for synthesis of 4-anilinoquinazolines

4-Chloroquinazolines (1 mmol) were dissolved in refluxing 2-propanol (20 ml) and the substituted aniline was added drop wise. The reaction mixture was refluxed for 3-4 hours, until the reaction was complete as indicated by TLC. The precipitate formed was filtered off and washed with 2-propanol (10 ml) and the ether (10 ml). If no precipitate was formed, the solvent was removed under reduced pressure to yield solid product. The product was recrystallized from 75 % ethanol.

***N*,2-Diphenylquinazolin-4-amine (98)**

Synthesized from aniline and 4-chloro-2-phenylquinazoline, yield 70%

Molecular weight: 297.35 g/mol

^1H NMR (DMSO- d_6) δ : 11.49 (s, 1H), 8.90 (d, $J = 8.3$ Hz, 1H), 8.39 – 8.34 (m, 2H), 8.31 (d, $J = 8.4$ Hz, 1H), 8.07 (t, $J = 7.3$ Hz, 1H), 7.88 – 7.84 (m, 2H), 7.80 (t, $J = 7.4$ Hz, 1H), 7.68 (t, $J = 7.3$ Hz, 1H), 7.62 (t, $J = 7.5$ Hz, 2H), 7.56 – 7.50 (m, 2H), 7.34 (t, $J = 7.4$ Hz, 1H).

^{13}C NMR (DMSO- d_6) δ : 159.10, 157.52, 137.23, 135.81, 133.18, 129.23, 129.08, 128.84, 128.07, 126.38, 124.60, 124.52, 112.96.

Anal. Calcd for $\text{C}_{20}\text{H}_{15}\text{N}_3$: C, 80.78; H, 5.08; N, 14.13. Found: C, 80.45; H, 5.23; N, 13.87.

***N*-(2-Bromophenyl)-2-phenylquinazolin-4-amine (99)**



Synthesized from 2-bromoaniline and 4-chloro-2-phenylquinazoline, yield 81 %.

Molecular weight: 376.25 g/mol

^1H NMR (DMSO- d_6) δ : 11.49 (s, 1H), 8.90 (d, $J = 8.3$ Hz, 1H), 8.39 – 8.34 (m, 2H), 8.31 (d, $J = 8.4$ Hz, 1H), 8.07 (t, $J = 7.3$ Hz, 1H), 7.88 – 7.84 (m, 2H), 7.80 (t, $J = 7.4$ Hz, 1H), 7.68 (t, $J = 7.3$ Hz, 1H), 7.62 (t, $J = 7.5$ Hz, 2H), 7.56 – 7.50 (m, 2H), 7.34 (t, $J = 7.4$ Hz, 1H).

^{13}C NMR (DMSO- d_6) δ : 159.10, 157.52, 137.23, 135.81, 133.18, 129.23, 129.08, 128.84, 128.07, 126.38, 124.60, 124.52, 112.96.

Anal. Calcd for $\text{C}_{20}\text{H}_{14}\text{BrN}_3$: C, 63.84; H, 3.75; N, 11.17. Found: C, 63.54; H, 4.15; N, 10.75.

***N*-(3-Bromophenyl)-2-phenylquinazolin-4-amine (100)**

Synthesized from 3-bromoaniline and 4-chloro-2-phenylquinazoline, yield 78 %.

Molecular weight: 376.25 g/mol

^1H NMR (DMSO- d_6) δ : 11.59 (s, 1H), 8.94 (d, $J = 8.1$ Hz, 1H), 8.44 – 8.38 (m, 2H), 8.33 (d, $J = 8.3$ Hz, 1H), 8.25 (s, 1H), 8.07 (t, $J = 7.6$ Hz, 1H), 7.94 – 7.86 (m, 1H), 7.81 (t, $J = 7.5$ Hz, 1H), 7.69 (t, $J = 7.3$ Hz, 1H), 7.62 (t, $J = 7.5$ Hz, 2H), 7.54 – 7.44 (m, 2H).

^{13}C NMR (DMSO- d_6) δ : 159.09, 157.50, 149.08, 139.01, 135.88, 133.18, 130.70, 129.21, 129.07, 128.64, 128.10, 126.92, 124.63, 123.07, 121.21, 113.06.

Anal. Calcd for $\text{C}_{20}\text{H}_{14}\text{BrN}_3$: C, 63.84; H, 3.75; N, 11.17. Found: C, 63.61; H, 4.05; N, 11.27.

***N*-(4-Bromophenyl)-2-phenylquinazolin-4-amine (101)**

Synthesized from 4-bromoaniline and 4-chloro-2-phenylquinazoline, yield 82 %.

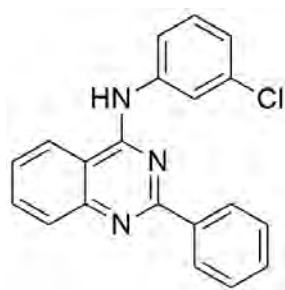
Molecular weight: 376.25 g/mol

^1H NMR (DMSO- d_6) δ : 11.57 (s, 1H), 8.93 (d, $J = 8.2$ Hz, 1H), 8.41 – 8.37 (m, 2H), 8.33 (d, $J = 8.1$ Hz, 1H), 8.07 (t, $J = 7.4$ Hz, 1H), 7.89 – 7.84 (m, 2H), 7.81 (t, $J = 7.5$ Hz, 1H), 7.74 – 7.70 (m, 2H), 7.68 (d, $J = 7.3$ Hz, 1H), 7.63 (t, $J = 7.5$ Hz, 2H).

^{13}C NMR (DMSO- d_6) δ : 159.03, 157.58, 150.03, 136.75, 135.86, 133.16, 131.69, 129.28, 129.12, 128.10, 126.38, 124.65, 118.42, 113.06.

Anal. Calcd for $\text{C}_{20}\text{H}_{14}\text{BrN}_3$: C, 63.84; H, 3.75; N, 11.17. Found: C, 63.67; H, 4.01; N, 10.94.

N-(3-Chlorophenyl)-2-phenylquinazolin-4-amine (102)



Synthesized from 3-chloroaniline and 4-chloro-2-phenylquinazoline, yield 69 %.

Molecular weight: 331.80 g/mol

^1H NMR (DMSO- d_6) δ : 11.56 (s, 1H), 8.93 (d, $J = 8.1$ Hz, 1H), 8.46 – 8.36 (m, 2H), 8.32 (d, $J = 8.1$ Hz, 1H), 8.11 – 8.02 (m, 2H), 7.87 (dd, $J = 8.1, 1.2$ Hz, 1H), 7.81 (t, $J = 7.6$ Hz, 1H), 7.69 (t, $J = 7.3$ Hz, 1H), 7.63 (t, $J = 7.5$ Hz, 2H), 7.55 (t, $J = 8.1$ Hz, 1H), 7.38 (dd, $J = 7.9, 1.3$ Hz, 1H).

^{13}C NMR (DMSO- d_6) δ : 159.12, 157.58, 138.94, 136.21, 135.85, 133.13, 132.94, 130.42, 129.17, 129.07, 128.08, 125.73, 124.61, 124.01, 122.70, 113.08.

Anal. Calcd for $\text{C}_{20}\text{H}_{14}\text{ClN}_3$: C, 72.40; H, 4.25; N, 12.66. Found: C, 72.29; H, 4.75; N, 12.37.

***N*-(3-Chloro-4-fluorophenyl)-2-phenylquinazolin-4-amine(103)**

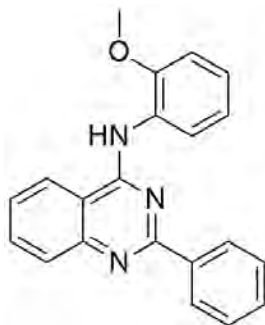
Synthesized from 3-chloro-4-fluoroaniline and 4-chloro-2-phenylquinazoline, yield 73 %.

Molecular weight: 349.79 g/mol

^1H NMR (DMSO- d_6) δ : 11.69 (s, 1H), 8.95 (d, $J = 8.0$ Hz, 1H), 8.38 (d, $J = 7.3$ Hz, 2H), 8.33 (d, $J = 8.0$ Hz, 1H), 8.20 (dd, $J = 6.8, 2.4$ Hz, 1H), 8.07 (t, $J = 7.6$ Hz, 1H), 7.89 (ddd, $J = 8.9, 4.2, 2.6$ Hz, 1H), 7.80 (t, $J = 7.7$ Hz, 1H), 7.69 (t, $J = 7.2$ Hz, 1H), 7.61 (dd, $J = 13.9, 6.6$ Hz, 2H), 7.57 (d, $J = 9.0$ Hz, 1H).

^{13}C NMR (DMSO- d_6) δ : 159.15, 157.54, 156.00, 154.05, 135.90, 134.57, 133.18, 129.19, 129.08, 128.12, 126.34, 124.98, 124.65, 119.30, 119.15, 117.06, 116.89, 112.96.

Anal. Calcd for $\text{C}_{20}\text{H}_{13}\text{ClFN}_3$: C, 68.67; H, 3.75; N, 12.01. Found: C, 68.52; H, 3.92; N, 11.89.

***N*-(2-Methoxyphenyl)-2-phenylquinazolin-4-amine(104)**

Synthesized from 2-methoxyaniline and 4-chloro-2-phenylquinazoline, yield 68 %.

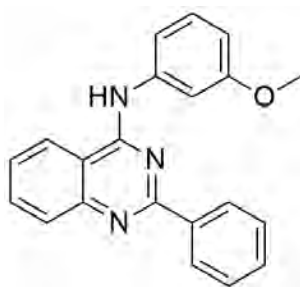
Molecular weight: 327.38 g/mol

^1H NMR (DMSO- d_6) δ : 11.39 (s, 1H), 8.82 (d, $J = 7.9$ Hz, 1H), 8.42 (d, $J = 8.2$ Hz, 1H), 8.27 (d, $J = 7.6$ Hz, 2H), 8.08 (t, $J = 7.7$ Hz, 1H), 7.81 (t, $J = 7.6$ Hz, 1H), 7.65 (t, $J = 7.3$ Hz, 1H), 7.61 – 7.51 (m, 3H), 7.43 (t, $J = 7.6$ Hz, 1H), 7.25 (d, $J = 8.2$ Hz, 1H), 7.11 (t, $J = 7.5$ Hz, 1H), 3.81 (s, 3H).

^{13}C NMR (DMSO- d_6) δ : 159.81, 157.21, 154.04, 150.05, 145.43, 135.93, 133.28, 129.17, 128.98, 128.93, 128.22, 127.83, 125.15, 124.47, 120.45, 112.47, 112.33, 55.92

Anal. Calcd for $\text{C}_{21}\text{H}_{17}\text{N}_3\text{O}$: C, 77.04; H, 5.23; N, 12.84. Found: C, 77.34; H, 5.14; N, 12.98.

***N*-(3-Methoxyphenyl)-2-phenylquinazolin-4-amine (105)**



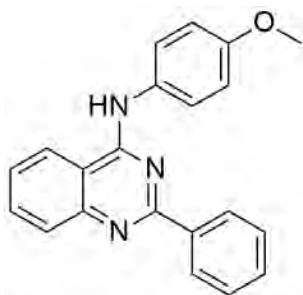
Synthesized from 3-methoxyaniline and 4-chloro-2-phenylquinazoline, yield 77 %.

Molecular weight: 327.38 g/mol

^1H NMR (DMSO- d_6) δ : 11.06 (s, 1H), 8.85 (d, $J = 8.2$ Hz, 1H), 8.42 (d, $J = 7.0$ Hz, 2H), 8.23 (d, $J = 8.2$ Hz, 1H), 8.02 (t, $J = 7.5$ Hz, 1H), 7.76 (t, $J = 7.4$ Hz, 1H), 7.64 (d, $J = 7.1$ Hz, 1H), 7.61 (d, $J = 8.0$ Hz, 2H), 7.50 (dd, $J = 8.0, 1.0$ Hz, 1H), 7.41 (t, $J = 8.1$ Hz, 1H), 6.87 (dd, $J = 8.2, 2.0$ Hz, 1H), 6.79 (dd, $J = 6.0, 2.8$ Hz, 1H), 3.82 (s, 3H).

^{13}C NMR (DMSO- d_6) δ : 160.11, 159.54, 158.80, 157.87, 154.93, 138.99, 135.23, 132.55, 130.57, 129.51, 128.93, 127.60, 124.28, 116.01, 113.65, 113.28, 111.61, 109.34, 107.39, 55.39.

Anal. Calcd for $\text{C}_{21}\text{H}_{17}\text{N}_3\text{O}$: C, 77.04; H, 5.23; N, 12.84. Found: C, 76.82; H, 5.06; N, 12.78.

***N*-(4-Methoxyphenyl)-2-phenylquinazolin-4-amine (106)**

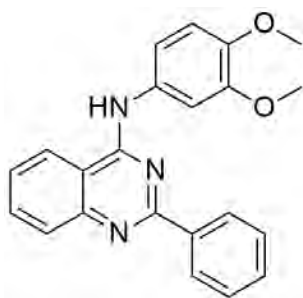
Synthesized from 4-methoxyaniline and 4-chloro-2-phenylquinazoline, yield 62 %.

Molecular weight: 327.38 g/mol

^1H NMR (DMSO- d_6) δ : 11.55 (s, 1H), 8.89 (d, $J = 8.2$ Hz, 1H), 8.43 – 8.26 (m, 3H), 8.06 (t, $J = 7.4$ Hz, 1H), 7.84 – 7.73 (m, 3H), 7.69 (t, $J = 7.3$ Hz, 1H), 7.62 (t, $J = 7.6$ Hz, 2H), 7.12 – 7.05 (m, 2H), 3.82 (s, 3H).

^{13}C NMR (DMSO- d_6) δ : 158.82, 157.65, 157.35, 135.78, 133.29, 129.82, 129.26, 129.08, 128.06, 125.98, 124.57, 114.01, 112.80, 55.50.

Anal. Calcd for $\text{C}_{21}\text{H}_{17}\text{N}_3\text{O}$: C, 77.04; H, 5.23; N, 12.84. Found: C, 76.91; H, 5.17; N, 12.81.

***N*-(3,4-Dimethoxyphenyl)-2-phenylquinazolin-4-amine(107)**

Synthesized from 3,4-dimethoxyaniline and 4-chloro-2-phenylquinazoline, yield 79 %.

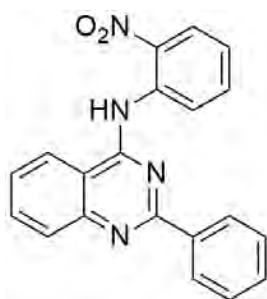
Molecular weight: 357.41 g/mol

^1H NMR (DMSO- d_6) δ : 11.10 (s, 1H), 8.81 (d, $J = 7.9$ Hz, 1H), 8.44 – 8.37 (m, 2H), 8.21 (d, $J = 7.2$ Hz, 1H), 8.02 (t, $J = 7.6$ Hz, 1H), 7.76 (t, $J = 7.6$ Hz, 1H), 7.64 (qd, $J = 14.5, 7.0$ Hz, 4H), 7.40 (dd, $J = 8.6, 2.3$ Hz, 1H), 7.08 (d, $J = 8.7$ Hz, 1H), 3.81 (d, $J = 5.0$ Hz, 6H).

^{13}C NMR (DMSO- d_6) δ : 158.51, 157.72, 148.49, 146.98, 135.27, 132.77, 130.71, 128.97, 127.70, 124.21, 116.09, 113.11, 111.72, 108.78, 55.88, 55.75.

Anal. Calcd for $\text{C}_{22}\text{H}_{19}\text{N}_3\text{O}_2$: C, 73.93; H, 5.36; N, 11.76. Found: C, 73.74; H, 5.50; N, 11.82.

N-(2-Nitrophenyl)-2-phenylquinazolin-4-amine (108)



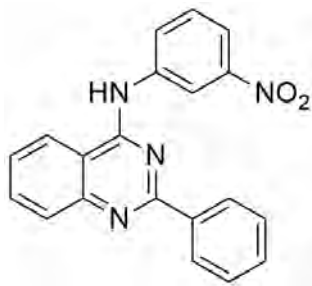
Synthesized from 2-nitroaniline and 4-chloro-2-phenylquinazoline, yield 83 %.

Molecular weight: 342.35 g/mol

^1H NMR (DMSO- d_6) δ : 11.82 (s, 1H), 8.54 – 8.47 (m, 1H), 7.94 (ddd, $J = 5.2, 4.3, 1.4$ Hz, 2H), 7.59 – 7.51 (m, 2H), 7.44 – 7.30 (m, 5H), 7.03 – 6.97 (m, 2H), 6.60 (ddd, $J = 8.4, 6.8, 1.3$ Hz, 2H).

^{13}C NMR (DMSO- d_6) δ : 165.96, 159.13, 151.40, 146.31, 137.68, 135.80, 134.26, 130.85, 130.47, 128.70, 128.11, 127.75, 127.09, 125.48, 123.44, 119.30, 115.59, 115.01.

Anal. Calcd for $\text{C}_{20}\text{H}_{14}\text{N}_4\text{O}_2$: C, 70.17; H, 4.12; N, 16.37. Found: C, 70.01; H, 3.98; N, 16.41.

***N*-(3-Nitrophenyl)-2-phenylquinazolin-4-amine (109)**

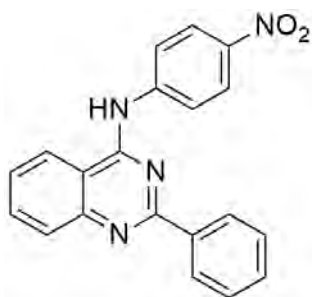
Synthesized from 3-nitroaniline and 4-chloro-2-phenylquinazoline, yield 89 %.

Molecular weight: 342.35 g/mol

^1H NMR (DMSO- d_6) δ : 11.43 (s, 1H), 9.12 (s, 1H), 8.90 (d, $J = 8.3$ Hz, 1H), 8.46 (d, $J = 7.2$ Hz, 2H), 8.35 (dd, $J = 8.1, 1.3$ Hz, 1H), 8.23 (d, $J = 8.0$ Hz, 1H), 8.12 (dd, $J = 8.2, 1.7$ Hz, 1H), 8.07 (t, $J = 7.8$ Hz, 1H), 7.86 – 7.77 (m, 2H), 7.67 (t, $J = 7.2$ Hz, 1H), 7.61 (t, $J = 7.4$ Hz, 2H).

^{13}C NMR (DMSO- d_6) δ : 158.96, 157.93, 147.97, 146.81, 139.17, 135.60, 132.74, 130.14, 129.49, 129.03, 127.90, 124.34, 119.88, 117.99, 113.34.

Anal. Calcd for $\text{C}_{20}\text{H}_{14}\text{N}_4\text{O}_2$: C, 70.17; H, 4.12; N, 16.37. Found: C, 69.87; H, 4.32; N, 16.73.

***N*-(4-Nitrophenyl)-2-phenylquinazolin-4-amine (110)**

Synthesized from 4-nitroaniline and 4-chloro-2-phenylquinazoline, yield 80 %.

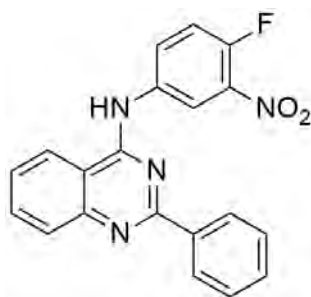
Molecular weight: 342.35 g/mol

^1H NMR (DMSO- d_6) δ : 11.21 (s, 1H), 8.84 (d, $J = 8.1$ Hz, 1H), 8.51 – 8.35 (m, 4H), 8.28 (d, $J = 8.7$ Hz, 2H), 8.17 (d, $J = 7.8$ Hz, 1H), 8.05 (t, $J = 7.8$ Hz, 1H), 7.79 (t, $J = 7.4$ Hz, 1H), 7.62 (d, $J = 7.5$ Hz, 3H).

^{13}C NMR (DMSO- d_6) δ : 158.89, 157.14, 148.13, 146.57, 140.35, 135.73, 132.16, 132.05, 130.85, 129.22, 128.78, 127.22, 126.19, 124.32, 120.78, 119.47, 112.39.

Anal. Calcd for $\text{C}_{20}\text{H}_{14}\text{N}_4\text{O}_2$: C, 70.17; H, 4.12; N, 16.37. Found: C, 70.25; H, 4.23; N, 16.43.

N-(4-Fluoro-3-nitrophenyl)-2-phenylquinazolin-4-amine (111)



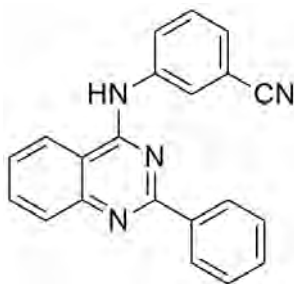
Synthesized from 4-fluoro,3-nitroaniline and 4-chloro-2-phenylquinazoline, yield 65 %.

Molecular weight: 360.34 g/mol

^1H NMR (DMSO- d_6) δ : 11.39 (s, 1H), 9.01 (d, $J = 4.6$ Hz, 1H), 8.85 (d, $J = 8.1$ Hz, 1H), 8.45 (d, $J = 7.4$ Hz, 2H), 8.37 – 8.27 (m, 1H), 8.20 (d, $J = 7.3$ Hz, 1H), 8.06 (t, $J = 7.7$ Hz, 1H), 7.86 – 7.70 (m, 2H), 7.64 (dt, $J = 15.0, 7.3$ Hz, 3H).

^{13}C NMR (DMSO- d_6) δ : 158.80, 157.98, 150.68, 136.45, 135.46, 133.67, 132.60, 130.94, 128.98, 127.81, 124.21, 120.50, 118.91, 118.74, 113.26.

Anal. Calcd for $\text{C}_{20}\text{H}_{13}\text{FN}_4\text{O}_2$: C, 66.66; H, 3.64; N, 15.55. Found: C, 66.61; H, 3.58; N, 15.60.

3-((2-Phenylquinazolin-4-yl)amino)benzonitrile (112)

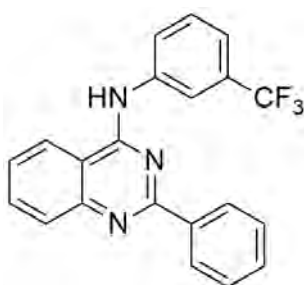
Synthesized from 3-aminobenzonitrile and 4-chloro-2-phenylquinazoline, yield 91 %.

Molecular weight: 322.36 g/mol

^1H NMR (DMSO- d_6) δ : 11.73 (s, 1H), 8.97 (d, $J = 8.3$ Hz, 1H), 8.43 – 8.36 (m, 3H), 8.32 (d, $J = 8.3$ Hz, 1H), 8.27 – 8.19 (m, 1H), 8.08 (t, $J = 7.4$ Hz, 1H), 7.88 – 7.66 (m, 4H), 7.61 (dd, $J = 10.4, 4.7$ Hz, 2H).

^{13}C NMR (DMSO- d_6) δ : 159.22, 157.65, 138.46, 135.93, 133.12, 130.23, 129.39, 129.16, 129.07, 128.98, 128.13, 127.52, 124.66, 118.57, 113.08, 111.60.

Anal. Calcd for $\text{C}_{21}\text{H}_{14}\text{N}_4$: C, 78.24; H, 4.38; N, 17.38. Found: C, 78.12; H, 4.46; N, 16.98.

2-Phenyl-*N*-(3-(trifluoromethyl)phenyl)quinazolin-4-amine (113)

Synthesized from 3-(trifluoromethyl)aniline and 4-chloro-2-phenylquinazoline, yield 69 %.

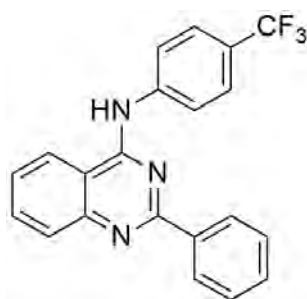
Molecular weight: 365.35 g/mol

^1H NMR (DMSO- d_6) δ : 11.66 (s, 1H), 8.96 (d, $J = 8.3$ Hz, 1H), 8.48 (s, 1H), 8.41 (dd, $J = 14.1, 6.9$ Hz, 2H), 8.32 (d, $J = 8.0$ Hz, 1H), 8.16 (d, $J = 8.3$ Hz, 1H), 8.08 (t, $J = 7.5$ Hz, 1H), 7.82 (t, $J = 7.7$ Hz, 1H), 7.76 (t, $J = 7.9$ Hz, 1H), 7.68 (dd, $J = 14.3, 7.2$ Hz, 2H), 7.60 (t, $J = 7.6$ Hz, 2H).

^{13}C NMR (DMSO- d_6) δ : 159.14, 157.61, 138.40, 135.84, 133.10, 130.02, 129.52, 129.27, 129.12, 128.99, 128.08, 127.70, 125.33, 124.59, 123.16, 122.18, 120.80, 113.14.

Anal. Calcd for $\text{C}_{21}\text{H}_{14}\text{F}_3\text{N}_3$: C, 69.04; H, 3.86; N, 11.50. Found: C, 68.74; H, 4.02; N, 11.70.

2-Phenyl-*N*-(4-(trifluoromethyl)phenyl)quinazolin-4-amine (114)



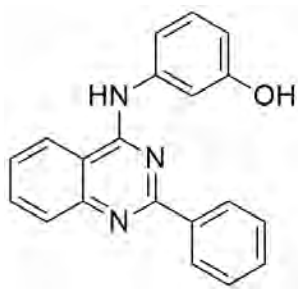
Synthesized from 4-(trifluoromethyl)aniline and 4-chloro-2-phenylquinazoline, yield 73 %.

Molecular weight: 365.35 g/mol

^1H NMR (DMSO- d_6) δ : 11.59 (s, 1H), 8.97 (d, $J = 8.2$ Hz, 1H), 8.46 – 8.39 (m, 2H), 8.32 (d, $J = 8.3$ Hz, 1H), 8.17 (t, $J = 9.6$ Hz, 2H), 8.08 (t, $J = 7.4$ Hz, 1H), 7.93 – 7.86 (m, 2H), 7.81 (dd, $J = 17.0, 9.6$ Hz, 1H), 7.73 – 7.59 (m, 3H).

^{13}C NMR (DMSO- d_6) δ : 159.16, 157.80, 141.35, 135.82, 132.97, 129.24, 129.10, 128.04, 125.97, 125.94, 125.47, 124.65, 124.17, 123.30, 113.23.

Anal. Calcd for $\text{C}_{21}\text{H}_{14}\text{F}_3\text{N}_3$: C, 69.04; H, 3.86; N, 11.50. Found: C, 69.15; H, 3.93; N, 11.45.

3-((2-Phenylquinazolin-4-yl)amino)phenol (115)

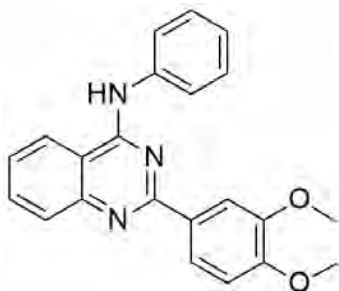
Synthesized from 3-aminophenol and 4-chloro-2-phenylquinazoline, yield 59 %.

Molecular weight: 357.41 g/mol

^1H NMR (DMSO- d_6) δ : 10.51 (s, 1H), 8.32 (s, 1H), 8.18 (dd, $J = 7.4, 1.6$ Hz, 1H), 7.75 (dd, $J = 7.7, 1.8$ Hz, 1H), 7.67 (td, $J = 7.3, 1.7$ Hz, 1H), 7.49 (td, $J = 7.8, 1.3$ Hz, 1H), 7.39 – 7.25 (m, 5H), 6.88 – 6.81 (m, 3H), 6.79 (dt, $J = 7.5, 1.8$ Hz, 1H).

^{13}C NMR (DMSO- d_6) δ : 161.59, 156.34, 154.82, 147.33, 142.26, 137.06, 131.26, 131.05, 130.57, 128.98, 126.24, 124.22, 122.59, 120.61, 119.35, 116.25, 115.03, 111.50.

Anal. Calcd for $\text{C}_{20}\text{H}_{15}\text{N}_3\text{O}$: C, 76.66; H, 4.82; N, 13.41. Found: C, 76.59; H, 5.03; N, 13.55.

2-(3,4-Dimethoxyphenyl)-*N*-phenylquinazolin-4-amine (116)

Synthesized from aniline and 4-chloro-2-(3,4-dimethoxyphenyl)quinazoline, yield 62 %.

Molecular weight: 357.41 g/mol

^1H NMR (DMSO- d_6) δ : 11.23 (s, 1H), 7.97 (dd, $J = 7.7, 16$ Hz, 1H), 7.70 (dd, $J = 7.5, 1.3$ Hz, 1H), 7.68 (td, $J = 7.2, 1.6$ Hz, 1H), 7.47 (td, $J = 7.7, 1.3$ Hz, 1H), 7.30 – 7.22 (m, 2H), 7.09 (t, $J = 7.8$ Hz, 2H), 6.87 (d, $J = 7.2$ Hz, 1H), 6.75 – 6.67 (m, 3H), 3.80 (d, $J = 11.4$ Hz, 6H).

^{13}C NMR (DMSO- d_6) δ : 161.82, 159.14, 152.81, 150.83, 148.62, 140.60, 135.32, 131.96, 131.05, 129.18, 126.22, 124.90, 123.72, 123.18, 119.55, 114.07, 113.26, 107.91, 56.12, 55.95.

Anal. Calcd for $\text{C}_{22}\text{H}_{19}\text{N}_3\text{O}_2$: C, 73.93; H, 5.36; N, 11.76. Found: C, 73.84; H, 5.53; N, 11.81.

***N*-(3-Bromophenyl)-2-(3,4-dimethoxyphenyl)quinazolin-4-amine (117)**



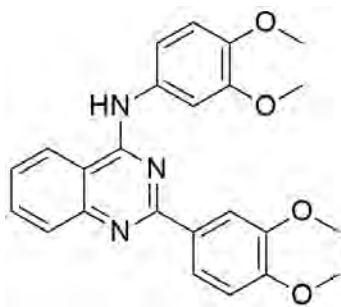
Synthesized from 3-bromoaniline and 4-chloro-2-(3,4-dimethoxyphenyl)quinazoline, yield 86 %.

Molecular weight: 436.30 g/mol

^1H NMR (DMSO- d_6) δ : 11.54 (s, 1H), 8.86 (d, $J = 8.2$ Hz, 1H), 8.43 (d, $J = 8.2$ Hz, 1H), 8.17 (t, $J = 1.8$ Hz, 1H), 8.12 (dd, $J = 8.6, 2.2$ Hz, 1H), 8.10 – 8.00 (m, 2H), 7.87 (ddd, $J = 7.8, 1.9, 1.2$ Hz, 1H), 7.77 (dd, $J = 11.4, 4.1$ Hz, 1H), 7.56 – 7.43 (m, 2H), 7.18 (d, $J = 8.7$ Hz, 1H), 3.88 (d, $J = 3.0$ Hz, 6H).

^{13}C NMR (DMSO- d_6) δ : 158.83, 156.74, 153.55, 148.92, 138.89, 135.93, 130.66, 128.88, 127.86, 127.07, 124.58, 123.59, 123.42, 121.21, 112.66, 112.08, 111.74, 56.07, 56.02.

Anal. Calcd for $\text{C}_{22}\text{H}_{18}\text{BrN}_3\text{O}_2$: C, 60.56; H, 4.16; N, 9.63. Found: C, 60.71; H, 3.89; N, 9.47.

***N*,2-Bis(3,4-dimethoxyphenyl)quinazolin-4-amine (118)**

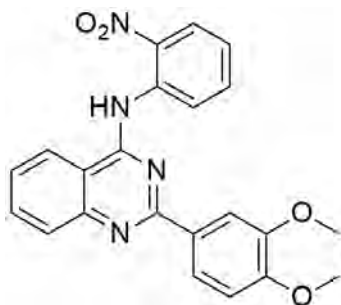
Synthesized from 3,4-dimethoxyaniline and 4-chloro-2-(3,4-dimethoxyphenyl)quinazoline, yield 53 %.

Molecular weight: 417.46 g/mol

^1H NMR (DMSO- d_6) δ : 11.43 (s, 1H), 8.81 (d, $J = 8.1$ Hz, 1H), 8.45 (d, $J = 8.2$ Hz, 1H), 8.15 – 8.08 (m, 2H), 8.07 – 8.01 (m, 1H), 7.77 (t, $J = 7.5$ Hz, 1H), 7.48 (d, $J = 2.4$ Hz, 1H), 7.38 (dd, $J = 8.6, 2.4$ Hz, 1H), 7.20 (d, $J = 8.4$ Hz, 1H), 7.09 (d, $J = 8.7$ Hz, 1H), 3.87 (d, $J = 4.3$ Hz, 6H), 3.80 (d, $J = 11.7$ Hz, 6H).

^{13}C NMR (DMSO- d_6) δ : 158.47, 156.48, 153.61, 148.88, 148.57, 147.49, 135.78, 130.03, 127.81, 124.43, 123.70, 117.02, 112.51, 112.31, 111.78, 111.59, 109.47, 56.06, 56.03, 55.91, 55.89.

Anal. Calcd for $\text{C}_{24}\text{H}_{23}\text{N}_3\text{O}_4$: C, 69.05; H, 5.55; N, 10.07. Found: C, 69.42; H, 5.68; N, 10.14.

2-(3,4-Dimethoxyphenyl)-*N*-(2-nitrophenyl)quinazolin-4-amine (119)

Synthesized from 2-nitroaniline and 4-chloro-2-(3,4-dimethoxyphenyl)quinazoline, yield 57 %.

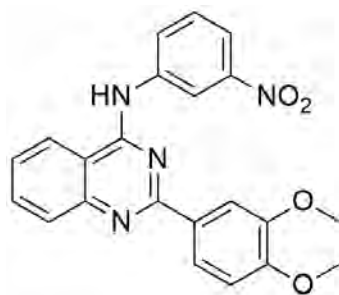
Molecular weight: 402.40 g/mol

^1H NMR (DMSO- d_6) δ : 11.15 (s, 1H), 8.14 – 8.09 (m, 1H), 8.06 (dd, $J = 14.6, 2.0$ Hz, 1H), 7.98 – 7.92 (m, 1H), 7.91 – 7.88 (m, 1H), 7.57 (ddd, $J = 8.1, 6.0, 2.2$ Hz, 1H), 7.38 (ddd, $J = 10.0, 6.1, 2.7$ Hz, 2H), 7.11 (d, $J = 8.5$ Hz, 1H), 7.00 (dd, $J = 8.6, 1.3$ Hz, 1H), 6.63 – 6.53 (m, 1H), 5.76 – 5.67 (m, 1H), 3.88 (s, 3H), 3.85 (s, 3H).

^{13}C NMR (DMSO- d_6) δ : 165.69, 158.99, 151.49, 148.80, 146.31, 135.80, 134.14, 130.30, 127.53, 126.58, 125.48, 123.41, 121.63, 119.30, 115.59, 114.73, 111.60, 111.13, 55.76, 55.63.

Anal. Calcd for $\text{C}_{22}\text{H}_{18}\text{N}_4\text{O}_4$: C, 65.66; H, 4.51; N, 13.92. Found: C, 65.39; H, 4.72; N, 14.11.

2-(3,4-Dimethoxyphenyl)-*N*-(3-nitrophenyl)quinazolin-4-amine (120)



Synthesized from 3-nitroaniline and 4-chloro-2-(3,4-dimethoxyphenyl)quinazoline, yield 72 %.

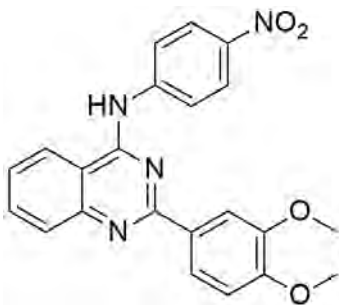
Molecular weight: 402.40 g/mol

^1H NMR (DMSO- d_6) δ : 11.60 (s, 1H), 8.93 (s, 1H), 8.86 (d, $J = 8.2$ Hz, 1H), 8.47 – 8.29 (m, 2H), 8.11 (dt, $J = 31.4, 9.8$ Hz, 3H), 7.80 (q, $J = 7.8$ Hz, 2H), 7.17 (d, $J = 8.6$ Hz, 1H), 3.86 (d, $J = 15.9$ Hz, 6H).

^{13}C NMR (DMSO- d_6) δ : 158.86, 157.03, 148.92, 147.91, 138.78, 135.86, 130.12, 127.80, 124.48, 123.62, 120.35, 118.53, 112.84, 112.01, 111.74, 56.04, 55.88.

Anal. Calcd for $C_{22}H_{18}N_4O_4$: C, 65.66; H, 4.51; N, 13.92. Found: C, 65.48; H, 4.62; N, 13.69.

2-(3,4-Dimethoxyphenyl)-*N*-(4-nitrophenyl)quinazolin-4-amine (121)



Synthesized from 4-nitroaniline and 4-chloro-2-(3,4-dimethoxyphenyl)quinazoline, yield 68 %.

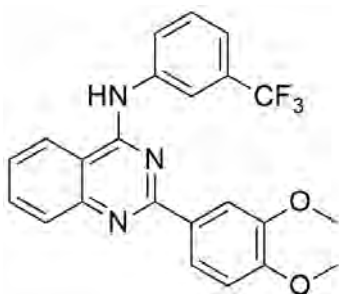
Molecular weight: 402.40 g/mol

^1H NMR (DMSO- d_6) δ : 11.54 (s, 1H), 8.86 (d, $J = 8.2$ Hz, 1H), 8.45 – 8.31 (m, 3H), 8.29 – 8.17 (m, 2H), 8.12 (dd, $J = 6.8, 2.1$ Hz, 2H), 8.06 (t, $J = 7.7$ Hz, 1H), 7.78 (t, $J = 7.7$ Hz, 1H), 7.20 (d, $J = 9.2$ Hz, 1H), 3.89 (d, $J = 12.0$ Hz, 6H).

^{13}C NMR (DMSO- d_6) δ : 158.70, 157.07, 153.30, 148.90, 144.03, 135.85, 127.74, 124.53, 124.46, 123.90, 123.57, 113.09, 112.00, 111.87, 56.00, 55.92.

Anal. Calcd for $C_{22}H_{18}N_4O_4$: C, 65.66; H, 4.51; N, 13.92. Found: C, 65.71; H, 4.32; N, 13.75.

2-(3,4-Dimethoxyphenyl)-*N*-(3-(trifluoromethyl)phenyl)quinazolin-4-amine (122)



Synthesized from 3-(trifluoromethyl)aniline and 4-chloro-2-(3,4-dimethoxyphenyl)quinazoline, yield 74 %.

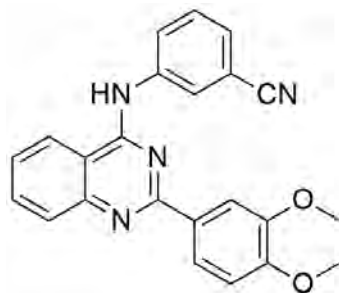
Molecular weight: 425.40 g/mol

^1H NMR (DMSO- d_6) δ : 11.62 (s, 1H), 8.87 (d, $J = 8.2$ Hz, 1H), 8.43 (d, $J = 7.9$ Hz, 1H), 8.31 (s, 1H), 8.18 (d, $J = 8.2$ Hz, 1H), 8.10 – 8.04 (m, 3H), 7.82 – 7.74 (m, 2H), 7.68 (d, $J = 7.7$ Hz, 1H), 7.16 (d, $J = 8.3$ Hz, 1H), 3.87 (d, $J = 9.8$ Hz, 6H).

^{13}C NMR (DMSO- d_6) δ : 158.99, 156.90, 153.56, 148.95, 138.23, 135.97, 130.02, 129.64, 129.39, 128.25, 127.89, 124.56, 123.65, 122.56, 120.99, 112.76, 112.19, 111.70, 56.07, 55.97.

Anal. Calcd for $\text{C}_{23}\text{H}_{18}\text{F}_3\text{N}_3\text{O}_2$: C, 64.94; H, 4.26; N, 9.88. Found: C, 64.72; H, 4.51; N, 9.69.

3-((2-(3,4-Dimethoxyphenyl)quinazolin-4-yl)amino)benzonitrile (123)



Synthesized from 3-aminobenzonitrile and 4-chloro-2-(3,4-dimethoxyphenyl)quinazoline, yield 89 %.

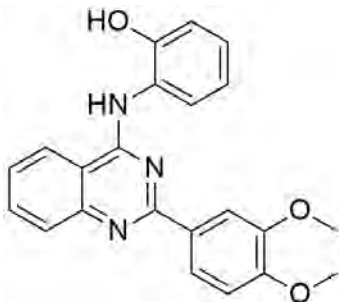
Molecular weight: 382.41 g/mol

^1H NMR (DMSO- d_6) δ : 11.07 (s, 1H), 8.32 (dd, $J = 7.1, 1.7$ Hz, 1H), 7.75 (dd, $J = 7.3, 1.5$ Hz, 1H), 7.69 (td, $J = 7.7, 1.6$ Hz, 1H), 7.54 (td, $J = 7.7, 1.3$ Hz, 1H), 7.31 (t, $J = 7.0$ Hz, 1H), 7.29 – 7.24 (m, 2H), 7.23 – 7.16 (m, 2H), 7.01 (dt, $J = 7.6, 1.5$ Hz, 1H), 6.89 (d, $J = 7.4$ Hz, 1H), 3.77 (d, $J = 2.4$ Hz, 6H).

^{13}C NMR (DMSO- d_6) δ : 159.99, 155.94, 152.18, 150.83, 147.62, 140.37, 133.29, 131.10, 131.00, 129.77, 127.38, 125.93, 125.11, 124.72, 122.81, 122.86, 118.39, 113.27, 112.31, 111.02, 108.65, 56.33, 55.61.

Anal. Calcd for $C_{23}H_{18}N_4O_2$: C, 72.24; H, 4.74; N, 14.65. Found: C, 71.88; H, 4.83; N, 14.71.

2-((2-(3,4-Dimethoxyphenyl)quinazolin-4-yl)amino)phenol (124)



Synthesized from 2-aminophenol and 4-chloro-2-(3,4-dimethoxyphenyl)quinazoline, yield 57 %.

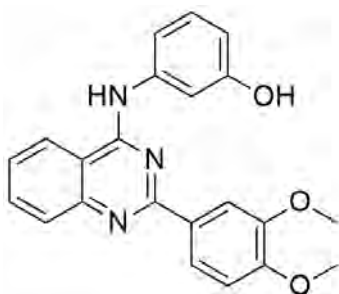
Molecular weight: 373.40 g/mol

^1H NMR (DMSO- d_6) δ : 10.15 (s, 1H), 8.34 (s, 1H), 7.94 (dd, $J = 6.9, 1.8$ Hz, 1H), 7.73 (dd, $J = 7.2, 1.3$ Hz, 1H), 7.69 – 7.63 (m, 1H), 7.39 (t, $J = 7.2$ Hz, 1H), 6.90 (d, $J = 7.1$ Hz, 2H), 6.88 (d, $J = 7.6$ Hz, 1H), 6.70 – 6.56 (m, 4H), 3.59 (d, $J = 3.1$ Hz, 6H).

^{13}C NMR (DMSO- d_6) δ : 161.54, 156.08, 152.65, 150.87, 148.01, 145.92, 132.74, 131.90, 130.49, 126.22, 125.34, 123.88, 123.10, 121.98, 121.00, 113.77, 111.24, 107.38, 56.29, 55.90.

Anal. Calcd for $C_{22}H_{19}N_3O_3$: C, 70.76; H, 5.13; N, 11.25. Found: C, 70.61; H, 5.34; N, 11.43.

3-((2-(3,4-Dimethoxyphenyl)quinazolin-4-yl)amino)phenol (125)



Synthesized from 3-aminophenol and 4-chloro-2-(3,4-dimethoxyphenyl)quinazoline, yield 60 %.

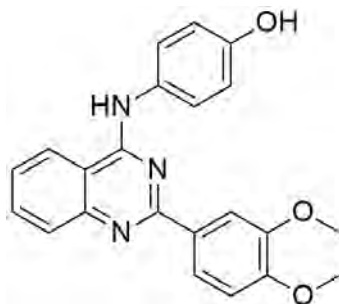
Molecular weight: 373.40 g/mol

^1H NMR (DMSO- d_6) δ : 11.32 (s, 1H), 9.75 (s, 1H), 8.81 (d, $J = 8.3$ Hz, 1H), 8.41 (d, $J = 8.2$ Hz, 1H), 8.16 (dd, $J = 8.6, 2.2$ Hz, 1H), 8.08 (d, $J = 2.2$ Hz, 1H), 8.07 – 8.01 (m, 1H), 7.77 (t, $J = 7.3$ Hz, 1H), 7.35 – 7.23 (m, 3H), 7.20 (d, $J = 8.7$ Hz, 1H), 6.76 (ddd, $J = 8.0, 2.3, 1.1$ Hz, 1H), 3.87 (d, $J = 2.8$ Hz, 6H).

^{13}C NMR (DMSO- d_6) δ : 158.65, 157.79, 156.52, 153.54, 148.89, 138.02, 135.82, 129.37, 127.80, 124.53, 123.55, 115.26, 113.62, 112.58, 112.23, 111.75, 56.07, 55.85.

Anal. Calcd for $\text{C}_{22}\text{H}_{19}\text{N}_3\text{O}_3$: C, 70.76; H, 5.13; N, 11.25. Found: C, 70.56; H, 5.28; N, 11.35.

4-((2-(3,4-Dimethoxyphenyl)quinazolin-4-yl)amino)phenol (126)



Synthesized from 4-aminophenol and 4-chloro-2-(3,4-dimethoxyphenyl)quinazoline, yield 57 %.

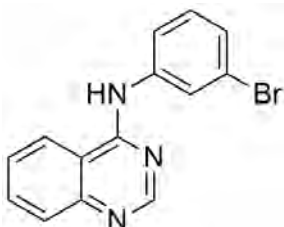
Molecular weight: 373.40 g/mol

^1H NMR (DMSO- d_6) δ : 11.37 (s, 1H), 9.72 (s, 1H), 8.76 (d, $J = 8.2$ Hz, 1H), 8.38 (d, $J = 8.3$ Hz, 1H), 8.11 – 7.97 (m, 3H), 7.75 (t, $J = 7.4$ Hz, 1H), 7.59 (d, $J = 8.8$ Hz, 2H), 7.20 (d, $J = 8.6$ Hz, 1H), 6.91 (d, $J = 8.8$ Hz, 2H), 3.87 (d, $J = 4.3$ Hz, 6H).

^{13}C NMR (DMSO- d_6) δ : 158.35, 156.39, 156.17, 153.53, 148.84, 135.71, 128.16, 127.76, 126.23, 124.38, 123.48, 115.21, 112.44, 112.19, 111.79, 56.05, 55.92.

Anal. Calcd for $C_{22}H_{19}N_3O_3$: C, 70.76; H, 5.13; N, 11.25. Found: C, 70.82; H, 5.21; N, 11.49.

***N*-(3-Bromophenyl)quinazolin-4-amine (127)**



Synthesized from 3-bromoaniline and 4-chloroquinazoline, yield 68 %.

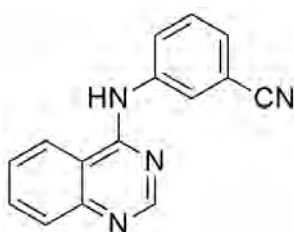
Molecular weight: 300.15 g/mol

^1H NMR (DMSO- d_6) δ : 11.89 (s, 1H), 9.03 (dd, $J = 8.4, 0.7$ Hz, 1H), 8.98 (s, 1H), 8.11 (ddd, $J = 8.4, 7.1, 1.2$ Hz, 1H), 8.07 (t, $J = 1.9$ Hz, 1H), 8.02 (dd, $J = 8.4, 0.8$ Hz, 1H), 7.86 (ddd, $J = 8.3, 7.1, 1.2$ Hz, 1H), 7.80 (ddd, $J = 8.0, 2.0, 1.0$ Hz, 1H), 7.52 (ddd, $J = 8.0, 1.9, 1.0$ Hz, 1H), 7.45 (t, $J = 8.0$ Hz, 1H).

^{13}C NMR (DMSO- d_6) δ : 160.08, 151.21, 139.09, 138.52, 136.41, 130.74, 129.32, 128.77, 127.40, 125.17, 123.82, 121.26, 120.05, 113.74.

Anal. Calcd for $C_{14}H_{10}BrN_3$: C, 56.02; H, 3.36; N, 14.00. Found: C, 55.88; H, 3.50; N, 13.75.

3-(Quinazolin-4-ylamino)benzonitrile (128)



Synthesized from 3-aminobenzonitrile and 4-chloroquinazoline, yield 71 %.

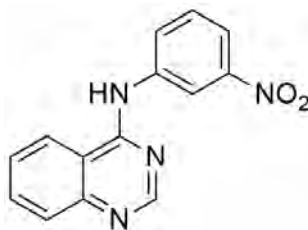
Molecular weight: 246.27 g/mol

^1H NMR (DMSO- d_6) δ : 12.07 (s, 1H), 9.07 (d, $J = 7.8$ Hz, 1H), 9.00 (s, 1H), 8.31 (t, $J = 1.8$ Hz, 1H), 8.16 – 8.09 (m, 2H), 8.03 (dd, $J = 8.4, 0.8$ Hz, 1H), 7.88 (ddd, $J = 8.3, 7.1, 1.1$ Hz, 1H), 7.78 (dt, $J = 7.7, 1.3$ Hz, 1H), 7.70 (t, $J = 8.0$ Hz, 1H).

^{13}C NMR (DMSO- d_6) δ : 160.19, 151.30, 139.32, 137.94, 136.52, 130.28, 130.03, 129.58, 128.85, 128.08, 125.20, 120.23, 118.47, 113.78, 111.65.

Anal. Calcd for $\text{C}_{15}\text{H}_{10}\text{N}_4$: C, 73.16; H, 4.09; N, 22.75. Found: C, 73.30; H, 4.28; N, 22.51.

***N*-(3-Nitrophenyl)quinazolin-4-amine (129)**



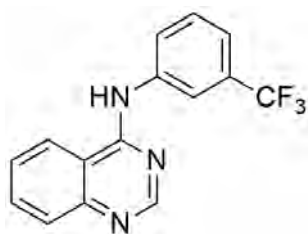
Synthesized from 3-nitroaniline and 4-chloroquinazoline, yield 79 %.

Molecular weight: 266.25 g/mol

^1H NMR (DMSO- d_6) δ : 12.08 (s, 1H), 9.07 (dd, $J = 8.4, 0.7$ Hz, 1H), 9.03 (s, 1H), 8.77 (t, $J = 2.1$ Hz, 1H), 8.31 (ddd, $J = 8.1, 2.1, 0.9$ Hz, 1H), 8.18 – 8.11 (m, 2H), 8.04 (dd, $J = 8.4, 0.8$ Hz, 1H), 7.89 (ddd, $J = 8.3, 7.1, 1.2$ Hz, 1H), 7.78 (t, $J = 8.2$ Hz, 1H).

^{13}C NMR (DMSO- d_6) δ : 160.20, 151.35, 147.92, 139.51, 138.31, 136.50, 130.86, 130.22, 128.85, 125.19, 120.93, 120.37, 119.21, 113.90.

Anal. Calcd for $\text{C}_{14}\text{H}_{10}\text{N}_4\text{O}_2$: C, 63.15; H, 3.79; N, 21.04. Found: C, 62.83; H, 3.91; N, 21.02.

***N*-(3-(Trifluoromethyl)phenyl)quinazolin-4-amine (130)**

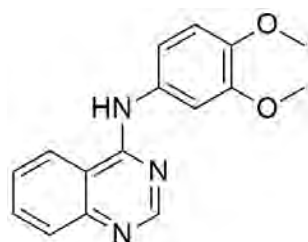
Synthesized from 3-(trifluoromethyl)aniline and 4-chloroquinazoline, yield 85 %.

Molecular weight: 289.26 g/mol

^1H NMR (DMSO- d_6) δ : 10.00 (s, 1H), 8.67 (s, 1H), 8.57 (d, $J = 8.0$ Hz, 1H), 8.34 (s, 1H), 8.25 (d, $J = 8.2$ Hz, 1H), 7.88 (ddd, $J = 8.2, 6.9, 1.2$ Hz, 1H), 7.82 (d, $J = 7.5$ Hz, 1H), 7.71 – 7.60 (m, 2H), 7.45 (d, $J = 7.7$ Hz, 1H).

^{13}C NMR (DMSO- d_6) δ : 157.73, 154.33, 149.86, 140.34, 133.37, 129.75, 129.52, 129.27, 128.05, 126.64, 125.63, 123.09, 119.80, 119.77, 118.17, 118.13, 115.30.

Anal. Calcd for $\text{C}_{15}\text{H}_{10}\text{F}_3\text{N}_3$: C, 62.28; H, 3.48; N, 14.53. Found: C, 62.00; H, 3.61; N, 14.38.

***N*-(3,4-Dimethoxyphenyl)quinazolin-4-amine (131)**

Synthesized from 3,4-dimethoxyaniline and 4-chloroquinazoline, yield 91 %.

Molecular weight: 281.31 g/mol

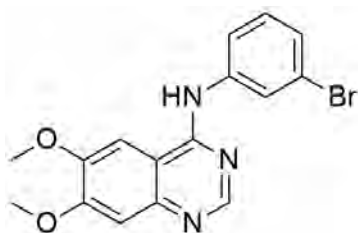
^1H NMR (DMSO- d_6) δ : 11.70 (s, 1H), 8.95 (d, $J = 8.3$ Hz, 1H), 8.88 (s, 1H), 8.12 – 8.04 (m, 1H), 7.98 (d, $J = 8.4$ Hz, 1H), 7.83 (dd, $J = 11.4, 4.2$ Hz, 1H), 7.39 (d, $J =$

2.4 Hz, 1H), 7.30 (dd, $J = 8.6, 2.4$ Hz, 1H), 7.05 (d, $J = 8.7$ Hz, 1H), 3.78 (d, $J = 13.4$ Hz, 6H).

^{13}C NMR (DMSO- d_6) δ : 159.71, 148.66, 147.72, 138.50, 136.20, 129.68, 128.63, 124.98, 119.67, 117.34, 113.54, 111.73, 109.68, 55.90, 55.86.

Anal. Calcd for $\text{C}_{16}\text{H}_{15}\text{N}_3\text{O}_2$: C, 68.31; H, 5.37; N, 14.94. Found: C, 68.52; H, 5.20; N, 15.27.

N-(3-Bromophenyl)-6,7-dimethoxyquinazolin-4-amine (132)



Synthesized from 3-bromoaniline and 4-chloro-6,7-dimethoxyquinazoline, yield 84 %.

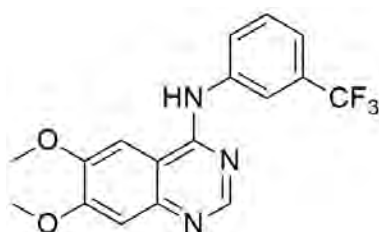
Molecular weight: 360.21 g/mol

^1H NMR (DMSO- d_6) δ : 11.32 (s, 1H), 8.86 (s, 1H), 8.30 (s, 1H), 8.02 (t, $J = 1.9$ Hz, 1H), 7.77 (ddd, $J = 7.9, 2.0, 1.1$ Hz, 1H), 7.49 (ddd, $J = 8.0, 1.9, 1.1$ Hz, 1H), 7.44 (t, $J = 8.0$ Hz, 1H), 7.34 (s, 1H), 4.01 (d, $J = 12.1$ Hz, 6H).

^{13}C NMR (DMSO- d_6) δ : 158.18, 156.52, 150.40, 138.91, 130.72, 128.79, 127.10, 123.50, 121.28, 107.62, 104.00, 100.38, 57.07, 56.61.

Anal. Calcd for $\text{C}_{16}\text{H}_{14}\text{BrN}_3\text{O}_2$: C, 53.35; H, 3.92; N, 11.67. Found: C, 53.07; H, 4.16; N, 11.49.

6,7-Dimethoxy-*N*-(3-(trifluoromethyl)phenyl)quinazolin-4-amine (133)



Synthesized from 3-(trifluoromethyl)aniline and 4-chloro-6,7-dimethoxyquinazoline, yield 90 %.

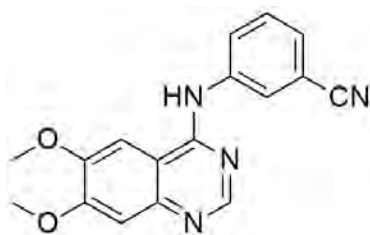
Molecular weight: 349.31 g/mol

^1H NMR (DMSO- d_6) δ : 11.74 (s, 1H), 8.87 (s, 1H), 8.46 (s, 1H), 8.17 (s, 1H), 8.11 (d, $J = 8.1$ Hz, 1H), 7.70 (t, $J = 7.9$ Hz, 1H), 7.66 – 7.61 (m, 1H), 7.39 (s, 1H), 4.01 (d, $J = 23.6$ Hz, 6H).

^{13}C NMR (DMSO- d_6) δ : 158.35, 156.59, 150.43, 138.15, 136.11, 129.94, 129.60, 129.34, 128.55, 122.48, 121.16, 121.13, 107.65, 104.39, 100.00, 57.25, 56.60.

Anal. Calcd for $\text{C}_{17}\text{H}_{14}\text{F}_3\text{N}_3\text{O}_2$: C, 58.45; H, 4.04; N, 12.03. Found: C, 58.39; H, 4.33; N, 12.19.

3-((6,7-Dimethoxyquinazolin-4-yl)amino)benzonitrile (134)



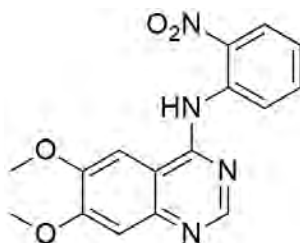
Synthesized from 3-aminobenzonitrile and 4-chloro-6,7-dimethoxyquinazoline, yield 83 %.

Molecular weight: 306.32 g/mol

^1H NMR (DMSO- d_6) δ : 11.39 (s, 1H), 8.87 (s, 1H), 8.29 (s, 1H), 8.27 (t, $J = 1.8$ Hz, 1H), 8.07 (ddd, $J = 8.1, 2.2, 1.2$ Hz, 1H), 7.75 (dt, $J = 7.7, 1.3$ Hz, 1H), 7.69 (dd, $J = 11.8, 4.1$ Hz, 1H), 7.33 (s, 1H), 4.01 (d, $J = 10.9$ Hz, 6H).

^{13}C NMR (DMSO- d_6) δ : 158.22, 157.87, 156.63, 150.48, 138.33, 130.29, 129.50, 129.22, 127.76, 118.54, 111.68, 107.70, 103.89, 57.09, 56.65.

Anal. Calcd for $\text{C}_{17}\text{H}_{14}\text{N}_4\text{O}_2$: C, 66.66; H, 4.61; N, 18.29. Found: C, 66.40; H, 4.93; N, 18.40.

6,7-Dimethoxy-*N*-(2-nitrophenyl)quinazolin-4-amine (135)

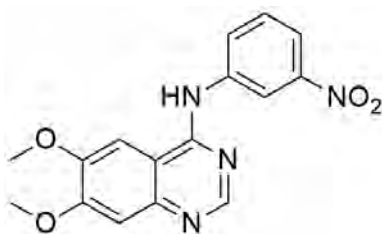
Synthesized from 2-nitroaniline and 4-chloro-6,7-dimethoxyquinazoline, yield 68 %.

Molecular weight: 326.31 g/mol

^1H NMR (DMSO- d_6) δ : 8.59 (s, 1H), 7.94 (dd, $J = 8.7, 1.5$ Hz, 1H), 7.41 – 7.32 (m, 4H), 7.28 (d, $J = 8.9$ Hz, 2H), 7.00 (dd, $J = 8.5, 1.3$ Hz, 1H), 6.60 (ddd, $J = 8.2, 6.8, 1.3$ Hz, 1H), 3.92 (d, $J = 16.1$ Hz, 6H).

^{13}C NMR (DMSO- d_6) δ : 164.58, 155.62, 149.97, 148.50, 146.65, 136.14, 130.82, 125.82, 119.64, 115.93, 110.57, 107.22, 101.24, 69.89, 56.46, 56.26.

Anal. Calcd for $\text{C}_{16}\text{H}_{14}\text{N}_4\text{O}_4$: C, 58.89; H, 4.32; N, 17.17. Found: C, 58.62; H, 4.52; N, 17.05.

6,7-Dimethoxy-*N*-(3-nitrophenyl)quinazolin-4-amine (136)

Synthesized from 3-nitroaniline and 4-chloro-6,7-dimethoxyquinazoline, yield 94 %.

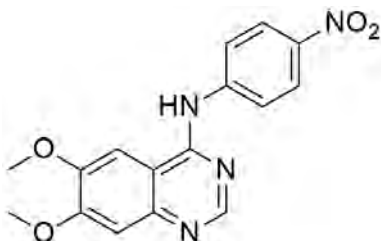
Molecular weight: 326.31 g/mol

^1H NMR (DMSO- d_6) δ : 11.13 (s, 1H), 8.87 (s, 1H), 8.70 (t, $J = 2.2$ Hz, 1H), 8.27 (ddd, $J = 8.1, 2.1, 0.9$ Hz, 1H), 8.19 (s, 1H), 8.11 (dd, $J = 8.2, 2.2$ Hz, 1H), 7.77 (t, $J = 8.2$ Hz, 1H), 7.31 (s, 1H), 4.01 (d, $J = 12.2$ Hz, 6H).

^{13}C NMR (DMSO- d_6) δ :

Anal. Calcd for $\text{C}_{16}\text{H}_{14}\text{N}_4\text{O}_4$: C, 58.89; H, 4.32; N, 17.17. Found: C, 59.00; H, 4.51; N, 17.26.

6,7-Dimethoxy-*N*-(4-nitrophenyl)quinazolin-4-amine (137)



Synthesized from 4-nitroaniline and 4-chloro-6,7-dimethoxyquinazoline, yield 83 %.

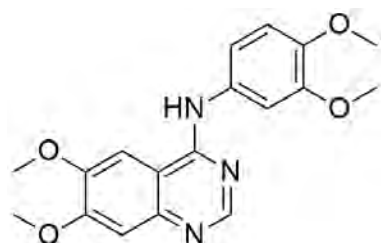
Molecular weight: 326.31 g/mol

^1H NMR (DMSO- d_6) δ : 10.94 (s, 1H), 8.58 (s, 1H), 8.06 (d, $J = 7.5$ Hz, 2H), 7.68 (s, 1H), 7.30 (s, 1H), 7.09 (d, $J = 7.5$ Hz, 2H), 3.72 (s, 3H), 3.59 (s, 3H).

^{13}C NMR (DMSO- d_6) δ : 158.72, 153.70, 152.39, 148.90, 147.76, 146.88, 141.27, 126.05, 119.22, 111.20, 107.53, 103.70, 56.23, 55.99.

Anal. Calcd for $\text{C}_{16}\text{H}_{14}\text{N}_4\text{O}_4$: C, 58.89; H, 4.32; N, 17.17. Found: C, 59.09; H, 4.41; N, 17.00.

***N*-(3,4-Dimethoxyphenyl)-6,7-dimethoxyquinazolin-4-amine (138)**



Synthesized from 3,4-dimethoxyaniline and 4-chloro-6,7-dimethoxyquinazoline, yield 76 %.

Molecular weight: 341.36 g/mol

^1H NMR (DMSO- d_6) δ : 11.08 (s, 1H), 8.75 (s, 1H), 8.18 (s, 1H), 7.29 (dd, $J = 8.7$, 5.1 Hz, 2H), 7.19 (dd, $J = 8.6$, 2.4 Hz, 1H), 7.05 (d, $J = 8.7$ Hz, 1H), 3.99 (d, $J = 5.0$ Hz, 6H), 3.79 (d, $J = 10.7$ Hz, 6H).

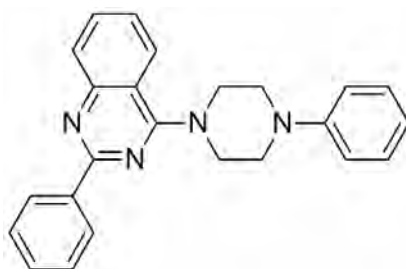
^{13}C NMR (DMSO- d_6) δ : 156.26, 150.24, 148.75, 147.48, 129.93, 117.35, 111.82, 109.74, 107.25, 103.85, 56.93, 56.56, 55.89.

Anal. Calcd for $\text{C}_{18}\text{H}_{19}\text{N}_3\text{O}_4$: C, 63.33; H, 5.61; N, 12.31. Found: C, 63.20; H, 5.72; N, 12.29.

7.1.2.15 General procedure for synthesis of 4-N-piperazinylquinazolines

To a solution of 4-chloro-2-phenylquinazoline (240 mg, 1 mmol) and K_2CO_3 (280 mg, 2 mmol) in refluxing 2-propanol (20 ml), the substituted N-phenyl-piperazine was added dropwise. The reaction mixture was refluxed for 10-12 hours, until the reaction was complete as indicated by TLC. The solvent was removed under reduced pressure and water was added to resulting solid and filtered under suction and washed with water. The resulting solid was recrystallized from 50 % ethanol.

2-Phenyl-4-(4-phenylpiperazin-1-yl)quinazoline (139)



Synthesized from 1-phenylpiperazine and 4-chloro-2-phenylquinazoline, yield 51 %.

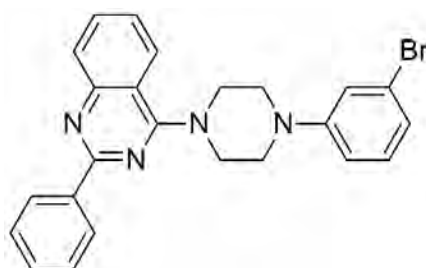
Molecular weight: 366.46 g/mol

^1H NMR (DMSO- d_6) δ : 8.57 – 8.44 (m, 2H), 8.09 (d, $J = 8.2$ Hz, 1H), 7.94 – 7.79 (m, 2H), 7.53 (dd, $J = 15.3, 7.1$ Hz, 4H), 7.25 (t, $J = 7.9$ Hz, 2H), 7.00 (d, $J = 8.1$ Hz, 2H), 6.81 (t, $J = 7.2$ Hz, 1H), 3.98 (m, 4H), 3.42 (m, 4H).

^{13}C NMR (DMSO- d_6) δ : 164.21, 158.28, 152.27, 150.94, 138.21, 133.08, 130.46, 129.15, 128.53, 128.09, 125.54, 125.46, 119.20, 115.58, 114.89, 49.19, 48.17.

Anal. Calcd for $\text{C}_{24}\text{H}_{22}\text{N}_4$: C, 78.66; H, 6.05; N, 15.29. Found: C, 78.40; H, 6.23; N, 15.18.

4-(4-(3-Bromophenyl)piperazin-1-yl)-2-phenylquinazoline (140)



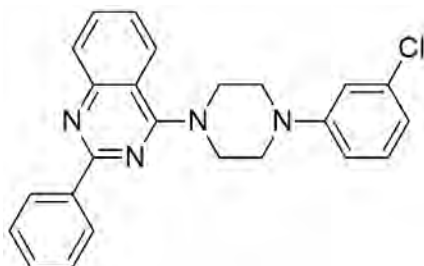
Synthesized from 1-(3-bromophenyl)piperazine and 4-chloro-2-phenylquinazoline, yield 54 %.

Molecular weight: 445.35 g/mol

^1H NMR (DMSO- d_6) δ : 8.50 (dd, $J = 7.7, 1.9$ Hz, 2H), 8.08 (d, $J = 7.7$ Hz, 1H), 7.90 (dd, $J = 8.4, 0.9$ Hz, 1H), 7.83 (ddd, $J = 8.3, 6.9, 1.2$ Hz, 1H), 7.57 – 7.46 (m, 4H), 7.22 – 7.15 (m, 1H), 7.13 (t, $J = 2.1$ Hz, 1H), 6.99 (dd, $J = 8.3, 2.1$ Hz, 1H), 6.94 (dd, $J = 7.8, 1.1$ Hz, 1H), 4.03 – 3.90 (m, 4H), 3.53 – 3.41 (m, 4H).

^{13}C NMR (DMSO- d_6) δ : 164.10, 158.26, 152.26, 138.19, 133.08, 130.93, 130.45, 128.52, 128.08, 125.52, 125.44, 122.71, 121.23, 117.42, 114.85, 114.10, 48.91, 47.47.

Anal. Calcd for $\text{C}_{24}\text{H}_{21}\text{BrN}_4$: C, 64.73; H, 4.75; N, 12.58. Found: C, 64.57; H, 4.69; N, 12.37.

4-(4-(3-Chlorophenyl)piperazin-1-yl)-2-phenylquinazoline (141)

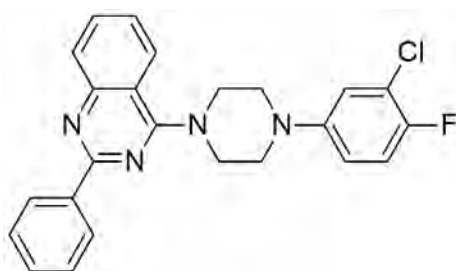
Synthesized from 1-(3-chlorophenyl)piperazine and 4-chloro-2-phenylquinazoline, yield 48 %.

Molecular weight: 400.90 g/mol

^1H NMR (DMSO- d_6) δ : 8.53 – 8.48 (m, 2H), 8.09 (dd, $J = 8.3, 0.8$ Hz, 1H), 7.90 (dd, $J = 8.4, 1.0$ Hz, 1H), 7.83 (ddd, $J = 8.3, 6.9, 1.3$ Hz, 1H), 7.56 – 7.49 (m, 4H), 7.27 – 7.22 (m, 1H), 7.00 (t, $J = 2.2$ Hz, 1H), 6.97 – 6.93 (m, 1H), 6.81 (ddd, $J = 7.9, 1.9, 0.7$ Hz, 1H), 4.01 – 3.95 (m, 4H), 3.51 – 3.44 (m, 4H).

^{13}C NMR (DMSO- d_6) δ : 164.12, 158.26, 152.27, 152.10, 138.19, 134.03, 133.09, 130.63, 130.46, 128.53, 128.09, 125.53, 125.45, 118.30, 114.86, 114.58, 113.69, 48.91, 47.47

Anal. Calcd for $\text{C}_{24}\text{H}_{21}\text{ClN}_4$: C, 71.90; H, 5.28; N, 13.98. Found: C, 72.06; H, 5.13; N, 13.82.

4-(4-(3-Chloro-4-fluorophenyl)piperazin-1-yl)-2-phenylquinazoline (142)

Synthesized from 1-(3-chloro,4-fluorophenyl)piperazine and 4-chloro-2-phenylquinazoline, yield 61 %.

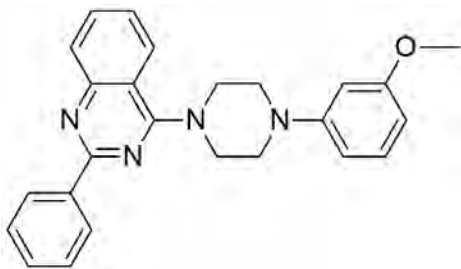
Molecular weight: 418.89 g/mol

^1H NMR (DMSO- d_6) δ : 8.55 – 8.45 (m, 2H), 8.07 (d, J = 8.2 Hz, 1H), 7.90 (d, J = 8.3 Hz, 1H), 7.83 (t, J = 7.5 Hz, 1H), 7.53 (dd, J = 14.9, 7.3 Hz, 4H), 7.27 (t, J = 9.1 Hz, 1H), 7.16 – 7.10 (m, 1H), 6.99 (d, J = 9.0 Hz, 1H), 3.96 (m, 4H), 3.41 (m, 4H).

^{13}C NMR (DMSO- d_6) δ : 164.17, 158.27, 152.26, 151.96, 150.07, 148.44, 138.18, 133.10, 130.47, 128.56, 128.53, 128.09, 125.57, 125.40, 117.10, 116.93, 116.80, 115.74, 115.69, 114.87, 48.99, 48.29.

Anal. Calcd for $\text{C}_{24}\text{H}_{20}\text{ClFN}_4$: C, 68.81; H, 4.81; N, 13.37. Found: C, 68.68; H, 5.04; N, 13.42.

4-(4-(3-Methoxyphenyl)piperazin-1-yl)-2-phenylquinazoline (143)



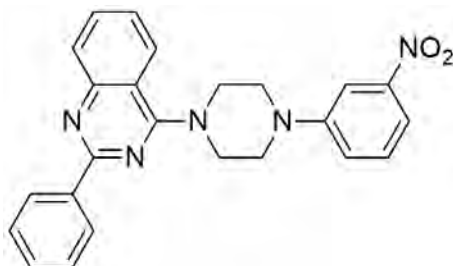
Synthesized from 1-(3-methoxyphenyl)piperazine and 4-chloro-2-phenylquinazoline, yield 57 %.

Molecular weight: 396.48 g/mol

^1H NMR (DMSO- d_6) δ : 8.22 (s, 1H), 7.99 (s, 1H), 7.81 (s, 1H), 7.69 – 7.52 (m, 2H), 7.44 (s, 1H), 7.39 – 7.31 (m, 2H), 7.26 (s, 1H), 7.07 (s, 1H), 6.48 (s, 1H), 6.37 (d, J = 30.4 Hz, 2H), 3.92 (s, 3H), 3.77 – 3.62 (m, 4H), 3.50 – 3.39 (m, 4H).

^{13}C NMR (DMSO- d_6) δ : 163.24, 160.28, 160.03, 154.59, 152.83, 136.73, 132.37, 131.86, 130.85, 130.16, 129.11, 128.80, 126.95, 126.00, 118.32, 109.86, 105.33, 101.11, 61.04, 48.98, 47.34.

Anal. Calcd for $\text{C}_{25}\text{H}_{24}\text{N}_4\text{O}$: C, 75.73; H, 6.10; N, 14.13. Found: C, 75.77; H, 6.23; N, 14.29.

4-(4-(3-Nitrophenyl)piperazin-1-yl)-2-phenylquinazoline (144)

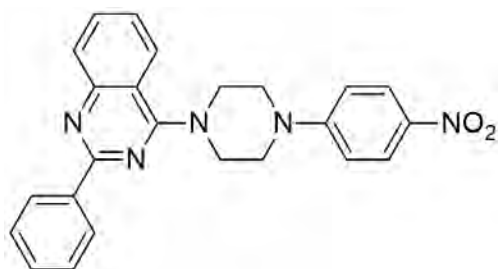
Synthesized from 1-(3-nitrophenyl)piperazine and 4-chloro-2-phenylquinazoline, yield 69 %.

Molecular weight: 411.46 g/mol

^1H NMR (DMSO- d_6) δ : 8.55 – 8.47 (m, 2H), 8.11 (d, $J = 7.6$ Hz, 1H), 7.91 (dd, $J = 8.4, 1.2$ Hz, 1H), 7.84 (ddd, $J = 8.3, 6.9, 1.3$ Hz, 1H), 7.71 (t, $J = 2.3$ Hz, 1H), 7.63 – 7.59 (m, 1H), 7.57 – 7.48 (m, 5H), 7.45 (dd, $J = 8.0, 2.2$ Hz, 1H), 4.08 – 3.95 (m, 4H), 3.64 – 3.53 (m, 4H).

^{13}C NMR (DMSO- d_6) δ : 164.08, 158.26, 152.27, 151.43, 149.04, 138.18, 133.11, 130.47, 130.37, 128.53, 128.09, 125.55, 125.47, 121.22, 114.85, 112.85, 108.32, 48.77, 47.21.

Anal. Calcd for $\text{C}_{24}\text{H}_{21}\text{N}_5\text{O}_2$: C, 70.06; H, 5.14; N, 17.02. Found: C, 70.27; H, 5.18; N, 17.11 .

4-(4-(4-Nitrophenyl)piperazin-1-yl)-2-phenylquinazoline (145)

Synthesized from 1-(4-nitrophenyl)piperazine and 4-chloro-2-phenylquinazoline, yield 64 %.

Molecular weight: 411.46 g/mol

^1H NMR (DMSO- d_6) δ : 8.51 (d, $J = 5.7$ Hz, 2H), 8.10 (d, $J = 8.3$ Hz, 3H), 7.97 – 7.76 (m, 2H), 7.52 (dd, $J = 12.4, 6.3$ Hz, 4H), 7.01 (d, $J = 9.0$ Hz, 2H), 4.18 – 3.98 (m, 4H), 3.78 (m, 4H).

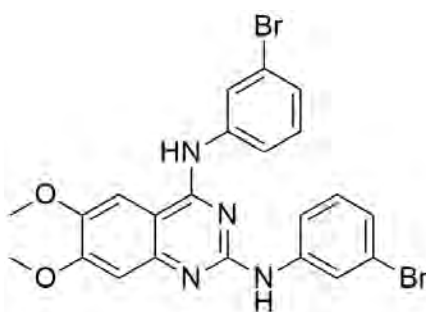
^{13}C NMR (DMSO- d_6) δ : 163.66, 158.20, 154.45, 152.30, 138.22, 137.01, 133.03, 130.45, 128.50, 128.09, 125.92, 125.56, 125.37, 114.73, 112.23, 48.20, 45.69.

Anal. Calcd for $\text{C}_{24}\text{H}_{21}\text{N}_5\text{O}_2$: C, 70.06; H, 5.14; N, 17.02 Found: C, 70.14; H, 5.19; N, 16.89.

7.1.2.16 General procedure for synthesis of N^2, N^4 -disubstituted quinazolines

2,4-dichloro-6,7-dimethoxyquinazoline (1 mmol) was dissolved in refluxing 2-propanol (20 ml) and the substituted aniline (2.5 mmol) was added drop wise. The reaction mixture was refluxed for 12-24 hours, until the reaction was complete as indicated by TLC. The precipitate formed was filtered off and washed with 2-propanol (10 ml) and ether (10 ml). The product was recrystallized from 75 % ethanol.

N^2, N^4 -Bis(3-bromophenyl)-6,7-dimethoxyquinazoline-2,4-diamine (146)



Synthesized from 3-bromoaniline and 2,4-dichloro-6,7-dimethoxyquinazoline, yield 58 %.

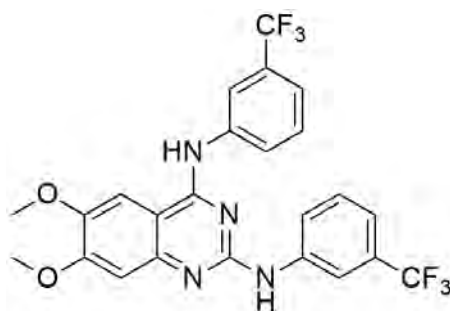
Molecular weight: 530.21 g/mol

^1H NMR (DMSO- d_6) δ : 12.05 (s, 1H), 10.17 (s, 1H), 7.64 (s, 1H), 7.38 (s, 1H), 7.30 (d, $J = 1.3$ Hz, 1H), 7.19 (ddt, $J = 9.8, 4.4, 2.7$ Hz, 5H), 6.88 – 6.73 (m, 1H), 6.65 (dt, $J = 7.1, 1.5$ Hz, 1H), 3.65 (s, 3H), 3.58 (s, 3H).

^{13}C NMR (DMSO- d_6) δ : 156.97, 155.67, 154.79, 150.42, 145.92, 145.53, 145.00, 130.05, 129.68, 125.54, 125.34, 124.03, 124.03, 122.90, 122.68, 120.78, 120.77, 111.61, 105.76, 101.76, 57.01, 55.39.

Anal. Calcd for $\text{C}_{22}\text{H}_{18}\text{Br}_2\text{N}_4\text{O}_2$: C, 49.84; H, 3.42; N, 10.57. Found: C, 49.79; H, 3.60; N, 10.39.

6,7-Dimethoxy- N^2,N^4 -bis(3-(trifluoromethyl)phenyl)quinazoline-2,4-diamine (147)



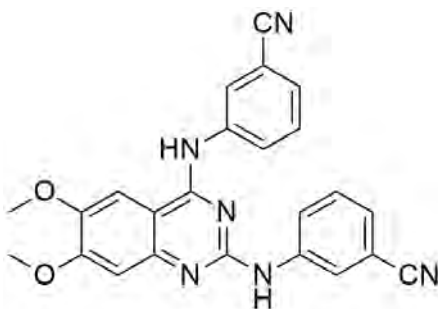
Synthesized from 3-(trifluoromethyl)aniline and 2,4-dichloro-6,7-dimethoxyquinazoline, yield 54 %.

Molecular weight: 508.42 g/mol

^1H NMR (DMSO- d_6) δ : 11.95 (s, 1H), 8.73 (s, 1H), 7.46 (s, 1H), 7.32 (s, 1H), 7.27 (d, $J = 1.4$ Hz, 1H), 7.12 – 6.97 (m, 3H), 6.82 (dd, $J = 3.2, 2.5$ Hz, 2H), 6.71 – 6.66 (m, 1H), 6.54 (ddd, $J = 5.9, 3.3, 1.7$ Hz, 1H), 3.54 (d, $J = 6.0$ Hz, 6H).

^{13}C NMR (DMSO- d_6) δ : 158.95, 156.07, 154.32, 149.26, 144.98, 143.04, 141.70, 134.50, 130.31, 128.82, 126.39, 126.07, 124.83, 123.92, 119.25, 118.78, 115.07, 110.54, 106.29, 103.88, 55.72, 54.89.

Anal. Calcd for $\text{C}_{24}\text{H}_{18}\text{F}_6\text{N}_4\text{O}_2$: C, 56.70; H, 3.57; N, 11.02. Found: C, 56.57; H, 3.70; N, 11.29

3,3'-((6,7-Dimethoxyquinazoline-2,4-diyl)bis(azanediyl))dibenzonitrile (148)

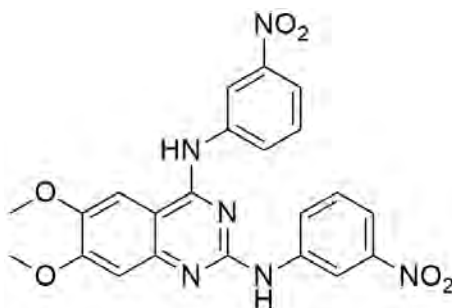
Synthesized from 3-aminobenzonitrile and 2,4-dichloro-6,7-dimethoxyquinazoline, yield 73 %.

Molecular weight: 422.44 g/mol

^1H NMR (DMSO- d_6) δ : 12.04 (s, 1H), 9.01 (s, 1H), 7.48 (s, 1H), 7.32 (s, 1H), 7.28 (ddd, $J = 6.9, 6.5, 4.3$ Hz, 3H), 7.09 (t, $J = 1.7$ Hz, 1H), 7.01 (ddd, $J = 7.3, 2.5, 1.3$ Hz, 2H), 6.71 (dt, $J = 7.1, 1.3$ Hz, 1H), 6.55 (dt, $J = 7.3, 1.7$ Hz, 1H), 3.68 (d, $J = 5.9$ Hz, 6H).

^{13}C NMR (DMSO- d_6) δ : 158.38, 156.40, 153.12, 150.61, 147.82, 141.30, 141.21, 133.50, 131.17, 130.06, 127.99, 125.31, 123.08, 121.47, 118.62, 116.57, 115.05, 110.33, 106.19, 101.22, 56.07, 55.31.

Anal. Calcd for $\text{C}_{24}\text{H}_{18}\text{N}_6\text{O}_2$: C, 68.24; H, 4.29; N, 19.89. Found: C, 68.33; H, 4.10; N, 20.05.

6,7-Dimethoxy- N^2, N^4 -bis(3-nitrophenyl)quinazoline-2,4-diamine (149)

Synthesized from 3-nitroaniline and 2,4-dichloro-6,7-dimethoxyquinazoline, yield 67 %.

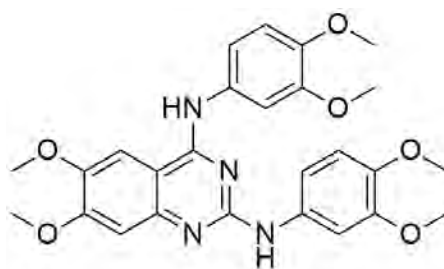
Molecular weight: 462.41 g/mol

^1H NMR (DMSO- d_6) δ : 12.08 (s, 1H), 8.93 (s, 1H), 7.85 – 7.78 (m, 4H), 7.34 – 7.28 (m, 2H), 7.10 (ddd, $J = 7.7, 4.9, 3.1$ Hz, 3H), 6.57 (s, 1H), 3.81 (d, $J = 4.9$ Hz, 6H).

^{13}C NMR (DMSO- d_6) δ : 159.07, 157.48, 155.40, 152.32, 149.02, 148.67, 145.05, 144.69, 143.91, 130.67, 128.38, 124.27, 123.11, 115.24, 114.30, 112.74, 110.61, 105.03, 103.22, 56.31, 55.82.

Anal. Calcd for $\text{C}_{22}\text{H}_{18}\text{N}_6\text{O}_6$: C, 57.14; H, 3.92; N, 18.17. Found: C, 56.80; H, 4.11; N, 18.24.

N^2, N^4 -Bis(3,4-dimethoxyphenyl)-6,7-dimethoxyquinazoline-2,4-diamine (150)



Synthesized from 3,4-dimethoxyaniline and 2,4-dichloro-6,7-dimethoxyquinazoline, yield 59 %.

Molecular weight: 492.52 g/mol

^1H NMR (CDCl_3) δ : 12.82 (s, 1H), 9.72 (s, 1H), 9.10 (s, 1H), 7.66 (s, 1H), 7.53 (d, $J = 2.2$ Hz, 1H), 7.46 (dd, $J = 8.6, 2.3$ Hz, 1H), 6.82 (dd, $J = 8.6, 2.4$ Hz, 1H), 6.56 (d, $J = 2.4$ Hz, 1H), 6.40 (dd, $J = 8.7, 1.9$ Hz, 2H), 6.29 (s, 1H), 4.07 (s, 3H), 3.82 (d, $J = 16.9$ Hz, 6H), 3.65 (d, $J = 4.5$ Hz, 6H), 3.58 (s, 3H).

^{13}C NMR (CDCl_3) δ : 157.08, 156.12, 150.47, 148.94, 148.81, 147.36, 146.89, 146.85, 134.75, 130.54, 129.15, 115.07, 114.97, 110.72, 110.61, 107.19, 104.20, 102.60, 97.71, 56.81, 56.13, 56.05, 56.03, 56.00, 55.92.

Anal. Calcd for $\text{C}_{26}\text{H}_{28}\text{N}_4\text{O}_6$: C, 63.40; H, 5.73; N, 11.38. Found: C, 63.21; H, 5.99; N, 11.50.

7.2 Biological testing

7.2.1 Materials

7.2.1.1 Chemicals

Chemicals	Manufacturer	Article number
Calcein-AM	Sigma	17783
Calcium chloride dihydrate	Merck	P 4901
Cyclosporin A	Sigma	C 3662
D-glucosemonohydrate	Merck	1040740500
Dimethylsulfoxid (DMSO)	Acros	AC19773
Disodium phosphate	Applichem	A4732
Doxorubicin	Fluka	44583
Genitacin (G418)	Sigma	G 9516
HEPES (free acid)	Applichem	A 3707
Hoechst 33342	Sigma	B 2261
Hydrochloric acid (0.5 M)	Grüssing	23204
Ko143	Tocris	3241
Magnesium sulfate heptahydrate	Applichem	A4101
Melsept SF	Braun	18907
Methanol	Merck	107018
Mitoxanthron	Sigma	M 6545
Pheophorbide A	Fontier Scientific Inc.	15664296
Potassium chloride	Merck	104936
Potassium phosphate	Applichem	A 3095
SN-38	TCI Europe N.V.	E0748
Sodium bicarbonate	Merck	106329
Sodium chloride	Merck	106404
Sodium hydroxide solution (1 M)	Grüssing	22195

7.2.1.2 Materials for cell culture and assays

Materials	Manufacturer	Article number
1.0-5.0 ml Bulk, Natural pipette tips	Starlab	I1009-5000
1.5 ml Amber microtubes with attached pp cap	Sarstedt	72690004
1.5 ml Neutral microtubes with attached pp cap	Sarstedt	72690001
2.0 ml MaxyClear microtubes	Axygen scientific	MCT-200-C
96 Well, clear PS microplate, flat bottom	Greiner bio-one	655098
96 Well, clear PS microplate, U-shape bottom	Greiner bio-one	650101
96F untreated black microwell SH plate	Nunc	237108
96-Well tissue culture plate , flat bottom with lid, sterile	Sarstedt	831835
CASYton solution	Schärfe System	43001
Conical test tube PP 15 ml, sterile	Nerbepplus GmbH	25027001
Conical test tube PP 50 ml, sterile	Nerbepplus GmbH	25707001
Cryos PP with screw cap, sterile	Greiner bio-one	123263
FACSClean	Becton Dickinson	340345
FACSFlow	Becton Dickinson	342003
FACSRinse	Becton Dickinson	340346
FACS-testtubes	Sarstedt	551579
Fetal bovine serum	Sigma	F 7524
Glass pasteur pipettes (230 mm)	VWR international	612-1702
Growth medium D-MEM 5671	Sigma	M 5650
Growth medium RPMI-1640	PAN Biotech GmbH	P0416500
L-Glutamine 200 mmol/l	Sigma	G 7513
Membrane filter 0.2 μ m, sterile	Whatman	10462200
Norm-Ject 10 ml syringe	Henke Sass Wolf	4100-000V0

Materials	Manufacturer	Article number
Norm-Ject 20 ml syringe	Henke Sass Wolf	4200-000V0
Penicillin-Streptomycin solution	Sigma	P0781
Serological pipette 10 ml, sterile	Sarstedt	86.1254.001
Serological pipette 25 ml, sterile	Sarstedt	86.1685.001
TipOne 0.1-10.0 μ l natural pipette tips	Starlab	S1111-3000
TipOne 101-1000 μ l natural pipette tips	Starlab	S1111-2020
TipOne 1-200 μ l yellow pipette tips	Starlab	S1111-0006
Tissue culture flasks, 175 cm ² , sterile, filter cap	Greiner bio-one	660175
Tissue culture flasks, 25 cm ² , sterile, filter cap	Greiner bio-one	690175
Tissue culture flasks, 75 cm ² , sterile, filter cap	Greiner bio-one	658175
Trypsin-EDTA solution	PAN Biotech GmbH	P100231SP

7.2.1.3 Instruments

Instruments	Manufacturer	Serial number
Accu-Jet suction pump	Brand	441938
Avanti centrifuge J-25	Beckman	JHY97G35
Axiovert 25 microscope	Zeiss	660197
CASY1 model TT	Schaerfe System	SC1 TT
CO ₂ cell	MMM Group	-
CO ₂ water jacket incubator	Forma Scientific	-
FACSCalibur	Becton Dickinson	E3231
FLUOstar Optima fluorescence plate reader	BMG Lab Technologies	4131164, 4132279
Laminar flow cabinet (model: Antares 48)	Steril S.p.A.	10155/1996
pH-Meter 744	Metrohm	20506
Pipette 0.1-2.5 μ l	Eppendorf	3638475

Instruments	Manufacturer	Serial number
Pipette 100-1000 μ l	Eppendorf	4741196
Pipette 20-200 μ l	Eppendorf	3534296
Pipette 2-20 μ l	Eppendorf	3407866
Pipette 500-5000 μ l	Eppendorf	3615095
POLARstar Galaxy fluorescence plate reader	BMG Lab Technologies	4030639
RH basic magnetic stirrer	IKA Labortechnik	3061661
Vacuum pump BVC21	Brand	08E12592
Vortex stirrer Minishaker	Vacuubrand	2.88069E+13
Waterbath type 1083	GFL	11530203

7.2.1.4 Buffers used for preparing cells for biological assays

1. Krebs-HEPES buffer (KHB)

In the current study, most of the cell based assays were performed using Krebs-HEPES buffer (KHB). KHB was prepared as described in Table 7.1. All the constituents were weighed so as to get 5X concentrated buffer solution.

Table 7.1: Preparation of Krebs-HEPES buffer (KHB)

Chemical	Molecular formula	Molecular weight (g/mol)	Conc. (mM) for 5X concentrated solution	Amount (g) required for 5X concentrated solution (500 ml)
Sodium chloride	NaCl	58.44	593	17.330
Potassium chloride	KCl	74.55	5.64	0.876
Potassium phosphate	KH ₂ PO ₄	136.09	6.00	0.408
Sodium bicarbonate	NaHCO ₃	84.01	21	0.882
D-glucose-mono-hydrate	C ₆ H ₁₂ O ₆ *H ₂ O	198.17	58.5	5.796
HEPES (free acid)	C ₈ H ₁₈ N ₂ O ₄ S	238.31	50	5.958

All substances were transferred to a 500 ml volumetric flask and dissolved in 450 ml of distilled water. The pH value of the solution was adjusted to 7.4 using 1.0 M

sodium hydroxide solution. After adjusting the pH, the volume of the solution was made up to 500 ml using distilled water. From this stock solution 100 ml aliquots were made and stored at -20°C .

To make a buffer solution for use in the assays, 100 ml of 5X concentrated buffer solution was transferred to a 500 ml volumetric flask and 650 μl of 1 M calcium chloride solution was added to give 2.50 mM concentration. To the resulting solution approximately 350 ml of distilled water was added, mixed well and 600 μl of 1M magnesium sulfate heptahydrate solution was added to give 1.20 mM final concentration. The volume of the solution was made up to 500 ml and mixed well. The solution was filtered using a membrane filter (pore size: 0.2 μm) and aliquots were prepared as required and stored at -20°C .

2. Phosphate buffered saline (PBS)

Before passaging the cells, the medium was removed and cells were washed once with phosphate buffered saline (PBS). PBS is suitable for washing cells being isotonic and nontoxic to cells. The buffer solution was prepared as described in Table 7.2.

Table 7.2: Preparation of phosphate buffered saline (PBS)

Chemicals	Molecular formula	Molecular weight (g/mol)	Concentration mmol/l	Amount (g) for 100 ml solution
Sodium chloride	NaCl	58.4	137	8.01
Potassium chloride	KCl	74.6	2.7	0.20
Monopotassium phosphate	KH_2PO_4	136.1	2.0	0.27
Disodium phosphate	Na_2HPO_4	141.9	10	1.44

All substances were transferred to a 1000 ml volumetric flask in the mentioned quantities and dissolved in 800 ml distilled water. The pH value was adjusted to 7.4 using 0.1 M sodium hydroxide solution and the volume was made up to 1000 ml with distilled water. The prepared buffer solution was sterilized before use in an autoclave at 121°C and 2 bar pressure for 20 minutes. It was stored at 4°C for further use.

7.2.2 Cell culture

7.2.2.1 Cell lines

Several different wild-type, resistant or transfected tumor cell lines were used for biological studies of the synthesized compounds.

1. MCF-7 and MCF-7 MX cell line:

The human breast cancer cell line MCF-7 MX was kindly provided by Dr. E. Schneider (Wadsworth Center, Albany, NY, USA). The cell line MCF-7 wt was originally selected from the mammary epithelial tissue of a Caucasian woman with adenocarcinoma. Cells were grown in RPMI-1640 medium supplemented with 20 % fetal bovine serum (FBS), 50 $\mu\text{g}/\text{ml}$ streptomycin, 50 U/ml penicillin G and 2 mM L-glutamine. To maintain the resistance in the BCRP expressing MCF-7 MX cell line, cells were intermittently incubated with 100 nM mitoxantrone for one passage.

2. MDCK wild type and MDCK BCRP cells:

The cell line MDCK wt and MDCK BCRP were received as a generous gift from Dr. A. Schinkel (The Netherlands Cancer Institute, Amsterdam, The Netherlands). MDCK BCRP cells were generated by transfection of the canine kidney epithelial cell line MDCKII with the human wild-type cDNA C-terminally linked to the cDNA of the green fluorescent protein (GFP). These cells were cultured in Dulbecco's modified eagle medium (DMEM) with 10 % fetal bovine serum (FBS), 50 $\mu\text{g}/\text{ml}$ streptomycin, 50 U/ml penicillin G and 2 mM L-glutamine.

3. A2780 and P-gp over-expressing A2780 adr cells:

Human ovarian carcinoma cell lines A2780 and the corresponding MDR1 over-expressing doxorubicin resistant A2780 adr cell line were purchased from ECACC (Nos. 93112519 and 93112520). The cell lines were grown in RPMI-1640 medium supplemented with 10 % FBS, 50 $\mu\text{g}/\text{ml}$ streptomycin, 50 U/ml penicillin G, and 300 mg/l L-glutamine. To maintain the P-gp overexpression in the A2780 adr cell line, intermittently cells were incubated with 1 μM doxorubicin for one passage.

4. 2008 wild type and overexpressing 2008 MRP1 cells:

The human ovarian cancer cell line 2008 MRP1 stably expressing MRP1 was a gift from Prof. Dr. Piet Borst (The Netherlands Cancer Institute, Amsterdam, The Netherlands). The cell line 2008 MRP1 was grown in the same medium as described for A2780 cells with addition of 400 $\mu\text{g}/\text{ml}$ G-418 (Geneticin) for maintaining ABCC1 overexpression.

7.2.2.2 Growing and subculturing of cells

All the cell lines used for biological testing of the synthesized compounds were cultivated in standard culture flasks of different capacities. Tissue culture flasks T25 (25 cm^2), T75 (75 cm^2) and T175 (175 cm^2) were used depending on the number of cells needed to perform assays. Cells were cultivated in an incubator maintained at 37 °C and 5 % CO_2 . The culture medium was changed every 2-3 days depending on cell confluence. In general the medium was changed when the phenyl red indicator present changed its color from pink to orange. In general for T25 flask 10 ml, for T75 flask 15-20 ml and for T175 flask 25-30 ml culture medium was used.

Subculturing of cells was done after a confluence of 80-90% was attained. For subculturing, first, the old medium was removed by aspiration and cells were washed with 3 ml of PBS buffer to remove floating dead cells and traces from culture medium. After this, 3 ml of trypsin-EDTA solution was added and incubated at 37 °C for 5-15 minutes depending on the cell line. The separation of cells from the surface of culture flasks was confirmed under the microscope. After incubation, 7 ml of culture medium was added and mixed well. The cell suspension was transferred to a 50 ml centrifugation tube and centrifuged at 1200 x g for 4 minutes at 4 °C. The trypsin containing medium was gently removed by aspiration and 10 ml fresh culture medium was added. Cells were re-suspended and depending on cell line and cell density, one to three ml of cell suspension was transferred into a new culture flask containing sufficient fresh growth medium. The rest of the cell suspension was used for performing assays.

7.2.2.3 Cryopreservation and defrosting of cells

For performing assays, most of the cell lines were used until a maximum passage number of 30. Hence it was necessary to have cell backups with lower passage numbers. To generate backups, cells were grown in T175 flasks and were harvested as described above. After centrifugation and removal of trypsin containing culture medium, cells were re-suspended in growth medium containing 10 % DMSO. After mixing well, cells were transferred into 1 ml cryovials. Cryovials were stored in -80 °C as fast as possible, to avoid toxic effect of DMSO. These cryovials were stored for one week at -80 °C and then transferred into liquid nitrogen tank (-190 °C) where longer storage of cells is possible.

For using cells with lower passage number, they were taken out of the nitrogen tank and defrosted at 37 °C in a water bath. Cells were transferred as fast as possible to T25 or T75 flasks filled with an adequate amount of fresh culture medium pre-warmed at 37 °C. Flasks were placed into the incubator. On the next day, old culture medium containing slight amount of DMSO was aspirated along with floating cells and replaced with fresh culture medium. Cells were cultured for 1-2 more passages before used in assays.

7.2.2.4 Cell counting using CASY1 model TT

For performing different cell based assays, the cell number was important. For this, 20 μ l of cell suspension was pipetted into 10 ml of sterile filtered Casy ton solution and analyzed with the CASY1 model TT cell counter using a 150 μ m capillary. The instrument measures the cell count along with the cell diameter. From this information and graphical presentation the status of the cells can be checked. For the measurement of cell count a cell size range of 8 μ m to 40 μ m was defined.

7.2.3 Assays

For the investigation of the synthesized compounds different cell based assays were applied. 10 mM stock solutions of the tested compounds were prepared in DMSO. Different dilutions of compounds were prepared in sterile filtered KHB. For some compounds with low solubility methanol was used for preparing 1 mM concentrations. The amount of methanol was chosen so that it did not exceed 5 % in the highest concentration used in the assay. The highest concentration of DMSO present in dilutions used for the assays was not more than 0.5 %.

7.2.3.1 Hoechst 33342 accumulation assay

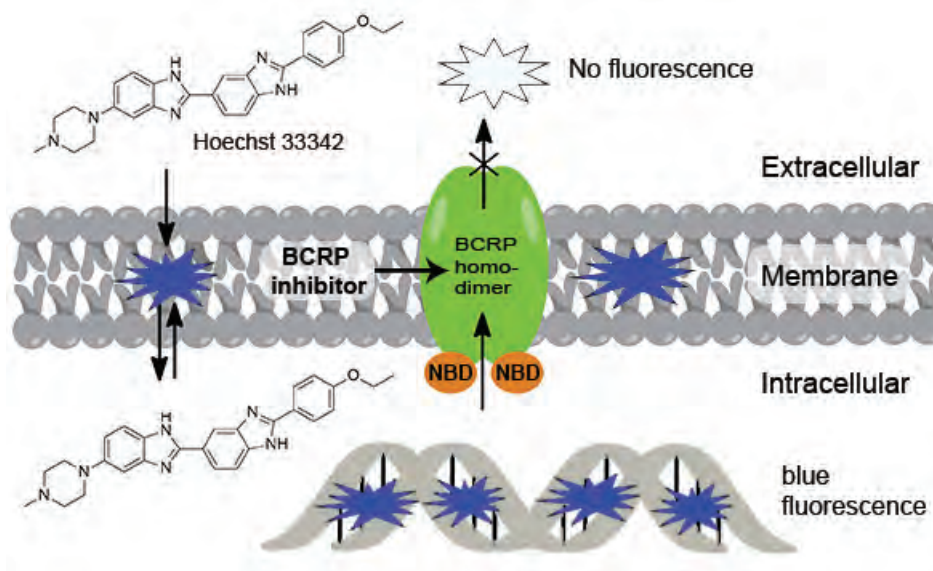


Figure 7.1: General principle of the Hoechst 33342 assay [58]

Hoechst 33342 is a fluorescent bisbenzimidazole derivative, which is primarily used as a cell permeable nucleic acid stain [225–227]. Hoechst 33342 has been found to bind to the minor groove of double-stranded DNA with more preference for adenine and thymine rich sequences which enhance fluorescence intensity [228, 229]. Hoechst 33342 shows fluorescence with an excitation maximum of 340 nm and an emission maximum of 450 nm [228] when bound to nucleotides. Unbound Hoechst 33342 shows fluorescence with an emission maximum 510–540 nm in very high concentrations. Hoechst 33342 has been found to be transported by the ABC transporters BCRP

and P-gp [230, 231]. Because of this, it shows less fluorescence in BCRP and P-gp overexpressing cells as compared to wild type cells. When BCRP or P-gp are inhibited by a modulator, the transport of Hoechst 33342 decreases leading to an increase in its total fluorescence. This increase in fluorescence can be used as a parameter to determine the extent of BCRP inhibition. In this study the Hoechst 33342 assay was used to investigate BCRP inhibition of all synthesized compounds.

Procedure: To investigate the inhibitory effect of synthesized compounds on BCRP, a Hoechst 33342 accumulation assay was performed as described earlier with small modifications [125, 232]. MDCK (BCRP) or MCF-7 (MX) cells were harvested after reaching a confluence of 80-90 % as described above (see section 7.2.2.2). The cell density was determined using a CASY1 model TT cell counter device. In general 3 million cells were needed per 96 well microplate. The required amount of cells from a 50 ml centrifugation tube was transferred to 2 ml microtubes and centrifuged at 7840 x g for 10-15 seconds. Cells were washed three times with Krebs-Hepes buffer (KHB) and seeded into black 96 well microplates at a density of approximately 20,000 cells per well in a volume of 90 μl . To this, 10 μl of the test compound in different concentrations was added to achieve a total volume of 100 μl . The general scheme used for pipetting compounds and different cells is shown in Figure 7.2.

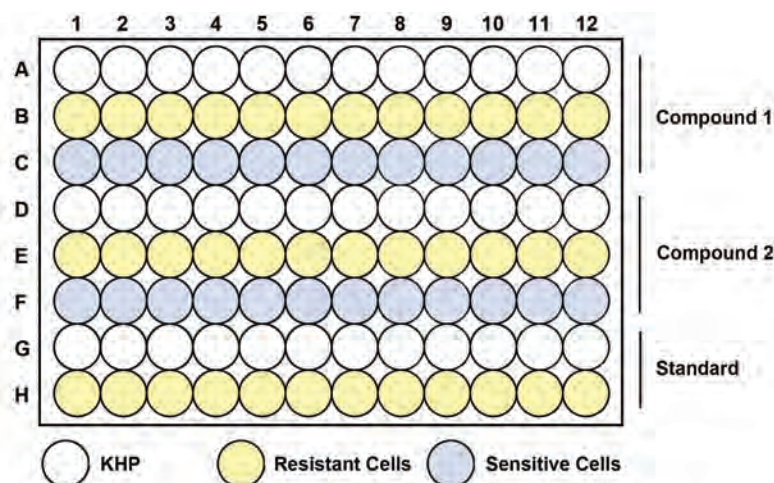


Figure 7.2: Arrangement of 96 well microplate for the Hoechst 33342 assay

The prepared 96 well plate was kept under 5 % CO₂ and 37 °C for 30 min. After this preincubation period, 20 μl of a 6 μM Hoechst 33342 solution (protected from

light) was added to each well yielding a final concentration of Hoechst 33342 of $1 \mu M$. Fluorescence was measured immediately in constant intervals (60 s) up to 120 min at an excitation wavelength of 355 nm and an emission wavelength of 460 nm using a 37 °C tempered BMG POLARstar OPTIMA or a FLUOstar OPTIMA microplate reader. Microplate reader parameters used for the assay are listed in Table 7.3.

Table 7.3: Parameters used for performing the Hoechst 33342 assay

Parameter	Value
Scanning mode	Plate
Incubation temperature	37 °C
Number of cycles	120
Cycle time	60 sec
Number of light flashes	10/sec
Interval between rows	0.5 sec
Measurement direction	horizontal
Excitation wavelength	355 nm
Emission wavelength	460 nm
Gain (for FLUOstar)	1700-1800
Gain (for POLARstar)	45-50
Required value	20 %

For the analysis of the data obtained from the assay, first the fluorescence of KHB was subtracted from the fluorescence reading obtained from MDCK cells. The average of fluorescence values in the steady state (from 100 min to 109 min) was calculated for each concentration and from these data concentration-response curves were generated by nonlinear regression using the four-parameter logistic equation in GraphPad Prism (v. 5.0, San Diego, CA, USA).

7.2.3.2 Pheophorbide A assay

Pheophorbide A is a chlorophyll-breakdown product and belongs to the chemical class of porphyrins. Pheophorbide A is present in various plant-derived foods and food supplements. BCRP plays an important role in transporting pheophorbide A and limiting its uptake from ingested food [233]. Pheophorbide A is a specific substrate of BCRP [104] and hence can be effectively used to investigate inhibitors of BCRP.

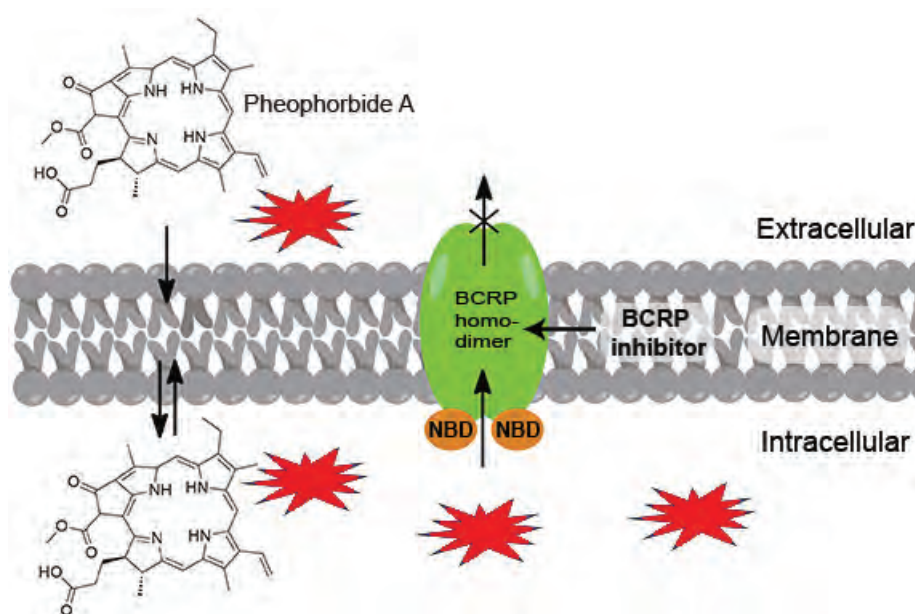


Figure 7.3: Principle of the pheophorbide A assay

Pheophorbide A shows fluorescence with an excitation maximum of 395 nm and emission maximum of 670 nm. This property makes it suitable for assessment with flow cytometry where fluorescence of pheophorbide A in individual cells is measured. Pheophorbide A diffuses easily through cell membranes and is accumulated inside cells. In case of cells with BCRP overexpression, pheophorbide A is transported outside the cell leading to a decrease in intracellular fluorescence. When BCRP is inhibited by modulators, pheophorbide A accumulation is increased which is reflected in increased intracellular fluorescence. This increase in fluorescence is proportional to the extent of BCRP inhibition.

Flow cytometry: The pheophorbide A assay was performed by flow cytometry where the fluorescence of single cells can be measured. For these experiments a Becton-Dickinson FACSCalibur was used (FACS: fluorescence activated cell sorting). With use of a very small nozzle and sheath fluid, cells are hydrodynamically brought in front of a laser light source, where one cell at a time passes the laser light. The optical system involves an argon laser with excitation wavelength of 488 nm and detectors for FSC (Forward angle light scatter), SSC (Side scatter) and fluorescence signals. Fluorescence signals can be detected in three different channels viz. FL1, FL2 and FL3 which have different wavelengths. For the pheophorbide A assay the FL3 channel was used which has a filter for 670 nm and longer wavelengths.

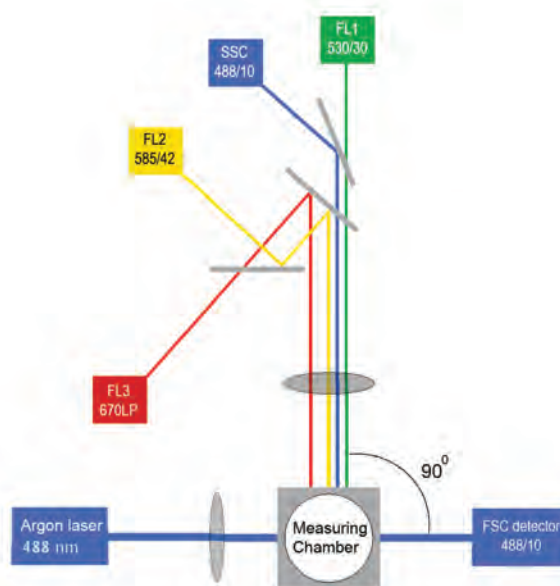


Figure 7.4: Schematic representation of a flow-cytometer [234]

Procedure: The pheophorbide A assay was performed as described earlier with small modifications [117, 235]. To perform the pheophorbide A assay, cells were prepared as described for the Hoechst 33342 assay (see section 7.2.3.1). Approximately 45,000 cells per well were seeded into U-shaped clear 96 well microplates in a volume of $160 \mu\text{l}$. To this, $20 \mu\text{l}$ of the test compound in different concentrations was added. The scheme used for preparing microplates for the pheophorbide A assay is shown in Figure 7.5.

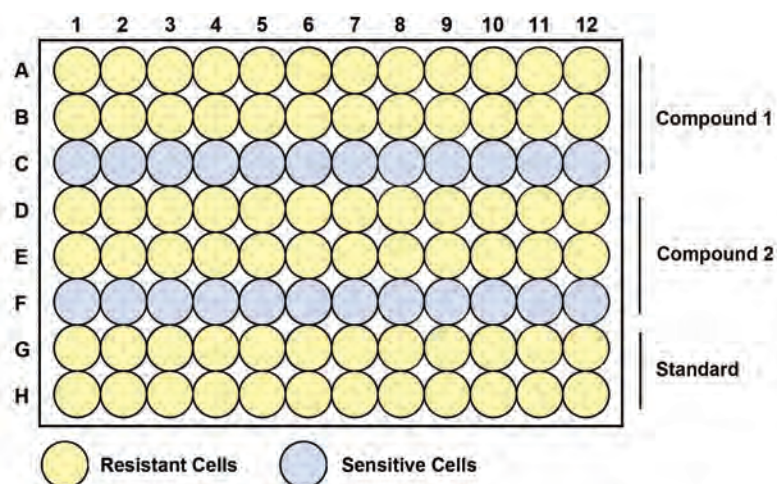


Figure 7.5: Arrangement of 96 well microplate for the pheophorbide A assay

The prepared 96 well plate was kept under 5 % CO₂ and 37 °C for 30 min. After this preincubation period, 20 µl of a 5 µM pheophorbide A solution (protected from light) was added to each well resulting in 0.5 µM end concentration. The 5 µM pheophorbide A solution was prepared freshly just before its use from a 1 mM stock solution. For this 15 µl pheophorbide A stock solution was dissolved in 2985 µl of KHB. After adding pheophorbide A solution into each well, plates were further incubated for 120 min. Before the measurements cells were again re-suspended using a multichannel pipette. Fluorescence was measured using a FACSCalibur flow-cytometer. Concentration-response curves were generated by nonlinear regression using the four-parameter logistic equation using GraphPad Prism (v. 5.0, San Diego, CA, USA).

7.2.3.3 Calcein AM accumulation assay

Calcein AM is an acetoxymethyl ester derivative of calcein. Calcein AM is a non-fluorescent and lipophilic compound which can diffuse through plasma membranes and can be hydrolyzed by unspecific esterases present in cells to the calcein anion [236]. In contrast to calcein AM, calcein shows strong green fluorescence. As calcein is rather hydrophilic, it can leave the cell only by active transport.

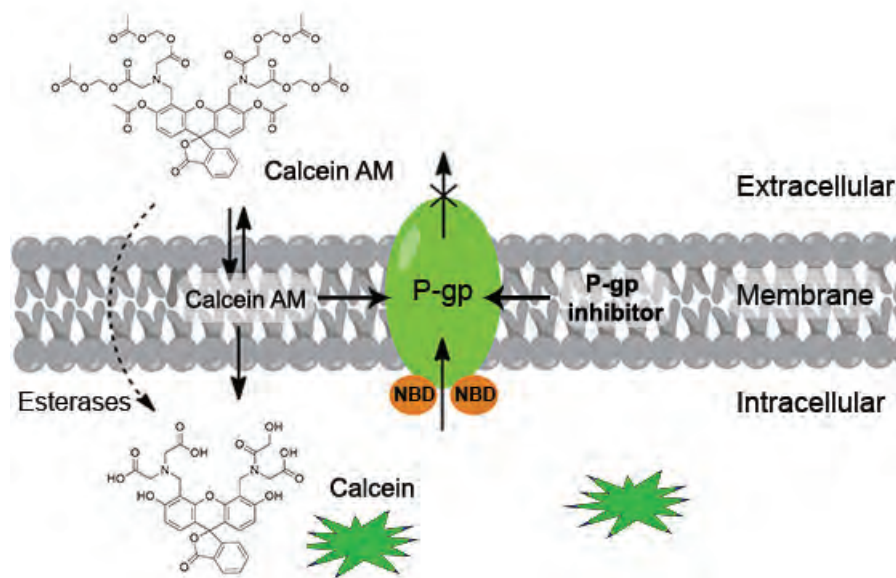


Figure 7.6: Principle of the calcein AM assay

Calcein AM has been found to be transported by the ABC transporter P-gp [237] as well as MRP1 [236]. This property can be used to assess inhibitors of P-gp and MRP1. In case of P-gp and MRP1 overexpressing cells, the intracellular fluorescence of calcein is much lower than in sensitive wild type cells, owing to transport of calcein AM outside the cell. When P-gp or MRP1 are inhibited by a modulator, this leads to an increased accumulation of calcein AM being hydrolyzed inside cells and hence increased fluorescence by calcein. This increase in fluorescence is proportional to the extent of inhibition of P-gp and MRP1 [157, 238].

In the current study, the calcein AM assay was used to screen all compounds at 10 μM concentration. Compounds showing significant inhibition in comparison to the standard cyclosporine A, were further investigated with a range of different concentrations to determine their IC_{50} values.

Procedure: For checking the selectivity of synthesized compounds towards BCRP, all compounds were further tested for their P-gp and MRP1 inhibition in the calcein-AM assay [235]. For this purpose A2780 adr cells for P-gp and 2008 MRP1 cells for MRP1 were used. After reaching a confluence of 80-90 %, subculturing was performed by adding 0.05 % trypsin and 0.02 % EDTA. Cells were prepared as described for the Hoechst 33342 assay (see section 7.2.3.1). Cells were seeded into colorless 96 well microplates at a density of approximately 30,000 cells in a volume of 90 μl per well. After this, 10 μl of the test compound was added, resulting in a final volume of 100 μl per well. The scheme for pipetting compounds and cells is shown in Figure 7.2. The prepared 96 well plates were preincubated for 30 min at 5 % CO_2 and 37 °C. After the preincubation period, 33 μl of a 1.25 μM calcein AM solution, which was protected from light, was added to each well. The fluorescence was measured immediately in constant time intervals (60 s) up to 90 min using an excitation wavelength of 485 nm and an emission filter of 520 nm with a 37 °C tempered BMG POLARstar OPTIMA or FLUOstar OPTIMA microplate reader. Microplate reader parameters used for the assay are listed in Table 7.5.

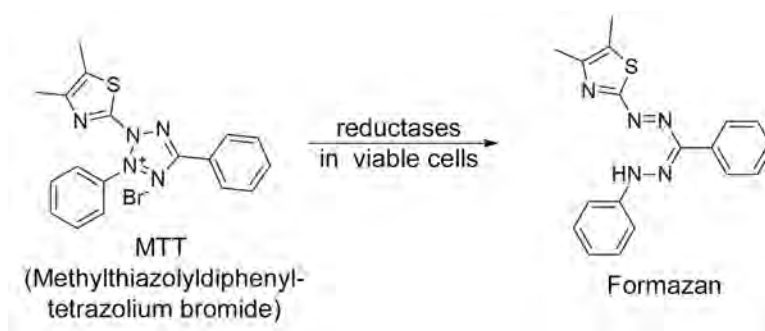
For calculation of inhibitory effects first, the fluorescence from KHB was subtracted from that of cells. From the obtained data, the first linear part of the generated fluorescence time curves was used to calculate the slope. The calculated slopes were plotted against logarithmic concentrations of tested compounds. The concentration-response curves were fitted with nonlinear regression using the four-parameter logistic equation in GraphPad Prism (v. 5.0, San Diego, CA, USA).

Table 7.5: Parameters used for performing the calcein AM assay

Parameter	Value
Scanning mode	Plate
Incubation temperature	37 °C
Number of cycles	90
Cycle time	60 sec
Number of light flashes	10/sec
Interval between rows	0.2 sec
Measurement direction	horizontal
Excitation wavelength	485 nm
Emission wavelength	520 nm
Gain (for FLUOstar)	1700-1800
Gain (for POLARstar)	40-45
Required value	20 %

7.2.3.4 MTT cytotoxicity assay

MTT (Methylthiazolyldiphenyl-tetrazolium bromide) is a yellow tetrazole which gets reduced in viable cells to formazan which is purple in color. As the formazan is insoluble in water it forms formazan crystals that can be visualized under the microscope. After solubilizing with DMSO, formazan color intensity can be quantified by measuring its absorbance at 544 nm.

**Figure 7.7:** Reduction of yellow MTT to purple formazan by cellular reductases

In the current study, the MTT assay was used for two purposes:

1. To enable future *in vivo* studies, it was important that the lead compounds are not cytotoxic. The most active compounds from each class were investigated for their cellular toxicity in MTT assays.

2. To prove the efficiency of lead compounds to sensitize BCRP overexpressing cells towards toxicity of well known anticancer and cytotoxic compounds. For this purpose the anticancer drug mitoxantrone and cytotoxic compounds SN-38 (7-Ethyl-10-hydroxy-camptothecin) and Hoechst 33342 were used. The shift of growth inhibition curves of these cytotoxic compounds towards lower concentrations (in presence of lead compounds) was studied by MTT cytotoxicity assay.

Procedure: The MTT assay was performed as described earlier with small modifications [239]. Cells were harvested as described before for the Hoechst 33342 assay (see section 7.2.3.1). Cells were seeded into 96-well tissue culture plates at a density of 2500 cells per well in a volume of 180 μl and were incubated at 5 % CO_2 at 37 $^\circ\text{C}$ for 6 h. Attachment of cells was controlled under the microscope and different concentrations of test compounds prepared in PBS were added to the cells to achieve the required final concentration in a final volume of 200 μl . Control experiments were performed with medium containing 1 % (v/v) of DMSO (positive control) and only PBS (negative control). A General schematic representation of pipetting cells and tested compounds is shown in Figure 7.8.

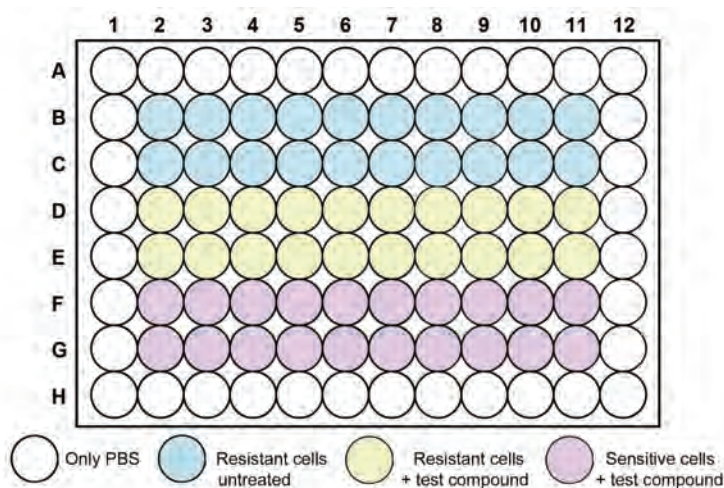


Figure 7.8: Preparation of 96 well tissue culture plates for the MTT cytotoxicity assay

After addition of the compounds, plates were incubated at 37 $^\circ\text{C}$ and 5 % CO_2 for 72 h. After the incubation period, 20 μl of a 5 mg/ml MTT solution was added to each well. Plates were further incubated for a period of about 1 h, after which the formation of purple colored formazan needles could be detected under the microscope. Then the supernatant was removed and the cells were lysed by addition of 100 μl DMSO per

well. Color intensity of formed formazan was determined spectrophotometrically by measuring the absorbance at 544 nm with background correction at 710 nm using a BMG POLARstar microplate reader. Cell viability was calculated as percentage of controls treated only with PBS. GI₅₀ values (growth inhibition concentration = concentration that produced a 50 % reduction of cell viability) were calculated by nonlinear regression analysis, assuming a sigmoidal concentration-response curve using GraphPad Prism (v. 5.0, San Diego, CA, USA).

7.2.3.5 IC₅₀ and GI₅₀ calculations using GraphPad Prism

In the current study different accumulation assays (Hoechst 33342, pheophorbide A and calcein AM) as well cytotoxicity assay (MTT) were performed. For all assays data are reported as IC₅₀ or GI₅₀ ± S.D. For this purpose the statistics software GraphPad Prism (version 5.0) was used. For calculating IC₅₀ and GI₅₀ concentration-response curves were generated using nonlinear regression with the four-parameter logistic equation (variable slope) and compared to the three-parameter logistic equation (fixed slope = 1). IC₅₀ is the concentration required to show 50 % inhibitory effect while GI₅₀ is the concentration which is required to show 50 % inhibition of cell growth. For the inhibitors where the maximum response was lower than that of the standard used, top values were fixed to the maximum response of the standard to generate concentration-response curves. The mathematical model of the logistic equation used for generating the concentration-response curves is:

$$Y = Bottom + \frac{Top - Bottom}{1 + 10^{((\log IC_{50} - \log X) * Hill\ slope)}}$$

Where, **X**: concentration of compound, **Y**: response, increasing or decreasing as X increases, **Bottom**: minimum baseline response, **Top**: maximum response, **Hill-slope**: steepness of the curve, **IC₅₀**: compound concentration to achieve 50 % of the maximum response

All the assays were performed in triplicate and hence data are represented as mean of values ± S.D. (standard deviation).

Bibliography

- [1] Gottesman, M. M.; Pastan, I. Biochemistry of multidrug resistance mediated by the multidrug transporter. *Annu. Rev. Biochem.* **1993**, *62*, 385–427.
- [2] Fojo, A. T.; Ueda, K.; Slamon, D. J.; Poplack, D. G.; Gottesman, M. M.; Pastan, I. Expression of a multidrug-resistance gene in human tumors and tissues. *Proc. Natl. Acad. Sci. U. S. A.* **1987**, *84*, 265–269.
- [3] Bodó, A.; Bakos, E.; Szeri, F.; Váradi, A.; Sarkadi, B. The role of multidrug transporters in drug availability, metabolism and toxicity. *Toxicol. Lett.* **2003**, *140-141*, 133–143.
- [4] van Vliet, E. A.; Redeker, S.; Aronica, E.; Edelbroek, P. M.; Gorter, J. A. Expression of multidrug transporters MRP1, MRP2, and BCRP shortly after status epilepticus, during the latent period, and in chronic epileptic rats. *Epilepsia* **2005**, *46*, 1569–1580.
- [5] Dassa, E.; Bouige, P. The ABC of ABCS: a phylogenetic and functional classification of ABC systems in living organisms. *Res. Microbiol.* **2001**, *152*, 211–229.
- [6] Holland, I. B.; Blight, M. A. ABC-ATPases, adaptable energy generators fuelling transmembrane movement of a variety of molecules in organisms from bacteria to humans. *J. Mol. Biol.* **1999**, *293*, 381–399.
- [7] Higgins, C. F. ABC transporters: from microorganisms to man. *Annu. Rev. Cell Biol.* **1992**, *8*, 67–113.
- [8] Sarkadi, B.; Ozvegy-Laczka, C.; Németh, K.; Váradi, A. ABCG2 – a transporter for all seasons. *FEBS Lett.* **2004**, *567*, 116–120.

- [9] Huls, M.; Russel, F. G. M.; Masereeuw, R. The role of ATP binding cassette transporters in tissue defense and organ regeneration. *J. Pharmacol. Exp. Ther.* **2009**, *328*, 3–9.
- [10] Szakács, G.; Paterson, J. K.; Ludwig, J. A.; Booth-Genthe, C.; Gottesman, M. M. Targeting multidrug resistance in cancer. *Nat. Rev. Drug Discov.* **2006**, *5*, 219–234.
- [11] Szakács, G.; Váradi, A.; Ozvegy-Laczka, C.; Sarkadi, B. The role of ABC transporters in drug absorption, distribution, metabolism, excretion and toxicity (ADME-Tox). *Drug Discov. Today* **2008**, *13*, 379–393.
- [12] Ozvegy, C.; Litman, T.; Szakács, G.; Nagy, Z.; Bates, S.; Váradi, A.; Sarkadi, B. Functional characterization of the human multidrug transporter, ABCG2, expressed in insect cells. *Biochem. Biophys. Res. Commun.* **2001**, *285*, 111–117.
- [13] Russel, F. G. M.; Masereeuw, R.; van Aubel, R. A. M. H. Molecular aspects of renal anionic drug transport. *Annu. Rev. Physiol.* **2002**, *64*, 563–594.
- [14] Schinkel, A.; Wagenaar, E.; Mol, C.; van Deemter, L. P-glycoprotein in the blood-brain barrier of mice influences the brain penetration and pharmacological activity of many drugs. *J. Clin. Invest.* **1996**, *97*, 2517.
- [15] Cordon-Cardo, C.; O'Brien, J.; Casals, D.; Rittman-Grauer, L.; Biedler, J.; Melamed, M.; Bertino, J. Multidrug-resistance gene (P-glycoprotein) is expressed by endothelial cells at blood-brain barrier sites. *Proc. Natl. Acad. Sci. USA* **1989**, *86*, 695–698.
- [16] Asperen, J.; Mayer, U.; Tellingen, O.; Beijnen, J. The functional role of P-Glycoprotein in the blood–Brain barrier. *J. Pharm. Sci.* **1997**, *86*, 881–884.
- [17] Wijnholds, J.; De Lange, E.; Scheffer, G.; Mol, C.; van der Valk, M.; Schinkel, A.; Scheper, R.; Breimer, D.; Borst, P. Multidrug resistance protein 1 protects the choroid plexus epithelium and contributes to the blood-cerebrospinal fluid barrier. *J. Clin. Invest.* **2000**, *105*, 279–285.
- [18] Rao, V.; Dahlheimer, J.; Bardgett, M.; Snyder, A.; Finch, R.; Sartorelli, A.; Piwnicka-Worms, D. Choroid plexus epithelial expression of MDR1 P glyco-

- protein and multidrug resistance-associated protein contribute to the blood–cerebrospinal-fluid drug-permeability barrier. *Proc. Natl. Acad. Sci. USA* **1999**, *96*, 3900–3905.
- [19] Cordon-Cardo, C.; O’Brien, J.; Boccia, J.; Casals, D.; Bertino, J.; Melamed, M. Expression of the multidrug resistance gene product (P-glycoprotein) in human normal and tumor tissues. *J. Histochem. Cytochem.* **1990**, *38*, 1277–1287.
- [20] Maliepaard, M.; Scheffer, G.; Faneyte, I.; van Gastelen, M.; Pijnenborg, A.; Schinkel, A.; van de Vijver, M.; Scheper, R.; Schellens, J. Subcellular localization and distribution of the breast cancer resistance protein transporter in normal human tissues. *Cancer Res.* **2001**, *61*, 3458–3464.
- [21] Suzuki, H. Role of ABC transporters in drug disposition. *Cell* **2004**, *36*, 175–178.
- [22] Glavinas, H.; Krajcsi, P.; Cserepes, J.; Sarkadi, B. The role of ABC transporters in drug resistance, metabolism and toxicity. *Curr. Drug Deliv.* **2004**, *1*, 27–42.
- [23] Schinkel, A.; Jonker, J. Mammalian drug efflux transporters of the ATP binding cassette (ABC) family: an overview. *Adv. Drug Delivery Rev.* **2012**,
- [24] Gottesman, M.; Fojo, T.; Bates, S. Multidrug resistance in cancer: role of ATP-dependent transporters. *Nat. Rev. Cancer* **2002**, *2*, 48–58.
- [25] Jekerle, V. Investigations of combined strategies to reverse P-glycoprotein- and BCRP-mediated Multidrug Resistance in Human Ovarian Cancer Cells and Xenograft Tumors. Ph.D. thesis, University of Bonn, **2006**.
- [26] Fojo, T.; Bates, S. Strategies for reversing drug resistance. *Oncogene* **2003**, *22*, 7512–7523.
- [27] Tan, B.; Piwnica-Worms, D.; Ratner, L. Multidrug resistance transporters and modulation. *Curr. Opin. Oncol.* **2000**, *12*, 450–458.
- [28] Ling, V.; Thompson, L. Reduced permeability in CHO cells as a mechanism of resistance to colchicine. *J. Cell. Physiol.* **1974**, *83*, 103–116.
- [29] Juliano, R. L.; Ling, V. A surface glycoprotein modulating drug permeability in Chinese hamster ovary cell mutants. *Biochim. Biophys. Acta* **1976**, *455*, 152–162.

- [30] Ling, V. Multidrug resistance: molecular mechanisms and clinical relevance. *Cancer Chemother. Pharmacol.* **1997**, *40*, 3–8.
- [31] Ishikawa, T.; Hirano, H.; Onishi, Y.; Sakurai, A.; Tarui, S. Functional evaluation of ABCB1 (P-glycoprotein) polymorphisms: high-speed screening and structure-activity relationship analyses. *Drug Metab. Pharmacokinet.* **2004**, *19*, 1–14.
- [32] Schinkel, A. H. The physiological function of drug-transporting P-glycoproteins. *Semin. Cancer Biol.* **1997**, *8*, 161–170.
- [33] Stenham, D. R.; Campbell, J. D.; Sansom, M. S. P.; Higgins, C. F.; Kerr, I. D.; Linton, K. J. An atomic detail model for the human ATP binding cassette transporter P-glycoprotein derived from disulfide cross-linking and homology modeling. *FASEB J.* **2003**, *17*, 2287–2289.
- [34] O'Mara, M. L.; Tieleman, D. P. P-glycoprotein models of the apo and ATP-bound states based on homology with Sav1866 and MalK. *FEBS Lett.* **2007**, *581*, 4217–4222.
- [35] Globisch, C.; Pajeva, I. K.; Wiese, M. Identification of putative binding sites of P-glycoprotein based on its homology model. *ChemMedChem* **2008**, *3*, 280–295.
- [36] Becker, J.-P.; Depret, G.; Van Bambeke, F.; Tulkens, P. M.; Prévost, M. Molecular models of human P-glycoprotein in two different catalytic states. *BMC Struct. Biol.* **2009**, *9*, 3.
- [37] Aller, S. G.; Yu, J.; Ward, A.; Weng, Y.; Chittaboina, S.; Zhuo, R.; Harrell, P. M.; Trinh, Y. T.; Zhang, Q.; Urbatsch, I. L.; Chang, G. Structure of P-glycoprotein reveals a molecular basis for poly-specific drug binding. *Science* **2009**, *323*, 1718–1722.
- [38] Higgins, C. F.; Gottesman, M. M. Is the multidrug transporter a flippase? *Trends Biochem. Sci.* **1992**, *17*, 18–21.
- [39] Sharom, F. J. The P-glycoprotein multidrug transporter. *Essays Biochem.* **2011**, *50*, 161–178.
- [40] Brinkmann, U.; Eichelbaum, M. Polymorphisms in the ABC drug transporter gene MDR1. *Pharmacogenomics J.* **2001**, *1*, 59–64.

- [41] Tsuruo, T.; Iida, H.; Tsukagoshi, S.; Sakurai, Y. Overcoming of vincristine resistance in P388 leukemia in vivo and in vitro through enhanced cytotoxicity of vincristine and vinblastine by verapamil. *Cancer Res.* **1981**, *41*, 1967–1972.
- [42] Pajeva, I.; Wiese, M. Structure–Activity Relationships of Tariquidar Analogs as Multidrug Resistance Modulators. *AAPS J.* **2009**, *11*, 435–444.
- [43] Thomas, H.; Coley, H. Overcoming multidrug resistance in cancer: an update on the clinical strategy of inhibiting p-glycoprotein. *Cancer control* **2003**, *10*, 159–159.
- [44] Krishna, R.; Mayer, L. Multidrug resistance (MDR) in cancer: mechanisms, reversal using modulators of MDR and the role of MDR modulators in influencing the pharmacokinetics of anticancer drugs. *Eur. J. Pharm. Sci.* **2000**, *11*, 265–283.
- [45] Cole, S.; Bhardwaj, G.; Gerlach, J.; Mackie, J.; Grant, C.; Almquist, K.; Stewart, A.; Kurz, E.; Duncan, A.; Deeley, R. Overexpression of a transporter gene in a multidrug-resistant human lung cancer cell line. *Science* **1992**, *258*, 1650.
- [46] Leslie, E.; Deeley, R.; Cole, S. Multidrug resistance proteins: role of P-glycoprotein, MRP1, MRP2, and BCRP (ABCG2) in tissue defense. *Toxicol. Appl. Pharmacol.* **2005**, *204*, 216–237.
- [47] Flens, M.; Zaman, G.; Van der Valk, P.; Izquierdo, M.; Schroeijs, A.; Scheffer, G.; Van Der Groep, P.; De Haas, M.; Meijer, C.; Scheper, R. Tissue distribution of the multidrug resistance protein. *Am. J. Pathol.* **1996**, *148*, 1237–1247.
- [48] Munoz, M.; Henderson, M.; Haber, M.; Norris, M. Role of the MRP1/ABCC1 multidrug transporter protein in cancer. *IUBMB Life* **2007**, *59*, 752–757.
- [49] Kruh, G. D.; Zeng, H.; Rea, P. A.; Liu, G.; Chen, Z. S.; Lee, K.; Belinsky, M. G. MRP subfamily transporters and resistance to anticancer agents. *J. Bioenerg. Biomembr.* **2001**, *33*, 493–501.
- [50] Rosenberg, M.; Mao, Q.; Holzenburg, A.; Ford, R.; Deeley, R.; Cole, S. The structure of the multidrug resistance protein 1 (MRP1/ABCC1) crystallization and single-particle analysis. *J. Biol. Chem.* **2001**, *276*, 16076–16082.

- [51] Gekeler, V.; Ise, W.; Sanders, K. H.; Ulrich, W. R.; Beck, J. The leukotriene LTD4 receptor antagonist MK571 specifically modulates MRP associated multidrug resistance. *Biochem. Biophys. Res. Commun.* **1995**, *208*, 345–352.
- [52] Zeng, H.; Chen, Z.; Belinsky, M.; Rea, P.; Kruh, G. Transport of Methotrexate (MTX) and Folates by Multidrug Resistance Protein (MRP) 3 and MRP1 Effect of Polyglutamylation on MTX Transport. *Cancer Res.* **2001**, *61*, 7225–7232.
- [53] Norman, B.; Gruber, J.; Hollinshead, S.; Wilson, J.; Starling, J.; Law, K.; Self, T.; Tabas, L.; Williams, D.; Paul, D. Tricyclic isoxazoles are novel inhibitors of the multidrug resistance protein (MRP1). *Bioorg. Med. Chem. Lett.* **2002**, *12*, 883–886.
- [54] Dantzig, A.; Shepard, R.; Pratt, S.; Tabas, L.; Lander, P.; Ma, L.; Paul, D.; Williams, D.; Peng, S.; Slapak, C.; Godinot, N.; Perry III, W. Evaluation of the binding of the tricyclic isoxazole photoaffinity label LY475776 to multidrug resistance associated protein 1 (MRP1) orthologs and several ATP-binding cassette (ABC) drug transporters. *Biochem. Pharmacol.* **2004**, *67*, 1111–1121.
- [55] Koley, D.; Bard, A. Inhibition of the MRP1-mediated transport of the menadione-glutathione conjugate (thiodione) in HeLa cells as studied by SECM. *Proc. Natl. Acad. Sci. USA* **2012**, *109*, 11522–11527.
- [56] Declèves, X.; Regina, A.; Laplanche, J. L.; Roux, F.; Boval, B.; Launay, J. M.; Scherrmann, J. M. Functional expression of P-glycoprotein and multidrug resistance-associated protein (Mrp1) in primary cultures of rat astrocytes. *J. Neurosci. Res.* **2000**, *60*, 594–601.
- [57] Bakos, E.; Homolya, L. Portrait of multifaceted transporter, the multidrug resistance-associated protein 1 (MRP1/ABCC1). *Pflugers Arch.* **2007**, *453*, 621–641.
- [58] Pick, A.-K. Funktionelle Untersuchungen des ABC-Transporters Breast Cancer Resistance Protein (BCRP). Ph.D. thesis, University of Bonn, **2011**.
- [59] Doyle, L.; Yang, W.; Abruzzo, L.; Krogmann, T.; Gao, Y.; Rishi, A.; Ross, D. A multidrug resistance transporter from human MCF-7 breast cancer cells. *Proc. Natl. Acad. Sci. USA* **1998**, *95*, 15665–15670.

- [60] Staud, F.; Pavek, P. Breast cancer resistance protein (BCRP/ABCG2). *Int. J. Biochem. Cell Biol.* **2005**, *37*, 720–725.
- [61] Wang, H.; Lee, E.; Cai, X.; Ni, Z.; Zhou, L.; Mao, Q. Membrane topology of the human breast cancer resistance protein (BCRP/ABCG2) determined by epitope insertion and immunofluorescence. *Biochemistry* **2008**, *47*, 13778–13787.
- [62] Özvegy, C.; Litman, T.; Szakács, G.; Nagy, Z.; Bates, S.; Váradi, A.; Sarkadi, B. Functional characterization of the human multidrug transporter, ABCG2, expressed in insect cells. *Biochem. Biophys. Res. Commun.* **2001**, *285*, 111–117.
- [63] Xu, J.; Liu, Y.; Yang, Y.; Bates, S.; Zhang, J. Characterization of oligomeric human half-ABC transporter ATP-binding cassette G2. *J. Biol. Chem.* **2004**, *279*, 19781–19789.
- [64] Fetsch, P.; Abati, A.; Litman, T.; Morisaki, K.; Honjo, Y.; Mittal, K.; Bates, S. Localization of the ABCG2 mitoxantrone resistance-associated protein in normal tissues. *Cancer Lett.* **2006**, *235*, 84–92.
- [65] Scharenberg, C.; Harkey, M.; Torok-Storb, B. The ABCG2 transporter is an efficient Hoechst 33342 efflux pump and is preferentially expressed by immature human hematopoietic progenitors. *Blood* **2002**, *99*, 507–512.
- [66] Zhou, S.; Morris, J.; Barnes, Y.; Lan, L.; Schuetz, J.; Sorrentino, B. Bcrp1 gene expression is required for normal numbers of side population stem cells in mice, and confers relative protection to mitoxantrone in hematopoietic cells in vivo. *Proc. Natl. Acad. Sci. USA* **2002**, *99*, 12339–12344.
- [67] Robey, R. W.; To, K. K. K.; Polgar, O.; Dohse, M.; Fetsch, P.; Dean, M.; Bates, S. E. ABCG2: a perspective. *Adv. Drug Deliv. Rev.* **2009**, *61*, 3–13.
- [68] Miyake, K.; Mickley, L.; Litman, T.; Zhan, Z.; Robey, R.; Cristensen, B.; Brangi, M.; Greenberger, L.; Dean, M.; Fojo, T.; Bates, S. Molecular Cloning of cDNAs Which Are Highly Overexpressed in Mitoxantrone-resistant Cells Demonstration of Homology to ABC Transport Genes. *Cancer Res.* **1999**, *59*, 8–13.

- [69] Ross, D.; Yang, W.; Abruzzo, L.; Dalton, W.; Schneider, E.; Lage, H.; Dietel, M.; Greenberger, L.; Cole, S.; Doyle, L. Atypical multidrug resistance: breast cancer resistance protein messenger RNA expression in mitoxantrone-selected cell lines. *J. Natl. Cancer Inst.* **1999**, *91*, 429–433.
- [70] Maliepaard, M.; van Gastelen, M. A.; de Jong, L. A.; Pluim, D.; van Waardenburg, R. C.; Ruevekamp-Helmers, M. C.; Floot, B. G.; Schellens, J. H. Overexpression of the BCRP/MXR/ABCP gene in a topotecan-selected ovarian tumor cell line. *Cancer Res.* **1999**, *59*, 4559–4563.
- [71] Yang, C.; Schneider, E.; Kuo, M.; Volk, E.; Rocchi, E.; Chen, Y. BCRP/MXR/ABCP expression in topotecan-resistant human breast carcinoma cells. *Biochem. Pharmacol.* **2000**, *60*, 831–837.
- [72] Diestra, J.; Scheffer, G.; Catala, I.; Maliepaard, M.; Schellens, J.; Scheper, R.; Germà-Lluch, J.; Izquierdo, M. Frequent expression of the multi-drug resistance-associated protein BCRP/MXR/ABCP/ABCG2 in human tumours detected by the BXP-21 monoclonal antibody in paraffin-embedded material. *J. Pathol.* **2002**, *198*, 213–219.
- [73] Krishnamurthy, P.; Ross, D.; Nakanishi, T.; Bailey-Dell, K.; Zhou, S.; Mercer, K.; Sarkadi, B.; Sorrentino, B.; Schuetz, J. The stem cell marker Bcrp/ABCG2 enhances hypoxic cell survival through interactions with heme. *J. Biol. Chem.* **2004**, *279*, 24218–24225.
- [74] Rajagopal, A.; Simon, S. Subcellular localization and activity of multidrug resistance proteins. *Mol. Biol. Cell* **2003**, *14*, 3389–3399.
- [75] Robey, R.; Honjo, Y.; Morisaki, K.; Nadjem, T.; Runge, S.; Risbood, M.; Poruchynsky, M.; Bates, S. Mutations at amino-acid 482 in the ABCG2 gene affect substrate and antagonist specificity. *Br. J. Cancer* **2003**, *89*, 1971–1978.
- [76] Rabindran, S.; Ross, D.; Doyle, L.; Yang, W.; Greenberger, L. Fumitremorgin C reverses multidrug resistance in cells transfected with the breast cancer resistance protein. *Cancer Res.* **2000**, *60*, 47–50.
- [77] Hazlehurst, L.; Foley, N.; Gleason-Guzman, M.; Hacker, M.; Cress, A.; Greenberger, L.; De Jong, M.; Dalton, W. Multiple mechanisms confer drug resistance

- to mitoxantrone in the human 8226 myeloma cell line. *Cancer Res.* **1999**, *59*, 1021–1028.
- [78] Litman, T.; Brangi, M.; Hudson, E.; Fetsch, P.; Abati, A.; Ross, D.; Miyake, K.; Resau, J.; Bates, S. The multidrug-resistant phenotype associated with overexpression of the new ABC half-transporter, MXR (ABCG2). *J. Cell Sci.* **2000**, *113*, 2011–2021.
- [79] Maliepaard, M.; van Gastelen, M. A.; Tohgo, A.; Hausheer, F. H.; van Waardenburg, R. C.; de Jong, L. A.; Pluim, D.; Beijnen, J. H.; Schellens, J. H. Circumvention of breast cancer resistance protein (BCRP)-mediated resistance to camptothecins in vitro using non-substrate drugs or the BCRP inhibitor GF120918. *Clin. Cancer Res.* **2001**, *7*, 935–941.
- [80] Rabindran, S.; He, H.; Singh, M.; Brown, E.; Collins, K.; Annable, T.; Greenberger, L. Reversal of a novel multidrug resistance mechanism in human colon carcinoma cells by fumitremorgin C. *Cancer Res.* **1998**, *58*, 5850–5858.
- [81] Nakatomi, K.; Yoshikawa, M.; Oka, M.; Ikegami, Y.; Hayasaka, S.; Sano, K.; Shiozawa, K.; Kawabata, S.; Soda, H.; Ishikawa, T.; Tanabe, S.; Kohno, S. Transport of 7-ethyl-10-hydroxycamptothecin (SN-38) by breast cancer resistance protein ABCG2 in human lung cancer cells. *Biochem. Biophys. Res. Commun.* **2001**, *288*, 827–832.
- [82] Rajendra, R.; Gounder, M.; Saleem, A.; Schellens, J.; Ross, D.; Bates, S.; Sinko, P.; Rubin, E. Differential effects of the breast cancer resistance protein on the cellular accumulation and cytotoxicity of 9-aminocamptothecin and 9-nitrocamptothecin. *Cancer Res.* **2003**, *63*, 3228–3233.
- [83] Sparreboom, A.; Gelderblom, H.; Marsh, S.; Ahluwalia, R.; Obach, R.; Principe, P.; Twelves, C.; Verweij, J.; McLeod, H. Diflomotecan pharmacokinetics in relation to ABCG2 421C>A genotype. *Clin. Pharmacol. Ther.* **2004**, *76*, 38–44.
- [84] Allen, J.; Brinkhuis, R.; Wijnholds, J.; Schinkel, A. The Mouse Bcrp1/Mxr/Abcp Gene Amplification and Overexpression in Cell Lines Selected for Resistance to Topotecan, Mitoxantrone, or Doxorubicin. *Cancer Res.* **1999**, *59*, 4237–4241.

- [85] Honjo, Y.; Hrycyna, C. A.; Yan, Q. W.; Medina-Pérez, W. Y.; Robey, R. W.; van de Laar, A.; Litman, T.; Dean, M.; Bates, S. E. Acquired mutations in the MXR/BCRP/ABCP gene alter substrate specificity in MXR/BCRP/ABCP-overexpressing cells. *Cancer Res.* **2001**, *61*, 6635–6639.
- [86] Sargent, J.; Williamson, C.; Maliepaard, M.; Elgie, A.; Scheper, R.; Taylor, C. Breast cancer resistance protein expression and resistance to daunorubicin in blast cells from patients with acute myeloid leukaemia. *Br. J. Haematol.* **2001**, *115*, 257–262.
- [87] Volk, E. L.; Schneider, E. Wild-type breast cancer resistance protein (BCRP/ABCG2) is a methotrexate polyglutamate transporter. *Cancer Res.* **2003**, *63*, 5538–5543.
- [88] Chen, Z.-S.; Robey, R. W.; Belinsky, M. G.; Shchaveleva, I.; Ren, X.-Q.; Sugimoto, Y.; Ross, D. D.; Bates, S. E.; Kruh, G. D. Transport of methotrexate, methotrexate polyglutamates, and 17beta-estradiol 17-(beta-D-glucuronide) by ABCG2: effects of acquired mutations at R482 on methotrexate transport. *Cancer Res.* **2003**, *63*, 4048–4054.
- [89] Wang, X.; Baba, M. The role of breast cancer resistance protein (BCRP/ABCG2) in cellular resistance to HIV-1 nucleoside reverse transcriptase inhibitors. *Antivir. Chem. Chemother.* **2005**, *16*, 213–216.
- [90] Wang, X.; Furukawa, T.; Nitanda, T.; Okamoto, M.; Sugimoto, Y.; Akiyama, S.-I.; Baba, M. Breast cancer resistance protein (BCRP/ABCG2) induces cellular resistance to HIV-1 nucleoside reverse transcriptase inhibitors. *Mol. Pharmacol.* **2003**, *63*, 65–72.
- [91] Robey, R. W.; Medina-Pérez, W. Y.; Nishiyama, K.; Lahusen, T.; Miyake, K.; Litman, T.; Senderowicz, A. M.; Ross, D. D.; Bates, S. E. Overexpression of the ATP-binding cassette half-transporter, ABCG2 (Mxr/BCrp/ABCP1), in flavopiridol-resistant human breast cancer cells. *Clin. Cancer Res.* **2001**, *7*, 145–152.
- [92] Zhou, L.; Schmidt, K.; Nelson, F. R.; Zelesky, V.; Troutman, M. D.; Feng, B. The effect of breast cancer resistance protein and P-glycoprotein on the brain

- penetration of flavopiridol, imatinib mesylate (Gleevec), prazosin, and 2-methoxy-3-(4-(2-(5-methyl-2-phenyloxazol-4-yl)ethoxy)phenyl)propanoic acid (PF-407288) in mice. *Drug Metab. Dispos.* **2009**, *37*, 946–955.
- [93] Burger, H.; van Tol, H.; Boersma, A.; Brok, M.; Wiemer, E.; Stoter, G.; Nooter, K. Imatinib mesylate (STI571) is a substrate for the breast cancer resistance protein (BCRP)/ABCG2 drug pump. *Blood* **2004**, *104*, 2940–2942.
- [94] Breedveld, P.; Zelcer, N.; Pluim, D.; Sönmezer, O.; Tibben, M. M.; Beijnen, J. H.; Schinkel, A. H.; van Tellinghen, O.; Borst, P.; Schellens, J. H. M. Mechanism of the pharmacokinetic interaction between methotrexate and benzimidazoles: potential role for breast cancer resistance protein in clinical drug-drug interactions. *Cancer Res.* **2004**, *64*, 5804–5811.
- [95] Nakagawa, R.; Hara, Y.; Arakawa, H.; Nishimura, S.; Komatani, H. ABCG2 confers resistance to indolocarbazole compounds by ATP-dependent transport. *Biochem. Biophys. Res. Commun.* **2002**, *299*, 669–675.
- [96] Haslam, I. S.; Wright, J. A.; O'Reilly, D. A.; Sherlock, D. J.; Coleman, T.; Simmons, N. L. Intestinal ciprofloxacin efflux: the role of breast cancer resistance protein (ABCG2). *Drug Metab. Dispos.* **2011**, *39*, 2321–2328.
- [97] Lin, X.; Skolnik, S.; Chen, X.; Wang, J. Attenuation of intestinal absorption by major efflux transporters: quantitative tools and strategies using a Caco-2 model. *Drug Metab. Dispos.* **2011**, *39*, 265–274.
- [98] Bachmeier, C.; Trickler, W.; Miller, D. Drug efflux transport properties of 2 , 7 -Bis (2-carboxyethyl)-5 (6)-carboxyfluorescein acetoxymethyl ester (BCECF-AM) and its fluorescent free acid, BCECF. *J. Pharm. Sci.* **2004**, *93*, 932–942.
- [99] Nezasa, K.; Tian, X.; Zamek-Gliszczynski, M.; Patel, N.; Raub, T.; Brouwer, K. Altered hepatobiliary disposition of 5 (and 6)-carboxy-2 , 7 -dichlorofluorescein in Abcg2 (Bcrp1) and Abcc2 (Mrp2) knockout mice. *Drug Metab. Dispos.* **2006**, *34*, 718–723.
- [100] Ebert, B.; Seidel, A.; Lampen, A. Identification of BCRP as transporter of benzo [a] pyrene conjugates metabolically formed in Caco-2 cells and its induction by Ah-receptor agonists. *Carcinogenesis* **2005**, *26*, 1754–1763.

- [101] Imai, Y.; Asada, S.; Tsukahara, S.; Ishikawa, E.; Tsuruo, T.; Sugimoto, Y. Breast cancer resistance protein exports sulfated estrogens but not free estrogens. *Mol. Pharmacol.* **2003**, *64*, 610–618.
- [102] Suzuki, M.; Suzuki, H.; Sugimoto, Y.; Sugiyama, Y. ABCG2 transports sulfated conjugates of steroids and xenobiotics. *J. Biol. Chem.* **2003**, *278*, 22644–22649.
- [103] Lee, Y.; Kusuhashi, H.; Jonker, J.; Schinkel, A.; Sugiyama, Y. Investigation of efflux transport of dehydroepiandrosterone sulfate and mitoxantrone at the mouse blood-brain barrier: a minor role of breast cancer resistance protein. *J. Pharmacol. Exp. Ther.* **2005**, *312*, 44–52.
- [104] Robey, R. W.; Steadman, K.; Polgar, O.; Morisaki, K.; Blayney, M.; Mistry, P.; Bates, S. E. Pheophorbide a is a specific probe for ABCG2 function and inhibition. *Cancer Res.* **2004**, *64*, 1242–1246.
- [105] Jonker, J.; Buitelaar, M.; Wagenaar, E.; Van Der Valk, M.; Scheffer, G.; Scheper, R.; Plösch, T.; Kuipers, F.; Elferink, R.; Rosing, H.; Beijnen, J.; Schinkel, A. The breast cancer resistance protein protects against a major chlorophyll-derived dietary phototoxin and protoporphyria. *Proc. Natl. Acad. Sci. USA* **2002**, *99*, 15649–15654.
- [106] Robey, R.; Fetsch, P.; Polgar, O.; Dean, M.; Bates, S. The livestock photosensitizer, phytoporphyrin (phylloerythrin), is a substrate of the ATP-binding cassette transporter ABCG2. *Res. Vet. Sci.* **2006**, *81*, 345–349.
- [107] Robey, R.; Steadman, K.; Polgar, O.; Bates, S. ABCG2-mediated transport of photosensitizers: potential impact on photodynamic therapy. *Cancer Biol. Ther.* **2005**, *4*, 187–194.
- [108] Mao, Q. Role of the breast cancer resistance protein (ABCG2) in drug transport. *AAPS J.* **2005**, *7*, 118–133.
- [109] Volk, E. L.; Farley, K. M.; Wu, Y.; Li, F.; Robey, R. W.; Schneider, E. Overexpression of wild-type breast cancer resistance protein mediates methotrexate resistance. *Cancer Res.* **2002**, *62*, 5035–5040.
- [110] de Bruin, M.; Miyake, K.; Litman, T.; Robey, R.; Bates, S. Reversal of resistance by GF120918 in cell lines expressing the ABC half-transporter, MXR. *Cancer Lett.* **1999**, *146*, 117–126.

- [111] Shiozawa, K.; Oka, M.; Soda, H.; Yoshikawa, M.; Ikegami, Y.; Tsurutani, J.; Nakatomi, K.; Nakamura, Y.; Doi, S.; Kitazaki, T.; Mizuta, Y.; Murase, K.; Yoshida, H.; Ross, D. D.; Kohno, S. Reversal of breast cancer resistance protein (BCRP/ABCG2)-mediated drug resistance by novobiocin, a coumermycin antibiotic. *Int. J. Cancer* **2004**, *108*, 146–151.
- [112] van Loevezijn, A.; Allen, J. D.; Schinkel, A. H.; Koomen, G. J. Inhibition of BCRP-mediated drug efflux by fumitremorgin-type indolyl diketopiperazines. *Bioorg. Med. Chem. Lett.* **2001**, *11*, 29–32.
- [113] Allen, J. D.; van Loevezijn, A.; Lakhai, J. M.; van der Valk, M.; van Tellingen, O.; Reid, G.; Schellens, J. H. M.; Koomen, G.-J.; Schinkel, A. H. Potent and specific inhibition of the breast cancer resistance protein multidrug transporter in vitro and in mouse intestine by a novel analogue of fumitremorgin C. *Mol. Cancer Ther.* **2002**, *1*, 417–425.
- [114] Erlichman, C.; Boerner, S. A.; Hallgren, C. G.; Spieker, R.; Wang, X. Y.; James, C. D.; Scheffer, G. L.; Maliepaard, M.; Ross, D. D.; Bible, K. C.; Kaufmann, S. H. The HER tyrosine kinase inhibitor CI1033 enhances cytotoxicity of 7-ethyl-10-hydroxycamptothecin and topotecan by inhibiting breast cancer resistance protein-mediated drug efflux. *Cancer Res.* **2001**, *61*, 739–748.
- [115] Houghton, P. J.; Germain, G. S.; Harwood, F. C.; Schuetz, J. D.; Stewart, C. F.; Buchdunger, E.; Traxler, P. Imatinib mesylate is a potent inhibitor of the ABCG2 (BCRP) transporter and reverses resistance to topotecan and SN-38 in vitro. *Cancer Res.* **2004**, *64*, 2333–2337.
- [116] Ozvegy-Laczka, C.; Hegedus, T.; Várady, G.; Ujhelly, O.; Schuetz, J. D.; Váradi, A.; Kéri, G.; Orfi, L.; Német, K.; Sarkadi, B. High-affinity interaction of tyrosine kinase inhibitors with the ABCG2 multidrug transporter. *Mol. Pharmacol.* **2004**, *65*, 1485–1495.
- [117] Pick, A.; Wiese, M. Tyrosine kinase inhibitors influence ABCG2 expression in EGFR-positive MDCK BCRP cells via the PI3K/Akt signaling pathway. *ChemMedChem* **2012**, *7*, 650–662.
- [118] Zhang, S.; Yang, X.; Morris, M. E. Flavonoids are inhibitors of breast cancer resistance protein (ABCG2)-mediated transport. *Mol. Pharmacol.* **2004**, *65*, 1208–1216.

- [119] Ahmed-Belkacem, A.; Pozza, A.; Muñoz-Martínez, F.; Bates, S. E.; Castanys, S.; Gamarro, F.; Di Pietro, A.; Pérez-Victoria, J. M. Flavonoid structure-activity studies identify 6-prenylchrysin and tectochrysin as potent and specific inhibitors of breast cancer resistance protein ABCG2. *Cancer Res.* **2005**, *65*, 4852–4860.
- [120] Hyafil, F.; Vergely, C.; Du Vignaud, P.; Grand-Perret, T. In vitro and in vivo reversal of multidrug resistance by GF120918, an acridonecarboxamide derivative. *Cancer Res.* **1993**, *53*, 4595–4602.
- [121] Furman, W. L.; Navid, F.; Daw, N. C.; McCarville, M. B.; McGregor, L. M.; Spunt, S. L.; Rodriguez-Galindo, C.; Panetta, J. C.; Crews, K. R.; Wu, J.; Gajjar, A. J.; Houghton, P. J.; Santana, V. M.; Stewart, C. F. Tyrosine kinase inhibitor enhances the bioavailability of oral irinotecan in pediatric patients with refractory solid tumors. *J. Clin. Oncol.* **2009**, *27*, 4599–4604.
- [122] Liu, X.-L.; Tee, H.-W.; Go, M.-L. Functionalized chalcones as selective inhibitors of P-glycoprotein and breast cancer resistance protein. *Bioorg. Med. Chem.* **2008**, *16*, 171–180.
- [123] Han, Y.; Riwanto, M.; Go, M.-L.; Ee, P. L. Modulation of breast cancer resistance protein (BCRP/ABCG2) by non-basic chalcone analogues. *Eur. J. Pharm. Sci.* **2008**, *35*, 30–41.
- [124] Zhang, S.; Yang, X.; Morris, M. E. Combined effects of multiple flavonoids on breast cancer resistance protein (ABCG2)-mediated transport. *Pharm. Res.* **2004**, *21*, 1263–1273.
- [125] Pick, A.; Müller, H.; Mayer, R.; Haenisch, B.; Pajeva, I. K.; Weigt, M.; Bönisch, H.; Müller, C. E.; Wiese, M. Structure-activity relationships of flavonoids as inhibitors of breast cancer resistance protein (BCRP). *Bioorg. Med. Chem.* **2011**, *19*, 2090–2102.
- [126] Bansal, T.; Jaggi, M.; Khar, R. K.; Talegaonkar, S. Emerging significance of flavonoids as P-glycoprotein inhibitors in cancer chemotherapy. *J. Pharm. Pharm. Sci.* **2009**, *12*, 46–78.
- [127] Ikegawa, T.; Ohtani, H.; Koyabu, N.; Juichi, M.; Iwase, Y.; Ito, C.; Furukawa, H.; Naito, M.; Tsuruo, T.; Sawada, Y. Inhibition of P-glycoprotein

- by flavonoid derivatives in adriamycin-resistant human myelogenous leukemia (K562/ADM) cells. *Cancer Lett.* **2002**, *177*, 89–93.
- [128] Zhang, S.; Yang, X.; Coburn, R. A.; Morris, M. E. Structure activity relationships and quantitative structure activity relationships for the flavonoid-mediated inhibition of breast cancer resistance protein. *Biochem. Pharmacol.* **2005**, *70*, 627–639.
- [129] Zhang, S.; Wang, X.; Sagawa, K.; Morris, M. E. Flavonoids chrysin and benzoflavone, potent breast cancer resistance protein inhibitors, have no significant effect on topotecan pharmacokinetics in rats or *mdr1a/1b* (-/-) mice. *Drug Metab. Dispos.* **2005**, *33*, 341–348.
- [130] Lemos, C.; Jansen, G.; Peters, G. J. Drug transporters: recent advances concerning BCRP and tyrosine kinase inhibitors. *Br. J. Cancer* **2008**, *98*, 857–862.
- [131] Nakamura, Y.; Oka, M.; Soda, H.; Shiozawa, K.; Yoshikawa, M.; Itoh, A.; Ikegami, Y.; Tsurutani, J.; Nakatomi, K.; Kitazaki, T.; Doi, S.; Yoshida, H.; Kohno, S. Gefitinib ("Iressa", ZD1839), an epidermal growth factor receptor tyrosine kinase inhibitor, reverses breast cancer resistance protein/ABCG2-mediated drug resistance. *Cancer Res.* **2005**, *65*, 1541–1546.
- [132] Nagashima, S.; Soda, H.; Oka, M.; Kitazaki, T.; Shiozawa, K.; Nakamura, Y.; Takemura, M.; Yabuuchi, H.; Fukuda, M.; Tsukamoto, K.; Kohno, S. BCRP/ABCG2 levels account for the resistance to topoisomerase I inhibitors and reversal effects by gefitinib in non-small cell lung cancer. *Cancer Chemother. Pharmacol.* **2006**, *58*, 594–600.
- [133] Gupta, D.; Jain, D.; Trivedi, P. Recent advances in chalcones as antiinfective agents. *Int. J. Chem. Sci.* **2010**, *8*, 649–654.
- [134] Tomar, V.; Bhattacharjee, G.; Kamaluddin,; Kumar, A. Synthesis and antimicrobial evaluation of new chalcones containing piperazine or 2,5-dichlorothiophene moiety. *Bioorg. Med. Chem. Lett.* **2007**, *17*, 5321–5324.
- [135] Viana, G.; Bandeira, M.; Matos, F. Analgesic and antiinflammatory effects of chalcones isolated from *Myracrodruon urundeuva* Allemão. *Phytomedicine* **2003**, *10*, 189–195.

- [136] Tuchinda, P.; Reutrakul, V.; Claeson, P.; Pongprayoon, U.; Sematong, T.; Santisuk, T.; Taylor, W. Anti-inflammatory cyclohexenyl chalcone derivatives in *Boesenbergia pandurata*. *Phytochemistry* **2002**, *59*, 169–173.
- [137] Anto, R.; Sukumaran, K.; Kuttan, G.; Rao, M.; Subbaraju, V.; Kuttan, R. Anticancer and antioxidant activity of synthetic chalcones and related compounds. *Cancer Lett.* **1995**, *97*, 33–37.
- [138] Miranda, C.; Stevens, J.; Ivanov, V.; McCall, M.; Frei, B.; Deinzer, M.; Buhler, D. Antioxidant and prooxidant actions of prenylated and nonprenylated chalcones and flavanones in vitro. *J. Agric. Food Chem.* **2000**, *48*, 3876–3884.
- [139] Sivakumar, P.; Seenivasan, S.; Kumar, V.; Doble, M. Synthesis, antimycobacterial activity evaluation, and QSAR studies of chalcone derivatives. *Bioorg. Med. Chem. Lett.* **2007**, *17*, 1695–1700.
- [140] Li, R.; Chen, X.; Gong, B.; Dominguez, J.; Davidson, E.; Kurzban, G.; Miller, R.; Nuzum, E.; Rosenthal, P. In vitro antimalarial activity of chalcones and their derivatives. *J. Med. Chem.* **1995**, *38*, 5031–5037.
- [141] Liu, M.; Wilairat, P.; Croft, S.; Tan, A.; Go, M. Structure–activity relationships of antileishmanial and antimalarial chalcones. *Bioorg. Med. Chem.* **2003**, *11*, 2729–2738.
- [142] Modzelewska, A.; Pettit, C.; Achanta, G.; Davidson, N.; Huang, P.; Khan, S. Anticancer activities of novel chalcone and bis-chalcone derivatives. *Bioorg. Med. Chem.* **2006**, *14*, 3491–3495.
- [143] Lawrence, N.; Patterson, R.; Ooi, L.; Cook, D.; Ducki, S. Effects of α -substitutions on structure and biological activity of anticancer chalcones. *Bioorg. Med. Chem. Lett.* **2006**, *16*, 5844–5848.
- [144] Bandgar, B.; Gawande, S.; Bodade, R.; Totre, J.; Khobragade, C. Synthesis and biological evaluation of simple methoxylated chalcones as anticancer, anti-inflammatory and antioxidant agents. *Bioorg. Med. Chem.* **2010**, *18*, 1364–1370.
- [145] Shibata, S. Anti-tumorigenic chalcones. *Stem Cells* **1996**, *12*, 44–52.

- [146] Kumar, S.; Hager, E.; Pettit, C.; Gurulingappa, H.; Davidson, N.; Khan, S. Design, synthesis, and evaluation of novel boronic-chalcone derivatives as antitumor agents. *J. Med. Chem.* **2003**, *46*, 2813–2815.
- [147] Lahtchev, K.; Batovska, D.; Parushev, S.; Ubiyvovk, V.; Sibirny, A. Antifungal activity of chalcones: A mechanistic study using various yeast strains. *Eur. J. Med. Chem.* **2008**, *43*, 2220–2228.
- [148] López, S.; Castelli, M.; Zacchino, S.; Dominguez, J.; Lobo, G.; Charris-Charris, J.; Cortés, J.; Ribas, J.; Devia, C.; Rodríguez, A.; Enriz, R. In vitro antifungal evaluation and structure–activity relationships of a new series of chalcone derivatives and synthetic analogues, with inhibitory properties against polymers of the fungal cell wall. *Bioorg. Med. Chem.* **2001**, *9*, 1999–2013.
- [149] Bois, F.; Beney, C.; Boumendjel, A.; Mariotte, A. M.; Conseil, G.; Di Pietro, A. Halogenated chalcones with high-affinity binding to P-glycoprotein: potential modulators of multidrug resistance. *J. Med. Chem.* **1998**, *41*, 4161–4164.
- [150] Bois, F.; Boumendjel, A.; Mariotte, A.; Conseil, G.; Di Pietro, A. Synthesis and biological activity of 4-alkoxy chalcones: potential hydrophobic modulators of P-glycoprotein-mediated multidrug resistance. *Bioorg. Med. Chem.* **1999**, *7*, 2691–2695.
- [151] Han, Y.; Riwanto, M.; Go, M.; EE, P. Modulation of breast cancer resistance protein (BCRP/ABCG2) by non-basic chalcone analogues. *Eur. J. Pharm. Sci.* **2008**, *35*, 30–41.
- [152] Boumendjel, A.; McLeer-Florin, A.; Champelovier, P.; Allegro, D.; Muhammad, D.; Souard, F.; Derouazi, M.; Peyrot, V.; Toussaint, B.; Boutonnat, J. A novel chalcone derivative which acts as a microtubule depolymerising agent and an inhibitor of P-gp and BCRP in in-vitro and in-vivo glioblastoma models. *BMC Cancer* **2009**, *9*, 242.
- [153] Claisen, L.; Claparede, A. Condensationen von ketonen mit aldehyden. *Chem. Ber.* **1881**, *14*, 2460–2468.
- [154] Schmidt, J. Ueber die Einwirkung von Aceton auf Furfurol und auf Bittermandelöl bei Gegenwart von Alkalilauge. *Berichte der deutschen chemischen Gesellschaft* **2006**, *14*, 1459–1461.

- [155] Klinkhammer, W. Design, Synthese und 3D-QSAR neuartiger P-gp-Modulatoren. Ph.D. thesis, University of Bonn, **2006**.
- [156] Martin, C.; Berridge, G.; Higgins, C. F.; Mistry, P.; Charlton, P.; Callaghan, R. Communication between multiple drug binding sites on P-glycoprotein. *Mol. Pharmacol.* **2000**, *58*, 624–632.
- [157] Essodaigui, M.; Broxterman, H. J.; Garnier-Suillerot, A. Kinetic analysis of calcein and calcein-acetoxymethylester efflux mediated by the multidrug resistance protein and P-glycoprotein. *Biochemistry* **1998**, *37*, 2243–2250.
- [158] Legrand, O.; Simonin, G.; Perrot, J.; Zittoun, R.; Marie, J. Pgp and MRP activities using calcein-AM are prognostic factors in adult acute myeloid leukemia patients. *Blood* **1998**, *91*, 4480–4488.
- [159] Qadir, M.; O’Loughlin, K. L.; Fricke, S. M.; Williamson, N. A.; Greco, W. R.; Minderman, H.; Baer, M. R. Cyclosporin A is a broad-spectrum multidrug resistance modulator. *Clin. Cancer Res.* **2005**, *11*, 2320–2326.
- [160] Stoclet, J.-C.; Schini-Kerth, V. Dietary flavonoids and human health. *Ann. Pharm. Fr.* **2011**, *69*, 78–90.
- [161] Erdman, J. W., Jr; Balentine, D.; Arab, L.; Beecher, G.; Dwyer, J. T.; Folts, J.; Harnly, J.; Hollman, P.; Keen, C. L.; Mazza, G.; Messina, M.; Scalbert, A.; Vita, J.; Williamson, G.; Burrowes, J. Flavonoids and heart health: proceedings of the ILSI North America Flavonoids Workshop, May 31-June 1, 2005, Washington, DC. *J. Nutr.* **2007**, *137*, 718S–737S.
- [162] Carratù, B.; Sanzini, E. Biologically-active phytochemicals in vegetable food. *Ann. Ist. Super. Sanita* **2005**, *41*, 7–16.
- [163] Steinberg, F. M.; Bearden, M. M.; Keen, C. L. Cocoa and chocolate flavonoids: implications for cardiovascular health. *J. Am. Diet. Assoc.* **2003**, *103*, 215–223.
- [164] Hollman, P. C.; Katan, M. B. Health effects and bioavailability of dietary flavonols. *Free Radic. Res.* **1999**, *31 Suppl*, S75–S80.
- [165] Hollman, P. C.; Katan, M. B. Dietary flavonoids: intake, health effects and bioavailability. *Food Chem. Toxicol.* **1999**, *37*, 937–942.

- [166] Böhm, H.; Boeing, H.; Hempel, J.; Raab, B.; Kroke, A. Flavonols, flavone and anthocyanins as natural antioxidants of food and their possible role in the prevention of chronic diseases. *Z. Ernährungswiss.* **1998**, *37*, 147–163.
- [167] Hollman, P. C.; Katan, M. B. Bioavailability and health effects of dietary flavonols in man. *Arch. Toxicol. Suppl.* **1998**, *20*, 237–248.
- [168] Chan, S.; Chang, Y.; Wang, J.; Chen, S.; Kuo, S. Three new flavonoids and antiallergic, anti-inflammatory constituents from the heartwood of *Dalbergia odorifera*. *Planta Med.* **1998**, *64*, 153–158.
- [169] Ramos, S. Effects of dietary flavonoids on apoptotic pathways related to cancer chemoprevention. *J. Nutr. Biochem.* **2007**, *18*, 427–442.
- [170] Butterweck, V.; Jürgenliemk, G.; Nahrstedt, A.; Winterhoff, H. Flavonoids from *Hypericum perforatum* show antidepressant activity in the forced swimming test. *Planta Med.* **2000**, *66*, 3–6.
- [171] Nöldner, M.; Schötz, K. Rutin is essential for the antidepressant activity of *Hypericum perforatum* extracts in the forced swimming test. *Planta Med.* **2002**, *68*, 577–580.
- [172] Kawai, M.; Hirano, T.; Higa, S.; Arimitsu, J.; Maruta, M.; Kuwahara, Y.; Ohkawara, T.; Hagihara, K.; Yamadori, T.; Shima, Y.; Ogata, A.; Kawase, I.; Tanaka, T. Flavonoids and related compounds as anti-allergic substances. *Allergol. Int.* **2007**, *56*, 113–123.
- [173] Wu, Y.; Wang, F.; Zheng, Q.; Lu, L.; Yao, H.; Zhou, C.; Wu, X.; Zhao, Y. Hepatoprotective effect of total flavonoids from *Laggera alata* against carbon tetrachloride-induced injury in primary cultured neonatal rat hepatocytes and in rats with hepatic damage. *J. Biomed. Sci.* **2006**, *13*, 569–578.
- [174] Kinjo, J.; Hitoshi, M.; Tsuchihashi, R.; Korematsu, Y.; Miyakoshi, M.; Murakami, T.; Niiho, D.; Mizutani, K.; Tanaka, T.; Nonaka, G.; Toshihiro, N.; Masafumi, O.; Hikaru, O. Hepatoprotective constituents in plants 15: protective effects of natural-occurring flavonoids and miscellaneous phenolic compounds as determined in an HepG2 cell cytotoxicity assay. *J. Nat. Med.* **2006**, *60*, 36–41.

- [175] Scambia, G.; Ranelletti, F. O.; Panici, P. B.; De Vincenzo, R.; Bonanno, G.; Ferrandina, G.; Piantelli, M.; Bussa, S.; Rumi, C.; Cianfriglia, M. Quercetin potentiates the effect of adriamycin in a multidrug-resistant MCF-7 human breast-cancer cell line: P-glycoprotein as a possible target. *Cancer Chemother. Pharmacol.* **1994**, *34*, 459–464.
- [176] Shapiro, A. B.; Ling, V. Effect of quercetin on Hoechst 33342 transport by purified and reconstituted P-glycoprotein. *Biochem. Pharmacol.* **1997**, *53*, 587–596.
- [177] Ferté, J.; Kühnel, J. M.; Chapuis, G.; Rolland, Y.; Lewin, G.; Schwaller, M. A. Flavonoid-related modulators of multidrug resistance: synthesis, pharmacological activity, and structure-activity relationships. *J. Med. Chem.* **1999**, *42*, 478–489.
- [178] Choi, C.-H.; Sun, K.-H.; An, C.-S.; Yoo, J.-C.; Hahm, K.-S.; Lee, I.-H.; Sohng, J.-K.; Kim, Y.-C. Reversal of P-glycoprotein-mediated multidrug resistance by 5, 6, 7, 3', 4'-pentamethoxyflavone (Sinensetin). *Biochem. Biophys. Res. Commun.* **2002**, *295*, 832–840.
- [179] Zhang, S.; Morris, M. E. Effects of the flavonoids biochanin A, morin, phloretin, and silymarin on P-glycoprotein-mediated transport. *J. Pharmacol. Exp. Ther.* **2003**, *304*, 1258–1267.
- [180] Kitagawa, S.; Nabekura, T.; Takahashi, T.; Nakamura, Y.; Sakamoto, H.; Tano, H.; Hirai, M.; Tsukahara, G. Structure-activity relationships of the inhibitory effects of flavonoids on P-glycoprotein-mediated transport in KB-C2 cells. *Biol. Pharm. Bull.* **2005**, *28*, 2274–2278.
- [181] Chan, K.-F.; Zhao, Y.; Burkett, B. A.; Wong, I. L. K.; Chow, L. M. C.; Chan, T. H. Flavonoid dimers as bivalent modulators for P-glycoprotein-based multidrug resistance: synthetic apigenin homodimers linked with defined-length poly(ethylene glycol) spacers increase drug retention and enhance chemosensitivity in resistant cancer cells. *J. Med. Chem.* **2006**, *49*, 6742–6759.
- [182] Wong, I. L. K.; Chan, K.-F.; Tsang, K. H.; Lam, C. Y.; Zhao, Y.; Chan, T. H.; Chow, L. M. C. Modulation of multidrug resistance protein 1 (MRP1/ABCC1)-mediated multidrug resistance by bivalent apigenin homodimers and their derivatives. *J. Med. Chem.* **2009**, *52*, 5311–5322.

- [183] Imai, Y.; Tsukahara, S.; Asada, S.; Sugimoto, Y. Phytoestrogens/flavonoids reverse breast cancer resistance protein/ABCG2-mediated multidrug resistance. *Cancer Res.* **2004**, *64*, 4346–4352.
- [184] Bennett, M.; Burke, A. J.; Ivo O’Sullivan, W. Aspects of the Algar-Flynn-Oyamada (AFO) reaction. *Tetrahedron* **1996**, *52*, 7163–7178.
- [185] Cummins, B.; Donnelly, D.; Eades, J.; Fletcher, H.; Cinnéide, F.; Philbin, E.; Swirski, J.; Wheeler, T.; Wilson, R. Oxidation of chalcones (AFO reaction). *Tetrahedron* **1963**, *19*, 499–512.
- [186] Gormley, T.; Osullivan, W. Flavanoid epoxides- XIII: Acid and base catalysed reactions of 2 -tosyloxychalcone epoxides. Mechanism of the algar-flynn-oyamada reaction. *Tetrahedron* **1973**, *29*, 369–373.
- [187] Stefan, K. Untersuchung von Chalkonen und Flavonoiden als BCRP-Inhibitoren. Master thesis, University of Bonn, **2011**.
- [188] Katayama, K.; Masuyama, K.; Yoshioka, S.; Hasegawa, H.; Mitsuhashi, J.; Sugimoto, Y. Flavonoids inhibit breast cancer resistance protein-mediated drug resistance: transporter specificity and structure-activity relationship. *Cancer Chemother. Pharmacol.* **2007**, *60*, 789–797.
- [189] Gabriel, S. Ueber das Chinazolin. *Chem. Ber.* **1903**, *36*, 800–813.
- [190] Abdel-Alim, A.-A. M.; El-Shorbagi, A.-N. A.; El-Gendy, M. A.; El-Shareif, H. A. Quinazolinone Derivatives of Biological Interest V. Novel 4 (3H)-Quinazolinones with Sedative-Hypnotic, Anticonvulsant and Antiinflammatory Activities. *Collect. Czech. Chem. Commun.* **1993**, *58*, 1963–1968.
- [191] Alagarsamy, V.; Salomon, V. R.; Vanikavitha, G.; Paluchamy, V.; Chandran, M. R.; Sujin, A. A.; Thangathiruppathy, A.; Amuthalakshmi, S.; Revathi, R. Synthesis, analgesic, anti-inflammatory and antibacterial activities of some novel 2-phenyl-3-substituted quinazolin-4 (3H) ones. *Biol. Pharm. Bull.* **2002**, *25*, 1432–1435.
- [192] Mikhalev, A.; Kon’shin, M.; Ovodenko, L.; Zaks, A. Synthesis, anti-inflammatory and analgesic activity of pyrido [2, 1-b] quinazoline derivatives. *Pharm. Chem. J.* **1995**, *29*, 124–126.

- [193] Iino, T.; Sasaki, Y.; Bamba, M.; Mitsuya, M.; Ohno, A.; Kamata, K.; Hosaka, H.; Maruki, H.; Futamura, M.; Nagata, Y.; Eiki, J.; Nishimura, T. Discovery and structure–activity relationships of a novel class of quinazoline glucokinase activators. *Bioorg. Med. Chem. Lett.* **2009**, *19*, 5531–5538.
- [194] Jatav, V.; Mishra, P.; Kashaw, S.; Stables, J. CNS depressant and anticonvulsant activities of some novel 3-[5-substituted 1, 3, 4-thiadiazole-2-yl]-2-styryl quinazoline-4 (3 H)-ones. *Eur. J. Med. Chem.* **2008**, *43*, 1945–1954.
- [195] Micale, N.; Postorino, G.; Grasso, S.; Zappalà, M.; Zuccala, G.; Ferreri, G.; De Sarro, G. Synthesis of Novel 3-(Alkylcarbamoyl)-2-aryl-1, 2-dihydro-6, 7-(methylenedioxy)-3H-quinazolin-4-ones as Anticonvulsant Agents. *Chem. Biodivers.* **2006**, *3*, 304–311.
- [196] Lemahieu, R. A. Quinazoline derivatives, process and intermediates for their preparation, medicaments containing them and their pharmaceutical use. 1981; EP Patent 0,027,268.
- [197] Kohno, S.; Murata, T.; Kinoshita, T.; Ohata, K. Effects of the new antiallergic drug 11-oxo-11H-pyrido [2, 1-b] quinazoline-2-carboxylic acid on type I allergic reactions. *Arzneim. Forsch.* **1986**, *36*, 1619–1627.
- [198] Guan, J.; Zhang, Q.; O’Neil, M.; Obaldia, N.; Ager, A.; Gerena, L.; Lin, A. J. Antimalarial activities of new pyrrolo [3, 2-f] quinazoline-1, 3-diamine derivatives. *Antimicrob. Agents Chemother.* **2005**, *49*, 4928–4933.
- [199] Thompson, P. E.; Bayles, A.; Olszewski, B. Antimalarial activity of 2, 4-diamino-6-[(3, 4-dichlorobenzyl) nitros-amino] quinazoline (CI-679 base) and CI-679 acetate. Laboratory studies in mice and rhesus monkeys. *Am. J. Trop. Med. Hyg.* **1970**, *19*, 12–26.
- [200] Shibata, S.; Satake, N.; Suh, T. K.; Ishida, Y.; Ueda, S.; Follmer, C.; Flores, F. Potent α -adrenoceptor blocking action of SGB-1534, a new quinazoline antihypertensive agent In vitro experiments. *Gen. Pharmacol. Vasc. Syst.* **1986**, *17*, 143–149.
- [201] Loev, B.; Jen, T.; McLean, R. A novel antihypertensive agent: 1, 2, 3, 5-tetrahydroimidazo [2, 1-b] quinazoline. *Cell. Mol. Life Sci.* **1971**, *27*, 875–875.

- [202] Jones, T. R.; Jackman, A. L.; Newell, D. R. Anti-cancer quinazoline derivatives. 1993; EP Patent 0,204,529.
- [203] El-Azab, A. S.; Al-Omar, M. A.; Abdel-Aziz, A. A.-M.; Abdel-Aziz, N. I.; El-Sayed, M. A.-A.; Aleisa, A. M.; Sayed-Ahmed, M. M.; Abdel-Hamide, S. G. Design, synthesis and biological evaluation of novel quinazoline derivatives as potential antitumor agents: Molecular docking study. *Eur. J. Med. Chem.* **2010**, *45*, 4188–4198.
- [204] Kreighbaum, W. E.; Comer, W. T. Anti-tumor quinazoline compounds. 1982; US Patent 4,343,940.
- [205] Chandrika, P. M.; Yakaiah, T.; Rao, A.; Narsaiah, B.; Reddy, N. C.; Sridhar, V.; Rao, J. V. Synthesis of novel 4, 6-disubstituted quinazoline derivatives, their anti-inflammatory and anti-cancer activity (cytotoxic) against U937 leukemia cell lines. *Eur. J. Med. Chem.* **2008**, *43*, 846–852.
- [206] Qian, L.; Shen, Y.; Chen, J.; Zheng, K. 3D-QSAR Study on a Series of Indolo [1, 2-b] quinazoline Derivatives with Anticancer Activity and their Molecular Design. *Acta. Phys. Chim. Sin.* **2006**, *22*, 1372–1376.
- [207] Ozvegy, C.; Váradi, A.; Sarkadi, B. Characterization of drug transport, ATP hydrolysis, and nucleotide trapping by the human ABCG2 multidrug transporter. Modulation of substrate specificity by a point mutation. *J. Biol. Chem.* **2002**, *277*, 47980–47990.
- [208] Chearwae, W.; Shukla, S.; Limtrakul, P.; Ambudkar, S. V. Modulation of the function of the multidrug resistance-linked ATP-binding cassette transporter ABCG2 by the cancer chemopreventive agent curcumin. *Mol. Cancer Ther.* **2006**, *5*, 1995–2006.
- [209] Polli, J. W.; Olson, K. L.; Chism, J. P.; John-Williams, L. S.; Yeager, R. L.; Woodard, S. M.; Otto, V.; Castellino, S.; Demby, V. E. An unexpected synergist role of P-glycoprotein and breast cancer resistance protein on the central nervous system penetration of the tyrosine kinase inhibitor lapatinib (N-3-chloro-4-[(3-fluorobenzyl)oxy]phenyl-6-[5-([2-(methylsulfonyl)ethyl]aminomethyl)-2-furyl]-4-quinazolinamine; GW572016). *Drug Metab. Dispos.* **2009**, *37*, 439–442.

- [210] Kodaira, H.; Kusuvara, H.; Ushiki, J.; Fuse, E.; Sugiyama, Y. Kinetic analysis of the cooperation of P-glycoprotein (P-gp/Abcb1) and breast cancer resistance protein (Bcrp/Abcg2) in limiting the brain and testis penetration of erlotinib, flavopiridol, and mitoxantrone. *J. Pharmacol. Exp. Ther.* **2010**, *333*, 788–796.
- [211] Deng, W.; Dai, C.-L.; Zhao, X.-q.; Ohnuma, S.; Liang, Y.-j.; Xiao, Z.-J.; Zeng, M.-S.; Ambudkar, S. V.; Fu, L.-w.; Chen, Z.-S. Abstract 5614: Tandutinib (MLN518/CT53518) targeted to stem-like cells by inhibiting the function of ATP-binding cassette subfamily G member 2. *Cancer Res.* **2012**, *72*, 5614–5614.
- [212] Yanase, K.; Tsukahara, S.; Asada, S.; Ishikawa, E.; Imai, Y.; Sugimoto, Y. Gefitinib reverses breast cancer resistance protein-mediated drug resistance. *Mol. Cancer Ther.* **2004**, *3*, 1119–1125.
- [213] Leggas, M.; Panetta, J. C.; Zhuang, Y.; Schuetz, J. D.; Johnston, B.; Bai, F.; Sorrentino, B.; Zhou, S.; Houghton, P. J.; Stewart, C. F. Gefitinib modulates the function of multiple ATP-binding cassette transporters in vivo. *Cancer Res.* **2006**, *66*, 4802–4807.
- [214] Agarwal, S.; Sane, R.; Gallardo, J. L.; Ohlfest, J. R.; Elmquist, W. F. Distribution of gefitinib to the brain is limited by P-glycoprotein (ABCB1) and breast cancer resistance protein (ABCG2)-mediated active efflux. *J. Pharmacol. Exp. Ther.* **2010**, *334*, 147–155.
- [215] Cruz-Lopez, O.; Conejo-García, A.; C Nunez, M.; Kimatrai, M.; E Garcia-Rubino, M.; Morales, F.; Gomez-Perez, V.; M Campos, J. Novel substituted quinazolines for potent EGFR tyrosine kinase inhibitors. *Curr. Med. Chem.* **2011**, *18*, 943–963.
- [216] Rewcastle, G. W.; Denny, W. A.; Bridges, A. J.; Zhou, H.; Cody, D. R.; McMichael, A.; Fry, D. W. Tyrosine kinase inhibitors. 5. Synthesis and structure-activity relationships for 4-[(phenylmethyl) amino]- and 4-(phenylamino) quinazolines as potent adenosine 5'-triphosphate binding site inhibitors of the tyrosine kinase domain of the epidermal growth factor receptor. *J. Med. Chem.* **1995**, *38*, 3482–3487.
- [217] Srivastava, S. K.; Kumar, V.; Agarwal, S. K.; Mukherjee, R.; Burman, A. C. Synthesis of quinazolines as tyrosine kinase inhibitors. *Anticancer Agents Med. Chem.* **2009**, *9*, 246–275.

- [218] Halsall, C. T.; Hennequin, L. F. A.; Plowright, A. T.; Storey, R.; Lennon, K. Quinazoline derivatives as tyrosine kinase inhibitors. 2006; US Patent App. 11/884,923.
- [219] Guo, J.; Zhang, X.; Wang, M.; Jiang, Y. Quinazoline derivatives as tyrosine kinase inhibitors. 2010; EP Patent 2,248,806.
- [220] Arora, A.; Scholar, E. M. Role of tyrosine kinase inhibitors in cancer therapy. *J. Pharmacol. Exp. Ther.* **2005**, *315*, 971–979.
- [221] Thompson, A. M.; Bridges, A. J.; Fry, D. W.; Kraker, A. J.; Denny, W. A. Tyrosine kinase inhibitors. 7. 7-Amino-4-(phenylamino)-and 7-amino-4-[(phenylmethyl) amino] pyrido [4, 3-d] pyrimidines: a new class of inhibitors of the tyrosine kinase activity of the epidermal growth factor receptor. *J. Med. Chem.* **1995**, *38*, 3780–3788.
- [222] Shewchuk, L.; Hassell, A.; Wisely, B.; Rocque, W.; Holmes, W.; Veal, J.; Kuyper, L. F. Binding mode of the 4-anilinoquinazoline class of protein kinase inhibitor: X-ray crystallographic studies of 4-anilinoquinazolines bound to cyclin-dependent kinase 2 and p38 kinase. *J. Med. Chem.* **2000**, *43*, 133–138.
- [223] Rewcastle, G. W.; Murray, D. K.; Elliott, W. L.; Fry, D. W.; Howard, C. T.; Nelson, J. M.; Roberts, B. J.; Vincent, P. W.; Showalter, H. H.; Winters, R. T.; Denny, W. Tyrosine kinase inhibitors. 14. Structure-activity relationships for methyl-amino-substituted derivatives of 4-[(3-bromophenyl) amino]-6-(methylamino)-pyrido [3, 4-d] pyrimidine (PD 158780), a potent and specific inhibitor of the tyrosine kinase activity of receptors for the EGF family of growth factors. *J. Med. Chem.* **1998**, *41*, 742–751.
- [224] Bridges, A. J.; Zhou, H.; Cody, D. R.; Rewcastle, G. W.; McMichael, A.; Showalter, H. H.; Fry, D. W.; Kraker, A. J.; Denny, W. A. Tyrosine kinase inhibitors. 8. An unusually steep structure-activity relationship for analogues of 4-(3-bromoanilino)-6, 7-dimethoxyquinazoline (PD 153035), a potent inhibitor of the epidermal growth factor receptor. *J. Med. Chem.* **1996**, *39*, 267–276.
- [225] Höglund, A. S.; Gray, J. C. Nucleotide sequence of the gene for ribosomal protein S2 in wheat chloroplast DNA. *Nucleic Acids Res.* **1987**, *15*, 10590.

- [226] Kubbies, M. Flow cytometric recognition of elastogen induced chromatin damage in G0/G1 lymphocytes by non-stoichiometric Hoechst fluorochrome binding. *Cytometry* **1990**, *11*, 386–394.
- [227] Crissman, H. A.; Wilder, M. E.; Tobey, R. A. Flow cytometric localization within the cell cycle and isolation of viable cells following exposure to cytotoxic agents. *Cancer Res.* **1988**, *48*, 5742–5746.
- [228] Parish, C. R. Fluorescent dyes for lymphocyte migration and proliferation studies. *Immunol. Cell Biol.* **1999**, *77*, 499–508.
- [229] Portugal, J.; Waring, M. J. Assignment of DNA binding sites for 4',6-diamidino-2-phenylindole and bisbenzimidazole (Hoechst 33258). A comparative footprinting study. *Biochim. Biophys. Acta* **1988**, *949*, 158–168.
- [230] Kim, M.; Turnquist, H.; Jackson, J.; Sgagias, M.; Yan, Y.; Gong, M.; Dean, M.; Sharp, J. G.; Cowan, K. The multidrug resistance transporter ABCG2 (breast cancer resistance protein 1) effluxes Hoechst 33342 and is overexpressed in hematopoietic stem cells. *Clin. Cancer Res.* **2002**, *8*, 22–28.
- [231] Shapiro, A. B.; Corder, A. B.; Ling, V. P-glycoprotein-mediated Hoechst 33342 transport out of the lipid bilayer. *Eur. J. Biochem.* **1997**, *250*, 115–121.
- [232] Müller, H.; Klinkhammer, W.; Globisch, C.; Kassack, M. U.; Pajeva, I. K.; Wiese, M. New functional assay of P-glycoprotein activity using Hoechst 33342. *Bioorg. Med. Chem.* **2007**, *15*, 7470–7479.
- [233] Jonker, J. W.; Buitelaar, M.; Wagenaar, E.; Van Der Valk, M. A.; Scheffer, G. L.; Scheper, R. J.; Plosch, T.; Kuipers, F.; Elferink, R. P. J. O.; Rosing, H.; Beijnen, J. H.; Schinkel, A. H. The breast cancer resistance protein protects against a major chlorophyll-derived dietary phototoxin and protoporphyria. *Proc. Natl. Acad. Sci. USA* **2002**, *99*, 15649–15654.
- [234] Müller, H. Funktionelle Untersuchungen des ABC-Transporters P-Glykoprotein. Ph.D. thesis, University of Bonn, **2007**.
- [235] Pick, A.; Müller, H.; Wiese, M. Structure-activity relationships of new inhibitors of breast cancer resistance protein (ABCG2). *Bioorg. Med. Chem.* **2008**, *16*, 8224–8236.

- [236] Feller, N.; Broxterman, H. J.; Währer, D. C.; Pinedo, H. M. ATP-dependent efflux of calcein by the multidrug resistance protein (MRP): no inhibition by intracellular glutathione depletion. *FEBS Lett.* **1995**, *368*, 385–388.
- [237] Homolya, L.; Holló, Z.; Germann, U. A.; Pastan, I.; Gottesman, M. M.; Sarkadi, B. Fluorescent cellular indicators are extruded by the multidrug resistance protein. *J. Biol. Chem.* **1993**, *268*, 21493–21496.
- [238] Tiberghien, F.; Loor, F. Ranking of P-glycoprotein substrates and inhibitors by a calcein-AM fluorometry screening assay. *Anticancer Drugs* **1996**, *7*, 568–578.
- [239] Mueller, H.; Kassack, M. U.; Wiese, M. Comparison of the usefulness of the MTT, ATP, and calcein assays to predict the potency of cytotoxic agents in various human cancer cell lines. *J. Biomol. Screen.* **2004**, *9*, 506–515.

List of Tables

1.1	Major ABC transporters and their localization in tissues	3
1.2	Substrates and inhibitors of P-gp	6
1.3	Substrates of MRP1	9
1.4	Tissue distribution and physiological role of BCRP	11
1.5	BCRP substrates	12
3.1	Synthesized chalcones and their inhibitory potencies against MCF-7 MX and MDCK BCRP cells in the Hoechst 33342 accumulation assay	29
3.2	Synthesized benzochalcones and their inhibitory potencies against MCF-7 MX and MDCK BCRP cells in the Hoechst 33342 accumulation assay	30
4.1	Synthesized flavones and their inhibitory potencies against MDCK BCRP cells in Hoechst 33342 and pheophorbide A accumulation assays.	49
4.2	Synthesized benzoflavones and their inhibitory potencies against MDCK BCRP cells in Hoechst 33342 and pheophorbide A accumulation assays.	50
4.3	Inhibitory potencies of selected flavonoids using A2780 adr and 2008 MRP1 cells in calcein AM assay.	55
5.1	Synthesized 2-phenyl-4-anilinoquinazolines and their inhibitory po- tencies against MDCK BCRP cells in Hoechst 33342 accumulation assays.	69
5.2	Synthesized 2-(3,4-dimethoxyphenyl)-4-anilinoquinazolines and their inhibitory potencies against MDCK BCRP cells in Hoechst 33342 and pheophorbide A accumulation assays.	71
5.3	Synthesized 4-anilinoquinazolines and their inhibitory potencies against MDCK BCRP cells in Hoechst 33342 and Pheophorbide A accumula- tion assays.	72

5.4	Synthesized 6,7-dimethoxy-4-anilinoquinazolines and their inhibitory potencies against MDCK BCRP cells in Hoechst 33342 and pheophorbide A accumulation assays.	73
5.5	Synthesized 4- <i>N</i> -piperazinylquinazolines and their inhibitory potencies against MDCK BCRP cells in Hoechst 33342 and pheophorbide A accumulation assays.	73
5.6	Synthesized <i>N</i> ² , <i>N</i> ⁴ -disubstituted quinazolines and their inhibitory potencies against MDCK BCRP cells in Hoechst 33342 and pheophorbide A accumulation assays.	74
5.7	Inhibitory potencies of selected quinazolines using A2780 adr and 2008 MRP1 cells in the calcein AM assay.	77
5.8	Inhibitory activity and cytotoxicity of the most potent quinazolines .	79
7.1	Preparation of Krebs-HEPES buffer (KHB)	188
7.2	Preparation of phosphate buffered saline (PBS)	189
7.3	Parameters used for performing the Hoechst 33342 assay	195
7.5	Parameters used for performing the calcein AM assay	200

List of Figures

1.1	Structural features of typical ABC transporters	3
1.2	Topological model of ABCB1 / P-gp	5
1.3	Hydrophobic vacuum cleaner and flippase models for substrate transport by P-gp	5
1.4	Topological model of MRP1	8
1.5	Topology model of BCRP	10
1.6	Selected inhibitors of BCRP	14
2.1	General structures of investigated chalcones and benzochalcones . . .	18
2.2	General structures of investigated flavones and benzoflavones	19
2.3	General structure of quinazoline type BCRP inhibitors and possible modifications	20
3.1	Structure of the chalcone scaffold	21
3.2	Structures of lead chalcones as P-gp and BCRP inhibitors	22
3.3	Mechanism involved in synthesis of the chalcone by Claisen-Schmidt condensation	24
3.4	Structural formula of Hoechst 33342	27
3.5	fluorescence–time curves of Hoechst 33342 in MDCK BCRP cells in presence of Ko143 and concentration–response curve for Ko143	27
3.6	Scatterplot of the pIC ₅₀ values determined in the Hoechst 33342 assay using MCF-7 MX and MDCK BCRP cells	28
3.7	Effect of different substituents on BCRP inhibition by chalcones . . .	32
3.8	Comparison of activities of chalcones and benzochalcones	32
3.9	Conversion of non-fluorescent calcein AM to fluorescent calcein by intracellular esterases	33
3.10	Effect of chalcones and benzochalcones on the accumulation of calcein AM in P-gp and MRP1 overexpressing cells	34

3.11	Effect of chalcone 28 on the GI_{50} of mitoxantrone in MCF-7 MX cells	36
3.12	Dose–response curve of SN-38 in presence of compound 43	36
3.13	Cytotoxicity of chalcones 11 , 28 and benzochalcone 43 in MDCK BCRP and sensitive cells	38
4.1	Basic structure of flavonoids	39
4.2	Subclasses of flavonoids	40
4.3	Structure-activity relationship of flavonoids for BCRP inhibition from published work	41
4.4	Mechanism involved in the synthesis of 3-hydroxyflavones	43
4.5	concentration-response curves of compound 74 and Ko143 obtained in the Hoechst 33342 assay	47
4.6	Structure of pheophorbide A	47
4.7	Concentration-response curve obtained from the fluorescence data for Ko143 using MDCK BCRP cells in the pheophorbide A assay	48
4.8	Scatterplot of pIC_{50} values of flavones and benzoflavones for BCRP inhibition obtained in the Hoechst 33342 assay and the pheophorbide A assay	52
4.9	Effect of different substituents on BCRP inhibitory activity of flavonoids	53
4.10	Effect of flavones and benzoflavones on accumulation of calcein in P-gp overexpressing A2780 adr cells	54
4.11	Effect of flavones and benzoflavones on accumulation of calcein in MRP1 overexpressing 2008 MRP1 cells	54
4.12	Cytotoxicity of selected flavonoids in the MTT assay using MDCK BCRP and sensitive MDCK cells	56
4.13	Shift in dose–response curves of SN-38 and Hoechst 33342 cytotoxicity in presence of compounds 74 and 81	57
5.1	General structure of quinazoline	59
5.2	Substrates and inhibitors of BCRP containing the quinazoline scaffold	60
5.3	Modifications of the quinazoline scaffold	61
5.4	Concentration-response curves of compound 109 and Ko143 obtained in the Hoechst 33342 assay.	70
5.5	Structural features of quinazolines as BCRP inhibitors	75
5.6	Scatterplot of pIC_{50} values for BCRP inhibition obtained in the Hoechst 33342 assay and the pheophorbide A assay	75

5.7	Influence of quinazolines on accumulation of calcein AM in P-gp and MRP1 overexpressing cells	76
5.8	Cytotoxicity of selected quinazolines in the MTT assay using MDCK BCRP and sensitive MDCK cells	78
5.9	Shift in dose–response curves of SN-38 and Hoechst 33342 cytotoxicity in presence of compounds 109 and 115	80
6.1	Overview of activity of flavonoids as BCRP inhibitors	83
7.1	General principle of the Hoechst 33342 assay	193
7.2	Arrangement of 96 well microplate for the Hoechst 33342 assay	194
7.3	Principle of the pheophorbide A assay	196
7.4	Schematic representation of a flow-cytometer	197
7.5	Arrangement of 96 well microplate for the pheophorbide A assay . . .	197
7.6	Principle of the calcein AM assay	198
7.7	Reduction of yellow MTT to purple formazan by cellular reductases .	200
7.8	Preparation of 96 well tissue culture plates for the MTT cytotoxicity assay	201

List of Algorithms

3.1	General reaction for synthesis of chalcones	24
3.2	General reaction involved in synthesis of benzochalcones	25
4.1	Synthesis of benzoflavones	42
4.2	Synthesis of 3-hydroxy flavones or benzoflavones from corresponding chalcones or benzochalcones	44
4.3	Synthesis of 3-methoxyflavones, 3-methoxybenzoflavones and poly- methyl derivatives of quercetin and morin	45
5.1	Synthesis of 2-phenyl-4-anilinoquinazolines	63
5.2	Synthesis of 2-(3,4-dimethoxyphenyl)-4-anilinoquinazolines	64
5.3	Synthesis of 4-anilinoquinazolines	65
5.4	Synthesis of 6,7-dimethoxy-4-anilinoquinazolines	66
5.5	Synthesis of 4- <i>N</i> -piperazinylquinazolines	67
5.6	Synthesis of 2,4-bis-anilinoquinazolines	67
6.1	Synthesis of chalcones, benzochalcones , flavones and benzoflavones .	82
6.2	Summary of synthetic routes used to prepare quinazolines	84

Publications

Research Articles

1. **Juvale, K.**; Pape, VF.; Wiese, M. Investigation of chalcones and benzochalcones as inhibitors of breast cancer resistance protein. *Bioorg. Med. Chem.* **2012**, *20*, 346-355.
2. **Juvale, K.**; Wiese, M. 4-Substituted-2-phenylquinazolines as inhibitors of BCRP. *Bioorg. Med. Chem. Lett.* **2012**, *22*, 6766-6769.
3. **Juvale, K.**; Stefan, K.; Wiese, M. Synthesis and biological evaluation of flavones and benzoflavones as inhibitors of BCRP/ABCG2. *Eur. J. Med. Chem.* (under review)
4. **Juvale, K.**; Wiese, M. Investigation of quinazolines as modulators of BCRP function and expression. (under Preparation)

Poster Presentations / conference abstracts

1. **Juvale, K.**; Wiese, M. Benzochalcones as selective inhibitors of BCRP, SFB-symposium, Vienna, Austria. (Sept. 2011).
2. **Juvale, K.**; Köhler, S.; Wiese, M. 7,8-Benzoflavones as potent inhibitors of Breast Cancer Resistance Protein (BCRP/ABCG2), 4th FEBS Special Meeting: ATP-Binding Cassette (ABC) Proteins, Innsbruck, Austria. (Mar. 2012).
3. Gallus, J.; **Juvale, K.**; Wiese, M. Investigation of pentamethoxy quercetin and pentamethoxy morin for their transport by BCRP, 4th FEBS Special Meeting: ATP-Binding Cassette (ABC) Proteins, Innsbruck, Austria. (Mar. 2012).
4. Spindler, A.; **Juvale, K.**; Wiese, M. Modulation of breast cancer resistance protein mediated multidrug resistance by quinazoline derivatives, 4th FEBS Special Meeting: ATP-Binding Cassette (ABC) Proteins, Innsbruck, Austria. (Mar. 2012).

Verfassererklärung

Hiermit erkläre ich, dass ich die vorliegende Arbeit selbständig verfasst habe. Ich habe keine anderen als die angegebenen Quellen und Hilfsmittel benutzt und die den verwendeten Werken wörtlich oder inhaltlich entnommenen Stellen als solche gekennzeichnet.

Bonn, März 2013

Kapil Juvale